



THE UNIVERSITY OF
WAIKATO
Te Whare Wānanga o Waikato

Research Commons

<http://waikato.researchgateway.ac.nz/>

Research Commons at the University of Waikato

Copyright Statement:

The digital copy of this thesis is protected by the Copyright Act 1994 (New Zealand).

The thesis may be consulted by you, provided you comply with the provisions of the Act and the following conditions of use:

- Any use you make of these documents or images must be for research or private study purposes only, and you may not make them available to any other person.
- Authors control the copyright of their thesis. You will recognise the author's right to be identified as the author of the thesis, and due acknowledgement will be made to the author where appropriate.
- You will obtain the author's permission before publishing any material from the thesis.

**EPISODIC, SEASONAL, AND LONG TERM
MORPHOLOGICAL CHANGES OF COROMANDEL
BEACHES**

A thesis
submitted in partial fulfilment
of the requirements for the degree
of
Master of Science in Earth and Ocean Sciences
at
The University of Waikato

by

ANDREW WOOD



The University of Waikato

2010

ABSTRACT

The Coromandel Peninsula was subject to subdivision and development primarily since the 1960's. Much of the development that has occurred now renders protection from the existing beach systems which have typically been altered by development. Coupled with huge populations during summer, the region is of national significance therefore an understanding of coastal impacts is paramount. Analysis of the spatial and temporal variation of beaches along the eastern Coromandel Peninsula from Whangapoua in the north to Whiritoa in the south provided results ranging from single storm events to decadal scale oscillations. Beach similarity was determined by measuring parameters such as beach length, beach connectivity to neighbouring beaches, aspect, and beach slope. The analysis of variability in beach face volumes was undertaken using an extensive beach profile database collected by R. Keith Smith, Ron Ovenden and a monitoring program maintained by Environment Waikato since 1978. The database had a higher-resolution sampling interval from 1996 until present (a maximum sampling frequency of approximately bimonthly).

Results showed that short term beach volume changes were explained by the beach classification devised from the Wright and Short (1984) model and available planform morphology data. Intermediate beaches overall had a greater range of variation, but had a higher frequency of low magnitude of change events. Reflective beaches had a higher frequency of large magnitude of change events and subsequently greater short term volume changes. Beaches adjacent to harbours and two outliers were identified which did not accord to the classification. The classification model maintained its applicability for seasonal scale beach response. Embayed beaches on the Coromandel Peninsula also exhibited beach rotation to varying degrees. Beaches with similar planform morphology showed similar long term beach rotation characteristics. A biennial oscillation related to the El Niño Southern Oscillation (ENSO) was evident as well as an interdecadal oscillation related to the Interdecadal Pacific Oscillation (IPO) was evident across the Peninsula. In particular, no beaches north of the Kuaotunu Peninsula showed a strong ENSO signal, and the strongest IPO

response was on beaches north of the Kuaotunu Peninsula. The IPO appeared to enter a long term negative phase indicating decadal scale persistence of La Niña events, therefore Coromandel beaches are likely to exhibit erosion dominant trends for the next 20 to 35 years.

Based on these results, 3 sediment transport and behavioural cells were defined, they were: beaches located north of the Kuaotunu Peninsula from Whangapoua to Otama with northerly orientations; Mercury Bay beaches including Opito Bay; and, easterly orientated beaches south of Mercury Bay.

ACKNOWLEDGEMENTS

First and foremost, my primary thanks go to my chief supervisor, Dr Karin Bryan for her enthusiasm, help, patience, and guidance throughout the project and my post graduate years. Your ever present willingness to help has made me a better scientist. Thanks also to Dr Giovanni Coco who had continual input with the project and was always happy to help where possible.

Thanks to Dr Vernon Pickett and Environment Waikato for making this project feasible with funding assistance. I also wish to thank Keith Smith firstly for pioneering an incredible dataset, but also for your ideas, enthusiasm and assistance throughout the thesis. Keith Smith and Ron Ovenden have developed the dataset into the colossus it is today!

A big thank you to the University of Waikato, the Department of Conservation and Environment Waikato (Dr Stella Frances Scholarship), and the NZ Coastal Society for financial assistance, the latter enabled attendance at the Coasts & Ports Conference in Wellington, and hopefully the first of many papers to come. You have helped in more ways than you can imagine!

Cheers to all my field assistants, I know a day in the sun on the beach at Raglan was tough work: Tracey, Emma, Dirk, Ben, Anais and Christien.

The company of the EOS grad students throughout, good times were had –Larry, Mel, Burgundy, Fantana. TCV and FNM did their best to distract me at crucial times and failed!

Dungeon crew – Bomber & Brendan Roddy, cheers for the many laughs! In particular help with drafts from Tracey Eyre

To my colleagues at CKL – Bevan Houlbrooke and Angela Bron...you guys put up with my endless requests thanks for your continued help, then kicked me out of my desk!

Last but not least, to the whanau cheers for the support the whole way through, in particular mum, dad, Emma, Red and Christine. You know it.

TABLE OF CONTENTS

Title page	Page
Abstract	i
Acknowledgements	iii
Table of Contents	v
List of Figures	vii
List of Tables	xi
	xv

Chapter 1 INTRODUCTION

1.1	MOTIVATION FOR THE STUDY	1
1.2	RESEARCH AIM AND OBJECTIVES	2
1.3	THESIS OUTLINE	2

Chapter 2 STUDY SITES AND THE BEACH PROFILE DATASET

2.1	STUDY SITES	5
2.1.1	Eastern Coromandel Peninsula	5
2.1.2	Ngarunui Beach, Raglan	9
2.2	EASTERN COROMANDEL PENINSULA GEOMORPHOLOGY	9
2.2.1	Beach Classification Parameters	11
2.2.1.1	<i>Whangapoua Beach and Matarangi Beach</i>	11
2.2.1.2	<i>Rings Beach</i>	12
2.2.1.3	<i>Kuaotunu West and Kuaotunu East Beaches</i>	12
2.2.1.4	<i>Otama Beach</i>	12
2.2.1.5	<i>Opito Bay</i>	13
2.2.1.6	<i>Wharekaho Beach</i>	13
2.2.1.7	<i>Buffalo Beach</i>	13
2.2.1.8	<i>Maramatotara Beach</i>	14
2.2.1.9	<i>Cooks Beach</i>	14
2.2.1.10	<i>Hahei Beach</i>	14
2.2.1.11	<i>Hot Water Beach</i>	14
2.2.1.12	<i>Tairua Beach and Pauanui Beach</i>	14
2.2.1.13	<i>Onemana Beach</i>	15
2.2.1.14	<i>Whangamata North and Whangamata South</i>	15
2.2.1.15	<i>Whiritoa</i>	16
2.2.2	Ngarunui Beach, Raglan	17
2.3	THE BEACH PROFILE DATASET	20
2.3.1	Data Collection at Ngarunui Beach, Raglan	21
2.3.2	Data / Sampling Error	22
2.4	WAVE DATA	22
2.5	SUMMARY	23

Chapter 3 SHORT TERM BEACH VARIATION

3.1	INTRODUCTION	25
-----	--------------	----

3.1.1	Why Study Short Term Beach Variation	25
3.1.2	Expected Outcomes	26
3.2	BACKGROUND: SHORT TERM BEACH VARIATION	26
3.2.1	Description and Definition of Short Term Beach Variation	26
3.2.2	Morphodynamics of Short Term Beach Variation	28
3.2.3	Forcing Mechanisms of Short Term Beach Variation	30
3.3	METHODS	32
3.3.1	Beach Volume Timeseries	32
3.3.2	Magnitude of Beach Volume Change	34
3.3.3	Exponential Decay versus the Intertidal Beach Slope	35
3.3.4	Short Term Variation in Wave Conditions	35
3.4	RESULTS	36
3.4.1	Short Term Observations	36
3.4.2	Beach Volume Change between Consecutive Surveys	38
3.4.3	Horizontal Beach Volume Segment Analysis	40
3.4.4	Standard Deviation of Horizontal Beach Volume Segments	44
3.4.5	Intertidal Beach Slope versus Mean Grain Size	46
3.4.6	Magnitude of Beach Volume Change	47
3.4.7	Exponential Decay versus Intertidal Beach Slope	52
3.4.8	The Impact of Wave Conditions on Short Term Beach Variation	54
3.4.9	Ngarunui Beach, Raglan	56
3.5	DISCUSSION	58
3.5.1	Observations of Beach Elevation Change	58
3.5.2	Beach Volume Change between Consecutive Surveys	60
3.5.3	Horizontal Beach Volume Segment Analysis	62
3.5.4	Standard Deviation of Horizontal Beach Volume Segments	63
3.5.5	Magnitude of Beach Volume Change	66
3.5.6	Exponential Decay versus Intertidal Beach Slope	69
3.5.7	Impact of Wave Conditions on Short Term Beach Variation	69
3.5.8	Ngarunui Beach, Raglan	70
3.6	SUMMARY	71

Chapter 4 SEASONAL VARIATION AND OSCILLATION

4.1	INTRODUCTION	73
4.1.1	The Importance of Seasonal Variation and Beach Oscillation	73
4.1.2	Expected Outcomes	74
4.2	BACKGROUND: SEASONAL OSCILLATION AND ROTATION	75
4.2.1	Seasonal Beach Variation – A Review	75
4.2.2	Beach Rotation – A Review	77
4.3	METHODS	79
4.3.1	Seasonal Variation in Beach Volumes	79
4.3.2	Beach Rotation and Oscillation	80
4.3.3	Seasonal Variation of Wave Conditions	82
	4.3.3.1 Beach Rotation versus Alongshore Wave Energy Flux	82
4.4	RESULTS	83
4.4.1	Beach Volume Variation on a Seasonal Scale	83
	4.4.1.1 Seasonal Variation- Intermediate Beaches	83
	4.4.1.2 Seasonal Variation - Reflective Beaches	84

4.4.1.3	<i>Seasonal Variation - Harbour Adjacent and Outlier Beaches</i>	85
	4.4.1.4 <i>Seasonal Variation - Lomb-Scargle Spectral Analysis</i>	86
4.4.2	Beach Rotation	87
4.4.3	Beach Rotation versus Wave Energy Flux	91
4.4.4	Seasonal Variation in Wave Height	94
4.5	DISCUSSION	96
4.5.1	Seasonal Variation – Intermediate Beaches	96
4.5.2	Seasonal Variation – Reflective Beaches	99
4.5.3	Seasonal Variation – Harbour Adjacent and Outlier Beaches	101
4.5.4	Beach Rotation	102
4.6	SUMMARY	106

Chapter 5 INTERANNUAL VARIATION

5.1	INTRODUCTION	109
5.1.1	The Importance of Interannual Variation	110
5.1.2	Expected Outcomes	110
5.2	BACKGROUND: INTERANNUAL VARIATION	111
5.2.1	Linear Analyses of Beach Variation	112
5.2.2	ENSO and IPO Impacts on Sandy Beach Systems	112
5.2.3	Non-stationary Timeseries Analysis Techniques	114
5.3	METHODS	115
5.3.1	Linear Trend Analysis	115
5.3.2	Spectral Analysis: Lomb-Scargle Fourier Transform	115
5.4	RESULTS	116
5.4.1	Linear Trend Analysis	116
	5.4.1.1 <i>Individual Profile Results</i>	116
	5.4.1.2 <i>Alongshore Variation</i>	118
	5.4.1.3 <i>Beach Average Results</i>	120
5.4.2	Observations: ENSO and IPO Trends on Beach Volume Variations	122
5.4.3	Spectral Analysis: Lomb-Scargle Fourier Transforms	124
	5.4.3.1 <i>ENSO and IPO Results</i>	124
	5.4.3.2 <i>Biennial Oscillations</i>	126
5.4.4	Interannual Variation of Wave Conditions	128
5.5	DISCUSSION	129
5.5.1	Linear Trend Analysis	129
	5.5.1.1 <i>Alongshore Variation</i>	130
5.5.2	Spectral Analysis: Lomb-Scargle Fourier Transforms	132
	5.5.2.1 <i>Biennial Trends and the ENSO</i>	132
	5.5.2.2 <i>IPO Impacts on Beach Volume Variations</i>	134
5.5.3	Coromandel Beaches – Coastal Hazards (Dahm & Gibberd, 2009)	136
	5.5.3.1 <i>Background and Introduction to the Report</i>	136
	5.5.3.2 <i>General Findings and Discussion</i>	137
	5.5.3.3 <i>Summary: Whangapoua Beach</i>	139
	5.5.3.4 <i>Summary: Matarangi Beach</i>	140
	5.5.3.5 <i>Summary: Rings Beach</i>	140
	5.5.3.6 <i>Summary: Kuaotunu East Beach</i>	140

5.5.3.7	<i>Summary: Opito Bay</i>	141
5.5.3.8	<i>Summary: Wharekaho Beach</i>	141
5.5.3.9	<i>Summary: Buffalo Beach</i>	141
5.5.3.10	<i>Summary: Maramatotara Beach</i>	142
5.5.3.11	<i>Summary: Hahei Beach</i>	142
5.5.3.12	<i>Summary: Tairua Beach</i>	142
5.5.3.13	<i>Summary: Whangamata North Beach</i>	143
5.5.3.14	<i>Summary: Whangamata South Beach</i>	143
5.5.4	Interannual Variation in Wave Conditions	143
5.6	SUMMARY	144

Chapter 6 CONCLUSIONS AND RECOMMENDATIONS

6.1	INTRODUCTION	147
6.2	BEACH CLASSIFICATION	148
6.3	SHORT TERM BEACH VARIATION	148
6.4	SEASONAL VARIATION AND OSCILLATION	150
6.5	INTERANNUAL BEACH VARIATIONS	151
6.5.1	Conclusions: Dahm and Gibberd (2009)	152
6.6	RECOMMENDATIONS FOR FURTHER RESEARCH	153

REFERENCES		159
-------------------	--	-----

APPENDICES

Appendix I:	Paper by Wood et al. (2009) from the proceedings of the Australasian Coasts and Ports Conference 2009	167
Appendix II:	Aerial photos and profile information	177
Appendix III:	Beach slope timeseries results	189
Appendix IV:	Beach elevation timeseries	199
Appendix V:	Individual profile results for horizontal segment analysis	209
Appendix VI:	Individual profile results for standard deviations of horizontal segment analysis	241
Appendix VII:	Individual profile beach volume timeseries results	249
Appendix VIII:	Individual profile magnitude of change results	263

LIST OF FIGURES

Figure 2.1. Site map illustrating the location of the Coromandel Peninsula on the north east coast of New Zealand's (inset).	7
Figure 2.2. 30 year wind hindcast data for nearshore regions at Matarangi (a), Opito Bay (b), Tairua (c), and Whangamata (d).	8
Figure 2.3. Schematic of the various beach classification parameters used (adapted from Hart & Bryan, 2008).	10
Figure 2.4. Beach length (solid black line) and average beach orientation (dashed blue line) for all beaches.	16
Figure 3.1. MSL change rate between consecutive surveys (from Yates et al., 2009).	31
Figure 3.2. A beach profile cross-section from the southern profile on Whangapoua Beach from 22-2-1998. The figure depicts the various regions used to calculate the dune volume (a); the upper beach volume area encompassing the “triangle” (c) and the corresponding area landward to a common datum (b); the intertidal beach volume encompassing the “triangle” (e) and the corresponding area landward to a common datum.	33
Figure 3.3. Timeseries of cross-shore elevation of beach topography from the central profile at Whangapoua (a), Matarangi (b), Tairua (c), and Pauanui (d) beaches.	37
Figure 3.4. Timeseries of beach volumes for the central profile on Whangapoua (a), Matarangi (b), Tairua (c), and Pauanui (d) beaches. The mean has been removed from the data. The black region illustrates above average beach volumes whilst the grey region illustrates below average beach volumes.	39
Figure 3.5. Timeseries of horizontal beach volume segments for the central profile at Whangapoua Beach. The data has been demeaned.	42
Figure 3.6. Timeseries of horizontal beach volume segments for the central profile from Matarangi Beach. The data has been demeaned.	42
Figure 3.7. Timeseries of horizontal beach volume segments for the central profile from Tairua Beach. The data has been demeaned.	43
Figure 3.8. Timeseries of horizontal beach volume segments for the central profile from Pauanui Beach. The data has been demeaned.	43
Figure 3.9. Standard deviation of horizontal beach volume segments at each site for intermediate beaches (black lines, a), reflective beaches (blue lines, b), harbour adjacent (solid red lines, c) and outlier beaches (dashed green lines, c).	45
Figure 3.10. Mean grain size versus the mean intertidal beach slope for each profile site (excluding the southern profile at Opito Beach). See text for definitions for of reflective beaches (blue stars), intermediate beaches (black circles), harbour adjacent beaches (red crosses), and outlier beaches (green squares).	47

- Figure 3.11.** Magnitude of beach volume change (logged x-axis) versus frequency of occurrence (y-axis) for intermediate beaches (solid black lines) and reflective beaches (dashed blue lines). Profile data was normalised and averaged for each beach. The logged x-axis illustrated an exponentially decaying relationship. 48
- Figure 3.12.** Magnitude of beach volume change (logged x-axis) versus frequency (y-axis) for harbour adjacent (solid red lines) and outlier beaches (dashed green lines). The logged x-axis illustrated an exponentially decaying relationship. 49
- Figure 3.13.** Magnitude of beach volume change (x-axis) versus frequency (y-axis) for intermediate (solid black lines) and reflective beaches (dashed blue lines). Erosion and accretion events were illustrated by negative and positive results respectively. 51
- Figure 3.14.** Magnitude of beach volume change (x-axis) versus frequency (y-axis) for harbour adjacent (solid red lines) and outlier beaches (dashed green lines). Erosion and accretion events were illustrated by negative and positive results respectively. 51
- Figure 3.15.** Decay constant k versus average intertidal beach slope all sites. See text for definitions for of reflective beaches (blue stars), intermediate beaches (black circles), harbour adjacent beaches (red crosses), and outlier beaches (green squares). The 3 profiles with reduced datasets were not considered for exponential decay analysis (refer text). 53
- Figure 3.16.** Average r^2 value for beach volume change versus time-averaged H_s between surveys for intermediate beaches (black bars, Whangapoua - Opito), reflective beaches (blue bars, hot Water - Whiritoa), harbour adjacent beaches (red bars, Matarangi – Whangamata South), and outlier beaches (green bars, Rings and Maramatotara). 55
- Figure 3.17.** Average r^2 value for beach volume change versus H_{max} between surveys for intermediate beaches (black bars, Whangapoua - Opito), reflective beaches (blue bars, hot Water - Whiritoa), harbour adjacent beaches (red bars, Matarangi – Whangamata South), and outlier beaches (green bars, Rings and Maramatotara). Note the different y-axis scale. 56
- Figure 3.18.** Demeaned beach volume timeseries for Rag1 (dashed green line), Rag2 (dash-dot red line), Rag3 (dotted blue line), and Rag4 (solid black line) at Ngarunui Beach, Raglan. The solid pink line with circle markers was the average volume across the four profiles. 57
- Figure 3.19.** Timeseries of the demeaned dune volume (a), upper beach volume (c), and intertidal beach volume (c) at the four survey sites Rag4 (solid black line), Rag3 (dotted blue line), Rag2 (dashed green line), and Rag1 (dash-dot red line). 58
- Figure 4.1.** Schematic identifying various beach rotation parameters and the wave energy flux direction (adapted from Ojeda & Guillen, 2008). 82
- Figure 4.2.** Average beach volume change through the year for intermediate beaches. All data have been demeaned. Beach volumes were averaged into 1.5 month groups through the calendar year beginning on January 1st. A

strong seasonal cycle is evident at all beach sites except Buffalo Beach and Cooks Beach. Otama Beach is identified as the dashed line with greatest amplitude. 84

Figure 4.3 Average beach volume change through the year for reflective beaches. The data have been demeaned. Beach volumes were averaged into 1.5 month groups through calendar the year beginning on January 1st. Hot Water Beach is the dashed line with smallest amplitude. 85

Figure 4.4. Average beach volume through the year for harbour adjacent beaches (solid red lines) and outlier beaches (dashed green lines). The data have been demeaned. Beach volumes were averaged into 1.5 month groups through the calendar year beginning on January 1st. Matarangi has a seasonal trend illustrated by the solid red line with the highest and lowest volume. 86

Figure 4.5. Beach rotation timeseries for all beaches with at least 3 profiles. Beaches are plotted from north to south, with panel labels (a) to (m) representing the 13 beaches from Whangapoua (a) to Whiritoa (m) identified below. The rotation component is illustrated in degrees. A positive slope indicates anti-clockwise rotation. Note there are 2 y-axes for clarity. The solid section of the respective y-axis depicts the y-axis limits. 88

Figure 4.6. Beach rotation timeseries for all embayed beaches. The rotation component is illustrated in degrees and a positive index/slope shows anti-clockwise rotation. The panel labels from Figure 4.5 above are maintained for simplicity and are explained in text. Note there are 2 y-axes for clarity. The solid section of the respective y-axis depicts the y-axis limits. 90

Figure 4.7. Time-averaged wave energy flux versus beach rotation at Tairua Beach (a), Whangapoua Beach (b), and Wharekaho Beach (c). The black line in each figure is the best fit line with the R-squared value identified in the top right. 93

Figure 4.8. The best fit R-squared value for each beach rotation coefficient versus time-averaged wave energy flux. The x-axis labels are defined in Section 2.1.1. 94

Figure 4.9. Seasonal variation of wave height for Matarangi (solid black line), Opito Bay (dotted blue line), Tairua (dashed green line), and Whangamata (dash-dot red line). The data was time-averaged into 1.5 month intervals through the calendar year. 95

Figure 4.10. The timing and frequency of storm wave events ($H_s > 3$ m) during the year at the Matarangi (a), Opito Bay (b), Tairua (c), and Whangamata (d) wave data sites. 96

Figure 4.11. Buffalo Beach and Cooks Beach seasonal change data for each profile on each beach. The figure illustrates the variation at these two intermediate beaches, with only the two northern most profiles on Cooks Beach (solid black line and dotted blue line) showing a seasonal trend. The remaining profiles from north to south are the dashed green line, dash-dot red line, and solid pink line with circle markers. 99

- Figure 4.12.** Significant wave height and direction at Matarangi (a), Opito Bay (b), Tairua (c), and Whangamata (d). The colourbar illustrates the frequency of the data. 103
- Figure 5.1.** 15- (blue bars) and 30- year (maroon bars) linear trend analysis for all profile sites. The profiles are plotted from north to south, left to right, and the x-axis labels are discussed in text. 120
- Figure 5.2.** 15- (blue) and 30-year (maroon) beach average volume change rates. The profiles are plotted from north to south, left to right, and the x-axis labels are discussed in text. The two arrows show apparent large scale sediment transport trends and are discussed in text. 121
- Figure 5.3.** Beach volume timeseries for the 3 Whangapoua Beach profiles from north to south (c) to (e). The beach profile data has been demeaned. The top two panels represent the ENSO (a) and IPO (b) indices for the same period with a 12-month running mean superimposed (black line). The black shading in (a) and (b) correspond to positive/warm periods where El Niño conditions dominate. The light grey shading in (a) and (b) correspond to negative/cool periods where La Niña conditions dominate. The red boxes (1 and 2) were discussed in text. 123
- Figure 5.4.** ENSO (top panel) and IPO (bottom panel) indices from 1979 to 2009 which encases the temporal variation of the beach profile dataset. Elevated beach volumes on the Coromandel Peninsula during the 1980's and the high resolution data from the mid 1990's are better attributed the IPO index. 124
- Figure 5.5.** An example power spectrum for Whangapoua Beach (CCS12, northernmost profile) produced using the Lomb-Scargle spectrum. The strongest signal has a frequency of 2.29×10^{-4} Hz (12 years) with a peak power of 25.8 % and greater than 99 % confidence. 126
- Figure 5.6.** Spectral power results for the biennial oscillation (a) and approximate 12 year oscillation (b). The arrows indicate the eastern end of the Kuaotunu Peninsula. Note the different y-axes between the upper and lower panels. The x-axis labels are discussed in text. 128
- Figure 5.7.** IPO phase shifts indicating the respective extreme conditions. From “Interdecadal Pacific Oscillation (IPO): a mechanism for forcing decadal scale coastal change on the northeast coast of New Zealand” by W. de Lange, 2000, *Journal of Coastal Research*, SI 34, p. 660. 136
- Figure 5.8.** Comparison of Whangapoua Beach volumes using the data in this thesis (solid black line) compared to the data used in Dahm and Gibberd (2009, dashed blue line). The horizontal dashed black lines represent one standard deviation above and below the mean. Three surveys exceeded two standard deviations from the mean, they were accretion events in 1992 and 2007, and the July 2008 erosion event. 139

LIST OF TABLES

Table 2-1. Beach classification data. See text for definitions.	18
Table 2-2. The four wave data sites and corresponding beaches to which the data is applied.	23
Table 3-1. The average standard deviation of demeaned beach volume (%) at each site. The standard deviations show the common variation of short term morphological change. The right hand column has ranked the beaches from lowest to highest standard deviation.	40
Table 3-2. Grouping of Coromandel Beaches according to the intertidal beach slope under the Wright and Short (1984) classification.	46
Table 3-3. Magnitude of change data for all beach sites. All data is displayed in $\text{m}^3 \cdot \text{m}^{-1} \cdot \text{day}^{-1}$. The right hand column shows the data ranked according the range of values where 1 was the lowest change rate.	52
Table 3-4. Percentiles of H_s (m) for the 30 year wave hindcast period at the four sites which represent the spatial variation of the Coromandel Peninsula.	54
Table 3-5. Harbours located adjacent to Coromandel beaches with corresponding harbour size and catchment size (Source: Mead & Moores, 2005).	64
Table 4-1. Seasonal oscillations evident in the beach profile data using Lomb-Scargle spectral analysis. The beaches and profiles are listed from north to south with the frequency in years and corresponding power in volume (%).	87
Table 4-2. The minimum, maximum and range of beach rotation coefficients for each beach analysed in this section.	89
Table 4-3. Seasonal wave height characteristics for the four sites analysed.	95
Table 5-1. Approximate 12 year spectral peaks within the beach profile data. The beaches and profiles are listed from north to south with the frequency in years and corresponding power in volume (%).	125
Table 5-2. Biennial oscillations evident within the beach profile data. The beaches and profiles are listed from north to south with the frequency in years and corresponding power in volume (%).	127
Table 5-3. Observed ENSO extremes on the northeast coast of New Zealand. From “Interdecadal Pacific Oscillation (IPO): a mechanism for forcing decadal scale coastal change on the northeast coast of New Zealand” by W. de Lange, 2000, <i>Journal of Coastal Research</i> , SI 34, p. 660.	134

CHAPTER ONE

INTRODUCTION

1.1 MOTIVATION FOR THE STUDY

The Coromandel Peninsula and its extensive white sandy beaches are among the most popular summer holiday destinations in New Zealand. The Coromandel has a diverse range of beach morphologies and were largely developed in the 1960's during periods of rapid subdivision in New Zealand as a result of improved road access. This significant land use change and extensive development has resulted in many beachfront settlements relying on the protection of the existing beach system from coastal processes. Continued development and increasing population pressure(s) has resulted in most beach regions becoming urbanised with numerous impacts on the pre-existing beach systems such as dune alteration, vegetation destruction, and lack of restrictions on beach pedestrian access which all contribute to degradation of beaches. Development was typically located on or close to the frontal dune and in many cases dunes were levelled to provide coastal views (Healy et al., 1981; Environment Waikato, 2002). As a result, numerous areas have been identified as erosion hotspots in which long term erosion trends coupled with short term storm impacts could lead to loss of property and infrastructure.

Monitoring subaerial beach variation on a large spatial scale is time consuming and can be expensive for local authorities to obtain high quality data. Regardless, there is a need to understand subaerial beach behaviour on the Coromandel to ensure the Regional Council (Environment Waikato; EW) has an adequate understanding of how beach morphology changes may impact the natural state of beaches and any potential impacts on development and infrastructure. There is limited published literature regarding Coromandel beach behaviour, with initial surveys and analysis by Healy et al. (1981) which classified the major sandy beaches of the eastern Coromandel based on limited survey data and historical shoreline analysis.

1.2 RESEARCH AIM AND OBJECTIVES

The primary aim of this research is to quantify the spatial and temporal variation of subaerial beach behaviour on the Coromandel Peninsula in order to provide EW with sufficient information on where to focus future monitoring efforts. This lead to the following objectives:

1. To describe the geomorphology and planform geometry of Coromandel beaches using the ArcGIS 1:50,000 topographic database coupled with surficial sediment sampling at each profile site;
2. To quantify the short term variation of subaerial beach systems on the Coromandel Peninsula and determine the forcing mechanisms which cause these short term changes;
3. To identify medium term oscillation(s) and variations of subaerial beaches on the Coromandel Peninsula and identify the beach response to medium term coastal processes; and
4. To determine the presence of interannual and long term behaviour of Coromandel beaches. This includes the determination of whether relationships were present between beach response and known climate variations.

Preliminary results of these objectives were published in the Proceedings of the Australasian Coasts and Ports Conference 2009 (Wood et al., 2009), attached as Appendix I.

1.3 THESIS OUTLINE

Following on from this chapter, the thesis is separated into chapters depending on the timescale of analysis. Firstly, **Chapter 2** consists of a description of the Coromandel Peninsula, the beach sites, of which the beaches were classified according to geomorphologic characteristics. A description of the beach profile dataset used in this thesis is also given, along with a background of Ngarunui Beach near Raglan which was used to compare east coast beach variation with short term west coast variation.

Chapter 3: Short Term Beach Variation

In Chapter 3, the short term variation of Coromandel beaches is analysed. The chapter describes how the analysis was performed and the key results in relation to the nearshore wave conditions and forcing mechanisms. The chapter described the methods, results, reviewed published literature, discussion, and conclusions of short term beach variation on the Coromandel Peninsula.

Chapter 4: Seasonal Variation and Oscillation

The timescale of analysis was increased to seasonal variation and medium term beach oscillations in Chapter 4. Seasonal changes in beach and wave conditions were explained, including beach rotation and the forcing mechanisms responsible for these coastal processes.

Chapter 5: Interannual Variation

Chapter 5 presented the spatial variation of long term morphological change on the Coromandel Peninsula. Comparisons to known climate oscillations were given using linear methods and non-stationary timeseries analysis. A comparison of the long term trends is made to a recent report by Dahm and Gibberd (2009) regarding coastal erosion and development setbacks on the Coromandel Peninsula.

Chapter 6: Conclusions and Recommendations

A summary of all the results and key findings summarising the spatial and temporal variation of Coromandel beaches was provided in Chapter 6. This chapter also outlined some suggestions for future research in order to better understand Coromandel beach morphodynamics and provide more detailed site specific information.

Following the main results and analyses, a full reference list was provided and further supporting information critical to the understanding of Coromandel beaches as follows:

- Appendix I: Paper by Wood et al. (2009) from the Proceedings of the Australasian Coasts and Ports Conference 2009;
- Appendix II: Aerial photos of all the profile sites at each beach and a table with the dates with which they were established and have data available from;
- Appendix III: Timeseries of intertidal beach slopes used to calculate average intertidal beach slope;
- Appendix IV: Timeseries plots of beach elevation through time;
- Appendix V: Horizontal segment results for each beach and profile;
- Appendix VI: Standard deviation of horizontal beach segments for each beach;
- Appendix VII: Demeaned beach volume timeseries for each beach and profile site with respective standard deviations.
- Appendix VIII: Magnitude of volume change individual beach and profile results.

Figure and table numbering within this thesis is chapter specific, with the first number representing the relevant chapter, and the second representing the figure / table number. For example, Figure 3.19 is the 19th figure in Chapter 3. Figures contained within appendices have the relevant appendix number in roman numerals as opposed to numerical digits, for example Figure VII.7 is the 7th figure in Appendix VII.

CHAPTER TWO

STUDY SITES AND THE BEACH PROFILE DATASET

2.1 STUDY SITES

This chapter describes the geomorphology of all beaches in this study, and the extensive beach profile dataset which has been gathered over the last 30 years across the eastern Coromandel Peninsula, and the interim data collected from Ngarunui Beach at Raglan. Other sites on the Coromandel Peninsula have been surveyed however the data were not available at the time of analysis.

2.1.1 Eastern Coromandel Peninsula

The eastern Coromandel Peninsula is located on the east coast of the North Island of New Zealand (Figure 2.1). The east coast of New Zealand is a lee coast from the prevailing westerly winds (Figure 2.2). As a result, the Coromandel Peninsula is relatively sheltered and the wave climate is described as storm dominated (Bradshaw, 1991; Gorman et al., 2003b). The dominant wave direction is from the north east. However, easterly storm conditions are not uncommon and have previously been determined to be primarily responsible for local beach erosion (Healy & Dell, 1987; Bradshaw, 1991). Tides are semi-diurnal and the maximum spring tidal range is approximately 1.8 m across the entire study site with a spring-neap variation of approximately 0.4 m (Land Information New Zealand; LINZ). The eastern Coromandel Peninsula coastline has been described as a headland-bay coast, comprised of a succession of steep rocky headlands separated by narrow shallow bays (McLean, 1979; Bradshaw, 1991). Most of the beaches are classified as “bayhead” or “pocket” beaches and are closed sedimentary systems meaning very little sediment input is received from littoral drift or terrigenous input from rivers (Bradshaw, 1991).

The Coromandel Peninsula is an uplifted horst block which is downtilted to the east (Healy et al., 1981). The steep and irregular topography of the Peninsula

reaches altitudes of up to 800 m with steep river valleys leading down to numerous embayments (Hume & Dahm, 1991). As a result, catchment areas are highly variable with the largest being Whitianga, Tairua, and Whangapoua at 492 km², 282 km², and 106 km² respectively (Mead & Moores, 2005). In numerous embayments, sea level rise of approximately 100 m during the Holocene resulted in considerable sedimentation and were almost entirely infilled. This infilling resulted in a complex of barrier ridges and estuarine deposits (e.g. Whangapoua, Otama, and Whiritoa, Healy et al., 1981).

Average annual precipitation is approximately 3000 mm.yr⁻¹, with individual high intensity events being associated with cyclonic systems (Ross et al., 1994). Large rain events have been measured to be greater than 550 mm in a single 24 hour period. These rainfall intensities can lead to very large runoff events from the steep catchment (Mead & Moores, 2005). The prevailing west to south-west winds (Figure 2.2) are associated with the passage of mid-latitude high pressure systems (Bradshaw, 1991). High velocity onshore-directed easterly and north-easterly winds occur during less frequent storm events which result in torrential orographically induced rainfall (Bradshaw, 1991).

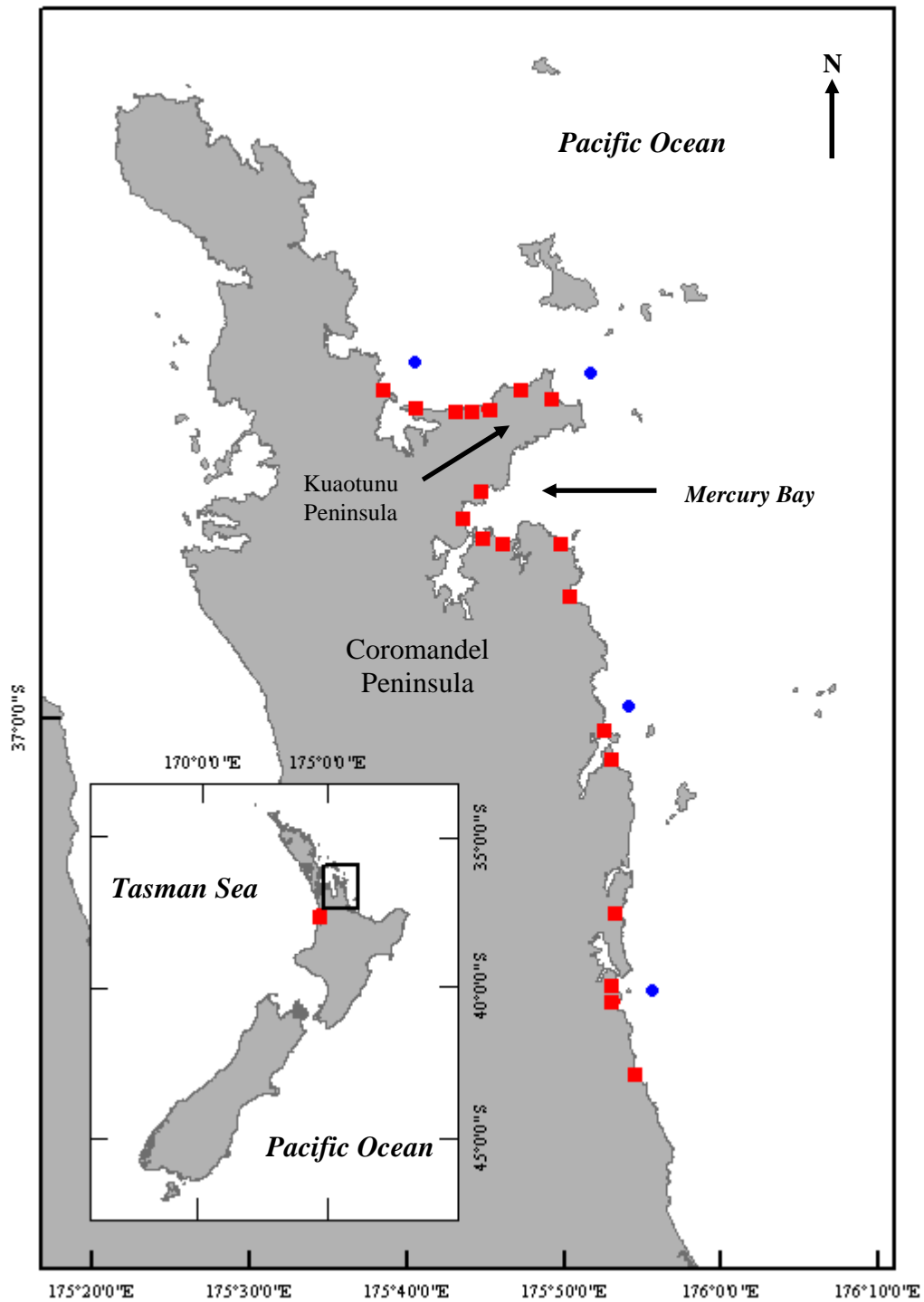


Figure 2.1: Site map illustrating the location of the Coromandel Peninsula on the north east coast of New Zealand's (inset). A list of the 19 Coromandel beaches (red squares) from north to south, left to right is given in text. Blue circles mark the wave data hindcast locations at Matarangi, Opito Bay, Tairua, and Whangamata (Table 2-2). The red square symbol in the inset is Ngarunui Beach, Raglan.

This study consists of 19 sandy beaches along the eastern Coromandel Peninsula (Figure 2.1) from Whangapoua in the north to Whiritoa in the South (refer below). A total of 61 profile sites are located across the 19 beaches (refer Appendix II).

Below is a list of the beaches from north to south (west to east) and subsequent x-axis labels used in Figure 2.4 throughout this thesis:

- Whangapoua (a)
- Matarangi (b)
- Rings (c)
- Kuaotunu West (d)
- Kuaotunu East (e)
- Otama (f)
- Opito Bay (g)
- Wharekaho (h)
- Buffalo (i)
- Maramaratotara (j)
- Cooks (k)
- Hahei (l)
- Hot Water (m)
- Tairua (n)
- Pauanui (o)
- Onemana (p)
- Whangamata North (q)
- Whangamata South (r)
- Whiritoa (s)

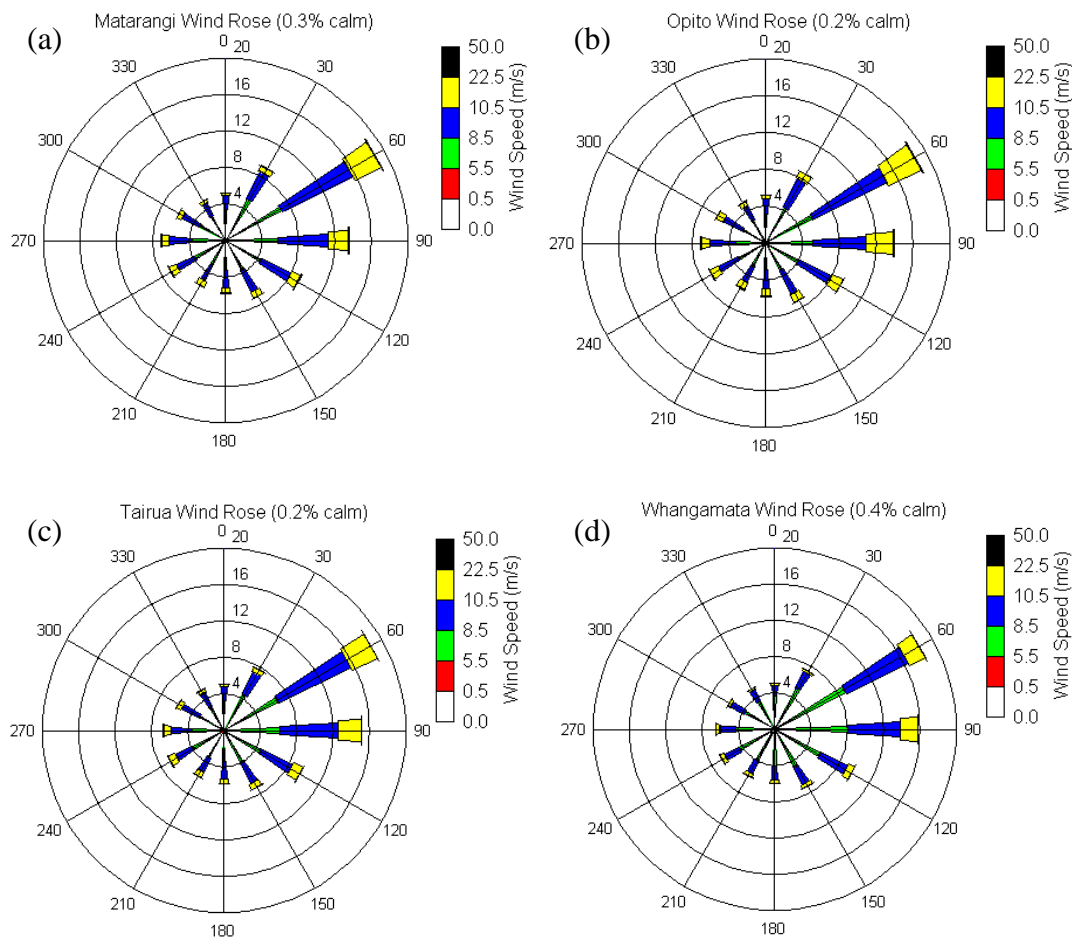


Figure 2.2: 30 year wind hindcast data for nearshore regions at Matarangi (a), Opito Bay (b), Tairua (c), and Whangamata (d). The numbers on the circumference of each panel represent the wind direction. The inner numbers on the vertical axes are percentages of the respective wind strength identified by the colour bar label. The locations from where the data are taken from are in Figure 2.1 (blue circles). The rose diagrams illustrate the consistency of the prevailing southwest to westerly winds which account for approximately one third of all wind conditions at each site.

2.1.2 Ngarunui Beach, Raglan

Ngarunui Beach is located near Raglan on the west coast of the North Island of New Zealand (Figure 2.1). There have been few studies carried out on west coast beaches of the Waikato Region. As a result, no long term datasets exist for wave and climate conditions. The west coast of New Zealand is a high energy swell dominated coast and has been described as a “river of sand” (Hart & Bryan, 2008), pertaining to the large scale sediment transport along the west coast of the North Island. In contrast to the east coast, Raglan has a large spring-neap tidal variation with a maximum spring tidal range of 2.8 m and a neap variation of 2.0 m (LINZ). The wave climate has an average significant wave height of 1.60 m with a mean period of 7.4 s. The mean wave direction was 68.3° and describes the direction to which waves are approaching. Scarfe (2008) used a NIWA wave hindcast model from 1979 – 2007 to derive the wave characteristics for the region. The location for the wave data was taken in 11 m water depth at the southern end of the beach adjacent to Manu Bay (refer Appendix II).

2.2 EASTERN COROMANDEL PENINSULA BEACH GEOMORPHOLOGY

Due to the spatial variation of the study site, a method of beach classification was required to identify beaches with similar geomorphologic characteristics. The following characteristics were used to initially classify beach systems and are summarised in Figure 2.3:

- Beach length;
- Beach orientation;
- Connection distance;
- Intertidal beach slope;
- Mean grain size; and
- The presence of offshore islands.

Beach lengths were calculated from the ArcGIS 1:50,000 topographic database from LINZ, defined as the length of the shoreline containing sand and inlet (e.g.

Hart & Bryan, 2008) and were shown in Figure 2.4. Beach orientation was calculated as the vector average of the orientation of the shoreline at both ends of the beach (e.g. Hart & Bryan, 2008) and were shown in Figure 2.4. Connection distance to the nearest beach (left and right looking seaward) was the approximate distance of coastline to the nearest beach (Figure 2.3), measured as the length of the two seaward sides of the triangle defined by the headland extent line and the beach separation line (Hart & Bryan, 2008). The intertidal beach slope was calculated using an average of the lowest three surveyed points above Mean Low Water Springs (MLWS) for the entire timeseries and expressed in radians. The effects of wave propagation on nearshore processes due to offshore islands were given a yes / no value depending on whether islands were located within 10 km of the beach or within the 50 m depth contour (whichever was closest to the shoreline; Table 2-1).

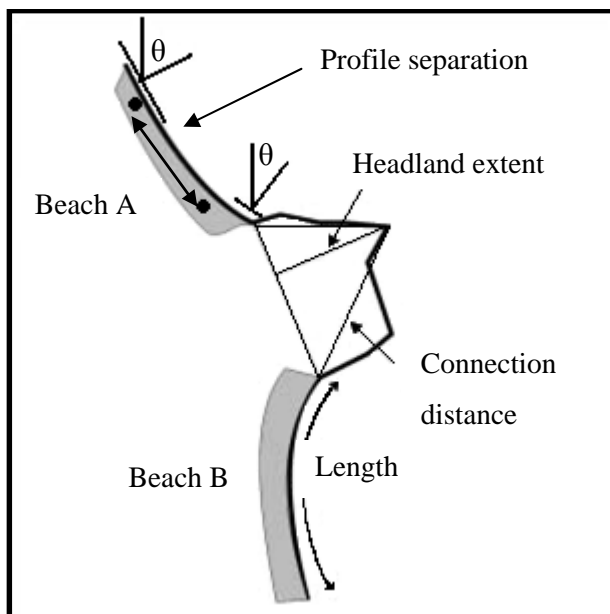


Figure 2.3: Schematic of the various beach classification parameters used (adapted from Hart & Bryan, 2008). See text for definitions.

Sediment samples to determine mean grain sizes were collected during a field excursion on the 25th and 26th of May 2009. Surficial sediment samples were obtained from the middle region of the intertidal zone at each profile site. Each sample was approximately 150 grams and comprised of sediment from the top 50-80 mm of the beach. Mean grain size characteristics were measured using the University of Waikato Rapid Sediment Analyser (RSA). The RSA uses

cumulative mass and measurement time to determine the settling velocity and size distribution (de Lange et al., 1997). Sediment samples were dried then passed through a 2 mm sieve to remove large shell fragments which were not a dominant part of the natural beach sediment. All sediment samples were sieved except for Maramaratotara (Figure 2.1 and Table 2-1) where shell material is the dominant beach sediment. Eastern Coromandel beaches are mainly sandy beaches comprising quartz, feldspars and volcanic glass, with minor quantities of calcite (shell material), heavy minerals (mainly titanomagnetite) and rock fragments (de Lange et al., 1997).

2.2.1 Beach Classification Parameters

The following sections provide a summary of the geomorphologic characteristics of each beach system from north to south. Figure 2.4 illustrates the respective beach length and average orientation for each beach. The location of each beach and the profile sites are illustrated in Figure 2.1 and aerial photos are attached as Appendix II. Timeseries of intertidal beach slope data are attached as Appendix III.

2.2.1.1 Whangapoua Beach and Matarangi Beach

Whangapoua Beach (Figure 2.1) is a pocket beach (1804 m, Table 2-1 & Figure 2.4) with headland barriers at each end. Whangapoua Beach is an intermediate sloped beach (Wright & Short, 1984) with a mean grain size of 322 μm (Table 2-1). A small estuary is located at the northern end of the beach. Pungapunga Island is a small island (2590 m^2) located toward the northern end of Whangapoua Beach approximately 150 m seaward of Mean High Water Springs (MHWS). Whangapoua Beach has three profile sites with separation distances between the three profiles of 377 m and 510 m. Matarangi Beach is a dune barrier beach located immediately east of Whangapoua Beach. Matarangi Beach is the longest (4618 m) and lowest gradient beach on the eastern Coromandel Peninsula and has a mean grain size of 275 μm (Table 2-1). Matarangi Beach abuts a headland at the eastern (basal) end and the spit extends to the west where it terminates at the

entrance to Whangapoua Harbour (distal end). Matarangi Beach has four profile sites with separation distances between the profiles of 481 m, 681 m, and 952 m.

2.2.1.2 *Rings Beach*

Rings Beach is a short pocket beach (627 m) with headland barriers at each end, and a small stream at the western end. Rings Beach has a mean grain size of 402 μm (Table 2-1) and has one profile site.

2.2.1.3 *Kuaotunu West and Kuaotunu East Beaches*

Kuaotunu West is an 1180 m long beach with a headland at the western end and a large rock outcrop at the eastern end. Kuaotunu West is an intermediate sloped beach with a mean grain size of 346 μm (Table 2-1) and a stream located centrally on the beach. Kuaotunu West has three profile sites with separation distances between the three profiles of 172 m and 349 m. Kuaotunu West Beach was mined for sand and gravel from approximately 1950 to 1980. Kuaotunu East is a 1205 m long beach with a headland at the eastern end and a large rock outcrop at the western end separating it from Kuaotunu West. Kuaotunu East is an intermediate sloped beach with a mean grain size of 427 μm (Table 2-1) and a stream at the eastern end of the beach. The relatively large grain size was caused by the presence of fine gravels in the sample which affected the sediment fall velocity calculation. Kuaotunu East has three profile sites with separation distances between the three profiles of 417 m and 291 m.

2.2.1.4 *Otama Beach*

Otama Beach is a 2275 m long beach with headland barriers at each end. Otama is an intermediate sloped beach with a mean grain size of 395 μm (Table 2-1). Otama Beach has a small estuary located at the eastern end of the beach and a small stream at the western end of the beach. Otama has two profile sites with a separation distance of 900m.

2.2.1.5 *Opito Beach*

Opito Beach is a 4417 m long beach with headland barriers at each end. Opito Beach is an intermediate sloped beach with a mean grain size of 252 μm (Table 2-1). A total of four small streams enter the Pacific Ocean across Opito Beach. Opito Beach has five profiles sites with separation distances between the five profiles of 894 m, 604 m, 485m, and 536 m. Opito Bay has a significant orientation change between the two ends of the beach. The northern end of the beach has an aspect of 99° and the southern end of the beach has an aspect of 310°, a total orientation change of 149°. The beach aspect was defined in Figure 2.3 as the vector average of the orientation of the shoreline at each end of the beach.

2.2.1.6 *Wharekaho Beach*

Wharekaho Beach is a 1539 m long with headland barriers at each end. Wharekaho Beach is an intermediate sloped beach with a mean grain size of 306 μm (Table 2-1). Titanomagnetite lag deposits were present in the sediment samples from Wharekaho Beach. Wharekaho Beach has two streams located the northern and southern ends of the beach. Wharekaho has three profile sites with separation distances between the three profiles of 719 m and 474 m.

2.2.1.7 *Buffalo Beach*

Buffalo Beach is a 3742 m long beach which terminates at a headland at the northern end of the beach and Whitianga Harbour at the southern end of the beach. Buffalo Beach is an intermediate sloped beach with a mean grain size of 197 μm (Table 2-1). In addition to Whitianga Harbour, Buffalo Beach has three streams which enter Mercury Bay (Figure 2.1). Buffalo Beach has five profile sites with separation distances between the five sites of 625 m, 709 m, 532 m, and 508 m. Buffalo Beach has 3 seawalls on various regions of the beach (refer Section 3.5.1).

2.2.1.8 *Maramaratotara Beach*

Maramaratotara Beach is a short pocket beach (1209 m) with headland barriers at each end. Maramaratotara is a steep beach with a mean grain size of 1072 μm (Table 2-1) and a stream located at the eastern end of the beach. The beach sediment is largely composed of shell fragments as opposed to all other beaches in this study which are predominantly sandy beaches with quartz-feldspar rich sand (de Lange et al. 1997). Maramaratotara Beach has one profile site.

2.2.1.9 *Cooks Beach*

Cooks Beach is a 2674 m long beach terminated by a headland at the western end and Purangi Estuary at the eastern end of the beach. A stream is also located at the western end of the beach. Cooks Beach is an intermediate sloped beach with a mean grain size of 204 μm (Table 2-1). Cooks Beach has five profile sites with separation distances between the five sites of 822 m, 793 m, 242 m, and 258 m.

2.2.1.10 *Hahei Beach*

Hahei Beach is a 1465 m long beach with headland barriers at each end. Hahei is an intermediate sloped beach with a mean grain size of 302 μm (Table 2-1). Hahei has two profile sites with a separation distance of 591 m.

2.2.1.11 *Hot Water Beach*

Hot Water Beach is an 1865 m long beach with headland barriers at each end. Hot Water Beach is a steep beach with a mean grain size of 430 μm (Table 2-1). Hot Water Beach has three streams located at the northern, central, and southern sections of the beach. Hot Water Beach has three profile sites with separation distances between the three sites of 817 m and 649 m.

2.2.1.12 *Tairua Beach and Pauanui Beach*

Tairua Beach is a 1511 m long beach with headland barriers at each end. Tairua Beach is a steep beach with a mean grain size of 427 μm (Table 2-1). Tairua

Beach has four profile sites with separation distances between the four sites of 179 m, 337 m, and 245 m. Pauanui Beach is a dune barrier located immediately south of Tairua Beach. The two beaches are separated by Paku hill and the entrance to Tairua Harbour. Pauanui Beach is a 2899 m long beach which abuts a headland at the southern (basal) end and the spit extends to the north where it terminates at the entrance to Tairua Harbour (distal end). The mean grain size is 246 μm (Table 2-1). Pauanui Beach has a stream located at the southern end of the beach and five profile sites with separation distances between the southern four sites of 614 m, 506 m, and 358 m. The benchmark for the northern most profile site is relatively new (established in 2004) and has not been surveyed to the local datum therefore no reference to the location or distance to the nearest profile can be given, hence why only three separation distances are given.

2.2.1.13 Onemana Beach

Onemana Beach is a 1088 m long pocket beach with headland barriers at each end. Onemana Beach is a steep beach with a mean grain size of 429 μm (Table 2-1). Onemana Beach has three streams located at the northern, central and southern sections of the beach. Onemana Beach has two profile sites with a separation distance between the two sites of 230 m.

2.2.1.14 Whangamata North and Whangamata South Beaches

Throughout this thesis Whangamata Beach has been analysed as two different beach systems. Although Whangamata Beach consists of one continuous shoreline between Whangamata Harbour in the north and Otahu River in the south, the beach is analysed as two separate beaches due to the significant orientation change north and south of Hauturu Island. The impact of Hauturu Island on wave refraction patterns and littoral drift has created a tombolo in the lee of the island, which has an impact on the behaviour to the north and south of the island (Healy et al., 1981). Whangamata North is a 2206 m long beach which terminates in the north at the entrance to Whangamata Harbour and the tombolo of Hauturu Island in the south. Whangamata North is an intermediate sloped beach with a mean grain size of 247 μm (Table 2-1). Whangamata North has two profile sites with a

separation distance between the two sites of 972 m. Whangamata South is an intermediate sloped beach with a mean grain size of 225 μm (Table 2-1). Whangamata South is a 1667 m long beach which terminates at the tombolo of Hauturu Island in the north and the entrance to the Otahu River in the south. Whangamata South has four profile sites with separation distances between the four sites of 286 m, 293 m, and 391 m.

2.2.1.15 Whiritoa Beach

Whiritoa Beach is a 1489 m long beach with headland barriers at each end. Whiritoa is a reflective beach with a mean grain size of 395 μm (Table 2-1) and a stream at each end of the beach. Whiritoa Beach has four profile sites with separation distances between the four sites of 283 m, 314 m, and 226 m. Beach sand from Whiritoa has a history of sand mining as evidenced by McLean (1979) and Healy et al. (1981).

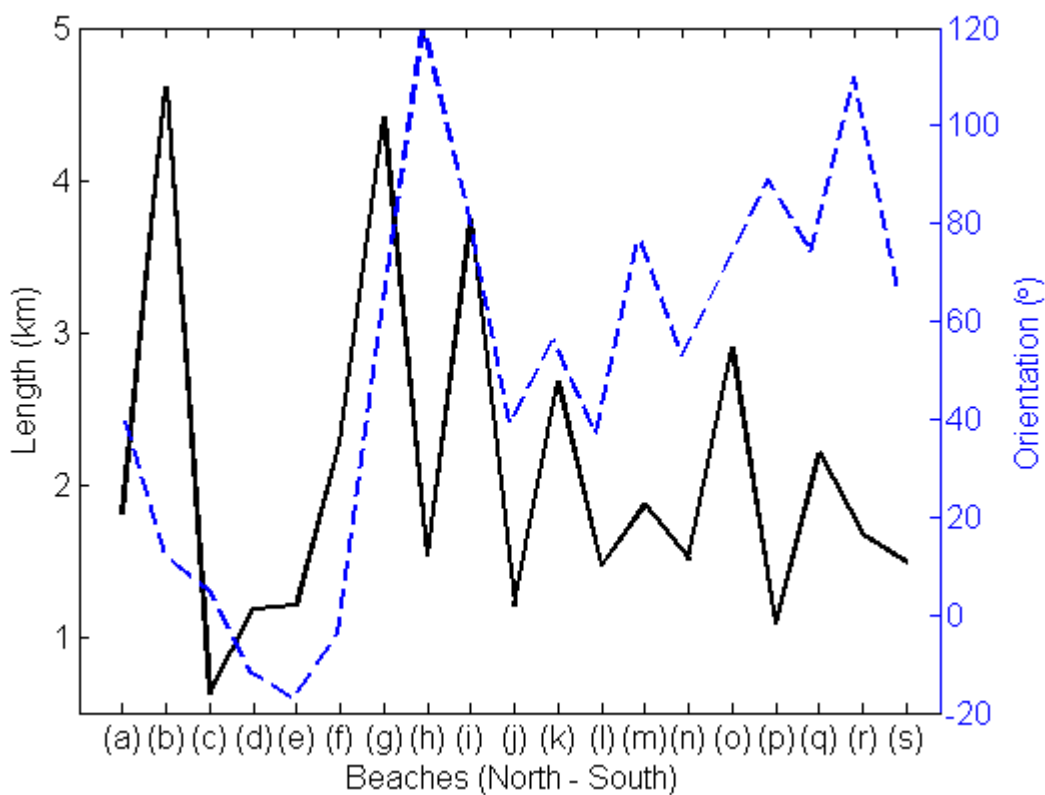


Figure 2.4: Beach length (solid black line) and average beach orientation (dashed blue line) for all beaches. The x-axis labels are discussed in Section 2.1.1.

2.2.2 Ngarunui Beach, Raglan

Whilst the main part of this thesis was to analyse the spatial and temporal variation of beaches located on the eastern Coromandel Peninsula, a comparison is also made to Ngarunui Beach at Raglan (Figure 2.1). Ngarunui Beach is a 5210 m long beach with headland barriers at each end. Following the definition of beach length in Hart and Bryan (2008), the beach length includes the inlet to Raglan Harbour and approximately 2400 m of beach to the north of the inlet. The dominant beach sediment is titanomagnetite with a mean grain size of 293 μm (Table 2-1). Sediment samples were obtained on the 23rd of January 2009 from the intertidal area of each profile site. Grain size analysis was undertaken using the University of Waikato Malvern Mastersizer-S because the dominant beach sediment is titanomagnetite which cannot be analysed in the RSA (de Lange et al., 1997). The Malvern Mastersizer-S calculates particle size using laser diffraction theory. Ngarunui Beach has four profile sites with separation distances between the four sites of 245 m, 205 m, and 251 m.

Table 2-1: Beach classification data. See text for definitions.

Beach Name	Length (m)	Average Orientation (°)	Intertidal Beach Slope	Mean Grain Size (µm)	Presence of Offshore Islands	Number of Profiles	Connectivity Index (m)
Whangapoua	1804	41	0.05	322	Yes	3	L: 1230 R: 990
Matarangi	4618	12	0.02	275	No	4	L: 990 R: 735
Rings	627	5	0.10	402	No	1	L: 735 R: 779
Kuaotunu West	1180	348	0.06	346	No	3	L: 779 R: 411
Kuaotunu East	1205	343	0.05	427	No	3	L: 411 R: 2348
Otama	2275	356	0.07	395	Yes	2	L: 2348 R: 809
Opito	4417	59	0.03	252	Yes	5	L: 2177 R: 1107
Wharekaho	1539	120	0.05	306	Yes	3	L: 3102 R: 2044
Buffalo	3742	83	0.02	197	Yes	5	L: 2044 R: 876
Maramatotara	1209	39	0.11	1072	Yes	1	L: 876 R: 1069
Cooks	2674	56	0.05	204	Yes	5	L: 338 R: 3870
Hahei	1465	37	0.07	302	Yes	2	L: 1144 R: 2838

Table 2-1 continued.

Beach Name	Length (m)	Average Orientation (°)	Intertidal Beach Slope	Mean Grain Size (µm)	Presence of Offshore Islands	Number of Profiles	Connectivity Index (m)
Hot Water	1865	77	0.11	430	Yes	3	L: 1156 R: 5890
Tairua	1511	53	0.12	427	Yes	4	L: 2571 R: 1389
Pauanui	2899	71	0.04	246	Yes	5	L: 1389 R: 5201
Onemana	1088	89	0.13	429	No	2	L: 3691 R: 949
Whangamata North	2206	74	0.04	247	No	2	L: 1178 R: 0
Whangamata South	1667	110	0.03	225	Yes	4	L: 0 R: 993
Whiritoa	1489	66	0.13	395	No	4	L: 174 R: 6157
Ngarunui Beach (Raglan)	5210	286	0.01	293	No	4	L: 2236 R: 446

2.3 THE BEACH PROFILE DATASET

Many of the profile sites were established in the summer of 1978-1979 after the renowned storms of 1978 (Hume, 1979) and were sporadically sampled by Environment Waikato (EW) using a level and staff. In addition, R. Keith Smith (Private Consultant) and Ron Ovenden (National Institute of Water and Atmospheric Research, NIWA) have been undertaking regular beach profile surveys of the Coromandel beaches since 1990 and have gathered an extensive database across the 61 profile sites. Each profile in the database has a specific name, for example the northern profile at Whangapoua Beach is CCS12. CCS stands for Coromandel Coastal Survey, the benchmark names of the original survey in which the number corresponds to the profile location (Healy et al., 1981). These surveys were undertaken using the Emery method (Emery, 1961). Not all sites were established in 1979, and further profile sites were established between 1979 and 2004 to increase the spatial variation of the database (Stewart, 2006). The profiles have been surveyed every 2 months since 1996 and 6-weekly more recently. Each survey begins from a known benchmark typically located landward of the dune crest. During each survey, points of interest such as the edge of vegetation line, the storm high water mark, the high water mark, and the extent of any saturated surface were measured where possible (Smith & Bryan, 2007). It is emphasised that surveys were often undertaken to measure specific storm damage, and never specific accretion periods. Therefore there is potential for the database to be skewed toward erosion dominated profiles.

The location of the benchmarks for each profile site are identified in Appendix II. Geodetic Datum 2000 was used for the survey for the Coromandel beach benchmarks as it was the only common datum encompassing the geographic area required (Stewart, 2002). The benchmark coordinates were converted to New Zealand Map Grid 1949 Projections and are all currently in use. The benchmark elevations are surveyed to Moturiki Mean Sea Level 1953 Datum which is RL 0.0 m (Stewart, 2006). The accuracy of the survey equipment used to locate the benchmarks was +/- 20 mm vertically and +/- 10 mm horizontally (Stewart, 2002). The beach profile database contains more than 5,500 profiles across 61 profile sites.

2.3.1 Data Collection at Ngarunui Beach, Raglan

Four new beach profile lines were established at Ngarunui Beach, Raglan. The beach profiling began in January 2009 and was surveyed on the same sampling cycle as the eastern Coromandel programme. Four beach profile lines were established along Ngarunui Beach with a spacing of approximately 200 m between each profile (refer Section 2.2.2). The location of the profile benchmarks are identified in Appendix II. There were several important considerations to be made when establishing the location of the beach profiles, including:

- the physical processes and impact of the Raglan Harbour entrance;
- the location of two EW camera operations which overlook the southern end of the beach; and
- human influences such as beach access locations.

A Nikon Electronic Total Station DTM-352 was used for beach profile surveying at Ngarunui Beach. The Total Station has precision of ± 10 mm at distances of up to 500 m. The total station was set up and levelled over a surveyed benchmark and the horizontal and vertical distance to the reflective prism was measured at points of interest across the profile line. The spacing of the measurements increased as the beach slope became more regular with distance from the dune region. Profiles were undertaken within an hour of low tide to ensure maximum excursion distances. All notable elevation changes were recorded along the profile and included the storm high water mark, high water mark, and the extent of any saturated surface where possible. All surveys were undertaken from the secondary benchmark (seaward most benchmark) with an annual survey encompassing the dune area landward to the primary benchmark. The profile benchmarks at Ngarunui Beach were surveyed using a real time kinetic global positioning system (GPS) to determine the location and elevation of the primary and secondary benchmarks and were surveyed to Mount Eden Circuit 2000 Datum. The elevations were surveyed to Moturiki Vertical Datum 1953, the same elevation datum as the east coast data.

2.3.2 Data / Sampling Error

The beach profile dataset is unique due to its large spatial and temporal extent, with relatively high sampling frequency since 1996. The Emery method used to collect the data has been the most widely applied method of beach surveying since its inception in the 1960's (Smith & Bryan, 2007). Original testing of the Emery method (Emery, 1961) calculated the average error in elevation between two points to be 0.035 feet (approximately 10.6 mm) with a maximum error of 0.18 feet (approximately 55 mm). These low values were not considered large enough to add significant error to the data presented.

2.4 WAVE DATA

There were no measured long term wave data available for the Coromandel Peninsula. A NIWA WAM (WAVE Model) hindcast was used to generate nearshore wave characteristics for four sites around the Coromandel Peninsula (Figure 2.1) from 1979 – March 2009. The wave hindcast model had a high correlation to measured wave buoy data for wave height data ($R = 0.88$, Gorman et al., 2003b). The buoy was located in 34 m water depth near Katikati, approximately 20 kilometres south from Whiritoa, the southernmost beach site. Four sites in 20 m water depth were chosen to encompass the spatial variation of the dataset with particular interest being given to areas with offshore islands or large bay features. These four sites were considered to provide sufficient spatial variation of wave climate variability along the Coromandel Peninsula. The wave data sites are outlined in Table 2-2 with the respective beaches to which the data was applied.

Table 2-2: The four wave data sites and corresponding beaches to which the data is applied.

Matarangi Wave Data	Opito Wave Data	Tairua Wave Data	Whangamata Wave Data
Whangapoua	Opito	Hahei	Onemana
Matarangi	Wharekaho	Hot Water	Whangamata North
Rings	Buffalo	Tairua	Whangamata South
Kuaotunu West	Maramaratotara	Pauanui	Whiritoa
Kuaotunu East	Cooks		
Otama			

2.5 SUMMARY

This thesis incorporates the study of a beach profile dataset with large spatial and temporal variation on the eastern Coromandel Peninsula of New Zealand. A total of 61 profile sites across 19 beaches with differing geomorphologic characteristics were discussed. The most dissipative beach on the Coromandel Peninsula, Matarangi, is to be compared to Ngarunui Beach at Raglan which is a dissipative beach located on the west coast of the Waikato region. The beach profiles were analysed and compared against wave hindcast data in order to determine the forcing mechanisms responsible for beach change on the eastern Coromandel Peninsula. The methodology used for the analysis of spatial and temporal variation of beach change on the Coromandel is provided within each individual chapter.

CHAPTER THREE

SHORT TERM BEACH VARIATION

3.1 INTRODUCTION

Beach systems on the Coromandel Peninsula have been subject to urbanisation and development pressures since the 1960's. The development has led to alteration of dune systems and typically resulted in a direct loss of sediment from the subaerial beach system which serves as a buffer from storm activity. Unfortunately this development was thriving at a time when the unstable nature of foreshores was not required to be taken into account in subdivision planning. As a result, significant property loss and damage during storms has occurred (Healy et al., 1981). The impact of storm activity combined with human alteration of the beach system has had detrimental effects on many Coromandel beaches. Adverse effects were often enhanced as the beaches were thought to be closed sedimentary systems, meaning they had very little sediment input from terrestrial sources or from sediment exchange between embayments via a nearshore littoral drift system (Healy et al., 1981). Due to the development on the Coromandel Coast and the potential impacts of storm wave conditions, the nature and distribution of short term beach variation on the Coromandel Peninsula needs to be understood.

3.1.1 Why Study Short Term Beach Variation

For the purpose of this study short term variation is considered to be variation that occurs on an approximate 6-weekly period. Variation between consecutive beach profile surveys are therefore the focus of this chapter. The prominent feature impacting beach systems in this timeframe is the occurrence of storm events. Understanding storm wave impacts on the eastern Coromandel Peninsula is paramount in order to understand the nature and distribution of the erosion hazard, which could provide vital information on beach systems and underpin management plans. Timeseries data derived from the beach profile database will be analysed to provide the understanding of short term beach variation.

3.1.2 Expected Outcomes

The impact of storm waves on subaerial beach systems are well documented in published literature (Komar, 1998), however little research has been undertaken on the Coromandel Peninsula. The variation of beach morphology across the Coromandel Peninsula (Chapter 2) showed the difficulty involved in analysis at the spatial scale considered here. As such, the following general assumptions of beach behaviour are anticipated to occur across the Coromandel Peninsula:

- Large wave events will erode subaerial beach profiles;
- Beaches will accrete during fair weather conditions;
- The Kuaotunu Peninsula will act as a boundary to sediment transport and beach behaviour (refer Figure 2.1); and
- A series of smaller sediment transport sub-cells will be identified in which beach behaviour will be similar.

The Kuaotunu Peninsula is hypothesised to be a barrier where local erosion / accretion events exhibit different behaviour due to the difference in orientation between beaches located to the north and south of the Peninsula (Figure 2.4 and Table 2-1). Beach behaviour is hypothesised to vary around the Peninsula, but several smaller behavioural sub-cells are hypothesised to be evident.

3.2 BACKGROUND: SHORT TERM BEACH VARIATION

3.2.1 Description and Definition of Short Term Beach Variation

Short term beach variation is often significant and perceived to be the largest degree of coastal change compared to larger temporal variation (Dolan et al., 1991). The primary reason is because the degree of change can actually be observed and quantified with relative ease. Interannual to interdecadal scale oscillations cause large scale coastal evolution (e.g. Bryan et al., 2008), however long term trends are not easily quantified. Shoreline erosion from a single storm wave event may cause a 50 % reduction in the subaerial beach volume (e.g. Whangapoua following the July 2008 storm event, Figure 3.4 c, Figure VII.1, and Appendix VII) and therefore lose its protective capacity, which renders the beach largely susceptible to further wave attack, and erosion of coastal properties

becomes probable (Bittencourt et al., 1997). The beach then appears depleted and in a dangerous state. Conversely, shoreline retreat of hundreds of metres can be observed from historical data and aerial photography (e.g. Crowell et al., 1991; Fenster et al., 1993; Bryan et al., 2008) but does not have the perception of an extreme consequence because coastal margins were largely undeveloped and the change rates were very slow, allowing mitigation measures to be implemented where appropriate. Coastal managers are targeted with the problem of quantifying annual exceedance probabilities (AEP) of erosion events for sandy beach environments to determine setback lines for development and infrastructure (Munoz-Perez & Medina, 2009). This highlights the need to understand short term variation of Coromandel Beaches.

Short term beach variation is observed by measuring changes in beach sediment volumes. Beach volumes are easily quantified using beach profile surveys. Continued surveying render timeseries of beach volume change and therefore provide the ability to quantify normal or extreme variation (e.g. Clarke & Eliot, 1988; Thom & Hall, 1991). Short term changes on sandy beaches also show a degree of cyclic behaviour (Dolan et al., 1991), and as a result, a minimum of 10 years data has been suggested to understand the true long term trend of short term variation and reduce the effect of high frequency oscillations (Eliot & Clarke, 1989).

Beach profile variation in the cross-shore direction is generally associated with advance and retreat of the beach profile. A healthy beach has a large sediment budget, a well developed berm, well vegetated dune region, and a steep beach face (Komar, 1998). Eroded beaches are typically flatter, with a low sediment budget, and faceted have dunes with vegetation slumping down the front (Komar, 1998). Variations in the alongshore direction are driven by the incoming wave direction, pressure gradients in the surf zone, alongshore variation in the wave height, infragravity wave oscillations, and the presence of rip currents (Quartel et al., 2008).

Beach volume change images the beach dynamics, expressing it by the variability of the beach profile with time (Bittencourt et al., 1997). There are numerous methods used to analyse beach volume change which could not be used in this thesis, for example empirical orthogonal function (EOF) analyses and wavelet analysis. These methods have proven useful in analysing short term beach variation, for example Eliot and Clarke (1982) used EOF and showed that up to 20 % of the variation on the beach face was aperiodic fluctuations attributed to individual storm events. Wavelet analysis by Reeve et al (2007) advanced further results from Plant et al. (1999) that less than 20 % of the variance occurred on temporal scales of less than one year. Short term variations cannot be accurately forecasted due to the chaotic and non-linear forcing mechanisms of winds and atmospheric conditions which ultimately drive wave conditions (Bittencourt et al., 1997; Reeve et al., 2007).

3.2.2 Morphodynamics of Short Term Beach Variation

Beach morphology changes in response to changing wave conditions were analysed in detail by Wright and Short (1983; 1984). Their qualitative beach classification model identified six morphological states for sandy beaches. The classification was based on several years' research, field sampling, and observations of numerous beaches on Australia's south eastern coast. Although the beach state classification of Wright and Short (1984) does not explicitly provide information on profile variation or volume changes, they are inherently linked because the same environmental factors which determine beach state also determine its variability. In addition to the profiling and observations, Wright and Short (1984) used a dimensionless fall parameter to determine beach state following Dean (1973) and Dalrymple and Thompson (1977), which is outlined below:

$$\Omega = H_b / w_s T \quad \text{Equation 3.1}$$

Where H_b is the breaking wave height, w_s is the sediment settling velocity (in $\text{m}\cdot\text{s}^{-1}$) and T is the wave period.

Short term changes in profile morphology, which in turn affect beach volume and beach behaviour (Wright & Short, 1984), occur due to erosion and accretion of the beach. Very seldom is a beach in a state of equilibrium because beaches and coastal processes are dynamic complex components of large scale non-linear interactions (Bittencourt et al., 1997). A beach will obtain a uniform or equilibrium state if it remains exposed for a long time to a steady state of wave conditions (Bittencourt et al., 1997). Short term beach erosion typically occurs, and is most significant during increased wave conditions due to winter storm events (Thom & Hall, 1991). Episodic storm events from tropical cyclone activity also affect southwest Pacific beaches (de Lange, 2000; Davidson & Turner, 2009). Quartel et al. (2008) describes the storm – post-storm model which is a qualitative description of morphological changes coupled to periods of erosion and accretion as shown by Dubois (1988); List and Farris (1999); Stive et al. (2002); and Miller and Dean (2007b).

The use of bulk statistical measures to analyse beach profile timeseries data is common in published literature. For example, Larson et al. (2003) measured variation in beach topography using the standard deviation of elevation at selected cross-shore locations from beach profile data. Limits of beach volume variations can then be used to define probability functions for certain degrees of beach erosion and accretion. The mean and standard deviation of beach volumes are simple, yet effective data. Larson et al. (2003) analysed beach profiles at Duck and showed that the greatest morphological change occurred at the MSL contour, with the dune being the most stable region. This behaviour was linked to wave impacts on the beach, in particular the shoreline behaviour and associated variations with the nearshore bar. Whilst Larson et al. (2003) state the improved ability of advanced statistical techniques to analyse morphological change, they recognise that many datasets do not satisfy the requirement of even temporal and spatial variation. Larson et al. (2003) therefore reinforce the applicability of bulk

statistics for analysing beach evolution and deriving simple empirical relationships to be used for predictive purposes.

3.2.3 Forcing Mechanisms of Short Term Beach Variation

Incoming wave energy causes erosion and accretion of sandy beaches. Wave parameters such as the height, period, steepness, and direction contribute to beach profile behaviour and determine whether a profile erodes or accretes (Ozolcer, 2008). In addition, storm events cause storm surge, increased wave set-up, increased wave runup, and high velocity winds, as well as increasing the wave height and steepness. These parameters create a significant increase in the erosive capabilities of waves and as a result beaches typically erode (Thom & Hall, 1991; Bittencourt et al., 1997; Quartel et al., 2008). However, continuous winter storms often cause erosion at a decreasing rate, to the point where a storm can cause beach accretion (e.g. Dail et al., 2000; Yates et al., 2009). This occurs when the equilibrium wave energy required to erode a beach increases following initial winter storm events, and subsequent winter and spring storm events do not possess a high enough equilibrium wave energy to erode a beach (Yates et al., 2009). A relationship between wave energy and shoreline position devised by Yates et al. (2009) is shown in Figure 3.1 in which the best fit line showing the observed average wave energy causing no MSL position change is of most importance. The relationship shows that lower wave energy is required to erode an accreted beach. As a beach erodes, the equilibrium wave energy required to continue eroding the beach increases.

Beach accretion is favoured under low energy wave conditions which encourage the nearshore movement of sediment from onshore directed bar velocities (Plant et al., 1999). If a beach has a nearshore bar, low energy wave conditions cause a landward shift of the bar which can weld with the subaerial beach face (Short, 1999; Aagaard et al., 2004). Swash zone sediment transport then drives sediment up the beach face to form a berm. Optimum beach face volume is achieved with a slightly landward sloping berm and a steep beach face. The limiting factor of profile accretion is usually the absence of a nearshore bar(s) which in turn allows

a greater amount of wave energy to impact, and potentially erode the beach face (Wright & Short, 1984; Dail et al., 2000; Harley, 2009b; Harley et al., 2009c).

Antecedent beach conditions are critical in determining beach response to storms (e.g. Wright & Short, 1984; Dail et al., 2000; Yates et al., 2009) with the presence of a nearshore bar(s) being paramount as they have been shown to dissipate up to 78 – 99 % of incoming wave energy (Carter & Balsillie, 1983; Dubois, 1988). For example, Harley et al. (2009c) produced an empirical model of beach response to storms using the storm wave direction, energy, and whether the antecedent beach conditions were barred or bar-less. Their model produced highly correlated results for beach width change versus cumulative wave energy at exposed and partially-exposed regions of the beach, but lower results for their sheltered site. This highlights the importance of antecedent profile conditions as the results were significantly reduced if their parameter for barred or bar-less conditions was removed.

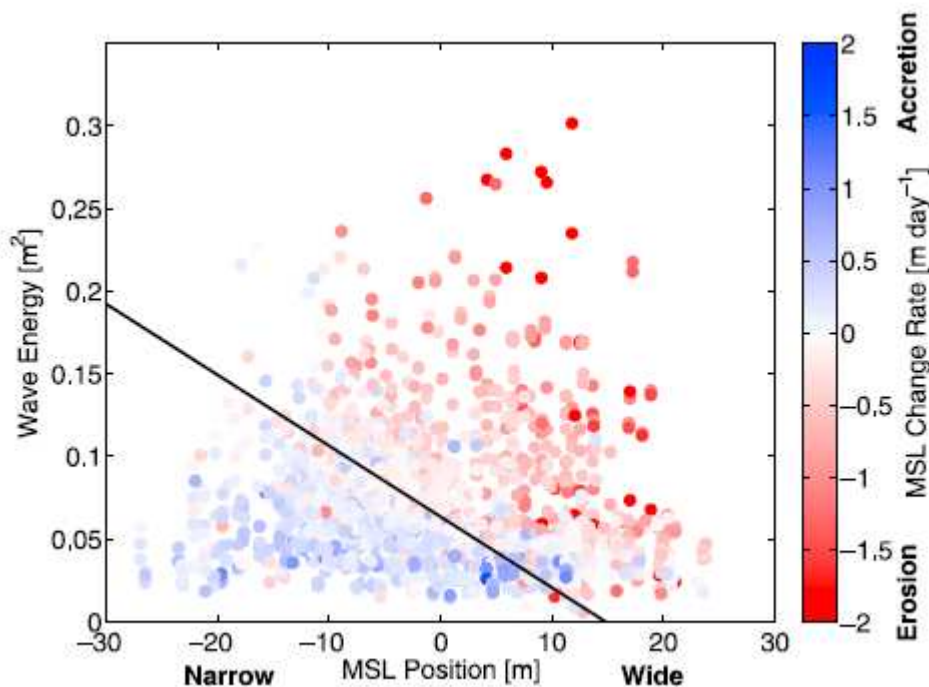


Figure 3.1: MSL change rate between consecutive surveys from “Equilibrium shoreline response: observations and modelling” by M.L. Yates et al., 2009, *Journal of Geophysical Research*, 114,C09014. Of particular interest is the equilibrium wave energy which is the best fit solid line to the observed wave energy causing no MSL position change.

3.3 METHODS

3.3.1 Beach Volume Timeseries

Raw beach profile data consisted of surveyed horizontal and vertical points from a known benchmark and extended seaward as far as possible, which was approximately mean sea level (MSL). A cross-section of the beach topography at a particular point in time was then created (Figure 3.2). Raw beach profile data was input into the Beach Profile Analysis Toolbox (BPAT) software. Upon verification in BPAT, the raw data was extracted in ASCII format for analysis with the Matlab software (Version 7.4.0 2009a). Computer algorithms were written to create time series data of the beach volume located seaward of a common benchmark. The subaerial beach volume is defined as the amount of sediment located seaward of a common datum and above MLWS (e.g. Clarke & Eliot, 1988). Each individual beach profile was interpolated at 1 m intervals in the cross-shore direction to enable analysis of the beach volume at a greater accuracy (Lacey and Peck, 1998). Common timeseries analysis methods including Fourier transforms, empirical orthogonal functions, and spectral analysis could not be undertaken due to the uneven sampling frequency of the dataset. Linear interpolation between surveys was considered too crude due to the uneven spacing of the dataset.

The subaerial beach profile was divided into horizontal beach segments to analyse beach sediment volumes at different elevations across the profile, comprising the intertidal area, the upper beach, and the dune region (Figure 3.2). The upper limit of the intertidal area was defined as MHWS (Relative Level (RL) 0.9 m) and the lower limit as MLWS (RL -0.9 m). The resulting “triangle” area under each beach profile (area (e) Figure 3.2) was evaluated as the seaward extent of the intertidal volume. The horizontal area from the intertidal zone landward to a common benchmark was then added to the triangle to quantify the advance or retreat of the profile (area (d) Figure 3.2). The maximum spring tidal range of 1.8 m was divided equally above and below MSL (RL 0.0 m) to provide a tidal amplitude of 0.9 m. If a particular profile did not extend as far as MLWS, the data were extrapolated to MLWS using the median slope of the last three surveyed points

for that particular profile (e.g. Lacey and Peck, 1998). One profile survey at Rings Beach did not contain 3 surveyed points within the intertidal region therefore linear interpolation was undertaken. The upper beach region extended from MHWS to RL 3.5 m and the volume was calculated using the same method as the intertidal area, noting the different elevation limits (areas (b) and (c) Figure 3.2). Visual observations by the beach profile surveyors indicate RL 3.5 m to be an average elevation where dune vegetation and storm debris are commonly located. This is considered to be an accurate limit for the upper extent of wave action. The dune area encompassed the volume of beach sediment above RL 3.5 m landward to a common benchmark (area (a) Figure 3.2). Beach volume timeseries were analysed using the percentage change in beach volume from the mean volume for the entire timeseries.

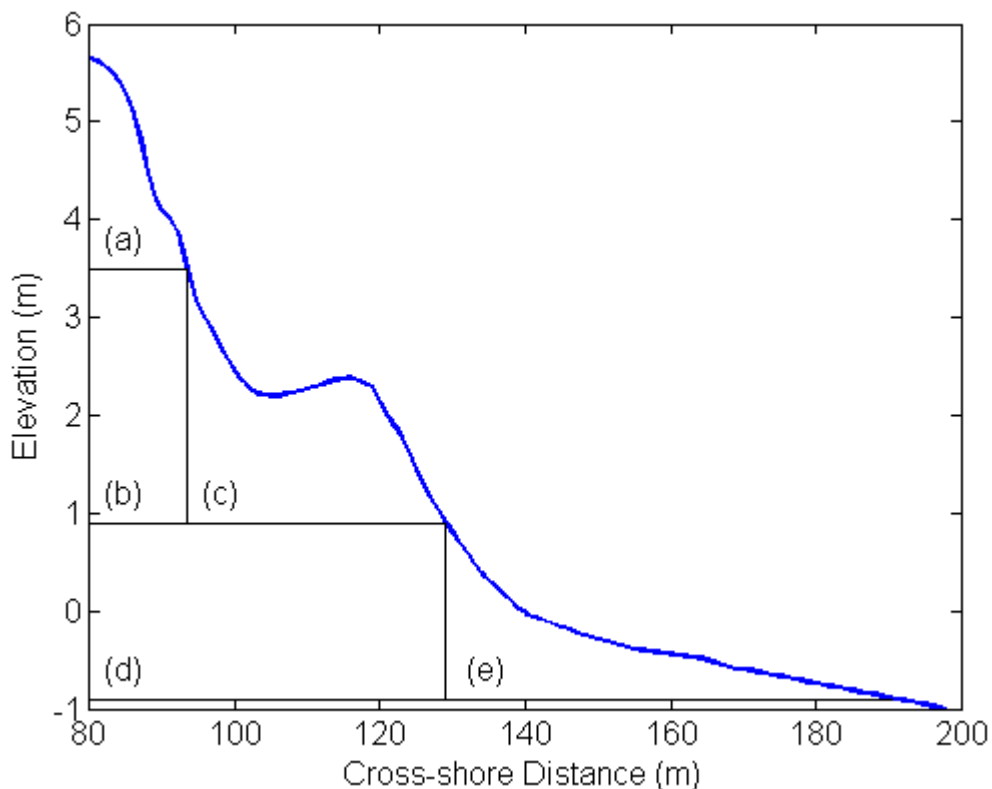


Figure 3.2: A beach profile cross-section from the southern profile on Whangapoua Beach from 22-2-1998. The figure depicts the various regions used to calculate the dune volume (a); the upper beach volume area encompassing the “triangle” (c) and the corresponding area landward to a common datum (b); the intertidal beach volume encompassing the “triangle” (e) and the corresponding area landward to a common datum (d).

3.3.2 Magnitude of Beach Volume Change

Beach volume change between surveys was analysed to produce change rates of erosion and accretion. The beach volume change divided by the number of days between profiles provided the rate of change in cubic metres per metre per day ($\text{m}^3 \cdot \text{m}^{-1} \cdot \text{day}^{-1}$). The data were then grouped into $0.2 \text{ m}^3 \cdot \text{m}^{-1} \cdot \text{day}^{-1}$ bins. Most profiles on each beach did not have an equal number of surveys. The frequency data were then normalised so the change rates could be compared directly between other profiles on the same beach. An example of the method is outlined below:

- Whangapoua has 3 profiles: CCS12, CCS11, and CCS11-1, with data of lengths 96; 93; and 90 respectively;
- CCS12 is the largest vector of change rates, of length 96;
- CCS12, CCS11, and CCS11-1 were grouped in $0.2 \text{ m}^3 \cdot \text{m}^{-1} \cdot \text{day}^{-1}$ bins from 0 to >4 , therefore containing frequency data within each bin e.g.;

 - Bin 1 = 27
 - Bin 2 = 19
 - Bin 3 = 11, and so on;

- In order to make them comparable they were converted to percentages;

 - Bin 1 = $27 / 96 * 100$
 - Bin 2 = $19 / 96 * 100$
 - Bin 3 = $11 / 96 * 100$, and so on;

- This was undertaken for each profile on Whangapoua Beach.

One profile at each of Tairua, Pauanui, and Whangamata Beaches were excluded from the analysis as the profile datasets were too small, having only been established in 2003, 2004, and 2002 respectively.

The beaches were then classified according to the Wright and Short (1984) classification. The initial classification used the average intertidal beach slope for each respective beach. All Coromandel Beaches were identified as intermediate or reflective beaches. The dimensionless fall parameter was also calculated using average wave height and period for the available data (Equation 3.1). The

breaking wave height was calculated using the mean H_s for all data from each site (Table 4-3) using the method of Gourlay (1992); w_s was calculated using the sediment grain size data collected; and the mean T for all data at each wave data site. Repeated calculations and observations of beach state could not be made as only one sediment sampling regime was available. The results therefore represent beach state approximations using the dimensionless parameter, and are not considered definitive. The parameter supplements the initial classification using beach slope data.

3.3.3 Exponential Decay versus the Intertidal Beach Slope

The magnitude of change data were expected to show a relationship with the frequency of occurrence as the largest events were expected occur less often. Least squares regression was used to find a best fit exponential curve for each beach (Equation 3.2).

$$f(x) = Ae^{-k\Delta v} \quad \text{(Equation 3.2)}$$

Where A is the beach volume at time zero, e is the exponential function, k is the decay constant, and Δv is the magnitude of change data. Of particular interest were the exponential decay constant (k) and the frequency of zero change (A). The resulting A and k values were compared to the average intertidal beach slope for each beach. The intertidal beach slope was calculated by averaging the slope of all available data points between MLWS and MHWS.

3.3.4 Short Term Variation in Wave Conditions

Large wave events can have a huge impact on subaerial beach change. The magnitude and duration of a storm event affects the magnitude of short term beach change. Analysis of the occurrence of storm events was undertaken. A storm wave event was defined as an event where the significant wave height (H_s) exceeded 3 m. This is a relatively low wave height, however the Coromandel Peninsula is a sheltered lee coast which does not receive frequent long period or

large swell waves, therefore is considered appropriate in this case. This is consistent with findings from Gorman et al. (2003a; 2003b) for the north east coast of the North Island of New Zealand who defined the 90th percentile significant wave height to be 2.93 m. The AEP storm waves of different magnitudes were developed for H_s events of 2 m, 3 m, and greater than 4 m.

The percentage change in beach volume was compared against the average and maximum H_s between consecutive surveys. H_s was time-averaged between the dates of consecutive beach profile surveys at each site. The maximum wave height during this period was also recorded. Least squares regression analysis was undertaken to determine the extent of any relationship present between the time-averaged wave data and the beach volume change.

3.4 RESULTS

3.4.1 Short Term Observations

The first method of analysis was to graph the beach profile variation through time. Figure 3.3 gives an example of beach profile elevation through time. This basic method of analysis can identify features such as:

- Variation of the MSL contour between profiles;
- The beach width;
- The beach slope; and,
- The extent of storm wave erosion on the beach.

The solid black line is the cross-shore location of the MSL contour through time (Figure 3.3). The MSL contour can vary up to 20 m between consecutive profiles. Figure 3.3 also showed large erosion events were more frequent than large accretion events. However, beaches typically recovered quickly from erosion events, as shown by the MSL contour which showed accretion following erosion events in most instances. The beach width can be approximated by analysing the distance from a known elevation (e.g. the horizontal black line for MSL contour) landward to a common cross-shore location. The intertidal beach slope was

analysed by comparing the cross-shore extent of the dark blue region in each panel which is approximately the spring tidal range. For example, the intertidal region at Whangapoua was approximately 35 m wide (the cross-shore location from 50 m – 85 m, Figure 3.3 a.) whereas at Matarangi (Figure 3.3 b.) the intertidal region was approximately 80 m wide (the cross-shore location from 120 m – 200 m). This showed that Matarangi had a much lower intertidal beach slope compared to Whangapoua. Storm activity was evident where landward retreat of a particular elevation level occurred to a large extent, or across more than one beach. An example of this was evident in July 2008 where the MSL contour for all four profiles retreated landward. Landward retreat of the upper beach and dune region also occurred at Whangapoua, Matarangi, and Tairua as shown by the reduction in the yellow / orange region. Beach profile elevations through time for all beaches and profiles are attached as Appendix IV.

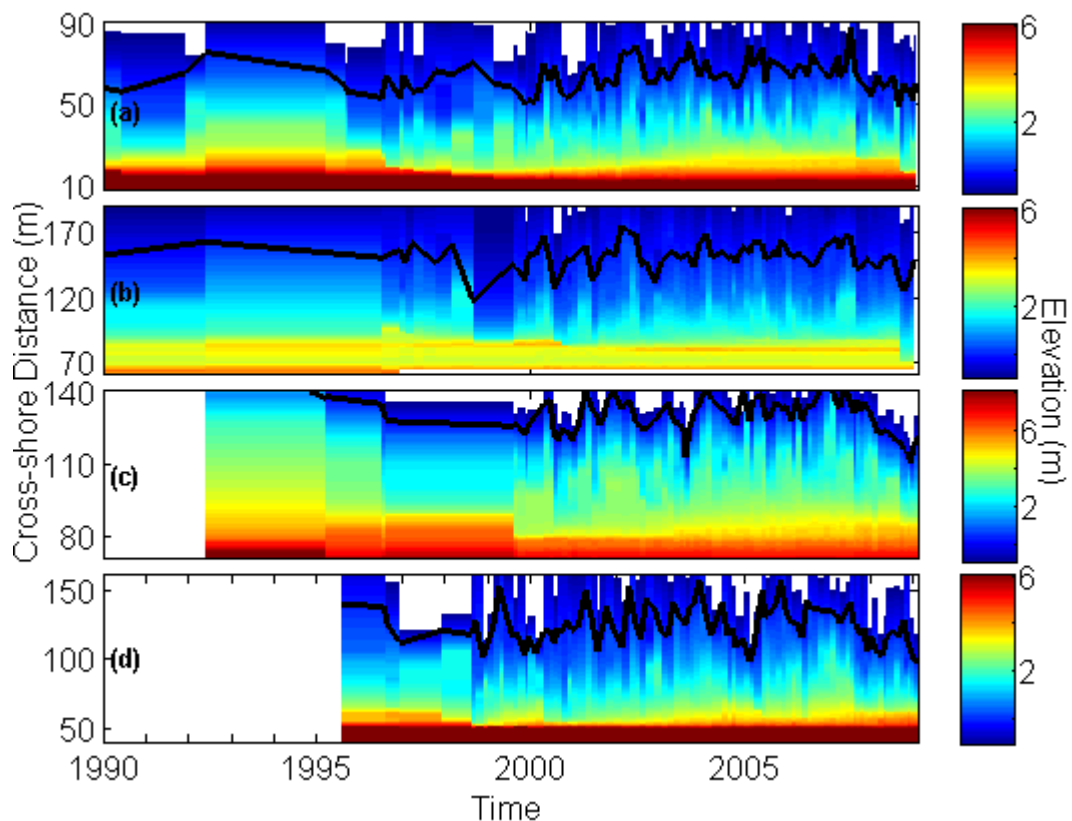


Figure 3.3: Timeseries of cross-shore elevation of beach topography from the central profile at Whangapoua (a), Matarangi (b), Tairua (c), and Pauanui (d) beaches. The solid black line in each panel represents the MSL contour. The colour bar on the right illustrates the elevations relative to MSL (RL = 0.0 m). A large uniform region in the x-axis direction represents a period where no surveys were undertaken e.g. 1992 – 1996 at Matarangi (b).

3.4.2 Beach Volume Change between Consecutive Surveys

Figure 3.4 showed example beach volume change data. Values above zero showed above average beach volumes and values below zero showed below average beach volumes. Beach volume change between consecutive surveys was analysed using a demeaned beach volume timeseries. Percentage changes were used because direct comparisons to the amount of beach sediment eroded or accreted could be made between any profile and / or beach, whereas raw volume changes would not enable this. The spatial variation of this study meant percentage changes were the best method for analysis, whereas many studies have used raw beach volume data as they did not encompass the same spatial variation (e.g. Dubois, 1988; Thom & Hall, 1991; Dail et al., 2000; Lizarraga-Arciniega et al., 2007). A key observation through most of the timeseries was that a volume change event of greater than approximately 25 % can be considered important because this magnitude of events was not a common occurrence. A volume change event of less than 25 % can be considered normal due to the regular occurrence.

Of interest was the frequent non-uniform behaviour between surveys on different beaches through time. Figure 3.4 showed that short term morphological change was not uniform between sites. For example, Box 1 showed that Whangapoua, Matarangi, and Tairua all increased in beach volume (Figure 3.4) then had a decrease, however Pauanui had very little change. Another example where non uniform behaviour was prevalent was identified in Box 4 (Figure 3.4), encasing a large storm wave event in July 2008. The percentage of sediment eroded from the pre-event volume was 36 %, 32 %, 14 %, and 7 % for the Whangapoua, Matarangi, Tairua and Pauanui profiles respectively.

Beach behaviour appeared to differ depending on the beach location. For example, Boxes 2 and 3 showed that Whangapoua and Matarangi had an increase in beach volume (Figure 3.4 a, b). During the same period, Tairua and Pauanui (Figure 3.4 c, d) showed similar behaviour, but it was different to the behaviour at Whangapoua and Matarangi. Large spikes of accretion in the timeseries were

most often attributed to berm formation, for example at the beginning of 1999 at Pauanui (Figure 3.4 d). This was evident when analysing the beach profile at that particular point in time. Short term morphological change events were also quantified by analysing the standard deviation of beach volume. Table 3-1 showed the standard deviation of volume at each beach. One standard deviation either side of the mean accounts for 68 % of the short term beach volume variation whilst two standard deviations account for 95 % of the variation. Demeaned beach volumes had a normal distribution therefore these bounds were applicable. The beaches in Table 3-1 were listed from north to south, and the right hand column showed the standard deviations ranked from lowest to highest. Beach volume timeseries with standard deviations for all sites are contained in Appendix VII.

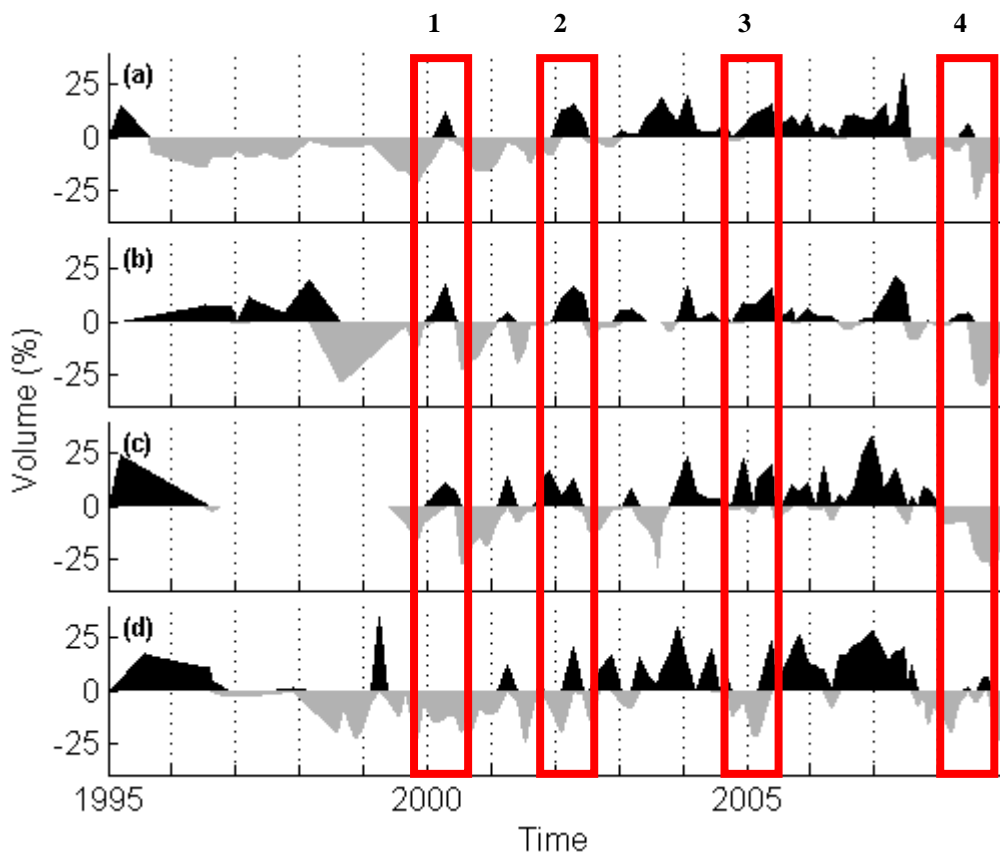


Figure 3.4: Timeseries of beach volumes for the central profile at Whangapoua (a), Matarangi (b), Tairua (c), and Pauanui (d) beaches. The data has been demeaned. The black region illustrates above average beach volumes whilst the grey region illustrates below average beach volumes. The red boxes are discussed in text.

Table 3-1: The average standard deviation of beach volume (%) for each site. The standard deviations show the degree of short term morphological change. The right hand column has ranked the beaches from lowest to highest.

Beach	One σ	Two σ's	Ranking
Whangapoua	14.0	28.1	11
Matarangi	13.3	26.7	8
Rings	4.83	9.66	1
Kuaotunu West	10.5	21.0	3
Kuaotunu East	13.6	27.1	10
Otama	17.4	34.8	18
Opito	11.4	22.8	6
Wharekaho	10.8	21.7	4
Buffalo	16.0	32.0	15
Maramaratotara	4.97	9.93	2
Cooks	17.5	34.9	19
Hahei	12.6	25.3	7
Hot Water	11.1	22.1	5
Tairua	16.0	31.9	14
Pauanui	16.7	33.4	17
Onemana	13.4	26.9	9
Whangamata North	14.9	29.7	13
Whangamata South	14.8	29.6	12
Whiritoa	16.4	32.9	16

3.4.3 Horizontal Beach Volume Segment Analysis

The beach profiles were divided into three horizontal beach segments comprising the intertidal area, the upper beach area, and dune region (Figure 3.2). Figures 3.5 to 3.8 showed the intertidal, upper beach, and dune volumes for the central profile located at Whangapoua, Matarangi, Tairua and Pauanui Beaches respectively. These four profiles are shown as examples. All profile sites are shown in Appendix V. In all four figures, the dune volume was illustrated as the raw dune volume ($\text{m}^3 \cdot \text{m}^{-1}$) with mean removed, whereas the intertidal and upper beach regions were illustrated as percentages. Raw data were considered most suitable for the dune volume analysis. For example, a volume change from $5 \text{ m}^3 \cdot \text{m}^{-1}$ to $4 \text{ m}^3 \cdot \text{m}^{-1}$ in the dune is a minor volume change (i.e. $1 \text{ m}^3 \cdot \text{m}^{-1}$), however when

represented as a percentage, a 20 % reduction implied a large amount of erosion occurred when this was not the case. This was deemed the most suitable method of analysing dune volume changes.

The primary observation between sites was the marked difference in behaviour at different elevations on the beach. Figures 3.5 to 3.8 showed that a large portion of beach volume change at all timescales occurred in the lower beach region, below the upper limit of wave action (RL 3.5 m) in the upper beach and intertidal zones. Most profile sites on the Coromandel Peninsula had little dune variation (Figures 3.5 – 3.8; Appendix V). Matarangi had very little data above RL 3.5 m therefore no data are plotted. Analysis showed that all sites (refer Appendix V) typically had similar short term trends of erosion and accretion between the upper beach and intertidal area. The four examples showed that this was evident, but was not as prevalent at Pauanui. At Whangapoua Beach the similarity in the behaviour between the upper beach and intertidal region is evident. The dune volume had very little volume variation except an erosion event in July 2008. At Matarangi, the short term behaviour for the entire timeseries was also very similar between the upper beach and intertidal region. Short term variation at Tairua was almost identical between the upper beach and intertidal region. The dune region was not subject to any large short term change events but long term trends were evident. Pauanui had no large short term change events evident in the dune region. The intertidal region at Pauanui had a relatively large degree of variation in short term profile variation compared to the upper beach region. The variation was also much greater when compared to the other 3 beach profiles plotted. The trends in the variation between the upper beach and intertidal region were similar, however the degree of variation was quite different, Pauanui and Tairua appeared to have a larger degree of variation than Whangapoua and Matarangi. This was evidenced by the latter two beaches having lower standard deviations (Table 3-1 and Figure 3.9).

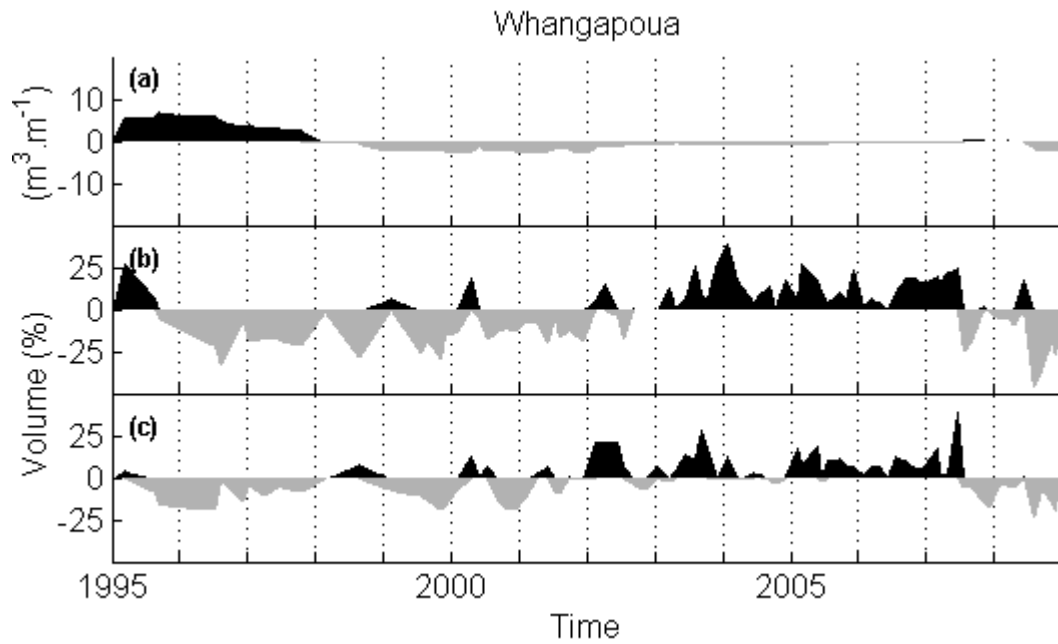


Figure 3.5: Timeseries of horizontal beach volume segments for the central profile at Whangapoua Beach. The data have been demeaned. Illustrated is the dune volume (a) above RL 3.5 m, the upper beach volume (b) between RL 3.5 m and RL 0.9 m, and the intertidal beach volume (c) between RL 0.9 m and RL -0.9 m. Note the different y axis limits and unit of measurement in the dune (a).

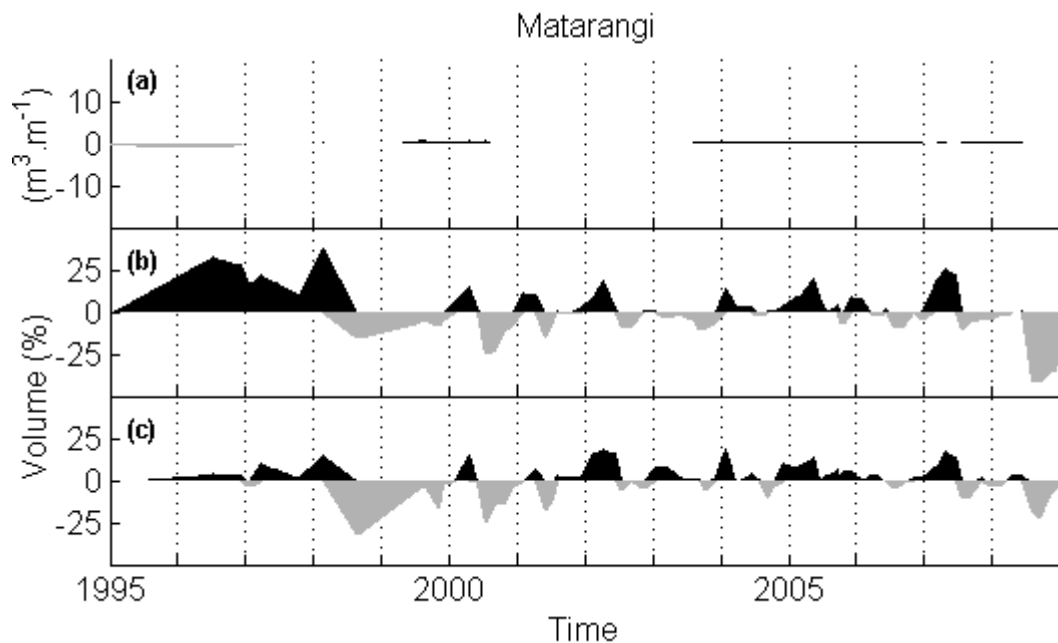


Figure 3.6: Timeseries of horizontal beach volume segments for the central profile from Matarangi Beach. The data have been demeaned. Illustrated is the dune volume (a) above RL 3.5 m, the upper beach volume (b) between RL 3.5 m and RL 0.9 m, and the intertidal beach volume (c) between RL 0.9 m and RL -0.9 m. Note the different y axis limits and unit of measurement in the dune (a).

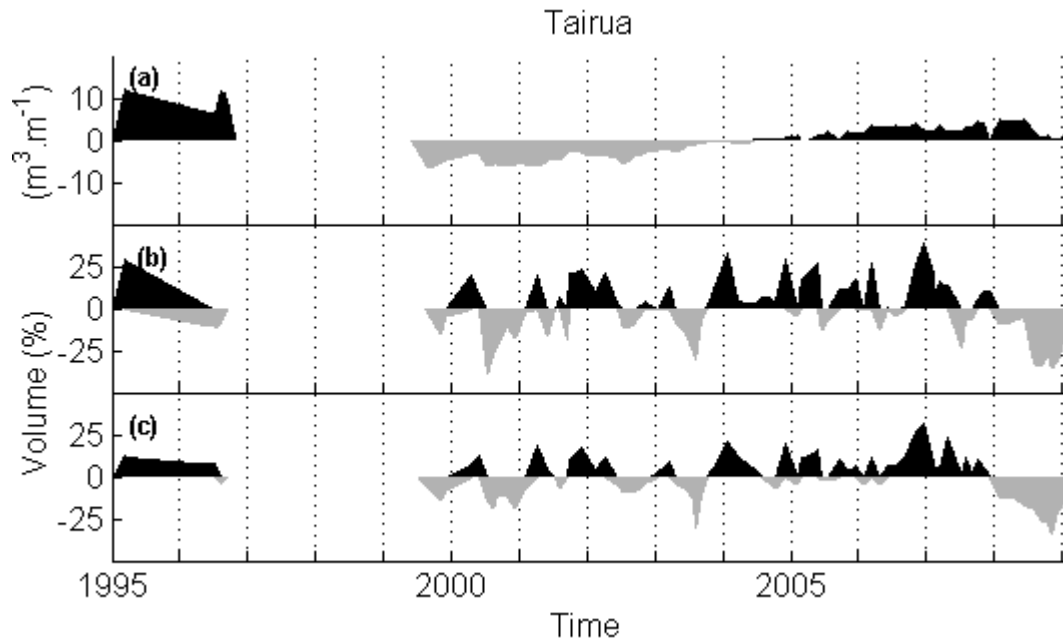


Figure 3.7: Timeseries of horizontal beach volume segments for the central profile from Tairua Beach. The data have been demeaned. Illustrated is the dune volume (a) above RL 3.5 m, the upper beach volume (b) between RL 3.5 m and RL 0.9 m, and the intertidal beach volume (c) between RL 0.9 m and RL -0.9 m. There is a lack of data from 1996 to 1999. Note the different y axis limits and unit of measurement in the dune (a).

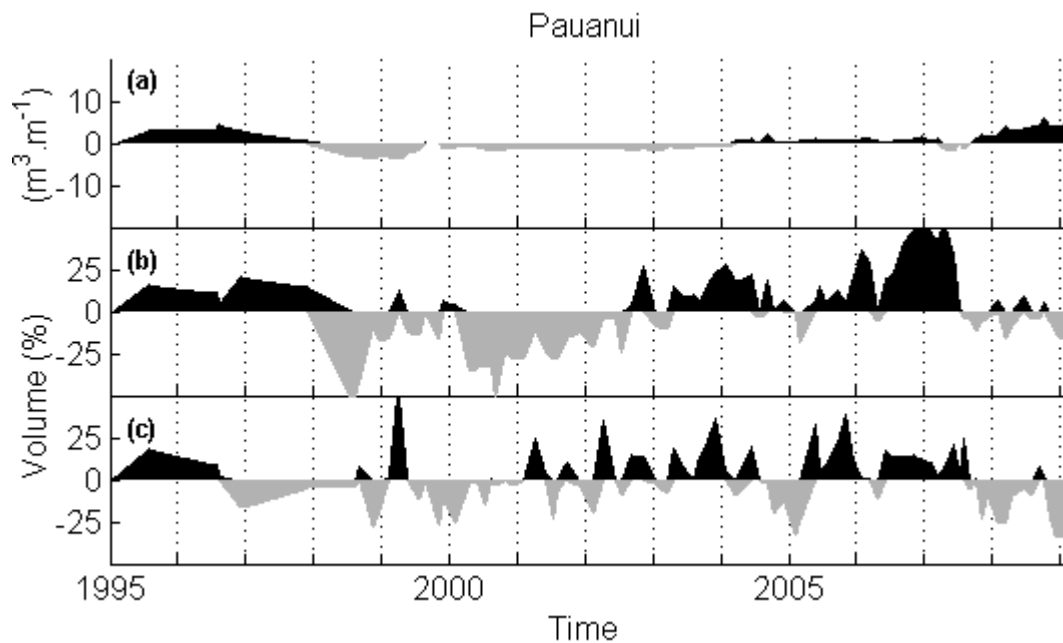


Figure 3.8: Timeseries of horizontal beach volume segments for the central profile from Pauanui Beach. The data have been demeaned. Illustrated are the dune volume (a) above RL 3.5 m, the upper beach volume (b) between RL 3.5 m and RL 0.9 m, and the intertidal beach volume (c) between RL 0.9 m and RL -0.9 m. Note the different y axis limits and unit of measurement in the dune (a).

3.4.4 Standard Deviation of Horizontal Beach Volume Segments

Figure 3.9 illustrates the average standard deviation of volume for each horizontal beach segment at each site. The beaches were grouped according to the mean intertidal beach slope and the dimensionless fall parameter to approximate the beach state according to Wright and Short (1984) (refer Section 3.3.2 and Table 3-2). It was evident across all beaches that the dune was the most stable region of the beach, illustrated by the lowest standard deviations. For intermediate beaches the standard deviation increased from the dune to the upper beach region to the intertidal region (Figure 3.9 a). Figure 3.9 (b) showed that the four reflective beaches had more variable upper beach regions than the respective intertidal region. This trend occurs on all four reflective beaches and 11 out of the 13 profiles on those four beaches (refer Appendix V). One profile at each of Hahei, Kuaotunu West, Kuaotunu East, and Otama Beaches also had a more variable upper beach region (refer Appendix V). These intermediate beaches were the four steepest intermediate beaches. Harbour adjacent beaches showed similar behaviour to intermediate beaches, and all have intermediate beach slopes (Wright & Short, 1984). Maramaratotara Beach (Figure 3.9 c) had a more variable upper beach region than the intertidal region. The intertidal region was the most variable region at Rings Beach (Figure 3.9 c). Both outlier beaches (Rings & Maramaratotara) had significantly lower standard deviations across the entire subaerial beach profile. A total of 6 profiles across the entire site did not contain dune volume data (i.e. above RL 3.5 m). This occurred at Buffalo Beach (3 profiles), Cooks Beach (2 profiles) and Opito Bay (1 profile).

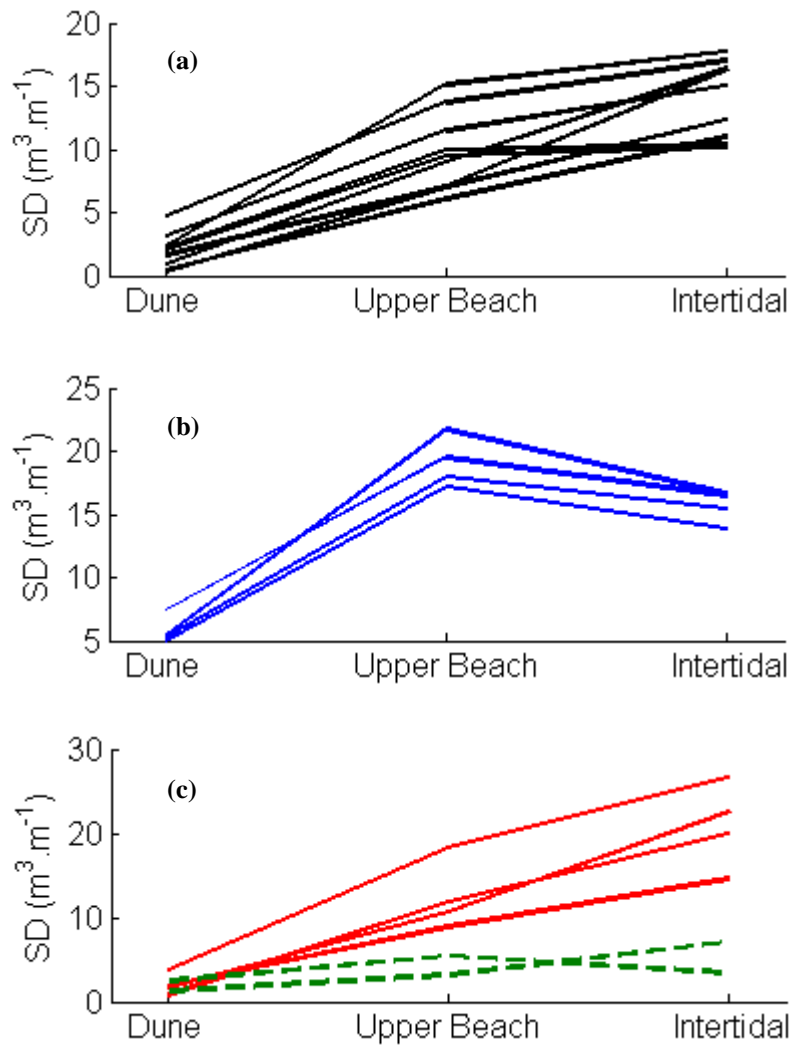


Figure 3.9: Standard deviation of horizontal beach volume segments at each site for intermediate beaches (black lines, a), reflective beaches (blue lines, b), harbour adjacent (solid red lines, c) and outlier beaches (dashed green lines, c).

The dimensionless fall parameter results were shown in Table 3-2. According to Wright and Short (1984), reflective beaches are characterised by parameters of less than one, intermediate beaches range from 1 to 6, and dissipative beaches are greater than 6. The reflective beaches had the lowest values and a narrow range from 2.2 to 2.9. The remaining beaches all ranged from 3.2 to 6.1. The result for Kuaotunu East (3.0) was not considered accurate due to the presence of gravels in the sediment sample which caused a high settling velocity and thus low dimensionless fall parameter. Maramaratotara Beach was also not considered as the settling velocity was not calculated for the calcite sediment.

Table 3-2: Grouping of Coromandel Beaches according to intertidal beach slope and dimensionless fall parameter (Wright and Short, 1984) with harbour adjacent and outliers additional to their classification. The dimensionless fall parameter is the number adjacent to each beach.

Intermediate	Reflective	Harbour Adjacent	Outliers
Whangapoua 4	Hot Water 2.2	Matarangi 4.7	Rings 3.2
Kuaotunu West 3.7	Tairua 2.6	Pauanui 4.5	Maramaratotara
Kuaotunu East 3.0	Onemana 2.7	Whangamata North 4.6	
Otama 3.3	Whiritoa 2.9	Whangamata South 5.1	
Opito 4.8			
Wharekaho 3.9			
Buffalo 6.1			
Cooks 5.9			
Hahei 3.7			

3.4.5 Intertidal Beach Slope versus Mean Grain Size

The mean intertidal beach slope for the 61 profiles sites was compared to the mean grain size for each profile. A sediment sample was not obtained from the southern profile site at Opito Beach therefore no comparison is made. Figure 3.10 showed the mean intertidal beach slope versus the mean grain size for each beach. Figure 3.10 showed that the reflective beaches (blue stars) had mean grain sizes ranging from 396 μm to 502 μm and average intertidal beach slopes from 0.11 to 0.13. The four reflective beaches showed a relatively narrow grouping for the relationship. The intermediate beaches (black circles) illustrated a larger degree of variation in both the mean grain size and intertidal beach slope. The intermediate beaches had mean grain sizes ranging from 197 μm to 427 μm and average intertidal beach slope from 0.02 to 0.07. The harbour adjacent beaches (red crosses) showed a relatively narrow grouping for the relationship. These beaches had mean grain sizes ranging from 225 μm to 275 μm and average intertidal beach slopes from 0.02 to 0.04. The two outlier beaches (green squares) had mean grain sizes of 402 μm and 1072 μm and average intertidal beach slopes of 0.10 and 0.11 for Rings and Maramaratotara respectively. A linear relationship was

evident between the mean grain size and intertidal beach slope data. Least squares regression analysis produced an R-squared value of 0.36. If Maramaratotara was excluded (mean grain size 1072 μm) from the analysis the R-squared value increased to 0.64.

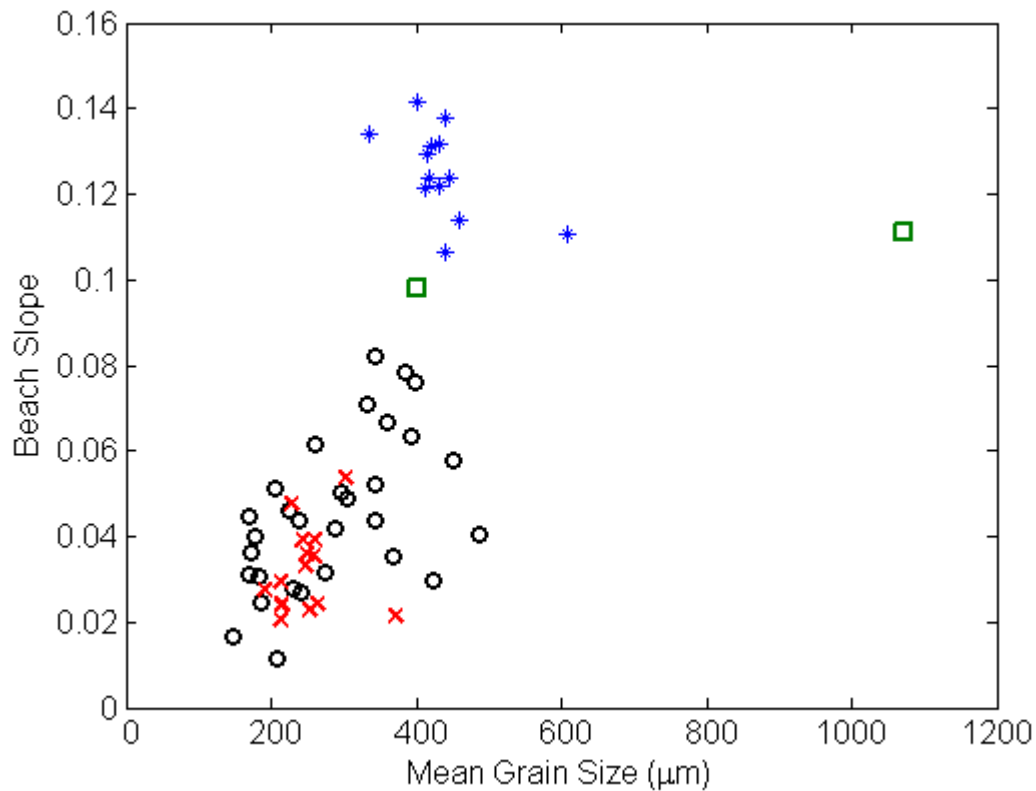


Figure 3.10: Mean grain size versus the mean intertidal beach slope for each profile site (excluding the southern profile at Opito Beach). See text for definitions of reflective beaches (blue stars), intermediate beaches (black circles), harbour adjacent beaches (red crosses), and outlier beaches (green squares).

3.4.6 Magnitude of Beach Volume Change

Beach volume change was further analysed by calculating the rate of volume change between consecutive beach profiles. Figure 3.11 illustrates the magnitude of beach volume change for all intermediate and reflective beaches on the Coromandel Peninsula (Table 3-2). The data in Figures 3.11 and 3.12 were all converted to positive integers. Figure 3.11 showed that intermediate sloped beaches had a high frequency of low magnitude events and a low frequency of large magnitude of change events. A large magnitude event was considered

greater than $1 \text{ m}^3 \cdot \text{m}^{-1} \cdot \text{day}^{-1}$ as a result. An increasing magnitude of beach volume change was associated with a decreasing frequency of occurrence. Figure 3.11 showed that reflective beaches had a low frequency of low magnitude events and a much higher frequency of larger magnitude of change events, with approximately 2 to 3 times more events between $0.8 \text{ m}^3 \cdot \text{m}^{-1} \cdot \text{day}^{-1}$ and $1.0 \text{ m}^3 \cdot \text{m}^{-1} \cdot \text{day}^{-1}$ than intermediate beaches.

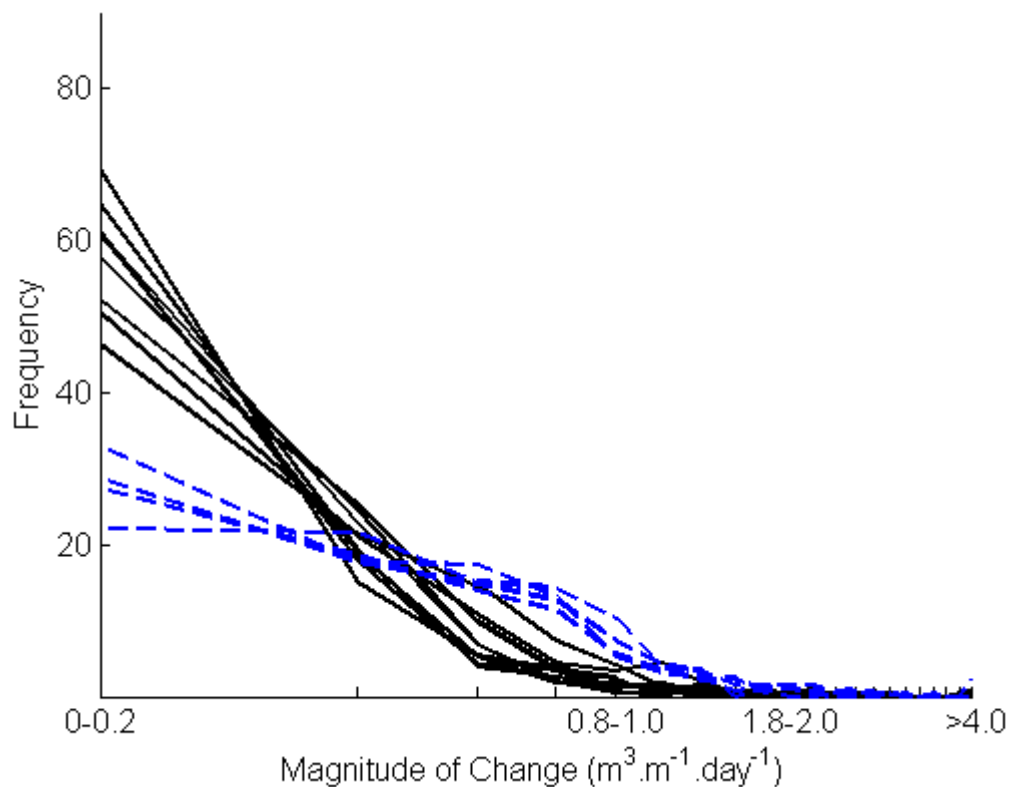


Figure 3.11: Magnitude of beach volume change (logged x-axis) versus frequency of occurrence (y-axis) for intermediate beaches (solid black lines) and reflective beaches (dashed blue lines). Profile data was normalised and averaged for each beach (refer 3.3.2). The logged x-axis illustrated an exponentially decaying relationship.

Figure 3.12 illustrated the magnitude of change for all other beaches on the Coromandel Peninsula. Rings Beach and Maramaratotara Beach were reflective beaches, however did not show the same behaviour as reflective beaches therefore were analysed as outliers (dashed green lines, Figure 3.12). Outlier beaches had the highest frequency of low magnitude events with only one large magnitude event between both beaches ($>1 \text{ m}^3 \cdot \text{m}^{-1} \cdot \text{day}^{-1}$). The two outlier beaches had one profile site at each beach, however their reflective state and analysis of the

individual profiles showed that these two beaches had the lowest degree of short term variation (Appendix VIII). Their behaviours were significantly different to the remaining reflective beaches. Conversely, the beaches plotted in red were intermediate beaches (Table 3-2) however they exhibited different behaviour to the remainder of the intermediate beaches. They had a relatively small frequency of low magnitude events and a higher frequency of larger magnitude events (Figure 3.12), similar to the behaviour of reflective beaches. These four beaches are located adjacent to three of the four largest harbours on the eastern Coromandel Peninsula (Table 3-5), therefore were here on termed 'harbour adjacent' beaches.

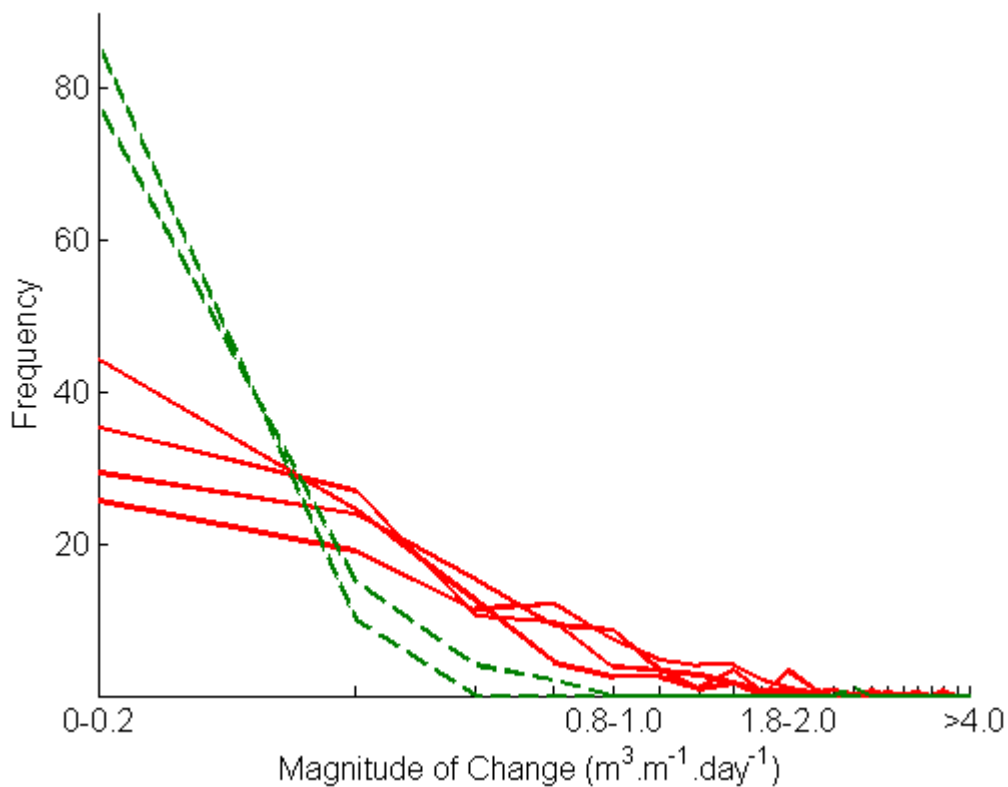


Figure 3.12: Magnitude of beach volume change (logged x-axis) versus frequency (y-axis) for harbour adjacent (solid red lines) and outlier beaches (dashed green lines). The logged x-axis illustrated an exponentially decaying relationship.

Raw magnitude of change data comprised positive and negative integers and were analysed with the same beach classification as above. Figure 3.13 showed the magnitude of change data for intermediate (black lines) and reflective beaches

(dashed blue lines). This further illustrated the difference in behaviour between intermediate and reflective beaches, and the similarity of behaviour within each beach classification. Intermediate beaches had approximately twice the frequency of low magnitude events than reflective beaches. Reflective beaches had a higher frequency of larger magnitude erosion and accretion events which confirms greater short term beach variation. Intermediate and reflective beaches both exhibited a normal distribution. The approximately equal distribution of erosion and accretion events suggested that intermediate and reflective beaches are relatively stable in the long term as the data were not skewed toward erosion or accretion events. Harbour adjacent beaches showed similar behaviour to reflective beaches (Figure 3.14). The magnitude of change data for each beach was shown in Table 3-3 with the maximum, minimum, mean, and range for each beach. The maximum value for Buffalo Beach was very high compared to other data and was because two profiles had large increases in beach volume on the 3rd and 4th of January 1997. This may be due to beach nourishment as consent to undertake such works had been given. The dates when work was actually undertaken are not available. The large beach volume increase and the short sampling interval caused the large result. The large value at Tairua beach was representative of the beach behaviour.

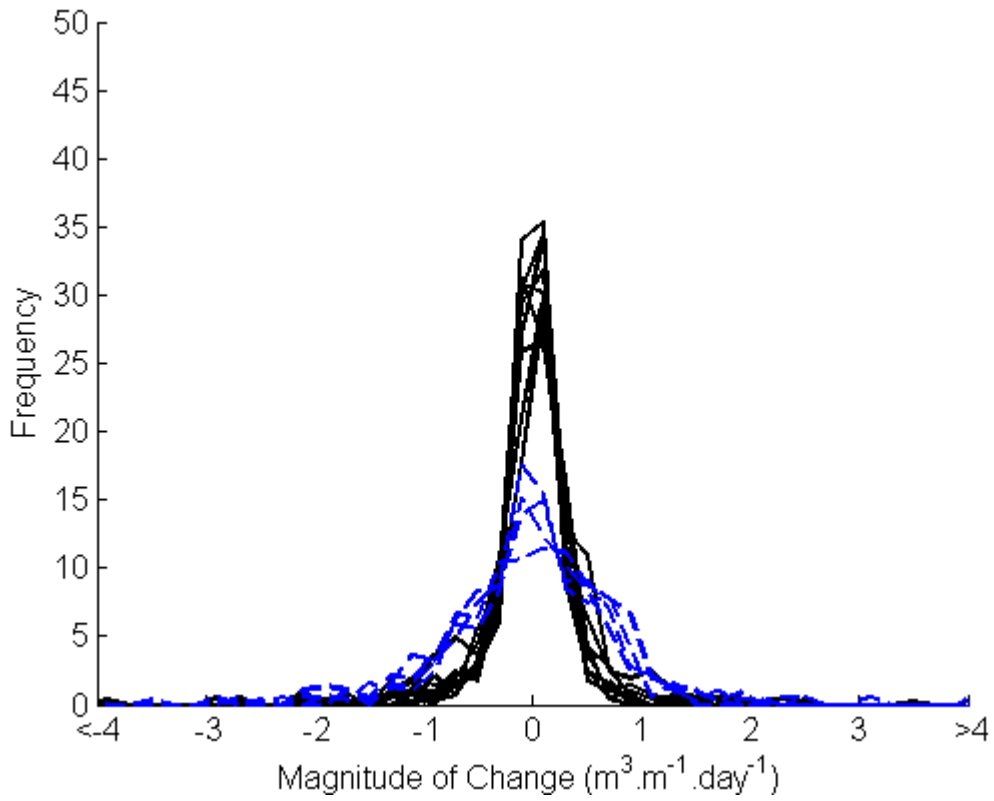


Figure 3.13: Magnitude of beach volume change (x-axis) versus frequency (y-axis) for intermediate (solid black lines) and reflective beaches (dashed blue lines). Erosion and accretion events were illustrated by negative and positive results respectively.

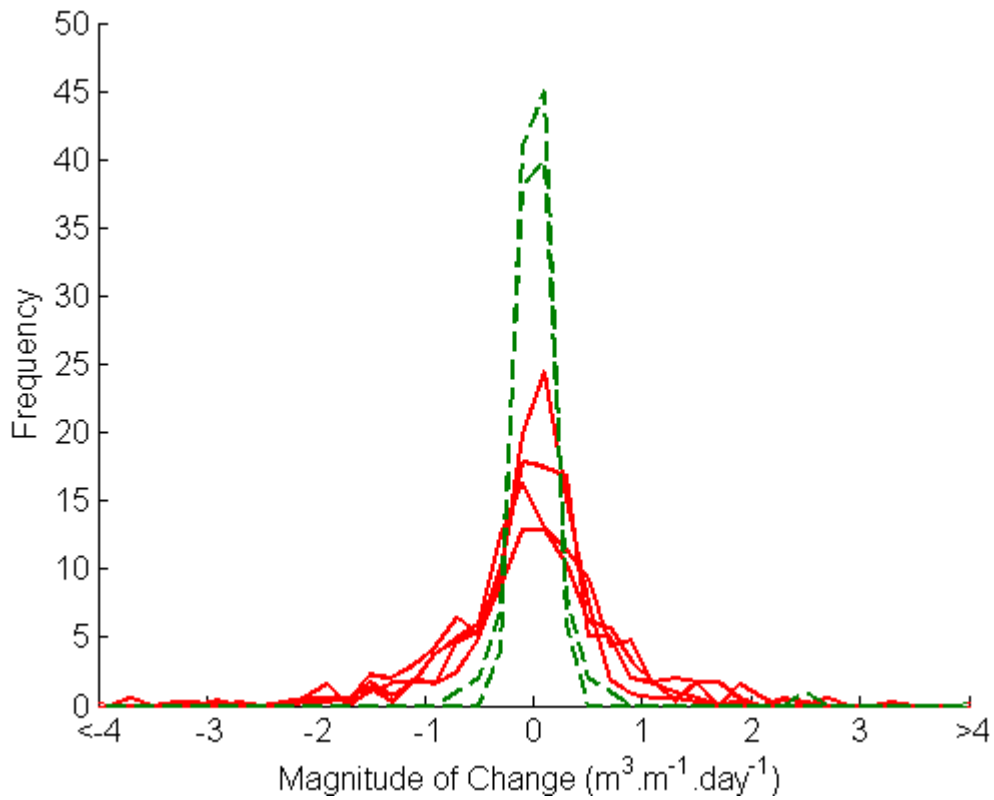


Figure 3.14: Magnitude of beach volume change (x-axis) versus frequency (y-axis) for harbour adjacent (solid red lines) and outlier beaches (dashed green lines). Erosion and accretion events were illustrated by negative and positive results respectively.

Table 3-3: Magnitude of volume change data for all beach sites. All data are displayed in $\text{m}^3 \cdot \text{m}^{-1} \cdot \text{day}^{-1}$. The right hand column shows the data ranked according the range of values with 1 being lowest.

Beach	Minimum	Maximum	Mean	Range	Rank
Whangapoua	-1.91	1.33	-0.02	3.24	9
Matarangi	-1.81	1.24	-0.02	3.05	8
Rings	-0.32	2.44	0.03	2.76	4
Kuaotunu West	-1.75	1.10	-0.01	2.85	5
Kuaotunu East	-1.22	1.05	0.00	2.27	3
Otama	-1.91	0.99	-0.03	2.90	7
Opito	-1.14	0.78	0.00	1.92	2
Wharekaho	-2.19	1.17	0.01	3.36	10
Buffalo	-1.46	16.6	-0.69	21.4	18
Maramaratotara	-0.70	0.62	0.00	1.32	1
Cooks	-1.91	0.94	-0.01	2.85	6
Hahei	-2.59	1.70	0.01	4.29	12
Hot Water	-2.79	1.82	0.01	4.61	13
Tairua	-16.9	4.94	-0.18	21.8	19
Pauanui	-2.44	2.33	0.44	4.78	15
Onemana	-2.20	2.81	-0.02	5.01	16
Whangamata North	-2.83	2.32	-0.01	5.15	17
Whangamata South	-2.22	1.39	-0.01	3.61	11
Whiritoa	-2.69	2.00	-0.02	4.69	14

3.4.7 Exponential Decay versus Intertidal Beach Slope

The magnitude of change results showed exponentially decaying relationships. A best fit exponential decay model was fitted using least squares regression to the magnitude of volume change data (Equation 3.2). The decay constant k was compared to the intertidal beach slope (Figure 3.15). A large decay constant meant there was less large magnitude of change events. Steep, reflective beaches

(blue stars) showed different behaviour to intermediate beaches (black circles) as illustrated by the narrow grouping of the decay constant (Figure 3.15). Reflective beaches were characterised by a narrow range of decay constants ($k = 1$ to $k = 2.5$) and steep beach slopes (0.11 to 0.14). Intermediate beaches had the highest variation of decay constants with k ranging from 3 to 11.7, excluding one outlier located at the northern end of Wharekaho Beach. The northern most profile on Wharekaho Beach had a decay constant of 18.5 which was larger than all other results. Intermediate beach slopes ranged from 0.012 to 0.08. Outliers (green squares) still showed different behaviour to the other reflective beaches with high decay constants ($k = 8$ and $k = 11$ for Maramaratotara and Rings respectively) and high beach slopes (0.10 and 0.11 for Rings and Maramaratotara respectively). Harbour adjacent beaches (red crosses) exhibited different behaviour to other intermediate beaches on the Coromandel Peninsula with low beach slopes (0.02 to 0.05) and decay constants ($k = 1.3$ to $k = 4.6$).

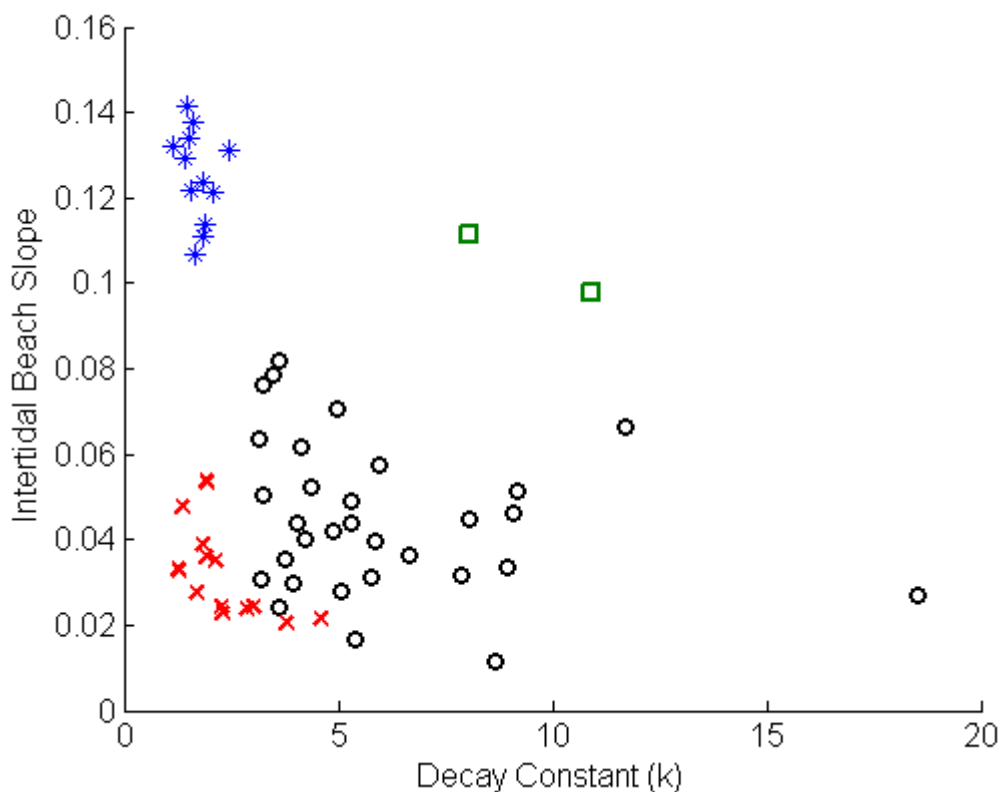


Figure 3.15: Decay constant k versus average intertidal beach slope all sites. See text for definitions of reflective beaches (blue stars), intermediate beaches (black circles), harbour adjacent beaches (red crosses), and outlier beaches (green squares). The 3 profiles with reduced datasets were not considered for exponential decay analysis (refer text).

3.4.8 The Impact of Wave Conditions on Short Term Beach Variation

A storm wave event was defined as an H_s greater than 3 m. Percentile results for the four wave data sites were shown in Table 3-4. Table 3-4 showed that the 3 m definition was nearest to the 99th percentile conditions at the four sites. The difference between the 90th and 95th percentile wave heights was small (approximately 0.4 m), however the difference between the 95th and 99th percentile heights was relatively large (approximately 1.0 m). The small difference between the 90th and 95th percentile values showed that wave heights in this range were not likely to be large storm events due to the relatively high frequency of occurrence. The 3 m justification for storm events was therefore considered sufficient and accounted for, on average, 3 to 4 storm days per year. This excluded preceding and proceeding wave heights near the 3 m level which were likely to be part of the same meteorological system or wave event. Further, the results in Table 3-4 were quite different at Matarangi and Opito Bay compared to Tairua and Whangamata. The latter two have higher results at all percentile levels indicating wave climate characterised by larger waves south of the Kuaotunu Peninsula. The Matarangi and Opito Bay sites were in the lee of the Mercury Islands which were likely to have decreased incoming wave energy.

Table 3-4: Percentiles of H_s (m) for the 30 year wave hindcast period at the four sites representing the spatial variation of the Coromandel Peninsula.

Site	Latitude	Longitude	50% (median)	90%	95%	99%	100% (max.)
Matarangi	-36.700	175.642	0.76	1.53	1.90	2.80	6.62
Opito Bay	-36.705	175.808	0.80	1.60	1.97	2.98	6.34
Tairua	-36.985	175.878	0.98	1.89	2.30	3.41	7.68
Whangamata	-37.217	175.908	0.87	1.75	2.15	3.16	7.24

Percentage change in beach volumes were compared against the mean H_s and H_{max} between surveys. Figure 3.16 illustrated the resulting R-squared values for beach volume versus average H_s . The largest R-squared values of 0.1 and 0.07 were observed at Wharekaho and Opito Beaches respectively. Figure 3.17

illustrated the R-squared values of beach volume versus H_{max} . The largest R-squared values of 0.19 and 0.18 were observed at Matarangi and Wharekaho Beaches respectively. Overall, volume versus H_{max} had larger R-squared values than mean H_s . Significance testing on the results showed that none of the data were significant at the 95 % level. Wharekaho Beach had the highest R-squared value in Figure 3.16 and the highest significance was a p-value of 0.53. Matarangi Beach had the highest R-squared value in Figure 3.17 and the highest significance was a p-value of 0.09.

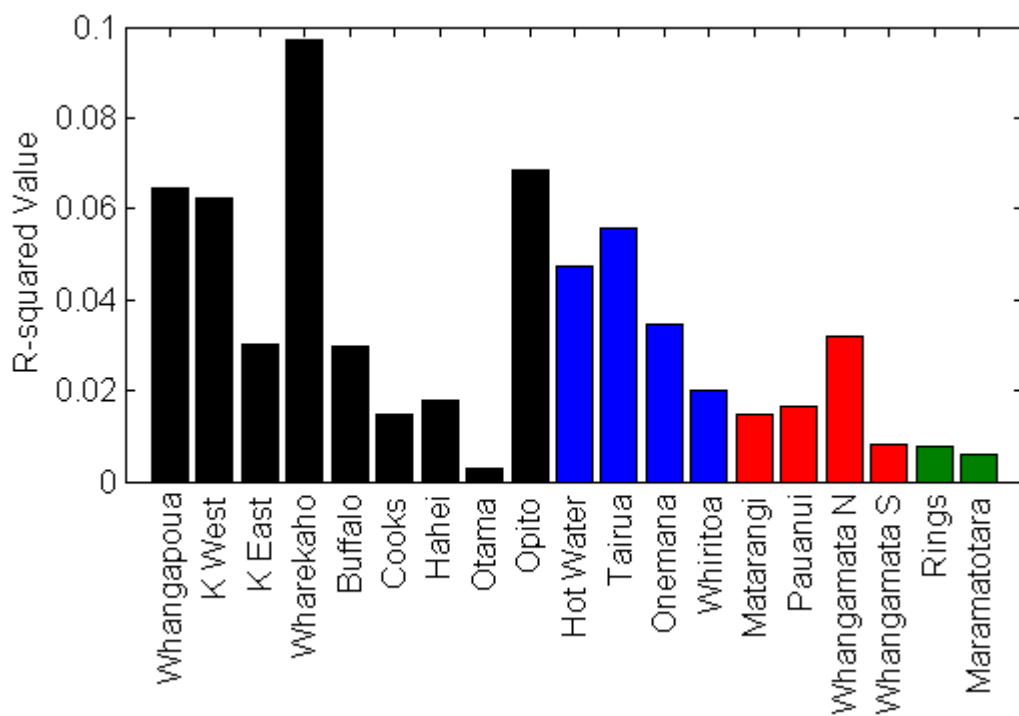


Figure 3.16: Average r^2 value for beach volume change versus time-averaged H_s between surveys for intermediate beaches (black bars, Whangapoua - Opito), reflective beaches (blue bars, hot Water - Whiritoa), harbour adjacent beaches (red bars, Matarangi - Whangamata South), and outlier beaches (green bars, Rings and Maramaratotara).

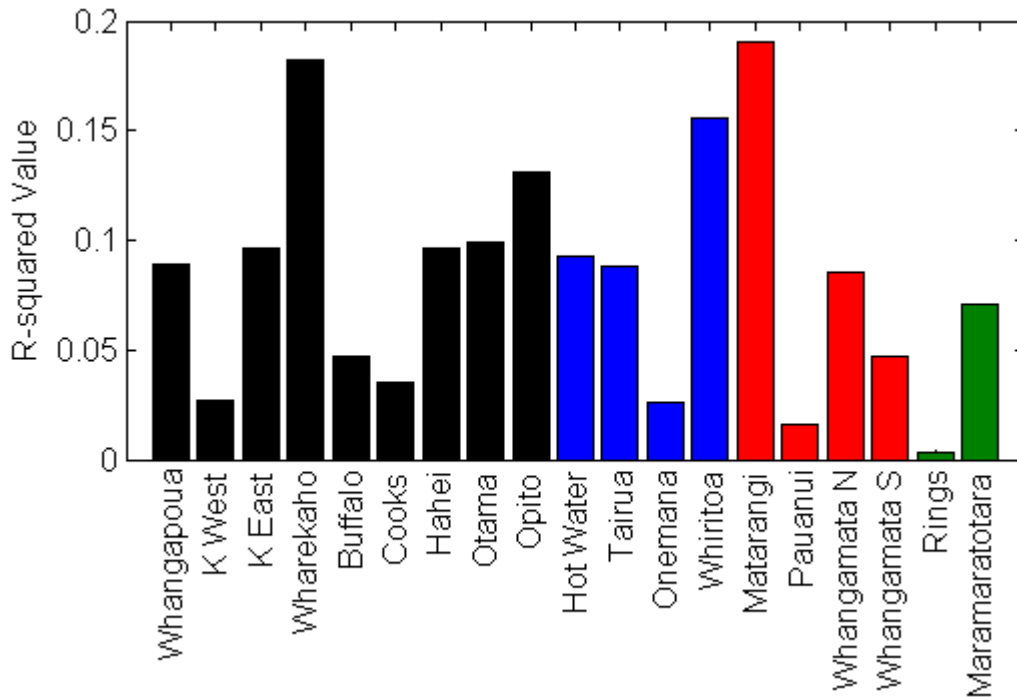


Figure 3.17: Average r^2 value for beach volume change versus H_{max} between surveys for intermediate beaches (black bars, Whangapoua - Opito), reflective beaches (blue bars, hot Water - Whiritoa), harbour adjacent beaches (red bars, Matarangi – Whangamata South), and outlier beaches (green bars, Rings and Maramaratotara). Note the different y-axis scale.

3.4.9 Ngarunui Beach, Raglan

Short term beach behaviour at Ngarunui Beach was analysed at four profile sites and 8 sampling dates during 2009 (Figure 3.18). The four sites were labelled Rag1 to Rag4 from south to north. The southern profile (Rag1, red dash-dot line) was relatively stable through the year. The maximum volume was 5 % and the minimum was -6 %. The profile showed erosion leading into the April and June profiles, then accretion leading into the July profile. The profile second from the south (Rag2, dashed green line) had similar short term behaviour to the southern profile (dash-dot red line) with similar volume changes at similar times during the year. The Rag3 profile (dotted blue line) was different as it showed an increase in volume from January to March, and decreased volumes in all other surveys except the July survey. The Rag4 profile (solid black line) had an unusual shape with a large spike of accretion in the September profile, then a greater amount of erosion in the following November profile. The accretion spike was a 600 mm increase in elevation across a majority of the profile compared to previous surveys. The profile also had unusual bed ripple formations between cross-shore distance 220

m and 240 m with elevation changes of 200 mm. These bedforms were not observed in any other survey on the beach for the duration of the surveying. The average beach volume through the year was also shown. Interim results showed the presence of a seasonal trend with accretion in the first and last 1.5 month intervals and erosion for the rest of the year. The large spike of accretion in the Rag4 September data affected the average result and subsequently showed a significant increase.

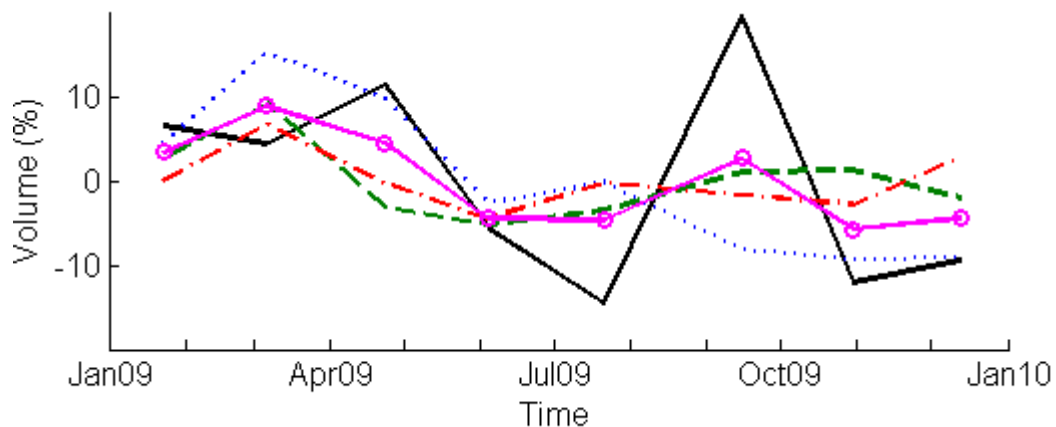


Figure 3.18: Demeaned beach volume timeseries for Rag1 (dashed green line), Rag2 (dash-dot red line), Rag3 (dotted blue line), and Rag4 (solid black line) at Ngarunui Beach, Raglan. The solid pink line with circle markers was the average volume across the four profiles.

Horizontal beach volume analysis was undertaken at Ngarunui Beach. Because the tidal range and wave climate is greater on the west coast (Bryan et al., 2007), the horizontal segment areas were changed. The intertidal volume was between RL -1.5 m and RL 1.5 m. The upper beach volume was between RL 1.5 m and RL 4 m, and the dune region was the area above RL 4 m. The intertidal region at all four profile sites (Figure 3.19 c) had similar erosion and accretion trends between surveys, excluding the large spike in the northernmost profile (Rag4, solid black line). The profiles had peak volumes in March and a general trend of erosion through to August. Three profiles eroded leading into the October surveys and accretion in the following December surveys. The Rag2 profile (dashed green line, Figure 3.19 c) had the opposite trend in the final two surveys.

In the upper beach region the southern two profiles (Rag1 and Rag2, dash-dot red and dashed green lines respectively) had accretion from April to October then erosion until the end of the year. The northern two profiles (Rag3 and Rag4, dotted blue and solid black lines, Figure 3.19 b) did not show similar trends with variation in the volume through the year. The large accretion spike affected the data, hence why the erosion at the end of the year appeared to be larger than other sites. The dune volumes (Figure 3.19 a) were similar at 3 profile sites, excluding the northernmost site (solid black line). There was a general trend of accretion through the year at these three sites. Standard deviations of elevation and magnitude of change data were not produced due to the short dataset available.

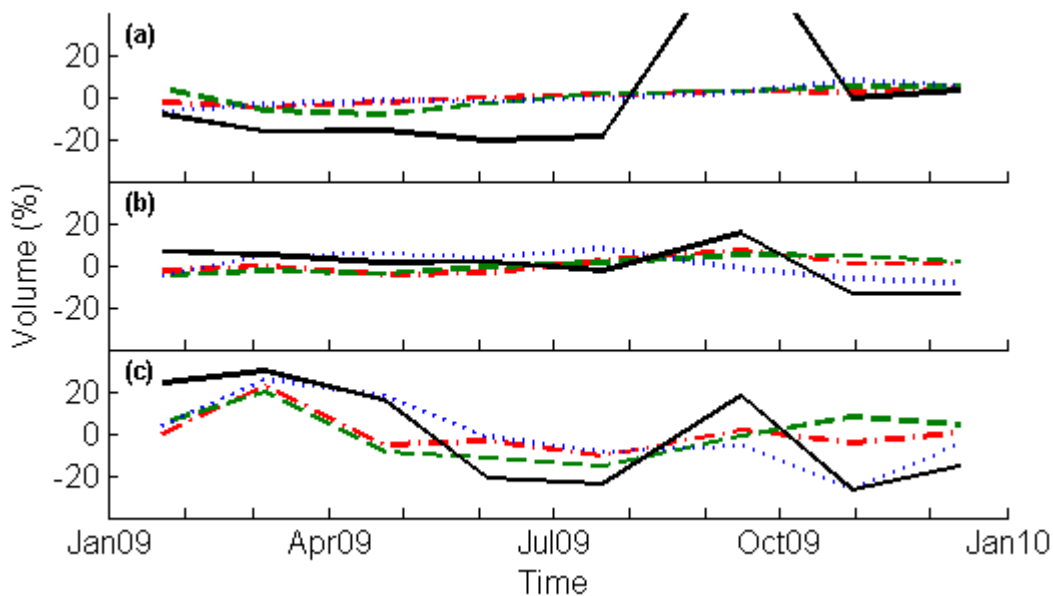


Figure 3.19: Timeseries of the demeaned dune volume (a), upper beach volume (b), and intertidal beach volume (c) at the four survey sites Rag4 (solid black line), Rag3 (dotted blue line), Rag2 (dashed green line), and Rag1 (dash-dot red line). The gap in the data in (a) is due to the value in September 2009 exceeding the y-axis limits. Increasing the axis limits would reduce the accuracy of the figure.

3.5 DISCUSSION

3.5.1 Observations of Beach Elevation Change

Figure 3.3 showed the temporal variation of beach elevation through time. These figures are commonplace in published literature especially for observing and analysing morphological change (e.g. Ranasinghe et al., 2004; Gunawardena et

al., 2008; Ojeda & Guillen, 2008). Short term beach variation was evident in Figure 3.3 but difficult to quantify. Erosion events were determined from the landward retreat of the MSL contour and / or the upper beach region. Large variations between consecutive surveys were prominent, however the overall location of the MSL contour remained relatively stable for the entire timeseries at most sites. The most significant variation was the uniform retreat of the MSL contour from mid 2007 to the start of 2009 in the four example timeseries shown. Most profiles on the eastern Coromandel Peninsula eroded following a storm wave event in July 2008. This storm event caused the largest amount of erosion at most Coromandel beaches for the entire timeseries. For example, the MSL contour was located at its most landward position at Whangapoua, Tairua, and Pauanui following this event. However, there was one previous event at Matarangi where the MSL contour was located further landward which occurred in 1998 (a further 7 m landward). Analysis of most sites showed that this July 2008 event was the largest in the timeseries. Landward retreat of more than one profile was due to storms because the spatial variation occurred across more than one beach. Short term natural shoreline variability was caused by waves, tides, and storm surge conditions, while short term human-induced changes were restricted to surf zone structures and shore nourishments (Stive et al., 2002). The large spatial variation of erosion events eliminates the probability of human influence in the data. The only approved beach alteration works across the entire Coromandel Peninsula in the timeframe considered are located on Buffalo Beach. Consents have been granted for beach and dune alteration works in the vicinity of CCS24 (northern profile) and CCS25-1 (central profile) on Buffalo Beach. Whilst these consented works were in place, details of the actual beach alteration are limited. There is also a seawall located between CCS25 and CCS25-1 (profile second from north), a second near CCS26 (profile second from south), and a third located south of CCS27 (southern profile). Overall, there is little human impact on Coromandel beaches with the largest cause of variation being associated with dune planting and beach restoration groups which occur infrequently and do not significantly affect volumes in the timeframe considered here.

3.5.2 Beach Volume Change between Consecutive Surveys

The non-uniform behaviour of subaerial beach systems on the Coromandel Peninsula was initially illustrated in Figure 3.4. Boxes 1 and 4 showed two occasions where the short term variation was uniform at more than one beach, but not across the Peninsula. This non-uniform behaviour was a common occurrence when analysing the available data (Appendix VII). In particular, Pauanui Beach was different to all other beaches in both boxes. Analysis of other profiles on Pauanui Beach showed a large degree of variation along the beach with very little uniform behaviour between profiles (Figure VII.15). Many beaches showed a large degree of similar variation in the alongshore direction. It can therefore be deemed that the behaviour at Pauanui is different to that occurring at Whangapoua, Matarangi, and Tairua. This shows support for sediment transport sub-cells. The non-uniform behaviour provides evidence that not one beach can be an indicator beach for short term variation on entire Peninsula. The behaviour identified in Boxes 1 and 4 illustrated the difference in behaviour between the northern and southern regions of the study site. With regard to the July 2008 storm event, it is interesting to note that the storm wave event had a larger H_s (mean H_s and H_{max}), longer duration and steeper waves at Tairua compared to the Matarangi wave data, however the northern two beaches (Whangapoua and Matarangi) had a greater amount of erosion. Further, the wave direction was predominantly north-easterly during this event, of which Whangapoua and Matarangi Beach are partially sheltered from. The major geophysical difference between the two systems is the beach orientation, however both systems were subjected to large storm waves therefore relatively uniform erosion would have been expected.

Boxes 2 and 3 further highlighted the difference in behaviour depending on the spatial location of beaches and profiles on the Coromandel Peninsula. Adjacent beaches exhibit similar behaviour within Boxes 2 and 3, yet it differs from behaviour exhibited at other regions of the Peninsula. This was evident through the data in Appendix VII. The difference in beach orientation is hypothesised to be a factor, however there is only 12° of variation between Whangapoua and Tairua beaches. This relatively low variation is not anticipated to cause a

significant variation in beach behaviour. However, beaches north of the Kuaotunu Peninsula are relatively sheltered from east to south easterly storm wave events, whereas Tairua is more exposed. As a result, the Kuaotunu Peninsula is hypothesised to be a barrier to sediment transport and beach behaviour on the Coromandel Peninsula because beaches north and south of the Kuaotunu Peninsula exhibit different behaviour (refer Chapter 5).

The standard deviations of beach volumes showed a large amount of variation between Coromandel beaches. Reflective and harbour adjacent beaches had greater short term variation in subaerial beach volumes, of which the large degree of variation on reflective beaches conforms to results published by Wright and Short (1984) and Dail et al. (2000). Intermediate beaches showed a greater range of short term variation, but overall undergo smaller volume changes which also conform to the Wright and Short (1984) classification, which suggest they change beach state relatively often. The standard deviations of harbour adjacent beaches showed a high degree of variation, as well as Buffalo and Cooks Beaches which are also adjacent to harbour entrances. Harbour adjacent beaches all had similar standard deviations and grain sizes, indicating that the sediment size and source has a large impact on Coromandel Beach behaviour. A study by Thom and Hall (1991) of a medium sand beach in southeast Australia had a standard deviation of beach volume of approximately 25 %. Cooks Beach had a standard deviation of 17.5 % which was the highest on the Coromandel Peninsula.

The dimensionless fall parameter (Wright & Short, 1984) was also used to classify the beaches (Table 3-2). The narrow range of results for the reflective beaches was considered sufficient to justify their classification as reflective beaches. It is acknowledged that a parameter of about 1 is required to classify a beach as reflective, however the average intertidal slope, coupled with the behaviour evident in this Chapter, suggest that the four beaches (Hot Water, Tairua, Onemana, and Whiritoa) are better attributed to reflective assemblages. It is hypothesised that a limited sediment supply of coarse grained sediment is an important factor of the reflective beach behaviour. Conversely, the intermediate

beaches had a large range of parameters and slopes, which accords well to intermediate beach variations.

3.5.3 Horizontal Beach Volume Segment Analysis

The most prominent short term trend within the horizontal segment analyses was the similarity in behaviour between the upper beach and intertidal beach volumes, and the stability of the dune region (Figures 3.5 to 3.8 and Appendix V). A large majority of cross-shore beach variation was restricted to the upper beach and intertidal region which was below the approximate storm high water mark and edge of vegetation line. This approximated line proved to be a good indicator of the upper limit of regular wave action, and shows that aeolian transport in the dune region is insignificant. A study of a microtidal sandy beach by Quartel et al. (2008) showed that the upper and lower beach regions (comparable elevations to those studied here) did not show the same similarity as identified at Whangapoua, Matarangi, and Tairua Beaches. Given the relatively uniform behavioural pattern between the upper beach and intertidal area on numerous different beach types in this study, it would be expected that this would occur on other beaches. The beach studied by Quartel et al. (2008) had a good correlation between the amount of beach change and the time-averaged wave height, whereas Coromandel Beaches showed poor correlations (refer Section 3.4.8). As a result, it is concluded that the beach considered by Quartel et al. (2008) differs from most Coromandel beaches and is better attributed to the harbour adjacent beach scenario with a high degree of short term variation. Figures 3.5 to 3.8 showed no regular short term variation in the dune region which was common for most Coromandel beaches (refer Appendix V). For example, Whangapoua Beach was subject to longer term trends with the most significant change occurring after the July 2008 storm. Matarangi Beach contained little dune data therefore no analysis was given. There was no regular short term variation at Tairua Beach and Pauanui Beach, however they were both subject to longer term dune volume trends. The spike in the Tairua dune volume timeseries in mid 1996 was not considered due to the 1.5 year gap in the data prior to 1996 and also the following survey.

The results presented here prove that the lower beach region comprising the upper beach and intertidal regions accounted for a large majority of variation in subaerial beach volumes. This conforms to results at the southern end of Tairua Beach which showed most variation also occurred in the intertidal beach region (Smith & Bryan, 2007). This study shows that this occurred across most Coromandel beaches (refer Appendix V). Coromandel beach variation is therefore largely confined to below the limit of regular wave action (RL 3.5 m).

3.5.4 Standard Deviation of Horizontal Beach Volume Segments

The standard deviations of horizontal beach volume segment results were grouped according to the Wright and Short (1984) classification. Rings Beach had an average slope of 0.098 therefore was considered to be reflective as the next steepest intermediate beach had a slope of 0.07. There were no dissipative beaches on the eastern Coromandel Peninsula. This classification does not mean Coromandel beaches were confined to any particular morphological state, but for the purpose of this thesis they were grouped according to average intertidal beach slopes and dimensionless fall parameters (Wright & Short, 1984). For example, Tairua has a steep average beach slope similar to reflective beaches in the Wright and Short (1984), although it is acknowledged the beach exists in various intermediate beach states (Bogle, 1999; Smith & Bryan, 2007; Gallop, 2009) and had a dimensionless fall parameter of 2.6. This was likely to occur on several Coromandel beaches.

There was an obvious difference in short term behaviour dependent on beach slope (Figure 3.9). Reflective beaches had different behaviour to intermediate beaches as evidenced by the standard deviation, magnitude of change results, and exponential decay. However, four intermediate beaches had behaviour which was similar to reflective beaches (Matarangi, Pauanui, Whangamata North, and Whangamata South). It was further identified that these four beaches were all located adjacent to harbour entrances. The respective harbours were 3 out of the 4 largest harbours on the eastern Coromandel Peninsula (Table 3-5). Due to the different short term behaviour evident in the data these four beaches were

classified as “harbour adjacent beaches”. The different behaviour was evident in all results in this Chapter. The high variability was particularly evident when analysing the individual volume timeseries. It is hypothesised that the behaviour is caused by storm events which cause an increase in eroded terrestrial and riverine sediment being ejected from the harbour. Groundwater variations due to storm precipitation have also been proven to impact subaerial beach volumes (Clarke & Eliot, 1988).

Table 3-5: Harbours located adjacent to Coromandel beaches with corresponding harbour and catchment size (Source: Mead & Moores, 2005).

Harbour / estuary (corresponding beach to which it applies)	Harbour area at high tide (x10⁶m²)	Catchment size (ha)
Whangapoua Harbour (Matarangi Beach)	13.1	106.56
Whitianga (Buffalo Beach)	15.6	492.01
Purangi River (Cooks Beach)	No data *	No data
Tairua Harbour (Pauanui Beach)	6.12	282.35
Whangamata Harbour (Whangamata North)	4.3	51.69
Otahu Estuary (Whangamata South)	Included in Whangamata Harbour	70.25

**Purangi estuary was stated as having the 5th largest area in hectares.*

Two further beaches exhibited different behaviour to all other beaches and were termed “outliers”. The main exception was Buffalo Beach which illustrated behaviour similar to the remaining intermediate beaches and is located adjacent to the largest harbour on the Peninsula. Cooks Beach is also located adjacent to Purangi Harbour, however it is small in comparison to the other harbours (Table 3-5). The two eastern profiles on Cooks Beach showed different behaviour

however it was not reflected in the behaviour of the entire beach. It is hypothesised that the smaller sized harbour only affects those profiles on the eastern end of the beach as shown in the raw volume data (refer Appendix VII).

The standard deviations of horizontal beach volume segments represented mean values for each beach (Figure 3.9). It was hypothesised that the standard deviation would increase with decreasing elevation, from the dune to upper beach to intertidal region. This hypothesis was based on the average limit of wave action being largely restricted to the lower beach region (below RL 3.5 m) as observed by the beach profile surveyors. Previous research had also shown increasing variation with decreasing elevation in the subaerial beach which provided further support for this hypothesis (e.g. Larson & Kraus, 1994; Larson et al., 2003; Quartel et al., 2008). This hypothesis was true across a majority of the Coromandel beaches. The dune region was the most stable region on all beaches due to minimal wave impacts and insignificant aeolian transport. Most dune volume data had no significant volume change events, and large temporal variations were the main factor of volume change. This was consistent with results of Larson et al. (2003) who found the lowest standard deviation of elevation (for the subaerial beach) at Duck was the dune region above 3.5 m elevation, and the greatest variation occurred about the MSL contour. The high variability of the shoreline at Duck was attributed to varying wave steepness during storm events. The stability of the dune was because of the lack of influence from waves and tides. Earlier research by Larson and Kraus (1994) analysed the same beach profile data at Duck and found the region of greatest variability to be around the MSL contour, and the most stable region of the subaerial beach was above 4 m elevation. These results confirm the hypothesis that the dune region would be the most stable region of the beach and that the intertidal region encompassing the MSL contour was the most variable region.

One significant difference in Coromandel beach behaviour was that all reflective beaches had more variable upper beach regions than the respective intertidal region (Figure 3.9). This variation occurred on 11 out of 13 profiles on the four

reflective beaches (Figures VI.13, VI.14, VI.16, and VI.19 Appendix VI). The results showed the largest amount of variation on reflective beaches was in the upper beach face. Wright and Short (1984) state that reflective beaches have little subaqueous sediment storage, therefore implying volume changes occur on the subaerial beach. The variation could also be due to the formation and subsequent erosion of berm features, however berms are not restricted to reflective beach systems. The steeper beaches in this study also had more coarse sediment than intermediate beaches (Figure 3.10). Because most sites are dominated by quartz feldsparic sand (Healy et al., 1981), this showed that the more coarse sediment on reflective beaches required greater wave energy to be transported. The wave energy does not vary between the intermediate and steep beach sites however steeper profiles cause energy released from wave breaking to be located closer to the shoreline. Wave energy on flatter beach profiles is dissipated further offshore through wave breaking. The resulting turbulence from breaking wave energy on reflective beaches is confined further up the beach face compared to intermediate beaches, hence increased wave runup (Wright & Short, 1984). Previous research showed that subharmonic edge waves are dominant on reflective beaches but had a reduced impact on intermediate beaches (Wright & Short, 1984). It is therefore hypothesised that complex swash zone interactions and infragravity wave oscillations may be responsible for the difference in behaviour between the upper beach and intertidal volumes on reflective beaches, ultimately caused by the steep beach face and relatively coarse sediment.

3.5.5 Magnitude of Beach Volume Change

The cycle of short term erosion and accretion was discussed by Clarke and Eliot (1988) and Dolan et al. (1991) who showed a need for long term datasets to adequately determine the degree of short term beach variation. Accretionary changes typically require a timeframe of several weeks to months whereas a single storm event can erode a beach of a large percentage of its volume in a very short period of time (e.g. hours to days), as identified at Whangapoua following the July 2008 storm event (refer Appendix VII). The morphology of a beach at any particular time is a function of its sediment characteristics, immediate and antecedent wave, tide and wind conditions, and the antecedent beach state (Wright

& Short, 1984). The wave, tide and wind conditions were very similar for the entire Coromandel Peninsula therefore Coromandel Beaches would be expected to undergo similar changes and have similar temporal variations of beach morphology changes. Antecedent beach conditions would not be expected to differ greatly between beaches because of the similar wave climate around the Coromandel, therefore sediment characteristics remain as a critical component of beach morphology on the Coromandel Peninsula. A linear relationship existed between grain size and beach slope, and if the obvious outlier in Figure 3.10 was excluded (Maramaratotara), the relationship had an R-squared value of 0.64. Increased sediment sizes were typically attributed to higher degrees of stability on the beach face, thus allowing increased beach slopes (Wright & Short, 1984). Increased beach slopes on the Coromandel Peninsula occurred on reflective and outlier beaches. Reflective beaches are also synonymous with relatively large subaerial sediment volumes (Wright & Short, 1984). The high degree of short term volume changes was described by Yates et al. (2009) who showed that accreted profiles required less wave energy to erode the beach face, therefore reflective beaches with higher subaerial beach volumes are relatively easily eroded (Figure 3.1).

The rate of change of subaerial beach volumes provided interesting results across most beaches in this study. Figures 3.11 and 3.13 illustrated a marked difference in behaviour between intermediate and reflective beaches. A study by Thom and Hall (1991) showed a maximum accretion rate of $0.27 \text{ m}^3 \cdot \text{m}^{-1} \cdot \text{day}^{-1}$ which is very low compared to the results for Coromandel beaches, except the outliers. The large degree of variation on reflective beaches was interesting because Wright and Short (1984) showed that reflective beaches were typical of lower sediment mobility compared to intermediate beaches because they were often sheltered systems. The results displayed here were conclusive that reflective beaches are more variable on a short term scale. The majority of sediment storage on reflective beaches is in the subaerial beach, implying that most morphological change occurs in the subaerial profile on reflective beaches. Therefore, high magnitude of change events lead to a direct loss of sediment from the subaerial profile, which in turn produce high standard deviations of beach volume within

the intertidal and upper beach region. According to Wright and Short (1984), it would be expected that repeated subaqueous profiling would yield relatively consistent volume results because a majority of the variation is in the subaerial profile with little subaqueous sediment storage.

Intermediate beaches have the greatest degree of variability, were typically comprised of medium grained sediment, and have a modest or meagre sediment supply (Wright & Short, 1984). The large range of standard deviations and magnitude of change results showed that intermediate beaches have a greater range of beach behaviour, and therefore beach states, consistent with Wright and Short (1984). This contrasts to the narrow range of behaviours shown by reflective beaches. Harbour adjacent beaches add a greater amount of variation to the intermediate beach systems. Harbour adjacent beaches did not show the same behaviour as the intermediate beaches. The differing behaviour was hypothesised to be due to episodic inputs of sediment from the harbour into the subaerial beach system and groundwater impacts (e.g. Clarke & Eliot, 1988). This is the obvious explanation regarding the behaviour, however Buffalo Beach is located adjacent to Whitianga Harbour which is the largest on the Coromandel Peninsula, but showed intermediate beach behaviour. However, analyses of the beach volume data along Buffalo Beach showed that the behaviour differs greatly between the profiles along the beach which is characteristic of harbour adjacent beaches.

The behaviour of the two outlier beaches was not been explained in this chapter. Both beaches had freshwater input which would suggest episodic inputs of sediment into the system. With regard to Rings Beach, it is the only reflective beach north of the Kuaotunu Peninsula, but is still subject to the same wave conditions. Therefore, a higher degree of short term variation similar to the reflective beaches would be expected. Maramaratotara Beach is a sheltered beach with coarse calcite sediment which could be a factor, however the behaviour is very similar to Rings Beach.

3.5.6 Exponential Decay versus Intertidal Beach Slope

The magnitude of change analysis resembled an exponentially decaying relationship. Reflective beaches showed a close grouping of intertidal beach slopes and decay constants. These results emphasised the similarity between reflective beaches. Intermediate beaches showed a large degree of variation in both beach slope and the decay constant which further emphasises the conformity to Wright and Short (1984). Harbour adjacent beaches interestingly had a relatively good grouping, given that they had exhibited a large degree of short term variation. Harbour adjacent beaches had relatively low intertidal beach slopes and decay constants compared to intermediate beaches. The outlier beaches continued to show different behaviour and could not be explained. An intermediate beach with a large decay constant was identified in Figure 3.15. This profile was the northern most profile on Wharekaho Beach (CCS22-1). The behaviour was attributed to the sheltered nature of the profile as shown by the aerial photo in Appendix II.

One profile at each of Tairua, Pauanui and Whangamata South Beaches were excluded as the respective datasets were too short to be compared against other profiles on the same beach.

3.5.7 Impact of Wave Conditions on Short Term Beach Variation

Storm wave events were the primary cause of beach erosion. Wave height conditions (time-averaged H_s and H_{max}) were analysed against the amount of short term beach volume change. It was hypothesised that short term changes in beach volume would be correlated to changes in H_s caused by storm waves. Figure 3.16 showed poor correlations between the time-averaged H_s and beach volume change. Slightly better results were achieved for beach volume change and H_{max} between surveys. These results conform to recent findings of Yates et al. (2009) who showed a weak correlation when using weekly to monthly averaged wave energy. A study of a reflective beach by Dail et al. (2000) also used time-averaged wave heights between surveys and produced low correlations with beach volume changes. The following conclusions were reached by Yates et al. (2009): 1) that

the timing of storm events was crucial to the beach response, rather than the amount of wave energy; and 2) that hourly averaged wave energy and antecedent beach conditions play a significant role in determining whether a beach eroded or accreted. As a result, it is considered that the time-averaging of wave data used in this thesis was over too long a period to yield strong correlations. The timing of storm events was also not considered. To more accurately determine short term beach response to storms, it is suggested that a greater detail of analysis is undertaken on shorter term wave events, in particular the timing of storm wave events and antecedent beach conditions.

3.5.8 Ngarunui Beach, Raglan

It was difficult to show conclusive evidence about the Ngarunui Beach data due to the short dataset available. The most interesting result was the large spike of accretion and elevation change identified in the Rag4 (northernmost) data in September 2009. Several hypotheses were drawn regarding the behaviour. The first was that a sand wave caused the significant elevation increase with a likely source being a pulse of sediment from the harbour mouth increased beach elevation prior to being transported offshore once subjected to larger ocean waves, that is, beyond the apparent sheltering of the ebb tidal delta. This would explain why it was not identified further down the beach. Further, increased wave conditions during winter may have resulted in a shift of sediment from the ebb tidal delta onto the beach. Alternatively, a rhythmic feature on the beach may have been evident, but was not studied further in this thesis. The aerial photo in Appendix II showed that the Rag4 profile is in the vicinity of the ebb tidal delta. The data showed a comparison to east coast beaches and many sandy beaches around the world, that most of the variation occurred within the intertidal zone, noting the increased spring tidal range of 3 m for the west coast (Bryan et al., 2007). The data did not show a relationship between the intertidal and upper beach region as identified on a majority of the east coast data. Overall, the data did not show any obvious similarities when compared visually to the 2008 data at the most dissipative east coast beach, Matarangi. The average beach volumes through the year showed the presence of a seasonal trend, although there were longer periods of erosion through the year compared to east coast beaches.

3.6 SUMMARY

Analysis of short term variations in beach behaviour on the Coromandel Peninsula showed four distinct beach classifications. The following conclusions were drawn from the short term analyses:

- Short term beach behaviour was not uniform on the Coromandel Peninsula with regard to erosion and accretion of subaerial beach profiles, however individual groups of beaches had a large degree of similarity;
- Reflective and harbour adjacent beaches are subject to greater volume changes and change rates on the short term timescale compared to intermediate beaches;
- Volume changes in the dune region were infrequent, whilst the intertidal and upper beach regions behaved in a similar manner;
- Reflective beaches had the greatest variation on the subaerial beach and also have more variable upper beach regions than intertidal regions;
- There was a linear relationship between mean grain size and intertidal beach slope on all Coromandel beaches except Maramaratotara which is dominated by calcite sediment. All other beaches are sandy beaches and were grouped relatively well according to beach state classification.
- Intermediate beaches had small volume change rates however the greater range of results suggest they had much greater variations in beach state. Outlier beaches had very little volume change. The grouping of beaches was further emphasised by the narrow grouping of decay constants for reflective and harbour adjacent beaches compared to intermediate beaches and outliers.
- Beach volume change was poorly correlated with time-averaged H_s and H_{max} between consecutive surveys. H_{max} yielded higher correlations than mean H_s .
- Ngarunui Beach did not show similar volume change behaviour to the most dissipative eastern Coromandel beach, Matarangi.

In summary, the beach state classification of Wright and Short (1984) appeared to be significant in determining the behaviour of eastern Coromandel beaches.

Results showed that intermediate beaches clearly exist in a greater range of beach states, but were subject to lower volume changes, and change rates, when compared to reflective beaches. Reflective beaches had relatively stable beach states, showed greater volume variations, greater volume change rates, and had more variable upper beach regions than intertidal regions. The Wright and Short (1984) classification is not applicable across the entire Peninsula however, as harbour adjacent beaches provided an anomaly to the behaviour of intermediate beaches, as well as the two outliers. The exact forcing mechanism of beach variation needs to be analysed further as time-averaged wave height and maximum wave height showed poor correlations to the volume change data.

CHAPTER FOUR

SEASONAL VARIATION AND OSCILLATION

4.1 INTRODUCTION

Analysis of the spatial and temporal variation of Coromandel beaches at a seasonal scale was undertaken in this chapter. Whilst short term variations were significant in the analysis of beach variation, underlying longer term processes may also be prevalent. One example is the typical annual variation of subaerial beach environments from a perceived, eroded profile during winter storm conditions to an accreted profile during fair weather summer conditions (e.g. Medina et al., 1994; Komar, 1998). The data used in this thesis enabled variation occurring on a 2-monthly (approximate) to an annual cycle to be identified. Variation occurring at this scale was termed seasonal variation for the purpose of this thesis.

4.1.1 The Importance of Seasonal Variation and Beach Oscillation

Seasonal variation can be a large component of subaerial beach system variation (Eliot & Clarke, 1982). Variation in beach morphology has long been documented as a response to equilibrium wave conditions as opposed to instantaneous wave conditions (e.g. Wright and Short, 1984). Previous studies have shown that beach morphology seldom responds to instantaneous changes in the wave conditions on beaches dominated by storms with intermittent and seasonal recovery patterns (Morton et al., 1995; Lee et al., 1998; Anthony, 1998; Jimenez et al., 2008; Yates et al., 2009). Therefore, analysis on a greater temporal scale was required to fully understand Coromandel beach behaviour. Analysis of the seasonal variation of beach volume changes will either prove or disprove the presence of seasonal trends on the Coromandel beaches. Knowledge of the extent of seasonal variation may be used to forecast future shoreline positions and provide data on whether certain levels of erosion or accretion can be considered normal or extreme (i.e. within acceptable limits) for planning purposes.

Beach rotation is an oscillatory, medium scale phenomenon which is characteristic of short, embayed beaches on lee coasts (e.g. Ranasinghe et al., 2004). Beach rotation occurs on a cycle that is greater than the sampling frequency of this dataset, but typically varies more often than an interannual or long term cycle. Therefore, it needs to be discernible from the underlying seasonal processes. Analysis of beach rotation was undertaken to determine if it occurred on Coromandel beaches.

4.1.2 Expected Outcomes

This chapter seeks to prove or disprove the following hypotheses relating to seasonal variation:

- Eastern Coromandel beaches erode during winter and accrete in summer due to seasonal variations in the wave conditions, particularly due to increased storm activity in winter; and
- Beach rotation is evident on embayed beaches on the Coromandel Peninsula.

It is hypothesised that eastern Coromandel Beaches will follow a typical erosion trend during winter followed by recovery and accretion of the beach during fair weather summer conditions. Justification for this hypothesis is a result of more energetic winter storms eroding sediment from the subaerial beach face (e.g. Eliot & Clarke, 1982; Dubois, 1988; Medina et al., 1994; Komar, 1998). If beach rotation is evident on embayed Coromandel beaches, it is expected that the orientation of the beach and the spatial variation of the beaches will be a key component of the extent of beach rotation. Beach rotation has been shown to occur on a large spatial scale in which the incident wave angle is critical, therefore Coromandel beaches may show similar behavioural patterns due to the variations in beach orientation around the Peninsula (Klein et al., 2002; Ranasinghe et al., 2004).

4.2 BACKGROUND: SEASONAL OSCILLATION AND ROTATION

4.2.1 Seasonal Beach Variation – A Review

Perhaps the most well documented literature on beach morphological change is the beach state classification model by Wright and Short (1983; 1984) and their work in the few years prior (e.g. Short, 1979a, 1979b, 1981; Short & Wright, 1981; Wright, 1981; Wright et al., 1982b). Wright and Short (1984) used daily observations of beach state over 3 years and varying environmental controls to devise their model. The study was undertaken across numerous Australian beaches with varying morphologies. Beach profiles and observations were the dominant methods of data collection. The classification comprises of two extreme morphological states, reflective and dissipative beaches, with four intermediate beach states in between. The beach state at any point in time is affected by near bottom currents in the surf zone which are driven by the incident wave conditions, subharmonic oscillations, infragravity oscillations, and mean longshore and rip currents. The actual morphology is a function of the sediment characteristics, immediate and antecedent waves, tide and wave conditions, and the antecedent beach state.

Of particular interest were the results of Wright and Short (1984) relating to seasonal changes in beach state. Each individual beach environment has a most common beach state which results from the average breaking wave conditions and prevailing sediment characteristics (Wright & Short, 1984). Repeated observations and surveys of beaches showed that the beach state varied largely with wave height when the sediment size remained the same (Wright & Short, 1984). This highlights how beach changes over short to medium term time scales were less dependent on the sediment characteristics, and more reliant on the wave conditions when compared with long term beach oscillations. Seasonal changes in the wave regime have been well documented as a driver of seasonal beach change as a result (Eliot & Clarke, 1982). Wave height therefore has a significant role in seasonal beach behaviour and results in a generalisation of beach and sediment characteristics. In particular, intermediate beaches, the most dominant state for eastern Coromandel beaches, were found to be favoured by wave heights of 1 –

2.5 m when composed of medium sand (Short, 1981). Reflective beaches occurred under low swell conditions or in sheltered compartments, and were often associated with coarse sediment (Wright & Short, 1984). The four reflective beaches in this study (Hot Water, Tairua, Onemana, Whiritoa) are all bound by relatively large headlands and thus situated within sheltered compartments which restricts the obliquity of incoming wave energy.

The dominant wave conditions on a seasonal scale affect the beach state and beach profile behaviour. The result is a dominant beach state which impacts the beach morphology and is often in phase with the seasonal wave climate (Wright & Short, 1984; Dubois, 1988). Increased storminess and wave heights in winter cause most sandy beaches to erode. The resulting eroded subaerial beach profile is typically referred to as a “bar profile”, “winter profile”, or “storm profile” (Winant et al., 1975; Eliot & Clarke, 1982; Clarke & Eliot, 1988; Dubois, 1988; Komar, 1998). Sediment is normally eroded from the subaerial beach and deposited in the nearshore where it forms a bar (Dubois, 1988; Quartel et al., 2008). Winter storm conditions typically last for a maximum of a few months and erosion of subaerial beach profiles often occurs at a uniform rate (e.g. Medina et al., 1994; Komar, 1998; Wood et al., 2009). When wave conditions subside, the beach begins to recover and a period of accretion dominates. The initial method of recovery has been suggested to be via the welding of the nearshore bar to the subaerial beach and was most often slower than the rate of erosion (e.g. Wright & Short, 1984; Dubois, 1988; Stive et al., 2002; Aagaard et al., 2004; Wood et al., 2009). This recovery continued until late summer and into autumn during periods of reduced wave energy until wave heights increased the following winter. The maximum subaerial beach volume coincided with late summer and autumn following prolonged periods of low wave heights. The resulting beach profile was typically termed a “berm profile”, “summer profile” or “swell/normal profile” (Winant et al., 1975; Eliot & Clarke, 1982; Dubois, 1988; Komar, 1998) and was initially identified by Shepard (1950) and Inman (1953). The total seasonal variation differs between every beach and alongshore region, for example, Clarke and Eliot (1988) showed that the average sediment transfer on a seasonal scale was 30 % at Warilla (New South Wales, Australia), with a maximum of 49 %.

Reflective beaches respond differently from intermediate beaches to a change in the wave conditions due to the slope of the beach face, the presence of nearshore bar(s), and the location of sediment storage. Reflective beaches typically have small subaqueous sediment storage, no nearshore bar system, and a steep beach face which means a large proportion of the wave energy is dissipated on the subaerial beach face (Wright & Short, 1984). Reflective beaches are typically more easily eroded as a result. Results presented by Yates et al. (2009) suggested that the first winter storms have the greatest erosion potential because of the large availability of sediment on the subaerial beach, therefore lower wave energy can erode the profile (refer Figure 3.1). Following peak seasonal volumes and the first winter storms, subsequent erosion events are the limiting factors of erosion change, and storm events can result in accretionary conditions (Yates et al., 2009). Once wave conditions subside, onshore sediment transport dominates and the bar begins to shift landward. After the bar has welded to the foreshore, swash zone sediment transport continuously deposits sediment in the swale until it is filled in. More sediment is added to the foreshore until a berm with a slight landward slope develops and the process begins again (Dubois, 1988).

The recovery rate of eroded profiles under low wave conditions can require weeks, months, or longer compared to the initial erosion which can occur in a matter of days (Wright & Short, 1984; Yates et al., 2009). The full sweep of variation from a dissipative state to a reflective state can occur, but does not on east Australian Beaches. Bar formation acts as a barrier to the incoming wave energy, where individual waves breaking on these bars may lose 78–99 % of their energy (Carter & Balsillie, 1983).

4.2.2 Beach Rotation – A Review

Beach rotation is a medium-term oscillation which is typical of short embayed beaches and has both high and low frequency cycles (Ranasinghe et al., 2004; Short & Trembanis, 2004; Ojeda & Guillen, 2008). Embayed beaches often exhibit beach rotation as they terminate at headlands at both ends, which is also suggested to be a precursor for headland bypassing because it enables the beach to

advance seaward, thus widening the surf zone (Ojeda & Guillen, 2008). Beach rotation is evident when there is a variation in the subaerial behaviour of a beach in the alongshore direction and results in opposite ends of the beach being out of phase, with a fulcrum point near the middle (Short et al., 1995; Short et al., 1999). This inverse relationship is most often identified when comparing beach width or beach volume data at opposite ends of an embayed beach (e.g. Klein et al., 2002; Ranasinghe et al., 2004; Short & Trembanis, 2004). It results from a shift in the alongshore sediment transport direction between the headland extremities on embayed beaches (Short & Masselink, 1999). The shift has been often attributed to periodic or long term changes in the wave climate, particularly the wave direction (Short & Masselink, 1999; Klein et al., 2002). However, rotation can occur on a range of timescales without any net gain or loss of sediment (Klein et al., 2002) and is a key process in understanding the morphodynamics of embayed beaches (Ojeda & Guillen, 2008). Beach rotation literature on New Zealand beaches is limited, with the only peer-reviewed work being that of Bryan et al. (2009) at Tairua Beach. Bryan et al. (2009) showed that beach rotation was evident at Tairua Beach and was clearly related to the dominance of northward and southward directed energy fluxes of greater than 3500 J.m^{-2} . The shoreline and barline at Tairua generally rotated in unison although the magnitude of variation in the shoreline was lower, hypothesised to be due to the reduction in surf zone energy levels at the shoreline compared with the bar.

It is documented that seasonal variations in the wave climate affect the degree of beach rotation and often results in seasonal rotation trends (Short & Masselink, 1999; Klein et al., 2002; Bryan et al., 2009). However, longer term oscillations of beach rotation have been shown to be correlated with the El Niño Southern Oscillation (ENSO) (Short et al., 1995; 2000; Ranasinghe et al., 2004; Harley, 2009a). It was first hypothesised by Short et al. (1995) using qualitative analysis of residual beach volumes and the Southern Oscillation Index (SOI) which is the ENSO index. This led to Ranasinghe et al. (2004) testing the hypothesis using quantifiable analysis of beach width data. They used mean monthly beach width data, as it was unrealistic to expect immediate beach response from changes in the SOI. Their results showed that there was a significant lagged response between

mean beach width and the SOI, with varying lag times between 3 months and 1.5 years depending on the location of the profile site on the beach. Further, Ranasinghe et al. (2004) produced a conceptual model of various stages of beach rotation and the processes governing beach rotation during ENSO phases. The conceptual model does not apply to the Coromandel beaches due to the different wave climates between the two regions. In summary, beach rotation is expected to be a key factor in this study due to the number of embayed beaches and the strong seasonal trend in storm wave events as evidenced by the above literature.

4.3 METHODS

4.3.1 Seasonal Variation in Beach Volumes

Seasonal trends and oscillations were largely undetected in the raw beach volume data therefore another method of analysis was required to determine the extent of seasonal variation on Coromandel beaches. Beach volume data were averaged at 1.5 month intervals through the calendar year beginning from January 1st as identified below (all dates are inclusive) as 1.5 months was the approximate sampling frequency for a majority of the dataset:

- January 1st to February 15th;
- February 16th to March 31st;
- April 1st to May 15th;
- May 16th to June 30th;
- July 1st to August 15th;
- August 16th to September 30th;
- October 1st to November 15th; and
- November 16th to December 31st.

The beach volume data were then grouped according to the date of survey. This enabled analyses of beach volumes at certain times of the year whilst encompassing the many years of data available. The entire dataset was used in the analysis as the sampling year was irrelevant when averaging data in the specified timeframes. Time-averaging of beach volume data is a common method of analysing medium term oscillations (e.g. Ranasinghe et al., 2004; Quartel et al.,

2008) and was considered suitable given the spatial and temporal variation of the dataset. The percentage change in beach volume from the mean was analysed to represent quantitative results on the extent of erosion or accretion throughout the year.

The grouping of beaches according to Wright and Short (1984) was maintained for the seasonal analysis. Seasonal variations in beach volumes depicted in this chapter were analysed as beach averages. Spectral analysis was also used on the volume data to identify significant seasonal oscillations in which the methodology is discussed in Section 5.3.2.

4.3.2 Beach Rotation and Oscillation

Beach rotation analysis required a minimum of three profiles on a beach in order to be considered in this study. This meant beaches had a profile located towards each end of the beach and a profile located at or near the central or fulcrum point (Figure 4.1 and Appendix II). Two beaches in this study only have one profile site (Rings and Maramaratotara, Figure 2.1; Figure II.3; Figure II.9) and a further four beaches have two profiles (Otama, Hahei, Onemana and Whangamata North). The following beaches satisfied these criteria and the number of profiles used in calculating the beach rotation is in brackets:

- Whangapoua (3);
- Wharekaho (3);
- Pauanui (4);
- Matarangi (4);
- Buffalo (5);
- Whangamata South (4);
- Kuaotunu West (3);
- Cooks (5);
- Whiritoa (4).
- Kuaotunu East (3);
- Hot Water (3);
- Opito (5);
- Tairua (3);

To quantify beach rotation, all profiles on a beach were required to have been surveyed on the same day. Tairua (CCS36-2), Pauanui (CCS38), and Whangamata South (CCS57-2) each contain one additional profile however the datasets only extend back to 2003, 2004, and 2002 respectively, therefore were

not included in the analysis. The profile excluded at Tairua is located on the southern half of the beach (second from the south), however the profile second from the north is located nearest the centre of the beach therefore the exclusion of the profile does not induce any bias by having two profiles located at one end of the beach. The profile excluded at Pauanui was located at the very northern end of the beach in the entrance to Tairua Harbour. The remaining four profiles encompass a good spatial variation along the beach (Figure II.14) and the exclusion of the profile does not induce any bias in the methodology. The profile excluded at Whangamata South is located relatively centrally, however the neighbouring profile was also close to the centre of the beach.

The seaward extent of each profile from its origin was related to the alongshore location. The degree of beach rotation was quantified by evaluating the intertidal beach volume with respect the alongshore location of each profile. For each time step the intertidal volume was plotted against the alongshore location of the profile. A best fit line using linear regression was fitted to each time step. The resulting linear equation had a slope component which was converted to degrees and used as the rotation coefficient. This method was considered accurate as an unstable or poor relationship between the profiles will give a low rotation coefficient, thus not indicating beach rotation. A strong rotation coefficient will only exist if there is a relatively large degree of variation between the intertidal beach volumes at each end of the beach and the profile(s) in between also contribute to a good fit. A positive beach rotation coefficient indicates a greater intertidal beach volume at the southern end of the beach (right hand side looking seaward), and anticlockwise rotation (Figure 4.1). The converse applies for a negative coefficient. A timeseries of the beach rotation coefficient was generated for each beach and compared to the spatial location of each site.

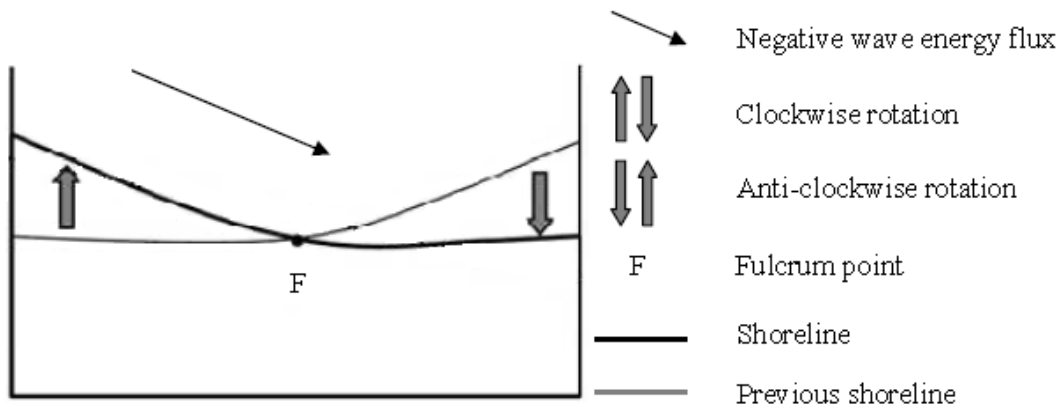


Figure 4.1: Schematic identifying various beach rotation parameters and the wave energy flux direction (adapted from Ojeda & Guillen, 2008).

4.3.3 Seasonal Variation of Wave Conditions

The wave data were evenly spaced at 3 hourly intervals at four sites from 1979 to March 2009 (Figure 2.1 and Table 2-2). To analyse seasonal variation in the wave climate, the data were grouped into 1.5 month intervals and averaged from 1995 to 2009 similar to the time of higher resolution survey data. The 1.5 month intervals used to group the beach volumes were maintained (refer Section 4.3.1). The data were compared between the four sites across the 1.5 month intervals to determine the extent of any seasonal variation present.

4.3.3.1 Beach Rotation versus Alongshore Wave Energy Flux

Wave data were time-averaged in order to analyse the potential forcing mechanisms of beach rotation on the Coromandel Peninsula. The wave energy flux was calculated and averaged between the time steps of the rotation data as it was a vector quantity with both cross-shore and alongshore components (Miller & Dean, 2007b). The wave energy flux was given by (Bryan et al., 2009):

$$E = \frac{1}{8} \cdot \rho \cdot g \cdot H_s^2 \cdot \sin \theta \quad \text{Equation 4.1}$$

Where ρ is the density of seawater (1025 kg.m^{-3}), g is the acceleration due to gravity (9.81 m.s^{-2}), H_s is the significant wave height in metres (m), and θ is the

angle of wave approach relative to beach orientation in radians where 0° was shore normal. The time-averaged wave energy flux data were compared to the beach rotation data to determine if a relationship existed between them. Least squares regression analysis was then undertaken. This method incorporated the incoming H_s and direction and compared it to the changing orientation of the subaerial beach face.

4.4 RESULTS

4.4.1 Beach Volume Variation on a Seasonal Scale

4.4.1.1 Seasonal Variation – Intermediate Beaches

Figure 4.2 illustrates the percentage change in beach volume through the calendar year for the intermediate sloped beaches. The beach classifications were maintained from Section 3.3.2. Volume data in this section were rounded to the nearest integer and were relative to the mean beach volume. Firstly, the figure illustrated that most intermediate beaches had a clear, albeit small, seasonal cycle with increased volumes in summer and decreased volumes in winter. The peak seasonal volume for intermediate beaches predominantly occurred in April and May. This period of above average beach volume was followed by uniform erosion of all beaches in July and the first half of August. There was a general trend of accretion from August to the end of the year. The overall extent of seasonal accretion reached a peak volume of approximately 5 % and a seasonal minimum of approximately -5 % to -7 % for most beaches. This equates to seasonal variation of approximately 10 % for most intermediate beaches. The behaviour at Otama beach was different as it had an average peak seasonal volume of 17 %, a seasonal minimum of -14 %, and an overall seasonal variation of 31 %. Buffalo Beach and Cooks Beach did not exhibit a seasonal trend.

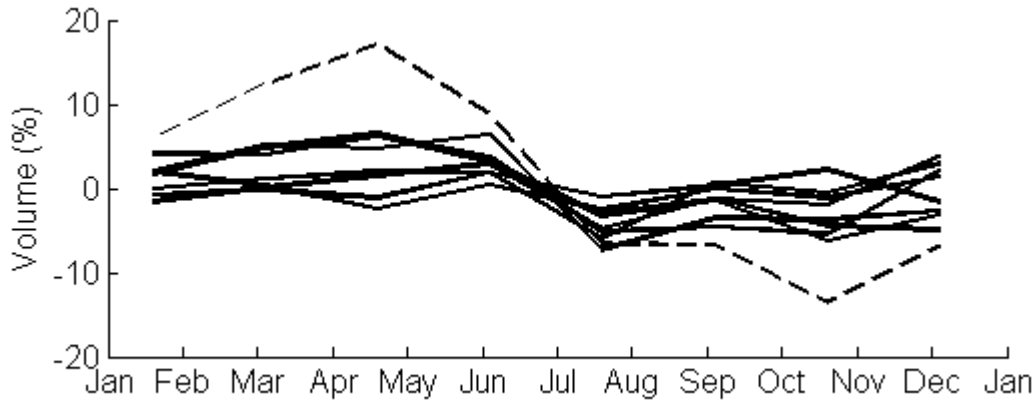


Figure 4.2: Average beach volume change through the year for intermediate beaches. All data have been demeaned. Beach volumes were averaged into 1.5 month groups through the calendar year beginning on January 1st. A strong seasonal cycle is evident at all beach sites except Buffalo Beach and Cooks Beach. Otama Beach is identified as the dashed line with greatest amplitude.

4.4.1.2 Seasonal Variation – Reflective Beaches

Figure 4.3 illustrates the seasonal variation in beach volume for the reflective beaches. Figure 4.3 showed that the peak seasonal volume of approximately 6 % to 8 % for 3 out of the 4 beaches (Tairua, Onemana, and Whiritoa) was reached in February to March. Hot Water Beach had a peak seasonal volume of 3 % from November to February. The seasonal minimum for all beaches occurred in July to August. Hot Water Beach had a seasonal minimum of -4 % whereas the other beaches had seasonal minimums of -7 % to -9 %. All four beaches eroded in a uniform manner in July and August. All four reflective beaches showed slight erosion from December to February. The overall seasonal variation was approximately 15 % for the reflective beaches except Hot Water Beach which had a lower seasonal variation of 7 %.

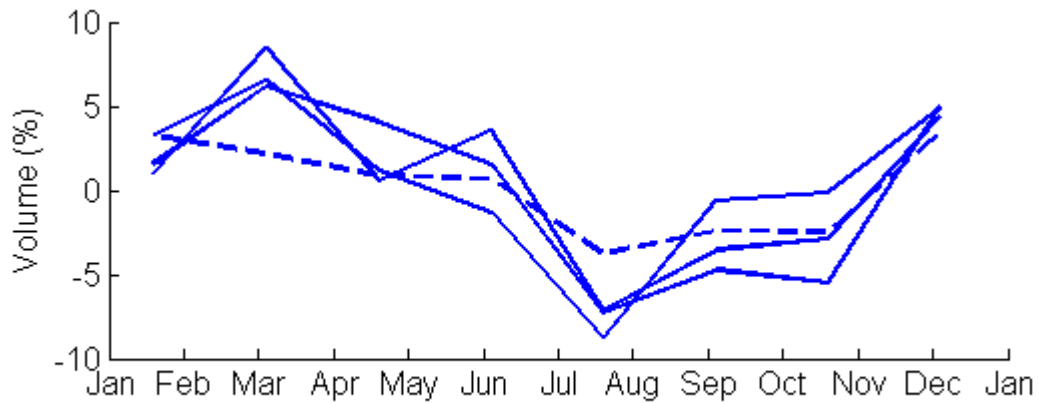


Figure 4.3: Average beach volume change through the year for reflective beaches. The data have been demeaned. Beach volumes were averaged into 1.5 month groups through calendar the year beginning on January 1st. Hot Water Beach is the dashed line with smallest amplitude.

4.4.1.3 Seasonal Variation – Harbour Adjacent and Outlier Beaches

Figure 4.4 showed all beaches adjacent to harbour mouths (red lines) and the two outlier beaches (dashed green lines). The figure highlighted the irregular behaviour of the harbour adjacent beaches which are all intermediate beaches. Matarangi was the only beach adjacent to a harbour which had a seasonal trend. Matarangi had a peak seasonal volume of 9 % in April to May and a seasonal minimum of -7 % in October to November, an overall seasonal variation of 16 %. The other 3 harbour adjacent beaches (Pauanui, Whangamata North, and Whangamata South) did not show a seasonal trend and had irregular volume change through the year. However, all harbour adjacent beaches showed uniform erosion in July and August. Excluding Matarangi, all harbour adjacent beaches each had average beach volume changes of less than 10 %.

The two outliers, Rings and Maramaratotara, showed a weak seasonal trend. Rings Beach had a peak seasonal volume of 2% in January to February and a seasonal minimum of -1 % in July to August, an overall seasonal variation of 4 % (accounting for integer values). Maramaratotara Beach had a peak seasonal volume of 2 % in May to June and a seasonal minimum of -1% in October to November, an overall variation of 3 %.

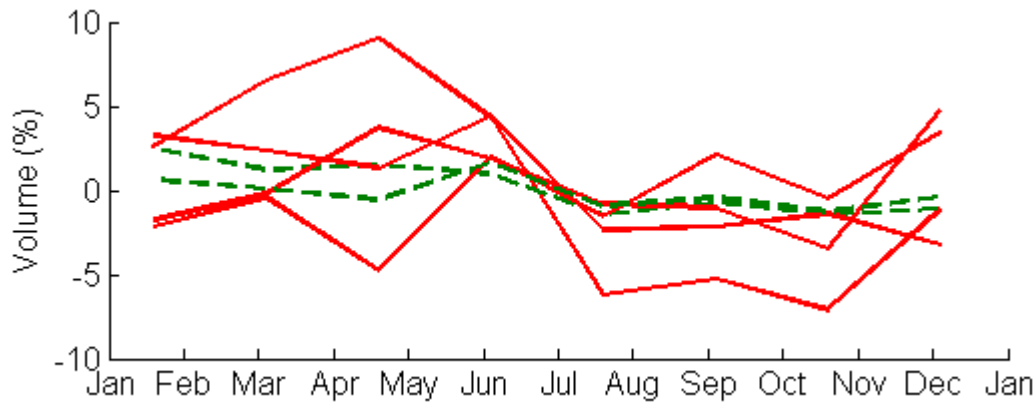


Figure 4.4: Average beach volume change through the year for harbour adjacent beaches (solid red lines) and outlier beaches (dashed green lines). The data have been demeaned. Beach volumes were averaged into 1.5 month groups through the calendar year beginning on January 1st. Matarangi has a seasonal trend illustrated by the solid red line with the highest and lowest volumes.

4.4.1.4 Seasonal Variation – Lomb-Scargle Spectral Analysis

Spectral analysis using the Lomb-Scargle method identified significant seasonal oscillations at some profile sites (Table 4-1). A description of the method and an example power spectrum are provided in Sections 5.3.2 and Figure 5.5 respectively. The spectral analysis identified significant oscillations in the raw volume data using approximately 8 profiles per year. These signals were therefore deemed to be the profiles with a consistent and strong seasonal trend. The corresponding spectral power also related relatively well to the seasonal signals identified above.

Table 4-1: Lomb-Scargle spectral analysis results for seasonal oscillations. The beaches and profiles are listed from north to south with the frequency in years and corresponding power in volume (%).

Beach/Profile Name (north to south)	Significant Frequency (Years)	Corresponding Power (%)
Matarangi CCS15	1.01	9.91
Matarangi CCS14	0.99	12.6
Matarangi CCS13	0.99	8.37
Kuaotunu West CCS19-4	1.00	11.3
Kuaotunu West CCS19-5	1.00	11.0
Kuaotunu East CCS20	0.99	9.66
Kuaotunu East CCS20-2	1.00	11.3
Otama CCS45	1.01	8.63
Otama CCS46	1.00	15.4
Opito CCS47-1	1.02	7.61
Opito CCS48-1	1.02	8.56
Onemana CCS53	1.01	8.81

4.4.2 Beach Rotation

Figure 4.5 illustrates beach rotation timeseries for the 13 beaches which have at least three profiles. The rotation component was displayed in degrees with a positive slope indicating anticlockwise rotation and a negative slope indicating clockwise rotation (Figure 4.1). The figure showed that several beaches appear to be rotating and several beaches which were not. A relatively flat timeseries does not show rotation. Matarangi, Opito, Buffalo, and Cooks Beaches had relatively flat timeseries which indicates that beach oscillation was dominant and not beach rotation. Matarangi, Buffalo, Cooks, Pauanui and Whangamata North and South Beaches are all adjacent to harbour entrances, therefore reducing the ability for rotation to occur as sediment is unlikely to be trapped against the harbour entrance. The profiles on Opito beach were unevenly spaced therefore were not considered for further analysis (Figure II.7). The panel labels in Figures 4.5 and 4.6 are maintained throughout the thesis. Beaches are labelled from north to south, Whangapoua (a) to Whiritoa (s) as follows:

- Whangapoua (a); • Wharekaho (h); • Tairua (n);
- Matarangi (b); • Buffalo (i); • Pauanui (o);
- Kuaotunu West (d); • Cooks (k); • Whangamata South (r);
- Kuaotunu East (e); • Hot Water (m); • Whiritoa (s).
- Opito (g);

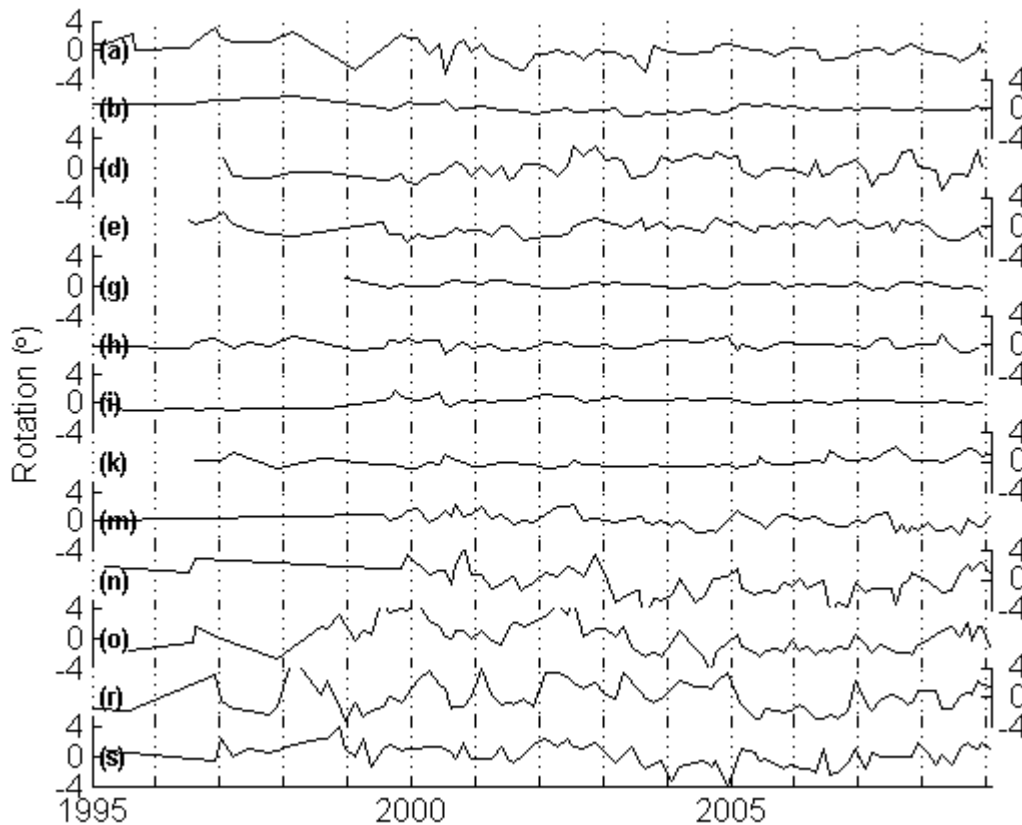


Figure 4.5: Beach rotation timeseries for all beaches with at least 3 profiles. Beaches are plotted from north to south, with panel labels (a) to (s) representing the 13 beaches from Whangapoua (a) to Whiritoa (s) identified in text. The rotation component is illustrated in degrees. A positive slope indicates anti-clockwise rotation. Note there are 2 y-axes for clarity. The solid section of the respective y-axis depicts the y-axis limits.

Table 4-2 showed the minimum, maximum, and range of beach rotation coefficients at each beach. The results showed that the shorter embayed beaches had higher rotation coefficients, those being Whangapoua, Kuaotunu West, Kuaotunu East, Hot Water, Tairua, and Whiritoa (Table 4-2 and Figure 4.5). Pauanui and Whangamata South also had high rotation coefficients but are harbour adjacent beaches therefore they were excluded from further analysis as they were not embayed beaches. It was hypothesised that a different parameter

caused the variation at Pauanui and Whangamata South. Figure 4.6 illustrates the beach rotation timeseries for short embayed beaches only. It was evident that the degree of rotation on these beaches was greater than those which were excluded (Figure 4.5).

Table 4-2: The minimum, maximum, and range of beach rotation coefficients for each beach analysed in this section.

Beach	Minimum	Maximum	Range
Whangapoua	-3.27	3.01	6.28
Matarangi	-1.13	1.78	2.91
Kuaotunu West	-3.17	2.75	5.93
Kuaotunu East	-2.13	1.80	3.92
Opito	-0.73	0.88	1.61
Wharekaho	-1.32	1.54	2.87
Buffalo	-1.14	1.52	2.66
Cooks	-0.83	2.01	2.84
Hot Water	-1.97	2.26	4.23
Tairua	-4.85	3.97	8.82
Pauanui	-4.44	5.67	10.11
Whangamata South	-3.41	5.31	8.73
Whiritoa	-4.17	3.95	8.12

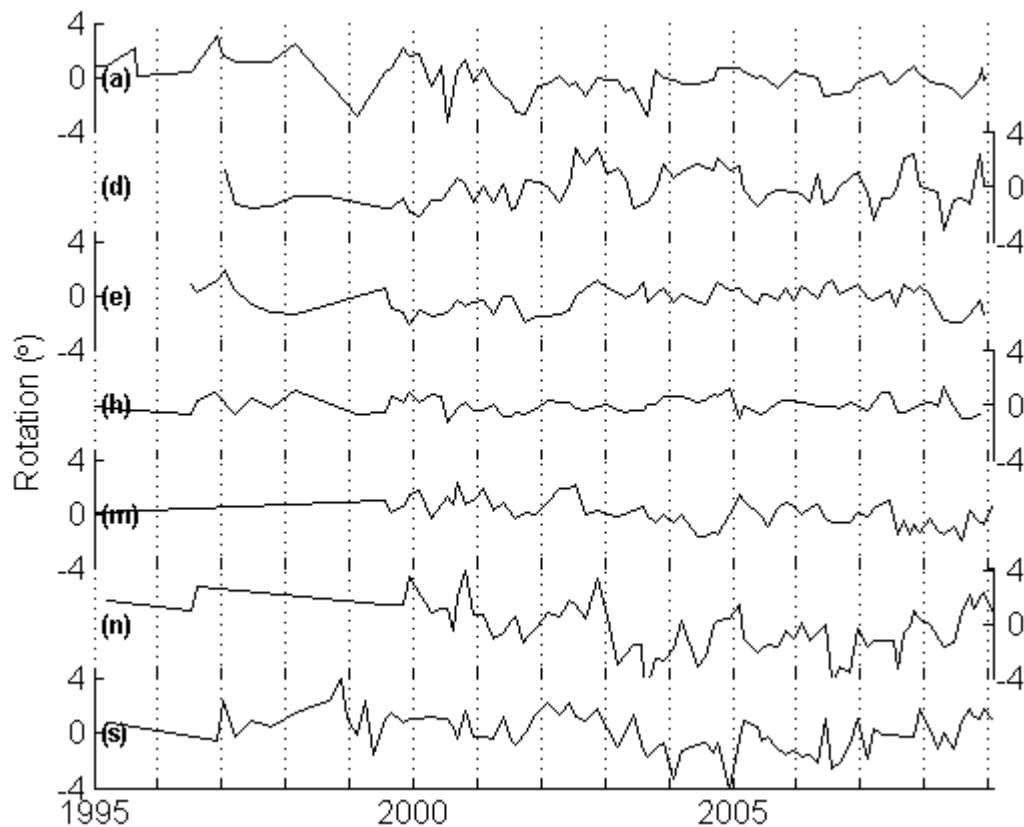


Figure 4.6: Beach rotation timeseries for all embayed beaches. The rotation component is illustrated in degrees and a positive index / slope shows anti-clockwise rotation. The panel labels from Figure 4.5 above are maintained for simplicity and are explained in text. Note there are 2 y-axes for clarity. The solid section of the respective y-axis depicts the y-axis limits.

Whangapoua (a) did not show a large degree of change or any obvious low frequency variation. For example, there was weak beach rotation from 2004 to the end of the timeseries. However, there were rotation events prior to 2004. Kuaotunu West (d) showed beach rotation for the entire timeseries with the prominence of several large rotation events of up to 4° in mid 2000, 2002, 2003, 2007, and 2008. It was apparent that a seasonal trend of anticlockwise rotation in winter and equal clockwise rotation in summer was dominant at Kuaotunu West. No long term trend of rotation was evident. Kuaotunu East (e) was relatively stable from 2003 to 2008, therefore had weak beach rotation, but did have rotation events similar and equal to those at Kuaotunu West in 1997, mid 2002, and 2008. Wharekaho Beach (h) had a relatively smooth timeseries and did not show a large degree of rotation, excluding several clockwise events in 2000, the beginning of 2005, and 2008. Hot Water Beach (m) showed rotation at both short- and long-term timescales and was subject to relatively frequent rotation events. For

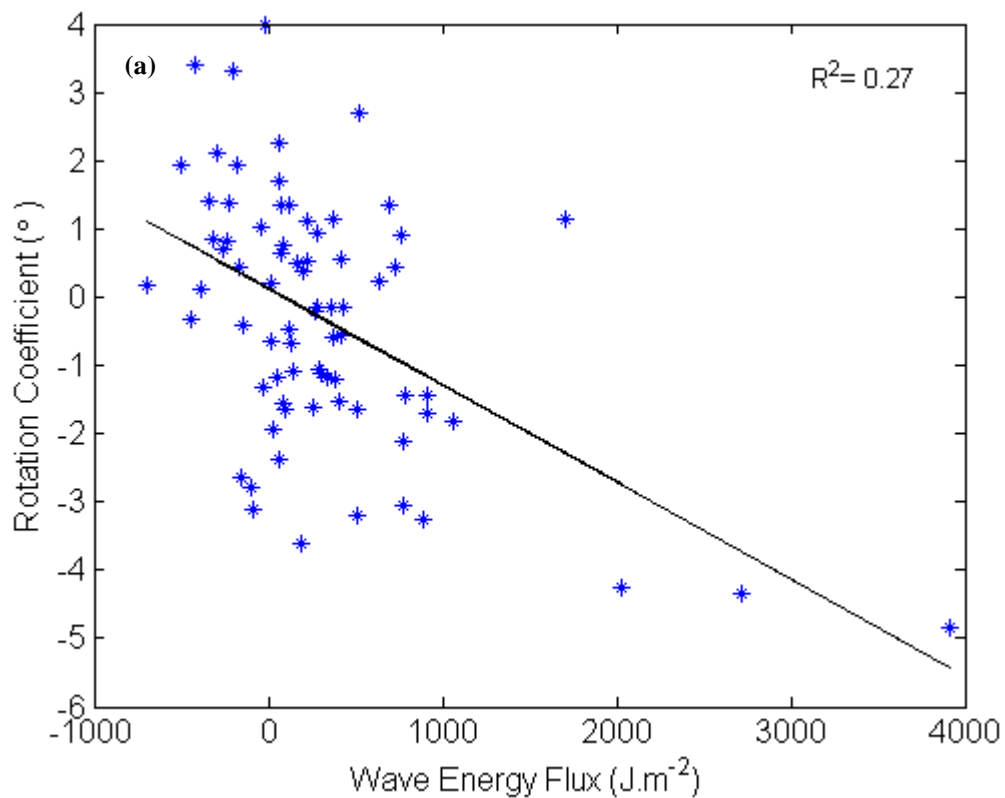
example, in 2002, 2004, and 2007, with low frequency rotation identified from 2000 to 2004 (clockwise), relative stability until mid 2007, and anticlockwise rotation until 2009. Tairua Beach (n) had similar low- and high-frequency rotation to Hot Water Beach, but to a larger degree. Tairua had frequent short term rotation events, as well as clockwise rotation from (at least) 2000 to 2004, and anticlockwise rotation from 2006 to 2009. From 2004 to 2006 no long term rotation was evident, however a small peak was evident in 2005. Whiritoa Beach (s) also showed the low frequency trend evident at Hot Water Beach and Tairua Beach, as well as high frequency beach rotation. The scale of beach rotation at Tairua and Whiritoa was greater than all other embayed beaches as evidenced by the degree of rotation change (Figure 4.6 and Table 4-2).

4.4.3 Beach Rotation versus Wave Energy Flux

Beach rotation was compared to the time-averaged wave energy flux. The wave energy flux was time-averaged between the profile survey dates and linear regression fitted to each set of data. The resulting R-squared values were shown in Figure 4.8. The overall relationship between the time-averaged wave energy flux and the beach rotation coefficient was poor across the entire Peninsula. Tairua had the highest relationship with an R-squared value of 0.27. The next highest relationships were Wharekaho and Whangapoua with R-squared values of 0.21 and 0.19 respectively which are still poor correlations. Only the Tairua result was significant at the 95 % confidence level.

Figure 4.7 illustrates the beach rotation coefficient versus wave energy flux at Tairua, Wharekaho and Whangapoua Beaches. The figure clearly showed that the largest wave energy events were associated with large rotation events. At Tairua, a wave energy flux event of 3915 J.m^{-2} was associated with a rotation coefficient of -4.8° . Figure 4.7 (a & b) showed that the largest wave energy events were associated with negative rotation coefficients (clockwise rotation, Figure 4.1). The slope of the best fit line also implied that if the wave energy flux was positive, the beach rotation coefficient was negative and vice versa.

The relationship between the wave energy flux and beach rotation at Whangapoua was similar to Tairua (Figure 4.7). However, the wave energy was significantly lower at Whangapoua as the largest event was only 1327 J.m^{-2} compared to 3915 J.m^{-2} at Tairua. Although the relationship was not as strong at Whangapoua ($R^2 = 0.19$), the slope of the best fit line confirms the similar behaviour between beach rotation and the wave energy flux on the two beaches. Wharekaho had an R^2 value of 0.21. However, the slope of the best fit line was opposite to that of Tairua and Whangapoua. The relationship suggests that negative wave energy fluxes were associated with clockwise rotation (refer to Section 4.5.4 below which discusses this matter further).



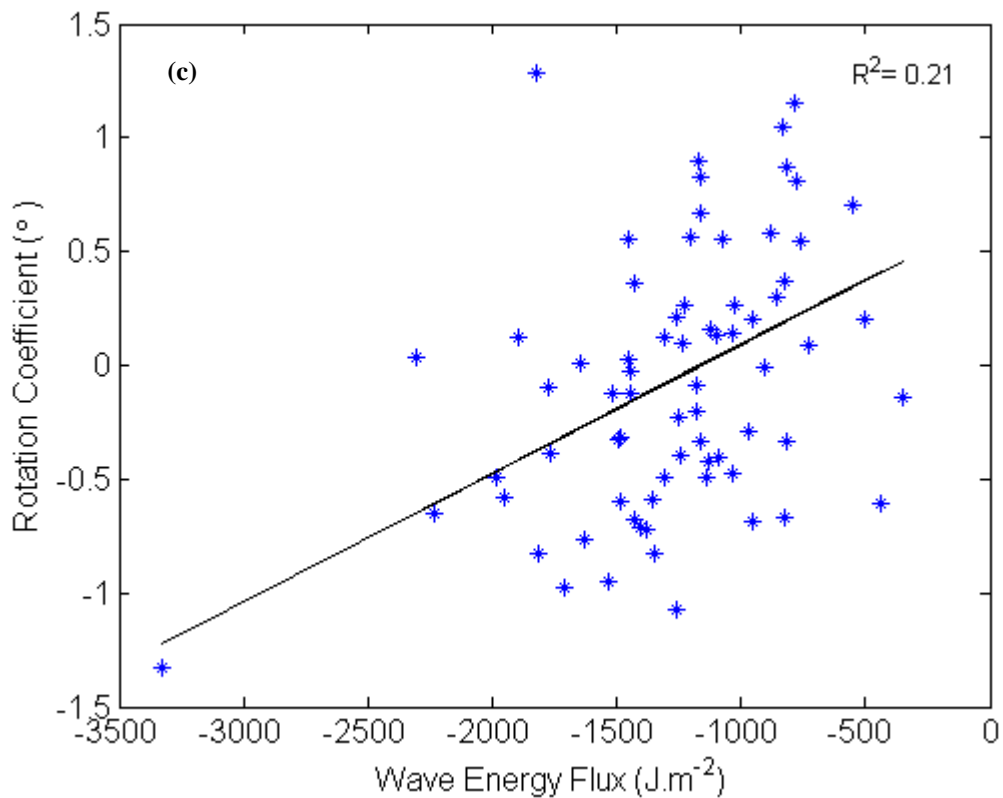
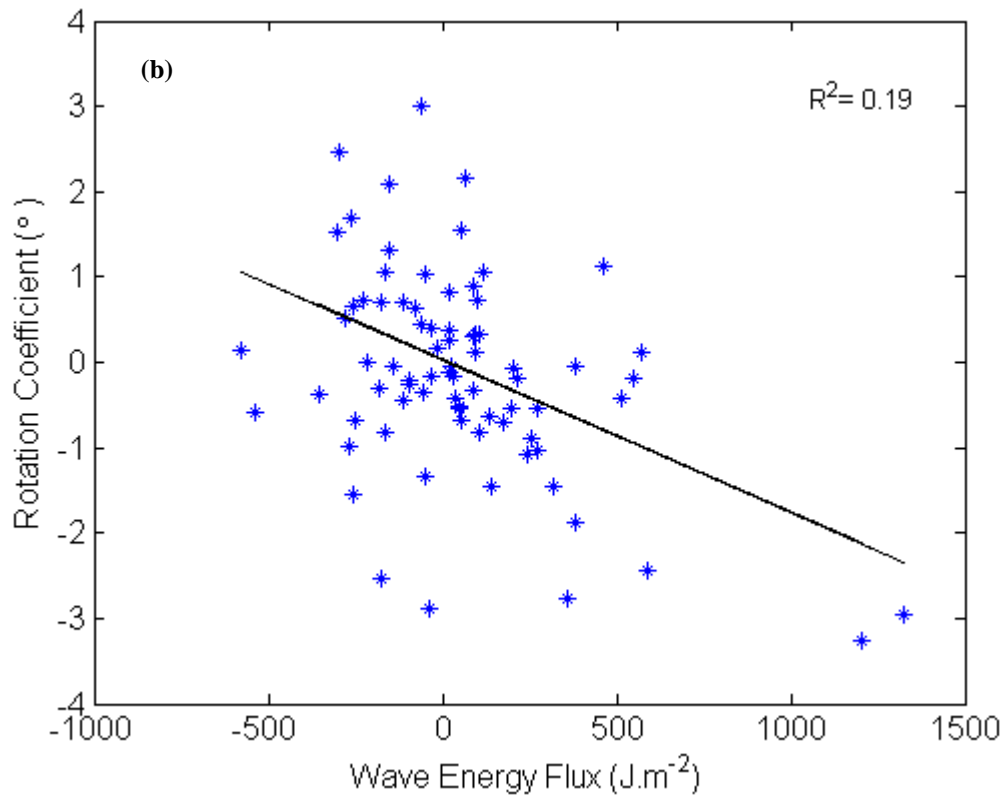


Figure 4.7: Time-averaged wave energy flux versus beach rotation at Tairua Beach (a), Whangapoua Beach (b), and Wharekaho Beach (c). The black line in each figure is the best fit line with the R-squared value identified in the top right.

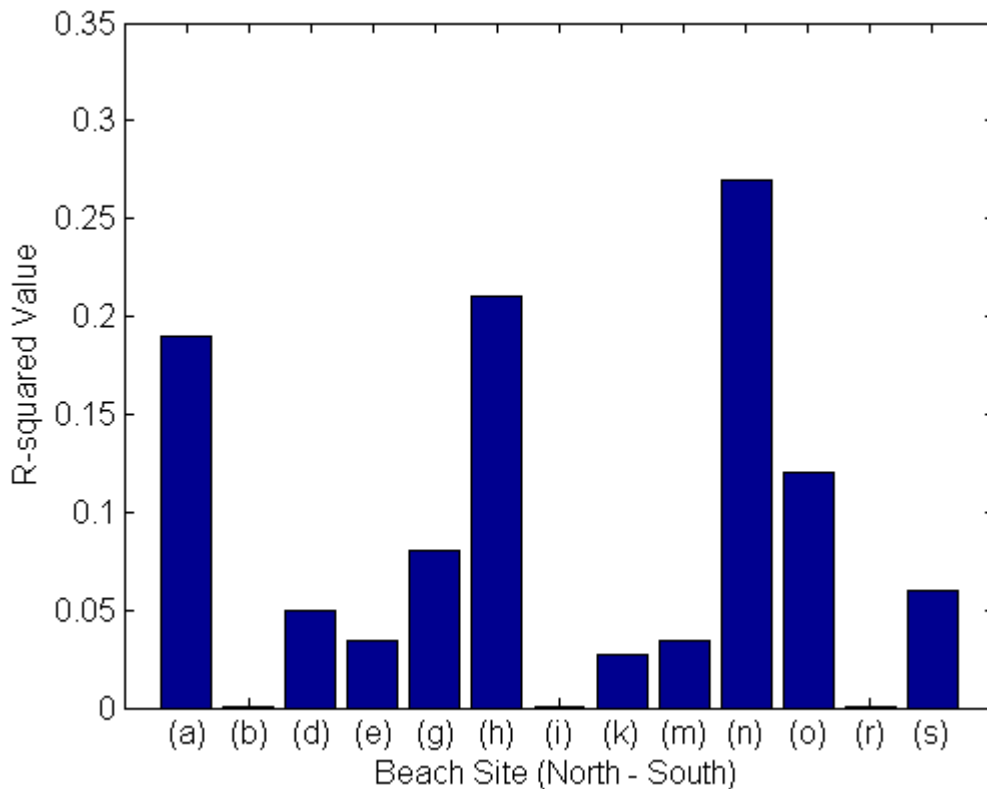


Figure 4.8: The best fit R-squared value for each beach rotation coefficient versus time-averaged wave energy flux. The x-axis labels are defined in Section 4.4.2.

4.4.4 Seasonal Variation in Wave Height

The methodology used to analyse the seasonal variation of beach volumes through the calendar year was also applied to the wave data. Table 4-3 and Figure 4.9 illustrate the mean seasonal H_s for the four sites. The average peak seasonal wave height was reached in February to March for all sites and ranged from 1.16 m at Matarangi to 1.42 m at Tairua. The average minimum seasonal wave height was reached during October to November for all sites and ranged from 0.84 m at Opito Bay to 1.05 m at Tairua. Overall the seasonal variation was relatively low with the major variation being a spike in the data occurring in July to August with a notable increase in the wave height.

Figures 4.10 illustrates the timing and frequency (n) of storm events ($H_s > 3$ m) through the year at the four sites. The definition of a storm wave event was described in Section 3.3.4. The figure showed there was a significantly higher frequency of storm wave events at all four sites in winter. The lowest frequency of

storm wave events occurred in late October and early November at all four sites. All four sites also showed a spike in the number of storm events during late February and early March. Matarangi (Figure 4.10 a) had the lowest frequency of storm events during the entire period whilst Tairua (Figure 4.10 c) had the highest.

Table 4-3: Seasonal wave height characteristics for the four sites analysed.

Site	Maximum (m)	Minimum (m)	Range (m)	Mean (m)
Matarangi	1.16	0.88	0.28	1.03
Opito Bay	1.17	0.84	0.33	1.04
Tairua	1.42	1.05	0.37	1.27
Whangamata	1.31	0.99	0.32	1.16

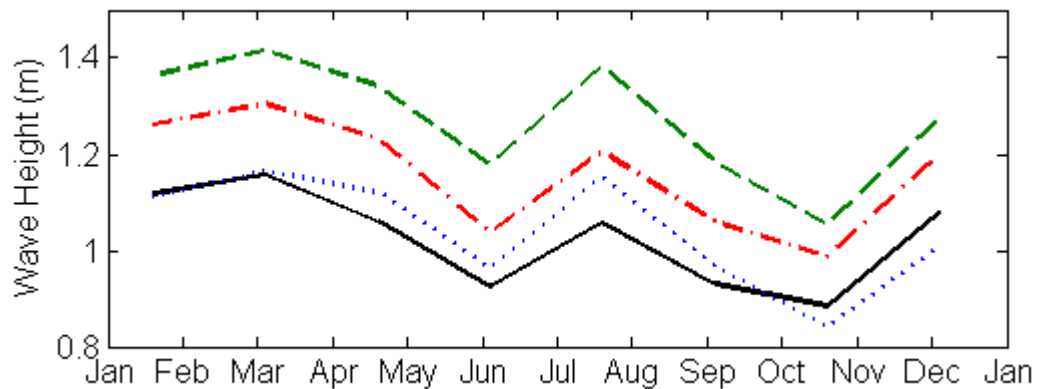


Figure 4.9: Seasonal variation of wave height for Matarangi (solid black line), Opito Bay (dotted blue line), Tairua (dashed green line), and Whangamata (dash-dot red line). The data was time-averaged into 1.5 month intervals through the calendar year using 30 years of available hindcast data.

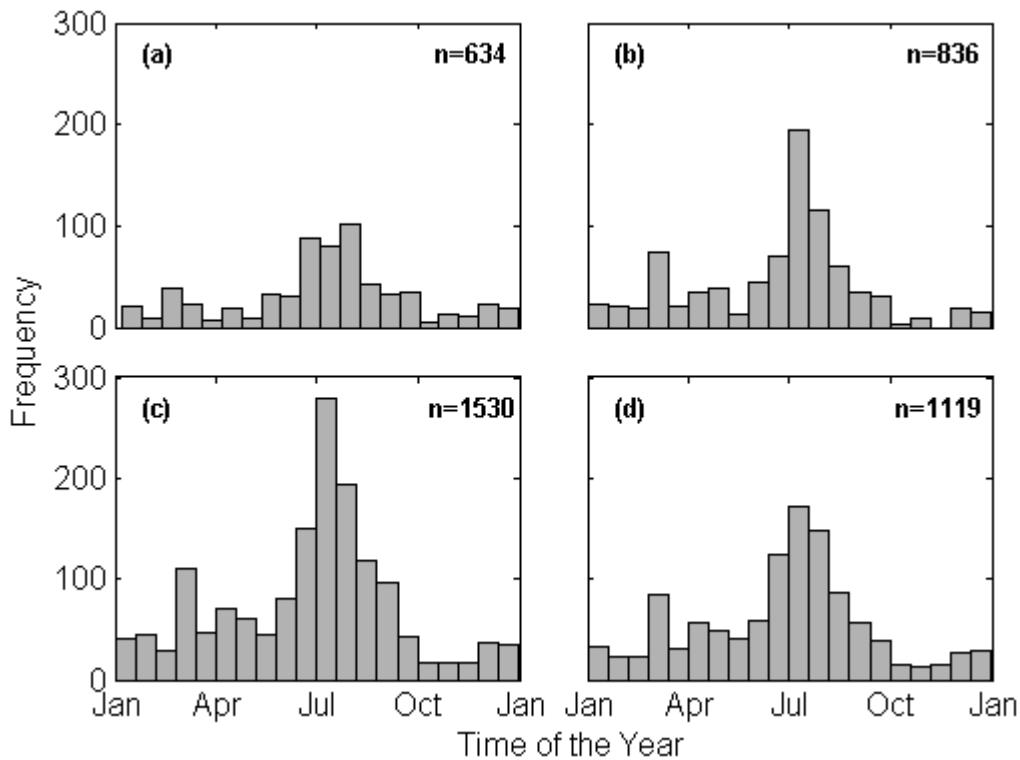


Figure 4.10: The timing and frequency (n) of storm wave events ($H_s > 3$ m) during the year at the Matarangi (a), Opito Bay (b), Tairua (c), and Whangamata (d) wave data sites. All axes are equal.

4.5 DISCUSSION

4.5.1 Seasonal Variation – Intermediate Beaches

Figure 4.2 showed that intermediate beaches on the Coromandel Peninsula had a moderate degree of seasonal variation of beach volumes with accretion in summer, autumn, spring, and erosion in winter. On average, the seasonal variation across most intermediate beaches was approximately 10 % of the total beach volume, which was much less than the 30 % identified by Clarke and Eliot (1988). The intermediate beaches also had uniform erosion in winter. This erosion corresponded to an increase in the average wave height and storm wave events in winter at all sites around the Coromandel Peninsula (Figures 4.9 & 4.10) which is common of many sandy beach systems worldwide (Clarke & Eliot, 1988; Komar, 1998; Stive et al., 2002). The eastern Coromandel Peninsula is a storm dominated wave environment (Bradshaw, 1991) where increased storminess in winter leads to erosion of subaerial beach profiles. However, it is interesting to note that Figure 4.9 showed a spike in the average wave height in February and March. Episodic cyclone activity in summer was considered to cause the increase. The episodic

events were unlikely to occur every year, however corresponded to erosion of reflective beaches, but not intermediate beaches. Buffalo Beach was the only intermediate beach which showed erosion during this period. Therefore a higher average wave height does not necessarily result in erosion of the subaerial beach profile (e.g. Yates et al., 2009). Cyclonic impacts in summer were more prominent at lower latitudes, for example, the east coast of Australia as studied by Davidson and Turner (2009) and less evident on the Coromandel Peninsula. Winter storms caused the greatest erosion which was associated with increased storminess. Results presented here conform to the findings of Yates et al. (2009) as the winter wave conditions lasted more than 6 weeks (Figure 3.1), however erosion of most beaches only occurred over a 6 week period (July – mid August). Initial winter storms caused the greatest erosion because they had the largest equilibrium wave energy compared to the end of winter when a higher wave energy equilibrium was required to erode beaches. The beach system studied by Clarke and Eliot (1988) was considered to be significantly different due to the morphological differences with Coromandel beaches. In particular, the seasonal variation of the beach (30 %) and the recovery rates following uniform erosion. Following the seasonal minimum in May to July, their study beach recovered quickly to record peak seasonal volumes in December. The wave climate of southeast Australia is much larger than the Coromandel Peninsula (Clarke & Eliot, 1988).

Otama Beach had a much larger seasonal variation of 31 %, similar to Clarke and Eliot (1988) for an east Australian intermediate embayed beach. The forcing mechanism(s) behind this very high degree of variation at Otama Beach were not evident. Otama Beach is located in relatively close proximity to Kuaotunu East (<2 km), has a similar orientation, and is sheltered from the northeast to southeast. Therefore, the behaviour should not be significantly different to other beaches as it is subjected to similar wave conditions. The large seasonal variation occurred on both profiles at Otama (Table 4-2) and was not a localised phenomenon at one particular section of the beach. A large spatial scale study of embayed beaches by Bowman et al. (2009) showed that sheltered embayed beaches tended to exhibit lower seasonal variations. Otama Beach is considered one of the most sheltered

pocket beaches in this study, therefore does not conform to the findings of Bowman et al. (2009). The seasonal behaviour at Otama could not be explained in this thesis.

There were two exceptions to the typical seasonal behaviour of intermediate beaches at Buffalo Beach and Cooks Beach. These beaches were identified as intermediate beaches in Chapter 3. However, the two beaches showed a different behaviour to the remaining intermediate beaches at the seasonal scale. They did not exhibit a seasonal cycle of accretion and erosion typical of summer and winter conditions, but showed irregularity throughout the year. No profiles on Buffalo Beach showed a seasonal signal (Figure 4.11). Conversely, it was interesting that the two western profiles on Cooks Beach showed a strong seasonal cycle (Figure 4.11), however the 3 eastern profiles and therefore the beach average did not. It was apparent that there is a certain point on the beach where variation in the beach behaviour differs in the alongshore direction. This could be due to a variation in the littoral drift system on the beach which may be inconsistent due to the orientation change of the beach. Another hypothesis is that sediment ejected from the harbour is only transported as far west as the first three profiles, thus affecting the subaerial beach volumes on these three profiles (similar to other harbour adjacent beaches), where it must then be transported offshore as they do not show a continuing trend of accretion. The aerial photo for Cooks Beach (Figure II.10) shows that the ebb tidal delta is located adjacent to the three eastern profiles. Although the delta is not permanent in size or location, it is likely that variations of the ebb tidal delta and the resulting sand bank may weld onto the subaerial beach at certain stages during the year causing variations in the subaerial beach volumes at these three profile sites (e.g. Aagaard et al., 2004). Both beaches were thus deemed complex systems due to the presence of harbour entrances, the complex wave interactions in Mercury Bay (due to the shape of the bay and the presence of a large bar in the middle of the bay; Steeghs, 2007), and the orientation changes (Buffalo Beach = 99°, Cooks Beach = 55°). Buffalo beach and Cooks Beach are deemed harbour adjacent beaches at the seasonal scale.

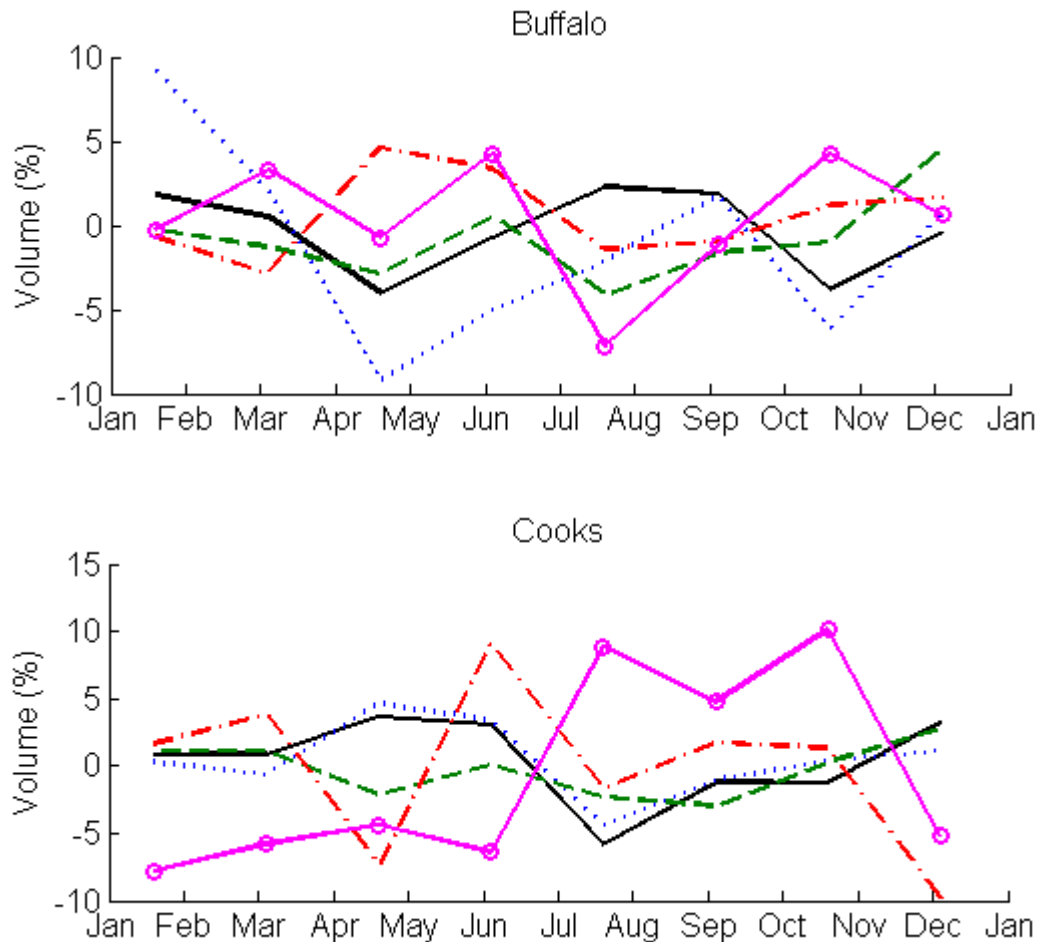


Figure 4.11: Buffalo Beach and Cooks Beach seasonal change data for each profile on each beach. The figure illustrates the variation at these two intermediate beaches, with only the two northern most profiles on Cooks Beach (solid black line and dotted blue line) showing a seasonal trend. The remaining profiles from north to south are the dashed green line, dash-dot red line, and solid pink line with circle markers.

4.5.2 Seasonal Variation – Reflective Beaches

Reflective beaches on the Coromandel Peninsula showed the strongest seasonal cycle of subaerial beach volumes (excluding Otama Beach). Three out of the four reflective beaches also had a greater seasonal variation than the intermediate beaches. Steeper beach profiles have a greater percentage of subaerial beach sediment storage (Wright & Short, 1984) which provides a greater amount of subaerial sediment which can accrete or erode throughout the year.

Of particular interest was that the peak seasonal volume for reflective beaches typically occurred earlier in the year compared to intermediate beaches. Three of

the reflective beaches had peak seasonal volumes in February to March, six weeks earlier than the majority of the intermediate beaches. This occurred during a period of above average wave heights (Figure 4.9). The following three months from April to June on average, had decreased wave heights. It would therefore be expected that the reflective profiles would continue to accrete until the increase in wave height observed in the July to August period. It was hypothesised that summer fair weather conditions would enable accretion of the subaerial beach system. However, on reflective beaches, the maximum seasonal volume is reached earlier, therefore sediment is more easily eroded (Wright & Short, 1984). The average increase in mean H_s in late summer appears to erode the subaerial beach and form a nearshore bar (Dubois, 1988). When the wave energy increased during winter, the subaerial beach was eroded and sediment deposited offshore (e.g. Dail et al., 2000). During the recovery months sediment initially replenishes the subaerial beach, followed by the nearshore bar region. This hypothesis would need to be tested for known bar locations, with direct comparisons made to the corresponding volume of the bar, subaerial beach, and wave conditions, preferably across more than one reflective beach in this study. Overall, the onset of the first winter storm events caused the greatest erosion as evidenced by the uniform erosion across the Coromandel Peninsula in July and August which corresponded to an increase in storm wave events. These results compared well to Yates et al. (2009) who showed that the more seaward (accreted) the profile, the lower the wave energy required for erosion (Figure 3.1). Therefore the first winter storms cause a large degree of uniform erosion across the Peninsula, and further winter storms, on average, do not have a high enough wave energy to continue eroding Coromandel beaches.

Following the seasonal minimum in July and August, reflective beaches had a faster recovery rate than intermediate beaches. This was identified by the reflective beaches reaching the mean beach volume earlier than intermediate beaches. This rapid recovery also had a negative impact on the reflective beaches, as they appeared to reach an equilibrium seasonal volume, because all reflective beaches showed erosion from December to February. As a result, reflective beaches appeared to have a greater ability to accrete and recover following an

erosion period, but also a greater ability to be eroded when sediment volumes were above average (Dail et al., 2000).

The causative factor for the relatively conservative behaviour at Hot Water Beach is unknown. The geomorphology of Hot Water Beach is very similar to Tairua and Whiritoa with regard to the respective beach lengths, orientation, intertidal beach slope, and mean grain size (Table 2-1). It was therefore anticipated that the beach systems would behave in relative unison similar to the rotation analysis. The difference in seasonal behaviour at Hot Water Beach was not explained in this thesis.

4.5.3 Seasonal Variation – Harbour Adjacent and Outlier Beaches

Harbour adjacent beaches showed irregular and inconsistent behaviour throughout the year. Matarangi was the exception and had a strong seasonal cycle. The only common feature between all the harbour adjacent beaches was uniform erosion in winter. The behaviour was attributed to the harbour adjacent nature of the beaches. Complex interactions of sediment ejected from estuaries, ebb tidal deltas, and groundwater impacts caused by hydraulic gradients in the water table, are some of the impacts which affect harbour adjacent beaches and were not analysed.

A study of seasonal shoreline change by Yates et al. (2009) identified a beach which had similar characteristics to Rings Beach and Maramaratotara Beach (steep, short and narrow) which showed a weak, barely detectable seasonal cycle. They hypothesised that the coarse grained sand on the beach and limited sand availability in the nearshore zone was sufficient to stabilise the beach. This may be applicable to Rings Beach and Maramaratotara Beach, however bathymetric surveying of the nearshore region would be required to confirm this hypothesis. Maramaratotara Beach has an erosion resistant substrate and the eastern end of the beach was previously mined, therefore may have limited sediment availability (Dahm & Gibberd, 2009).

4.5.4 Beach Rotation

Results showed that beach rotation occurred on embayed beaches on the eastern Coromandel Peninsula which accords to other published work for embayed beaches (e.g. Klein et al., 2002; Ranasinghe et al., 2004; Ojeda & Guillen, 2008). However rotation was not prominent or uniform across all embayed beaches on the Coromandel Peninsula. For example, Whangapoua Beach did not show constant rotation on a short or long term scale. It is suggested that unusual wave refraction patterns due to the Mercury Islands, and nearby Pungapunga Island which is 150 m offshore from the northern profile on Whangapoua Beach, cause non-uniform wave energy along the beach. Whangapoua Beach has a similar orientation to Tairua Beach, but was the only beach with a north-eastern aspect located north of the Kuaotunu Peninsula. Figure 4.12 (a) showed that waves north of the Kuaotunu Peninsula approach from a more northerly direction and there was also a much narrower range of approach directions compared to the other sites. Published literature on beach rotation forcing mechanisms states that wave direction is the primary forcing mechanism of beach rotation (Short & Masselink, 1999; Klein et al., 2002; Ranasinghe et al., 2004; Short & Trembanis, 2008). Therefore, the narrow approach direction of waves at Whangapoua Beach is likely to be the reason why it did not rotate. However, the 3 large rotation events in 1999, 2000, and 2003 were unexplained. Section 4.4.3 (Figure 4.7) showed that Whangapoua was one of only 3 beaches to show any relationship with the wave energy flux (although not significant). The two largest wave energy flux events in Figure 4.7 were likely to have caused the relationship as the remaining data appeared unrelated. One of the main problems with linear regression is that when data are clustered, some results will have more influence on the regression than others (Dolan et al., 1991). This was likely to be the case at Whangapoua Beach. The two large rotation events in 2000 and 2003 occurred at the same time as the two largest time-averaged wave energy flux events. Rotation at Whangapoua Beach was therefore limited to short term events. Analysis of the wave energy flux at a shorter timescale with increased profile surveying may improve the understanding of beach rotation at Whangapoua Beach.

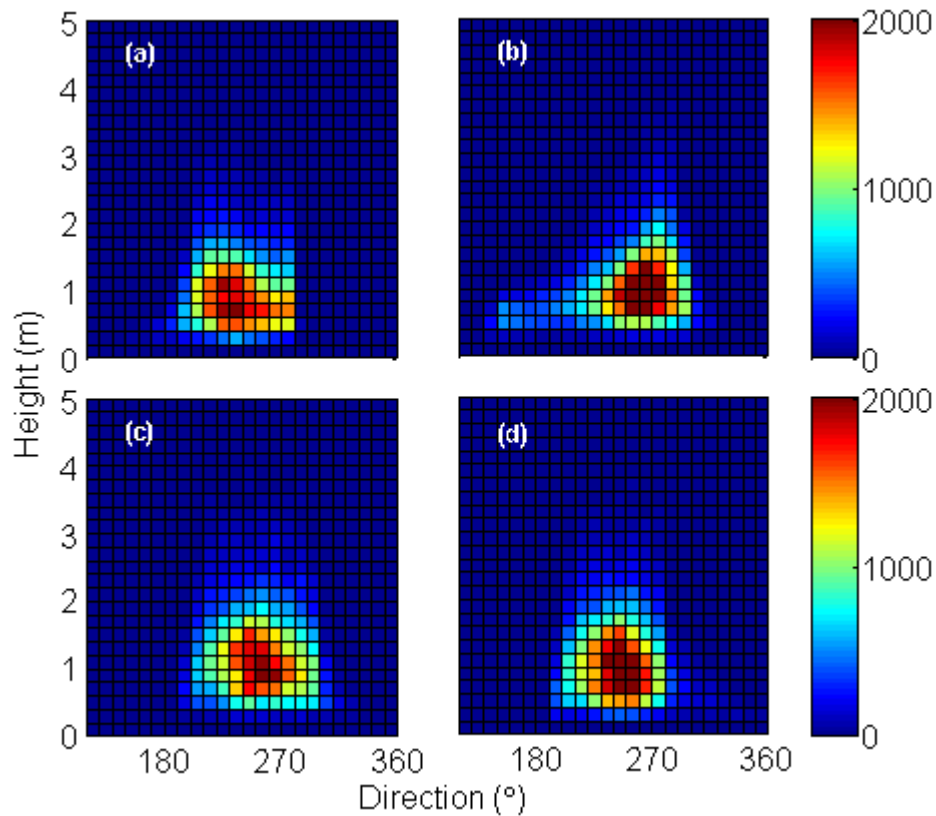


Figure 4.12: Significant wave heights and directions at Matarangi (a), Opito Bay (b), Tairua (c), and Whangamata (d) from 1995 to 2009. The colourbar illustrates the frequency of the data. The wave direction is the direction the waves are travelling to.

Interesting results were obtained at Pauanui Beach and Whangamata South Beach which had the highest and third highest range of rotation coefficients of all beaches. The data suggest that these beaches rotated to quite a large degree, however previous research showed that rotation is confined to embayed beaches (Short & Masselink, 1999). Pauanui Beach and Whangamata South Beach are harbour adjacent beaches. Therefore a contradiction exists between the data which suggest beach rotation occurs and literature which states it should not (Short & Masselink, 1999; Ranasinghe et al., 2004; Short & Trembanis, 2008). A logical hypothesis would suggest that sediment pulses ejected from the harbours and transported in the alongshore direction (e.g. sand waves) were causing the rotation data shown (e.g. Fenster & Dolan, 1993). Figure 4.5 showed that the rotation coefficient on Whangamata South Beach rotates around an equilibrium planform (i.e. 0° or shore-normal), whereas at Pauanui Beach long term rotation trends were evident, and similar to those at neighbouring Tairua Beach. The Whangamata

South data therefore conform to the above hypothesis whereas the Pauanui data does not. It is suggested that complex wave refraction patterns around Shoe and Slipper Islands are a key factor affecting behaviour on Pauanui Beach in the alongshore direction, coupled with impacts from the harbour may cause alongshore rhythmic features that affect the results. Author observations have also identified rip currents which are likely to affect the alongshore variation.

Several studies have been done on individual or several naturally embayed beaches (e.g. Klein et al., 2002; Ranasinghe et al., 2004), however the spatial scale of the analysis considered here appears unprecedented. Accordingly, the rotation behaviour of Hot Water, Tairua, and Whiritoa Beaches was very interesting. These 3 beaches are all steep, coarse grained beaches with an east to northeast orientation and all showed similar trends of long term beach rotation behaviour. Klein et al. (2002) suggested that beaches with similar planform morphology and hydrodynamic characteristics would exhibit similar beach rotation behaviour. Their study of 3 adjacent beaches showed that short-term beach rotation processes can differ significantly between reflective, intermediate, and dissipative beaches, as well between beaches with different degrees of curvature and exposure to the incident waves. The 3 adjacent beaches studied by Klein et al. (2002) showed differing behaviour due to their different morphological characteristics. Hot Water, Tairua, and Whiritoa Beaches conform to their hypothesis for beaches with similar morphology and wave conditions as these systems have similar geomorphology (Table 2-1). However, contrasting evidence from this study was illustrated at Kuaotunu West and Kuaotunu East Beaches. These two beaches are located immediately adjacent to each other and have almost identical lengths, orientations, average intertidal slopes, mean grain size, and wave climate, yet the beach rotation results were not particularly similar. It is acknowledged that several events between the beaches such as anticlockwise rotation in 2002, and clockwise rotation at the beginning of 2005 and 2008 were similar, however they were all individual events. There were at least an equal number of events where rotation was the opposite between the beaches (e.g. mid 2003, mid 2006, and mid 2008). The rotation at Kuaotunu West appeared to be seasonally dominant as there was strong anticlockwise rotation in winter and

clockwise rotation in summer. Kuaotunu East did not show a strong seasonal cycle. The differing behaviour between two similar beaches was not explained in this thesis.

Wharekaho Beach showed weak rotation for a large majority of the timeseries. Due to the orientation, the sheltered nature of the beach, and the dominant incoming wave direction (Figure 4.12), most of the incoming wave energy would be refracted and therefore arrive from a relatively uniform direction. Wave direction was the primary forcing mechanism of beach rotation (Short & Masselink, 1999; Ojeda & Guillen, 2008), therefore little to no variation in the wave direction would not cause beach rotation. The beach orientation (120°) also explained the inverse relationship between rotation and wave energy flux.

Figure 4.7 showed the 3 beaches with the strongest relationship between beach rotation and the wave energy flux (Tairua, Whangapoua, and Wharekaho). Tairua was the only beach which showed a significant relationship between beach rotation and the time-averaged energy flux. Because the relationship was still poor (R-squared = 0.27), the analysis of beach rotation and the wave energy flux were poorly correlated at the timescale analysed here. These results conform to Yates et al. (2009) who showed that time-averaging the wave energy yields very poor correlations to the degree of beach change, in their case, with the MSL contour. Although their analysis was not directly applicable to beach rotation, the MSL contour is a significant factor when analysing rotation, therefore the results of Yates et al. (2009) were considered applicable. A key example was the comparison by Yates et al. (2009) of two timeseries with equal wave energy, yet the timing of wave events differed within the two timeseries, and showed contrasting degrees of erosion and accretion. The analysis showed that the timing of the wave energy impact was much more significant than the average energy (Yates et al., 2009). This explained why the methods used in this thesis did not provide significant results, and that a more detailed analysis of the wave energy is required to determine the impact of waves on beach rotation, as suggested by Yates et al. (2009). A study on Tairua Beach by Bryan et al. (2009) showed that

beach rotation occurred in response to large wave energy fluxes, which were only partially evident in this thesis due to the timescale of analysis in this thesis. It is concluded that the temporal variation used to average wave data in this thesis was too great to yield a relationship. However, the results of events greater than 3500 J.m^{-2} coupled with strong rotation are encouraging as they conform to Bryan et al. (2009) for Tairua beach. Shorter timescales of analysis used by Bryan et al. (2009) have shown to yield strong results to beach rotation.

Overall, beach rotation occurred on embayed beaches on the Coromandel Peninsula, however, not all beaches were similar. Only the beach rotation trends were identified within this research, not the forcing mechanism (although an attempt was made) or individual site characteristics (e.g. Klein et al., 2002; Ranasinghe et al., 2004; Short & Trembanis, 2004).

4.6 SUMMARY

Analysis of the medium term behaviour of beach systems on the Coromandel Peninsula showed some results that were typical of sandy beaches worldwide, results that further emphasised the efficacy of the classification made in Chapter 3, and some interesting and unpredictable results on individual beaches. The following conclusions can be drawn from the medium term analyses:

- Eastern Coromandel beaches showed a reasonable degree of seasonal volume variations. The behaviour was typically dependent on beach state and therefore beach slope and grain size;
- Seasonal volume variations differed between intermediate and reflective beaches. Reflective beaches had a greater amount of seasonal variation. Reflective beaches also reached the peak seasonal volumes earlier in the year compared to intermediate beaches. Otama Beach and Hot Water Beach were outliers out in each respective classification by showing higher- and lower-than expected volume variations respectively;
- Harbour adjacent beaches had irregular behaviour through the year. Matarangi Beach was the exception and had a strong seasonal cycle.

Buffalo Beach and Cooks Beach were identified as intermediate beaches in Chapter 3 but behaved similar to the harbour adjacent beaches at the seasonal scale;

- Outlier beaches had seasonal signals, however they were very small. These two beaches continue to show a different behaviour to all other Coromandel beaches;
- Beach rotation was evident at most embayed Coromandel beaches. Some similar beach systems (i.e. the 3 reflective assemblages analysed) showed similar low frequency oscillations, however it was not uniform around the Coromandel Peninsula;
- The time-averaged wave energy flux studied was not related to beach rotation. Wave energy flux variations on a shorter time scale with higher resolution rotation data have proved to be effective (Bryan et al., 2009); and
- A seasonal variation in wave height existed with higher average H_s in winter. Increased wave heights identified in late summer were not expected. There was also a significant increase in the number of storm events in winter. Seasonal variations in the wave climate account for the seasonal variation in beach volumes on intermediate and reflective beaches on the Coromandel Peninsula.

CHAPTER FIVE

INTERANNUAL VARIATION

5.1 INTRODUCTION

Interannual variations are oscillations or trends which occur at frequencies of more than once per year. In particular, long term trends in beach behaviour greater than the typical “summer-winter” profile (Komar, 1998). Interannual to climatic scale oscillations in weather patterns have featured in published literature, however the predictive tools for the subsequent impacts on coastal processes and coastal management are lacking, and considerable effort has been expended to develop predictive tools for long term variation (Capobianco et al., 1999). In the New Zealand context, the El Niño Southern Oscillation (ENSO) is one such trend that has received considerable attention due to the scale of impacts that can affect coastal processes in the south Pacific (e.g. Salinger et al., 2001). ENSO, along with the Interdecadal Pacific Oscillation (IPO, also known as Pacific Decadal Oscillation) are known to cause variation in weather and climate regimes in the southern Pacific (e.g. Zhang et al., 1997; de Lange, 2000; Salinger et al., 2001; Harley, 2009b). The IPO has been characterised as consisting of a sequence of climatic regime shifts associated with interacting bidecadal and pentadecadal oscillations (Minobe, 1997; 1999). As a result, the IPO is a consequence of interacting oscillations as opposed to a single oscillation in itself (de Lange, 2000). Interannual to climatic scale variations in weather patterns are well documented due to their signals preserved in ice cores, tree ring data, and geological evidence (de Lange, 2000). However the impacts of these variations on subaerial beach systems are relatively scarce due to the lack of suitable data. The aim of this chapter is to identify any relationship between subaerial beach behaviour and interannual climate variations on eastern Coromandel Peninsula beaches.

5.1.1 The Importance of Interannual Variation

Variations of weather and climate patterns impact wave and sea conditions, and can therefore affect coastal processes and subaerial beach behaviour. Historical shoreline changes are typically large because coastal processes have a greater amount of time between observations to impact beach environments. Climate variations affect the frequency and intensity of wind stress, waves, rainfall, groundwater, sea level elevation, and ocean temperatures and pressures. All of these factors impact subaerial beaches through various mechanisms. The IPO and ENSO represent irregular, but coherent sets of fluctuations in atmospheric and oceanic circulation patterns (de Lange, 2000). In particular, ENSO affects the number of extratropical cyclones generated to the north of New Zealand, which affects the number of storm events affecting the northeast coast. The IPO is a longer term recurring pattern of ocean-atmosphere variations over the north Pacific with reversals of the index identified around 1925, 1947, 1977, (Mantua et al., 1997; Minobe, 1997; Zhang et al., 1997; Mantua & Hare, 2002) and most recently around 2008. Work presented by Mantua and Hare (2002) showed existence of IPO impacts in the southern hemisphere and that the 20th century IPO signal was most energetic at two general periodicities, one from 15 – 25 years and the other from 50 – 75 years, although the mechanisms causing IPO variability are unclear. The IPO modulates the frequency and intensity of ENSO extremes, therefore affecting storm frequency on the northeast coast. The positive (warm) and negative (cool) phases of IPO favour El Niño and La Niña conditions respectively. ENSO has an inverse relationship in which positive and negative phases favour La Niña and El Niño conditions respectively. Many climate anomalies associated with the IPO are broadly similar to ENSO variations, although the impacts are generally not as extreme (Latif & Barnett, 1996; Mantua et al., 1997; Minobe, 1997; Mantua & Hare, 2002).

5.1.2 Expected Outcomes

The primary aim of this chapter is to identify the presence of interannual variation of subaerial beach behaviour on the Coromandel Peninsula. This was achieved by proving or disproving the following hypotheses:

- Interannual trends of erosion or accretion will be similar between eastern Coromandel beaches; and,
- Coromandel beach behaviour will be related to ENSO and IPO variations due to variations of weather patterns and the wave climate;

5.2 BACKGROUND: INTERANNUAL VARIATION

Interannual beach variation incorporates morphological changes which occur less frequently than a seasonal oscillation. They do not include extreme events which may occur, for example, once every decade on average. Low frequency oscillations have been identified on sandy beaches worldwide, however results and analyses on the impact of such variations are relatively new, but are becoming increasingly prevalent in the literature due to the availability of larger datasets (e.g. Stive et al., 2002; Wijnberg, 2002; Short & Trembanis, 2004; Reeve et al., 2007; Davidson & Turner, 2009). Interannual behaviour is typically driven by climatic variations and oscillations which in turn affect sea level pressures, sea surface temperatures, wind, and ultimately wave conditions (Mantua & Hare 2002; Rooney & Fletcher, 2005).

Long term trend analysis initially used linear techniques and historical shoreline position data to develop shoreline change rates for temporally-poor data (Crowell et al., 1991; Dolan et al., 1991; Fenster & Dolan, 1993). This method is still applicable as some sites do not have other data available (e.g. Bryan et al., 2008). Many long term datasets now provide the ability to analyse interannual behaviour, but are still restricted to decadal scale behaviour because of the lack of high resolution data (Larson et al., 2003). Shoreline position and beach profile data show zones of maximum beach variability which are critical for coastal management purposes (Clarke & Eliot, 1988). However, long term datasets which identify beach profile envelopes can only ever increase with time. Advanced statistical methods now dominate long term trend analysis because computer programmes can quickly determine peak frequency oscillations and the significance of the results relatively easily. Some of high resolution datasets with large temporal and spatial variations exist at Narrabeen Beach in Australia, Duck

in the U.S, Germany, and The Netherlands (Larson & Kraus, 1994; Larson et al., 2003; Miller & Dean, 2007; Reeve et al., 2007; Gunawardena et al., 2008). These quality datasets were fairly unique as data collection has been the biggest problem because it was traditionally time consuming and required a lot of human input (Short & Trembanis, 2004).

5.2.1 Linear Analyses of Beach Variation

Linear regression and variations of the method were often used to quantify long term beach morphology changes (e.g. Dolan et al., 1991). When applied to long term datasets, the results were simple and easy to understand because the long term trend was explicit, and were often used to determine coastal hazard setbacks (Fenster et al., 1993). The significance of the result was also easily obtained. Rate of change data are effective because analysis of the forcing mechanism is not required to quantify the variation (Dolan et al., 1991). However, forcing mechanisms are now a pre-requisite for many model inputs (e.g. Davidson & Turner, 2009). One disadvantage of linear regression was that some results would have more influence on the regression if a majority of the remaining data were clustered. This was easily rectified by applying linear regression techniques to different timescales of data, for example when analysing more recent trends in shoreline change (Dolan et al., 1991).

5.2.2 ENSO and IPO Impacts on Sandy Beach Systems

ENSO affects the frequency of tropical cyclones which affect New Zealand. A negative ENSO index favours El Niño conditions which cause a northward shift of the westerly wind belt, thus increasing the incidence of south westerly winds affecting New Zealand (de Lange, 2000). The Coromandel Peninsula is a lee coast to the prevailing west to southwest winds, therefore increased winds from this direction favour accretionary conditions due to the prominence of offshore winds. A positive ENSO index favours La Niña conditions which cause a southward shift of the subtropical cyclone belt therefore increasing the incidence of northerly quarter winds (de Lange, 2000). Onshore winds favour erosion dominated conditions for northeast facing beaches in New Zealand. The IPO modulates the

frequency and intensity of ENSO events which results in decadal scale persistence of El Niño or La Niña conditions. The IPO has similar impacts to ENSO but has 3 key distinguishable characteristics: the oscillatory period is much longer; the IPO is more prominent at higher latitudes whereas ENSO is more pronounced in the tropics; and, the mechanisms causing IPO variability are not known whereas ENSO variations are relatively well understood (Mantua et al., 1997; Zhang et al., 1997; de Lange, 2000; Mantua & Hare, 2002; Rooney & Fletcher, 2005).

ENSO has been linked with beach morphology changes at many beaches around the Pacific. Decadal scale analysis of spit morphology at Ohiwa Spit on the northeast coast of New Zealand showed that periods of erosion and accretion loosely corresponded to the IPO index with sustained ENSO behaviour during the respective IPO trend (Bryan et al., 2008). Inverse trends were also evident on a west coast spit. The analysis undertaken by Bryan et al. (2008) used historical shoreline maps and various short term datasets to identify the relationships. Sandy beach systems on Australia's east coast have been shown to be coupled with ENSO behaviour by Clarke and Eliot (1988) with variations in beach volume occurring at periods of 3 to 6 years. Further research which has identified similar scale oscillations in beach volume data were presented by Lacey and Peck (1998) and Bittencourt et al., (1997). Results from the latter authors showed a significant oscillation of 29 months at all 3 of their profile sites which was most prominent in the lower beachface. Oscillations on the order of 2.5 years were also shown to occur on the south-eastern coast of Australia by Clarke and Eliot (1988). This oscillation was attributed to the stratospheric Quasi-biennial Oscillation of approximately 26 to 27 months as identified by (Quiroz, 1981; Labitzke, 1982; van Loon et al., 1982; cited in Clarke & Eliot, 1988). Oscillations on this scale were attributed to wave climate variations caused by ENSO oscillations by these authors. Significant oscillations at this scale were identified on numerous Coromandel beaches (Table 5-2).

Lacey and Peck (1998) also identified a long term oscillation on the scale of 11 to 14 years at 5 out of their 7 study sites, however they stated that such long term

variations were beyond the limits of the spectral analysis performed on their data. Beach rotation has been shown to have a significant lagged correlation with the Southern Oscillation Index (SOI, also known as ENSO) due to shifts in the modal wave direction (Short et al., 1995; cited in Ranasinghe et al., 2004). This occurred at greater than the seasonal scale of typical rotation with the opposite impacts identified at more than one beach on eastern Pacific equatorial beaches (Lizarraga-Arciniega et al., 2007). These results show that ENSO cycles not only impact beach oscillation, but also the rotation component due to ENSO driven variations in the wave climate (Harley, 2009a; 2009b).

5.2.3 Non-stationary Timeseries Analysis Techniques

Beach volume timeseries with uneven temporal variations are relatively sparse in published literature because most analysis relates to evenly spaced data. Many datasets contain uneven data early on which were often disregarded and the focus placed on the high resolution, evenly spaced data. The earliest methods of non-stationary analysis comprised of linear trend analysis being applied to different segments of data to identify interannual variations. This method provided results similar to running means. The Lomb-Scargle (refer 5.3.2) method analyses unevenly spaced data using spectral analysis without interpolating between data points. It is therefore applicable to apply to timeseries data which don't have even temporal spacing, but still includes all available data to determine spectral peaks (Lomb, 1976; Scargle, 1982; Ruf, 1999; Goikoetxea, et al., 2009). There is no known published literature regarding the applicability of this method to analyse coastal processes, however the method has been used to analyse paleoclimatic and sea surface temperature data (Schulz & Stattegger, 1997; Goikoetxea et al., 2009). Datasets with uneven temporal variation have typically been interpolated with linear function to provide evenly spaced datasets (e.g. Larson & Kraus, 1994; Miller & Dean, 2007; Ojeda & Guillen, 2008).

5.3 METHODS

5.3.1 Linear Trend Analysis

The uneven spacing of the dataset limited the statistical analyses that could be used on the data. Firstly, linear regression was undertaken on each set of individual beach profile data to determine the long term linear trend. A positive trend illustrated accretion and a negative trend illustrated erosion. The gradient of the line showed the rate of change of volume per day and was converted to percent per year. The percentage change in volume was used so comparisons between profiles and beaches could be made.

Due to the temporal variation of the dataset with many profiles spanning approximately 30 years with sporadic sampling from 1979 to 1995, two linear trends for each profile site were developed. The first covered the entire timeseries available at each profile site and the second covered the higher resolution data from 1995 until the beginning of 2009. Dolan et al. (1991) showed that extreme values are likely to affect linear trend results because a greater weighting is placed on them. Most data prior to 1990 were surveyed in summer and therefore were highly likely to have above average beach volumes. This could have an impact of displaying a false decreasing linear trend for the timeseries. Hence, a linear trend was developed for the higher resolution data from 1995 until 2009.

5.3.2 Spectral Analysis: Lomb-Scargle Fourier Transform

Spectral analysis is a timeseries analysis technique which identifies the frequency of significant oscillations within data. The Lomb-Scargle periodogram uses Fourier transforms and was designed to fit unevenly spaced timeseries unlike standard spectral analysis techniques (Goikoetxea et al., 2009). The Lomb-Scargle method restricts all calculations to actually measured values, therefore producing more accurate results. This avoids possible bias results created by interpolation between unevenly spaced data (Ruf, 1999). Calculations used for the Lomb-Scargle method were well presented in Ruf (1999) as well as the original papers by Lomb (1976) and Scargle (1982). It was described most simply by Ruf (1999) in which the maximum oscillation of the Lomb-Scargle periodogram occurred at

the same period that minimises the sum of squares in a fit of a sine wave to the data (Lomb, 1976; Scargle, 1982).

A programme developed for the Matlab software was used for the analysis (Shoelson, 1999). Lomb-Scargle analysis showed peak oscillations and significant frequencies at various levels of confidence. The corresponding power of the signal showed which frequencies were strongest in the data. The minimum period was set to 100 days (<0.01 Hz) for the analysis. The default value for the window overlap of 4 was used. Increasing the window overlap provided more accurate results, however significantly increased the analysis time. For example, the window overlap was increased from 4 to 8 and the power increased slightly from 25.8 to 26.6 for Whangapoua CCS12 (Table 5-1). Decreasing the window overlap from 4 to 1 reduced the power of the resulting frequency from 25.8 to 18. The Lomb-Scargle analysis used a consistent window overlap value of 4 as a result which was considered suitable as outlined by the test case and within the programme (Shoelson, 1999). Only results with greater than 95 % confidence are retained, however a number of additional results which had greater than 50 % confidence are discussed.

Spectral analysis was also performed on the IPO and ENSO data to identify peak oscillation periods. IPO data were provided by Nathan Mantua and obtained from <http://jisao.washington.edu/pdo/PDO.latest>. ENSO data were provided by NIWA.

5.4 RESULTS

5.4.1 Linear Trend Analysis

5.4.1.1 Individual Profile Results

Figure 5.1 shows the volume change rate for the 15 year (blue bars) and 30 year (maroon bars) trend. All 61 profile sites are displayed from north to south, left to right. The length of the bar shows the sum of the 15- and 30-year trends whereas the lengths of the individual colours represent the values attributed to each trend. Firstly, there was an obvious difference between the 15- and 30-year trends. The

15 year trends had a much greater variability as shown by the longer blue bars and thus, higher rates of change. For the 15 year data, 25 profiles had a positive change rate and 36 profiles had a negative change rate. For the 30 year data, 24 profiles had a positive change rate and 37 profiles had a negative change rate. A total of 10 profiles had change rates greater than 2 % per year for the last 15 years as follows:

- Matarangi Beach CCS16 (b) western profile 2.3 %;
- Opito Beach CCS48-1 (g) southern profile -2.0 %;
- Buffalo Beach CCS25 (i) profile second from north -4.1 %;
- Buffalo Beach CCS25-1 (i) central profile -2.5 %;
- Cooks Beach CCS31 (k) central profile -2 %;
- Cooks Beach CCS31-1 (k) profile second from south 5.1 %;
- Hot Water Beach CCS34 (m) southern profile -3.1 %;
- Pauanui Beach CCS39-2 (o) profile second from south -2.3 %;
- Pauanui Beach CCS40-1 (o) southern profile -2.8 %; and
- Whiritoa Beach CCS63 (s) southern profile -3 %.

Pauanui Beach CCS39-1 is the central profile on the beach, however the northern most profile was not considered (refer 5.4.1.2 below). A total of 15 profiles had change rates greater than 1 % per year for the 30 year trend, with 6 profiles greater than 2 % as follows:

- Kuaotunu East CCS21 (e) eastern profile -2.5 %;
- Buffalo Beach CCS25 (i) profile second from north -3.1 %;
- Buffalo Beach CCS25-1 (i) central profile -3.3 %;
- Cooks Beach CCS31 (k) central profile -2.2 %;
- Cooks Beach CCS31-1 (k) profile second from south 3 %; and
- Whiritoa Beach CCS63 (s) southern profile -3.5 %.

Further, it was evident that several profiles had opposing trends at these two timescales. All of those profiles had low change rates at both the 15- and 30-year scale therefore were considered insignificant. The profile with the greatest amount

of accretion was second from the southern end of Cooks Beach (k, CCS31-1) with an accretion rate of 5.1 % per year for the last 15 years and 3 % for the last 30 years. This was a significant increase in subaerial beach volume at both time scales. Interestingly, the neighbouring central profile at Cooks Beach (CCS31) showed a significant rate of long term erosion of -2 % for the last 30 years and was the only Cooks Beach site showing long term erosion. These two profiles had a separation distance of 241 m which was considered a small spacing for such contrasting results. The central profile at Cooks Beach had strong cyclic patterns in the volume timeseries which appeared to exaggerate the erosion trend as the beach was accreting toward an apparent peak volume at the end of the timeseries (Figure VII.11). Elevated beach volumes in the late 1980's and early 1990's, followed by erosion until 2004 contributed to the negative linear trend.

5.4.1.2 Alongshore Variation

North of the Kuaotunu Peninsula, it was evident at Whangapoua (a), Matarangi (b), Kuaotunu West (d), and Kuaotunu East (e) Beaches that there was a general trend of accretion at the western ends of the beaches and erosion at the eastern end of the beaches (Figure 5.1). This trend of an increasing amount of erosion towards the southern (eastern) end of beaches was also evident at Opito Beach (g), Tairua Beach (n), and Whiritoa Beach (s). This behaviour presents two possible hypotheses which are discussed in section 5.5.1. The first is that a nearshore littoral system is evident between adjacent beaches with erosion downdrift of headlands. The second is that long term beach rotation is occurring with large scale realignment of shoreline orientations.

Long term erosion of entire beaches was evident at Opito Beach, Buffalo Beach, and Whiritoa Beach. Interesting variation in the alongshore direction was also evident at Pauanui Beach. The northernmost profile on Pauanui Beach was not considered due to the short dataset and therefore not discussed. Figure 5.1 showed that the northern two profiles had long term accretion trends whilst the southern two profiles had long term erosion trends. The rate of erosion at the southern end

exceeded the rate of accretion at the northern end at both the 15- and 30-year scale which indicates a long term adjustment of the shoreline orientation.

Harbour adjacent beaches also showed interesting trends. All of the profiles at Matarangi, Buffalo, Cooks, Pauanui, and Whangamata South Beaches showed long term accretion rates (or reduced erosion rates) in the profiles located nearest to the harbour entrances. Buffalo Beach and Cooks Beach were classified as intermediate beaches in Chapter 3 but showed harbour adjacent behaviour in Chapter 4. Therefore, this trend occurred on all eastern Coromandel Peninsula beaches which were located adjacent to a harbour mouth, except Whangamata North.

One profile at each of Tairua (CCS36-2 second from the south, n), Pauanui (CCS38 northernmost, o), and Whangamata South (CCS57-2 second from the south, r) beaches had short datasets which were not considered in the long term analyses. Below is a list of the beaches from north to south and subsequent x-axis labels used in Figures 5.1 and 5.2.

- Whangapoua (a)
- Matarangi (b)
- Rings (c)
- Kuaotunu West (d)
- Kuaotunu East (e)
- Otama (f)
- Opito (g)
- Wharekaho (h)
- Buffalo (i)
- Maramaratotara (j)
- Cooks (k)
- Hahei (l)
- Hot Water (m)
- Tairua (n)
- Pauanui (o)
- Onemana (p)
- Whangamata N (q)
- Whangamata S (r)
- Whiritoa (s)

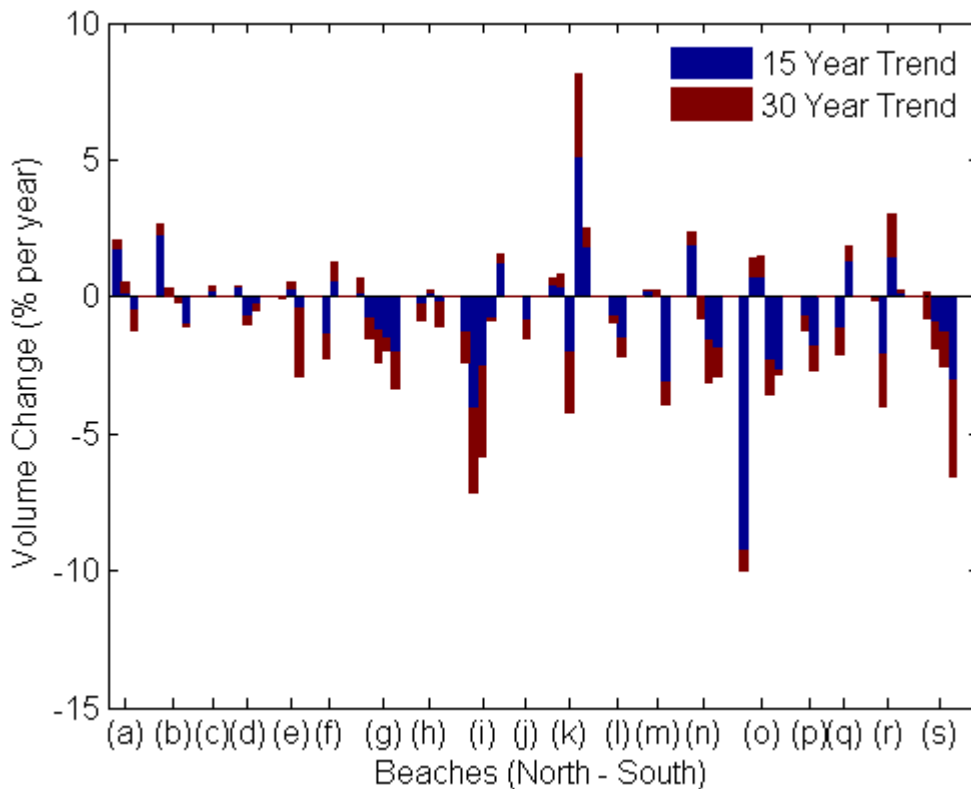


Figure 5.1: Linear trend analysis for all profile sites. Blue bars represent the 15 year trend and maroon bars represent the 30 year trend. The profiles are plotted from north to south, left to right, and the x-axis labels are discussed in text.

5.4.1.3 Beach Average Results

Figure 5.2 shows the average change rate for each beach for the 15- and 30-year trends. Overall it was evident that most beaches had long term trends of erosion at both the 15- and 30-year scale. Firstly, it was identified that there was a large degree of variation of erosion and accretion trends across the Peninsula. The 15- and 30-year trends were similar in most instances, however the magnitudes differed as the 15 year trend was typically greater than the 30 year trend. The beaches with the highest erosion rates at both the 15- and 30-year timeframe were: Opito Beach (g); Buffalo Beach (i); Maramaratotara Beach (j); Onemana Beach (p); and Whiritoa Beach (s). These beaches all had erosion trends greater than 0.5 % per year, which equates to a minimum of 15 % of the entire beach volume over 30 years. The trends at Buffalo Beach and Whiritoa Beach were approximately 1.5 % per year. Beaches with the strongest accretion trend were Whangapoua Beach (15 year trend, a), Cooks Beach (k) and Whangamata South Beach (r), and were all greater than 0.5 %. Matarangi Beach (b) and Rings Beach (c) also

showed accretion trends, but at a reduced rate. The remaining beaches were described as having no distinctive or strong long term trend of erosion or accretion because of the relatively small change rate, they were: Kuaotunu West Beach (d); Otama Beach (f); and Whangamata North Beach (q).

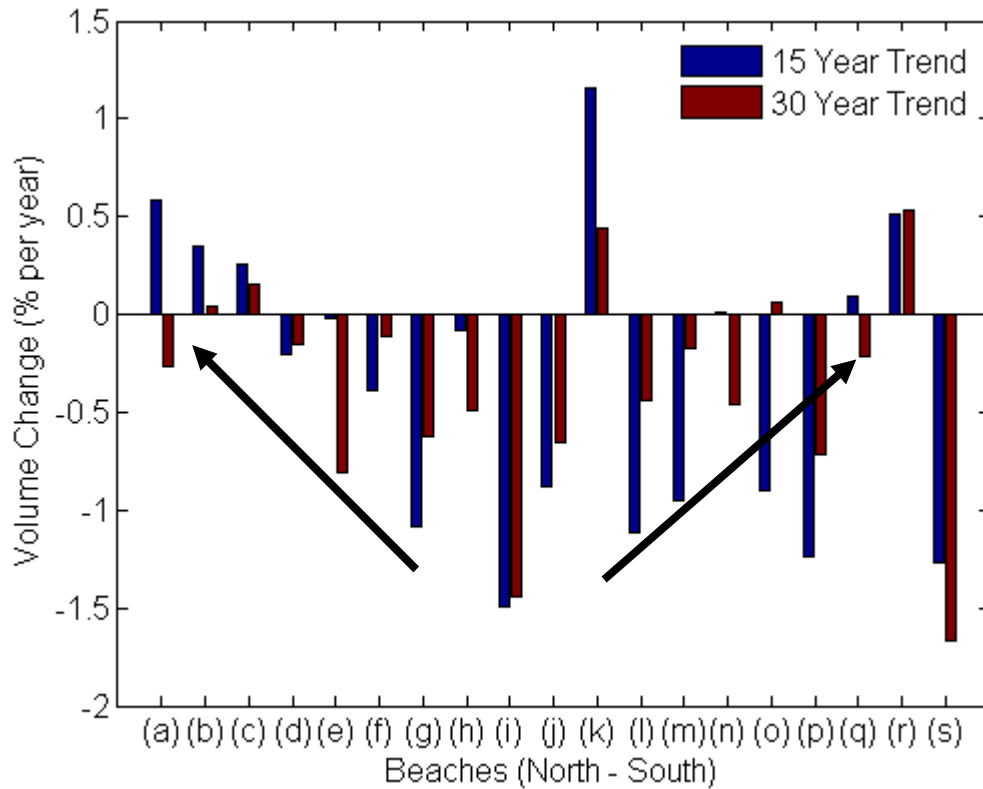


Figure 5.2: Beach average volume change rates. Blue bars represent the 15 year trend and maroon bars represent the 30 year trend. The profiles are plotted from north to south, left to right, and the x-axis labels are discussed in text. The two arrows show apparent large scale sediment transport trends and are discussed in text.

It was apparent that large scale trends were evident in Figure 5.2. Opito Beach (g) is located at the end of the Kuaotunu Peninsula. All beaches west (north) of Opito Beach, (a) to (g), showed a net increase in beach volume change rates from east to west as indicated by the arrow in Figure 5.2. This was indicative of large scale sediment transport to the west along the northern Kuaotunu Peninsula. When referring back to Figure 5.1, it was evident that the respective beach profile had net accretion from east to west. This suggests that headland bypassing maybe evident, with headlands acting as natural groins and downdrift erosion at the eastern end of the beaches. South of the Kuaotunu Peninsula, beaches in Mercury

Bay did not appear to be consistent with the large scale observations. South of Mercury Bay it was apparent that a net increase in beach volume change rates occurred from north to south, Hahei (l) to Whiritoa (s), as indicated by the right hand arrow in Figure 5.2. Onemana Beach (p) and Whiritoa Beach (s) did not conform to these observations. Further, all beaches south of Mercury Bay had an increasing rate of erosion toward the southern end of the respective beach, except Whangamata North and Whangamata South. The alongshore variations may also be indicative of long term rotation trends, particularly beaches north of Opito and south of Hahei. Most of these beaches showed opposing trends of erosion and accretion from one end of the beach to the other (Figure 5.1). This behaviour is discussed further in Section 5.5.1.2.

Linear trend analysis showed that ENSO had no long term trend whereas the IPO was decreasing from 1980 to 2009 which was similar to most beach volume trends.

5.4.2 Observations: ENSO and IPO Trends on Beach Volume Variations

The first method used to determine if a relationship existed between the beach volume data and known climate variations were to compare it against the ENSO and IPO indices. Figure 5.3 illustrates a beach volume timeseries for all three profile sites at Whangapoua Beach and the corresponding ENSO and IPO indices. All beach and profile sites are shown in Appendix VII. The ENSO and IPO trends were similar from 1995 to 2009, accounting for the inverse relationship. A majority of the beach volume trends from 1995 – 2009 were broadly similar to the ENSO (inversely) and IPO indices and trend line. Box 1 in Figure 5.3 illustrates that if the IPO index was in a negative (cool) phase there were predominantly below average beach volumes. Box 2 illustrates that for the following positive (warm) IPO phase the corresponding beach volumes were above average. It is also apparent that the trend continued after Box 2 until 2009. ENSO fluctuations were more frequent than the IPO, and the longer term response rate of the beach volumes across the Peninsula suggest a better correlation to the IPO (Figure 5.4). Most of the available profile data prior to 1995 had higher volumes when

compared to post 1995 data. Pre 1995 volumes at many sites were more than 20 % above the respective mean volume, indicating accretionary conditions which were more consistent with the positive IPO phase from 1980 to 1995 as opposed to the more frequent ENSO variations. Overall, the long term volume trends appear to show a better correlation with the IPO index for the period which data was available. This does not imply that ENSO is not significant. Perhaps the most interesting result was that the two largest recorded erosion events on the eastern Coromandel Peninsula in recent times, which occurred in 1978 (Hume et al., 1992; Dahm & Gibberd, 2009) and 2008, coincided with the last two major shifts of the IPO phase, from negative to positive around 1978, and the following shift to a negative phase which was apparent around 2008 (Figure 5.4; Minobe, 1997).

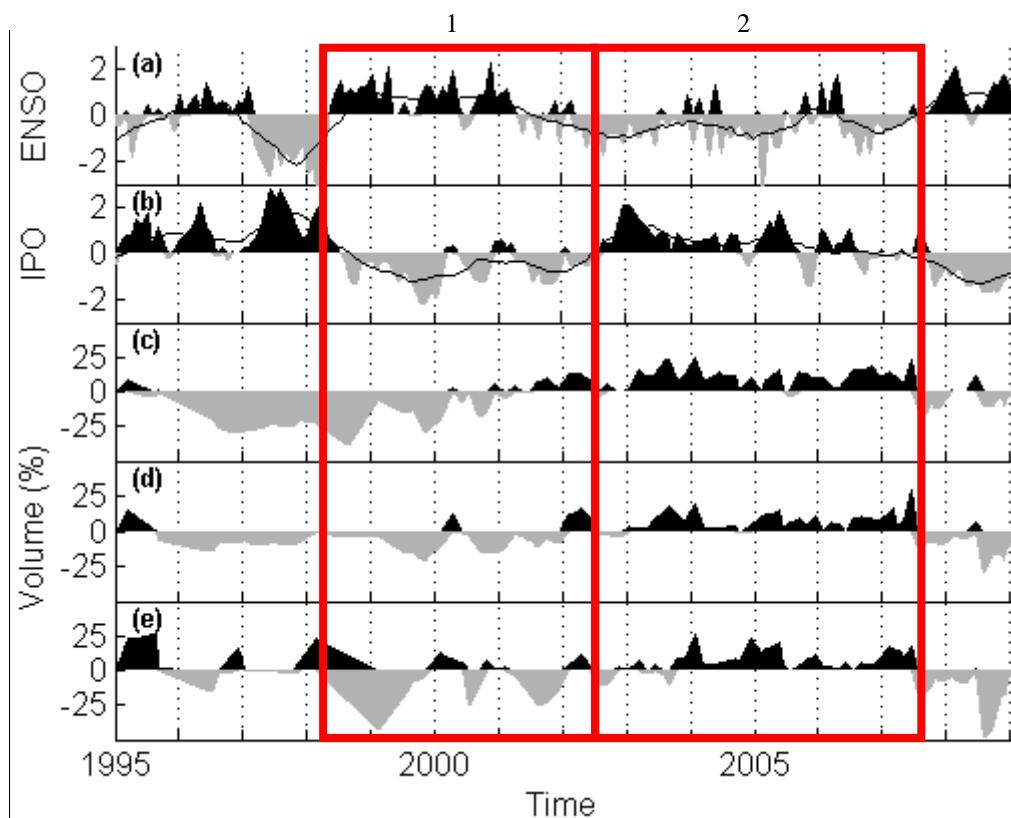


Figure 5.3: Beach volume timeseries for the three Whangapoua Beach profiles from north to south (c) to (e). The beach profile data have been demeaned. The top two panels represent the ENSO (a) and IPO (b) indices for the same period with a 12-month running mean superimposed (black lines). The black shading of the positive ENSO index (a) corresponds to La Niña dominant conditions. The grey shading of the ENSO index (a) corresponds to El Niño dominant conditions. The black shading in (b) corresponds to positive / warm periods where El Niño conditions dominate. The light grey shading in (b) corresponds to negative / cool periods where La Niña conditions dominate. The red boxes (1 and 2) are discussed in text.

Figure 5.3 shows that all three Whangapoua Beach profiles oscillated in a similar manner to the IPO. Peak volumes were achieved in approximately 2004. All three profiles also appeared to be decreasing from a previous peak just prior to 1995. However, the lower resolution data prior to 1995 made analysis difficult. This showed an approximate 12 year oscillation of beach volumes which was similar to the recent IPO index. In comparison, analysis of the ENSO trend in Figure 5.4 showed frequent peaks with approximate 5 year spacing which were not prevalent in the data.

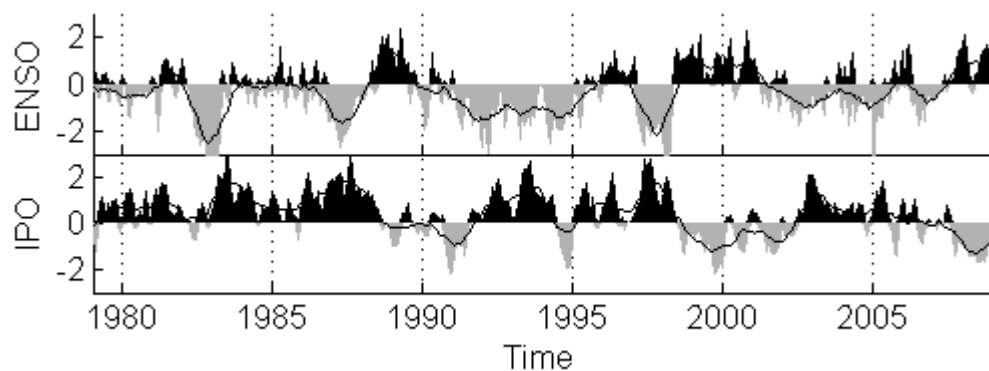


Figure 5.4: ENSO (top panel) and IPO (bottom panel) indices from 1979 to 2009 which encases the temporal variation of the beach profile dataset. Elevated beach volumes on the Coromandel Peninsula during the 1980's and the high resolution data from the mid 1990's are better attributed the IPO index.

5.4.3 Spectral Analysis: Lomb-Scargle Fourier Transforms

5.4.3.1 ENSO and IPO Results

Table 5-1 showed the Lomb-Scargle spectral analysis results for all sites which had a significant frequency of 12 years ± 3 years. The results showed that the oscillation was more prominent on beaches north of the Kuaotunu Peninsula. A power spectrum from Whangapoua Beach is shown in Figure 5.5. The 12 year period was initially determined from qualitative analysis of apparent beach volume and IPO oscillations (Appendix VII). Many beaches showed peak volumes in approximately 2004 and the early 1990's. Spectral analysis using the Lomb-Scargle method on the IPO data returned only one significant oscillation of 9.1 years for the entire dataset (1900 to 2009). The ENSO data returned one significant oscillation of 10.2 years. Because the profile data had a lower

resolution prior to 1995 the previous peak in the approximate 12 year oscillation was difficult to identify, hence the relatively large error bounds of ± 3 years. Peaks were evident in the IPO (positive) and ENSO (negative) data in approximately 1994 and 2004. Several large ENSO variations were not evident in most volume data therefore observations suggest a better long term relationship with the recent IPO trend. Regardless, 19 profile sites (31 %) showed significant trends similar to the recent IPO and ENSO oscillations with 95 % confidence. A further 5 profile sites showed a significant frequency oscillation within these bounds at greater than 50 % confidence.

Table 5-1: Approximate 12 year spectral peaks within the beach profile data. The beaches and profiles are listed from north to south with the frequency in years and corresponding power in volume (%).

Beach/Profile Name (north to south)	Significant Frequency (Years)	Corresponding Power (%)
Whangapoua CCS12	12.0	25.8
Whangapoua CCS11	12.0	17.9
Whangapoua CCS11-1	8.59	10.7
Matarangi CCS16	13.3	17.9
Matarangi CCS15	9.21	13.1
Rings CCS18	10.9	10.9
Kuaotunu West CCS19-4	15.8	10.4
Kuaotunu West CCS19-1	9.31	9.47
Kuaotunu East CCS20	11.9	10.4
Kuaotunu East CCS21	12.4	11.1
Otama CCS45	13.3	16.2
Buffalo CCS26	15.0	13.2
Cooks CCS31-2	14.4	17.3
Hot Water CCS34	15.0	9.36
Tairua CCS37	12.0	19.0
Pauanui CCS38-1	10.3	23.9
Pauanui CCS39-1	10.8	12.4
Whangamata North CCS56	14.8	9.01
Whiritoa CCS63	10.6	8.01

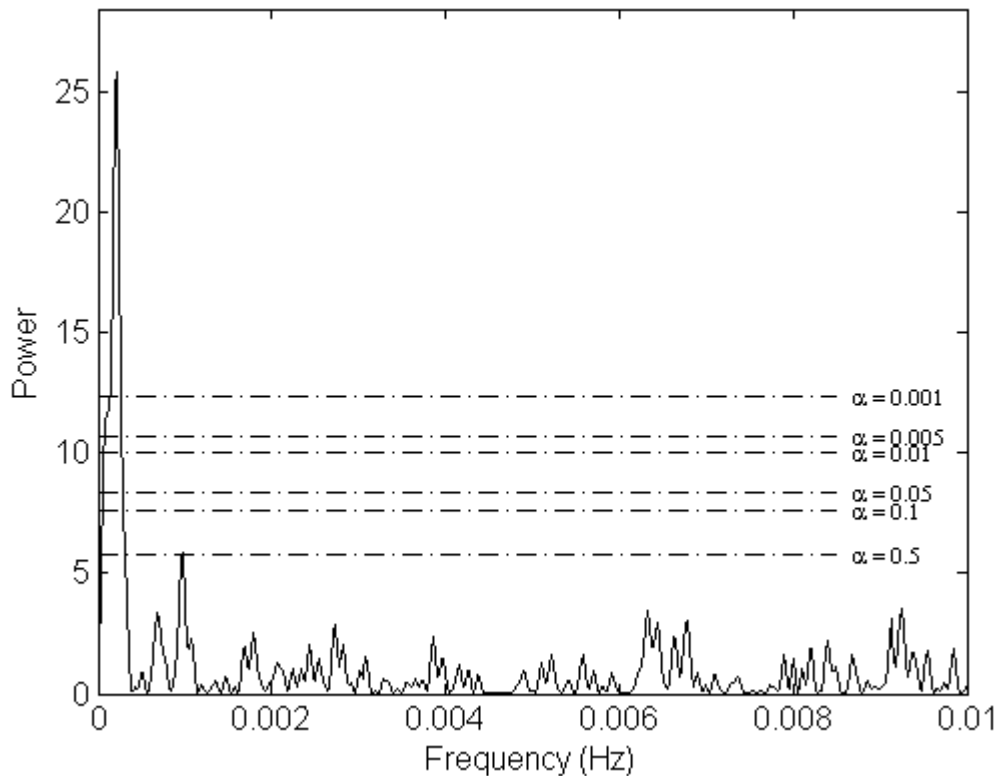


Figure 5.5: An example power spectrum for Whangapoua Beach (CCS12, northernmost profile) produced using the Lomb-Scargle spectrum. The strongest signal has a frequency of 2.29×10^{-4} Hz (12 years) with a peak power of 25.8 % and greater than 99 % confidence.

5.4.3.2 Biennial Oscillations

Lomb-Scargle spectral analysis showed 13 profile sites which had a significant frequency of 2.5 years \pm 0.5 years (Table 5.2). A further 23 sites were identified as having a frequency of 2.5 years \pm 0.5 years at greater than 50 % confidence. This approximate biennial oscillation was only apparent in beaches south of the Kuaotunu Peninsula, including Opito Bay which is situated at the end of the Peninsula. All but one of the 13 sites had an oscillation between 2.2- and 2.5-years. Opito, Wharekaho, Buffalo, and Cooks Beaches all had relatively large orientation changes, however Hahei, Hot Water, and Whiritoa Beaches are all relatively short embayed beaches. The only apparent similarity between the sites was that they were sandy Coromandel beaches south of the Kuaotunu Peninsula with a general east to northeast orientation. This suggests a large scale oscillation which affected beach volumes on a biennial scale regardless of the beach type.

Table 5-2: Biennial oscillations evident within the beach profile data. The beaches and profiles are listed from north to south with the frequency in years and corresponding power in volume (%).

Beach/Profile Name (north to south)	Significant Frequency (Years)	Corresponding Power (%)
Opito CCS49	2.44	9.69
Opito CCS49-1	2.37	8.86
Opito CCS48-1	2.43	9.08
Wharekaho CCS22-1	2.23	13.2
Wharekaho CCS22	2.28	10.1
Wharekaho CCS23	2.30	8.67
Buffalo CCS25-1	2.31	10.8
Cooks CCS29	2.23	9.61
Hahei CCS32	2.27	12.7
Hahei CCS33	2.50	9.95
Hot Water CCS34	2.45	8.72
Whangamata South CCS57-3	2.86	11.2
Whiritoa CCS61	2.41	8.92

The results in Tables 5-1 and 5-2 were also shown in Figure 5.6. Figure 5.6 illustrates that there was a difference in behaviour on the interannual scale dependent on the spatial location of the beach. The arrow in each respective panel identified the end of the Kuaotunu Peninsula between Otama Beach (f) and Opito Beach (g). There was a clear distinction in the spectral analysis results on beaches located north and south of the Kuaotunu Peninsula. All beaches north of the Kuaotunu Peninsula had a significant oscillation of approximately 12 years and none of these beaches showed the biennial oscillation of approximately 2.5 years. The 12 year oscillation was evident at 7 beaches south of the Kuaotunu Peninsula, of which only Pauanui Beach (o) showed the oscillation at more than one profile. Conversely, the biennial trend was prominent from Opito Bay (g) southward to Hot Water Beach (m), including beaches in Mercury Bay. Only 2 profiles outside this region showed the biennial oscillation, with one profile at each of Whangamata South (r) and Whiritoa Beaches (s).

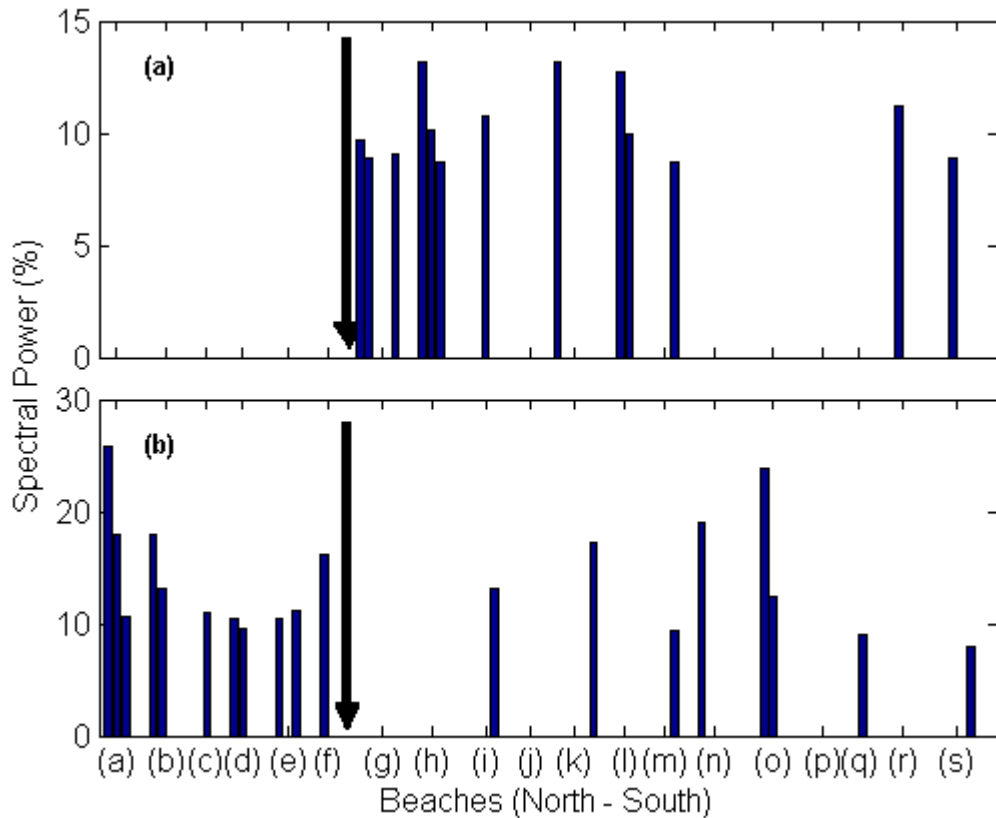


Figure 5.6: Spectral power results for the biennial oscillation (a) and approximate 12 year oscillation (b). The arrows indicate the eastern end of the Kuaotunu Peninsula. Note the different y-axes between the upper and lower panels. The x-axis labels are discussed in text.

5.4.4 Interannual Variation of Wave Conditions

Lomb-Scargle spectral analysis was also performed on the wave height data as the method was also suitable for evenly spaced timeseries (Ruf, 1999; Goikoetxea et al., 2009). Analysis of the wave data from 1979 to 2009 produced similar results between sites. The strongest 3 periods at each site consisted of a 40.2 year oscillation, a 10.98 year oscillation, and a seasonal oscillation. The 40.2 year oscillation was strongest at all four sites. The 10.98 year oscillation was second strongest at Matarangi and Whangamata, and third strongest at Opito and Tairua, behind the seasonal signal. This oscillation was likely to be ENSO or IPO forced due to the similarity of the results and the higher resolution data available.

5.5 DISCUSSION

5.5.1 Linear Trend Analysis

Erosion trends were prevalent at both the 15- and 30-year timescale at many Coromandel beaches. Such large scale behaviour is typically attributed to climatic oscillations affecting wave conditions around New Zealand (Goring & Bell, 1999; de Lange & Gibb, 2000; Salinger et al., 2001). Localised erosion is often attributed to features such as rip currents, wave refraction, beach rotation, and human impacts (Stive et al., 2002). Percentage change rates provided information on the varying degrees of long term coastal change. The 15 year trend data was more variable due to the shorter timeframe, however should be representative of recent trends due to the high resolution data. The 15 year trends were predominantly greater than 30 year trend. This was typical of longer duration data being more representative of the true long term trend, thus reducing the impacts of shorter term oscillations, such as seasonal variations and ENSO impacts, of which the former can be a large source of error in linear change rates (Smith & Zarillo, 1990; Dolan et al., 1991). The 30 year data obviously encase a greater timescale, however the early data were lower resolution. Further, most profiles before 1990 were surveyed in late summer during peak volume periods. Least squares regression used these data early in the timeseries which were likely to exaggerate the long term erosion trend. The long term erosion trends would not be as prominent if early winter data were available, as it would reduce the impact of earlier surveys on the high resolution, clustered data. It is reiterated that surveys were often undertaken to measure specific storm damage, and never specific accretion periods. Therefore there is potential for the data to be skewed toward erosion dominant trends. Early data points in long term datasets have been proven to affect clustered data where the temporal spacing is large (Dolan et al., 1991). The temporal variations discussed by Dolan et al., (1991) were in the order of 30 years, therefore the same error is not considered to significantly affect the results presented here. As a result, the linear trends were considered worst case scenarios for the last 30 years.

Cooks Beach had the fastest accretion rate and showed interesting results in the alongshore direction. Four out of five profiles on Cooks Beach had prominent accretion trends whereas the central profile had an erosion trend. Analysis of the individual profile data showed that the central profile had very strong oscillatory behaviour. There was an erosion trend from the early 1990's to 2004 followed by recovery until 2009. Because the next peak volume in the oscillatory cycle had not been reached, the profile showed a strong erosion trend even though it had strong accretion since 2004. The southern (eastern) two profiles appear to follow the same trend, however both had larger degrees of short term variation which masked the oscillatory pattern (Appendix VII). Cyclic patterns have proven to be a weakness of linear regression techniques which was evident at Cooks Beach (Smith and Zarillo, 1990).

The spatial variation of the dataset enabled large scale observations to be made. For example, all beaches north of the Kuaotunu Peninsula except Kuaotunu East had a relatively stable or accretionary linear trend. Further, only the eastern profile at Kuaotunu East Beach had a significant erosion trend. Beaches north of the Kuaotunu Peninsula had the most stable long term trends, which was attributed to the northerly quarter orientation of the beaches, the sheltering effect of the Mercury Islands from dominant northeast waves, and easterly storms which have been shown to be a primary cause of beach erosion (Healy & Dell, 1987; Bradshaw, 1991). The anomaly at the eastern end of Kuaotunu East only occurred in the 30 year trend. The profile had a strong erosion trend from 1981 to 2009 which was exacerbated by 3 large erosion events in 2006, 2007 and the largest event in 2008. There has been a 45 m landward shift of the MSL contour since 1981 and complete erosion of a 4.5 m high foredune.

5.5.1.1 Alongshore Variation

Figure 5.1 showed that beaches north of the Kuaotunu Peninsula had a trend of net increasing volume change rates from east to west. This implied that there was a sediment transport sub-cell with net littoral drift to the west from Otama to Whangapoua (Figure 5.1 f to a). The connectivity index between these beaches

was much lower when compared to beaches south of the Kuaotunu Peninsula which supports these findings (Table 2-1). This suggested that sediment transport between and along beaches was feasible with rip currents, beach rotation events, and storm events all contributing to headland bypassing of sediment (Short & Masselink, 1999; Masselink & Pattiaratchi, 2001; Holman et al., 2006; Ojeda & Guillen, 2008). The individual profile trends showed further evidence for headland bypassing. All profiles sites at the eastern end of beaches (downdrift side) north of the Kuaotunu Peninsula showed erosion, with net accretion toward the western end. This was an indicator of the littoral drift direction with headlands acting as groins. The behaviour at Whangapoua Beach was likely to be a combination of littoral drift and impacts from the ebb tidal delta of Whangapoua Harbour. Coromandel estuaries are continuously infilling, therefore a continued ejection of sediment from Whangapoua Harbour could be expected to be added to the nearshore drift (Mead & Moores, 2005). An early study of Coromandel beaches by Healy et al. (1981) suggested Coromandel Beaches were closed sedimentary systems with very little sediment exchange between beaches, although the region from Otama to the west was identified as a separate, complex region. Kuaotunu East was previously hypothesised to be eroding due to net westward littoral drift and was compensating for sand extraction from Kuaotunu West up until the 1970's (Healy et al., 1981). The results presented here show evidence for a nearshore littoral drift system to the west along beaches located north of the Kuaotunu Peninsula. However, an alternative hypothesis regarding this behaviour could be long term beach rotation and realignment of the shoreline orientation. Beach rotation was evident at Whangapoua, Kuaotunu West, and Kuaotunu East, whereas Matarangi and Rings Beaches were not considered (refer Section 4.4.2). Long term rotation trends were evident in the results in Chapter 4, however they were largely unimportant due to the small trends. Whiritoa Beach had the highest long term rotation trend suggesting clockwise rotation of 0.2 degrees per year from 1995 to 2009.

A similar trend south of the Kuaotunu Peninsula and Mercury Bay was evident in the linear trend results. It was apparent that a net increase in volume change rates from north to south occurred from Hahei Beach to Whangamata South Beach.

Notably, Onemana and Whiritoa did not conform to this trend. The trend south of the Kuaotunu Peninsula was not as prominent. The difference was attributed to the larger connectivity index between beaches south of the Kuaotunu Peninsula (refer Table 2-1). Further, beach profile data for all beaches north of the Kuaotunu Peninsula were analysed, whereas south of Mercury Bay there are 12 sandy beaches between Hahei and Whiritoa which were not analysed in this thesis. This meant that all sediment exchange north of the Kuaotunu Peninsula was measured. The additional sandy beaches south of the Kuaotunu Peninsula could be sources or sinks of sediment, which may explain the less dominant trend. These results suggest sediment exchange between Coromandel beaches on a relatively large spatial scale which were attributed to beach orientation changes for the differing transport directions. However, south of Mercury Bay, evidence for large scale transport southward contradicts the individual profile results in which Hahei, Hot Water, Pauanui, Onemana, and Whiritoa Beaches show increasing erosion toward the southern end of the respective beach. Whangamata North and South Beaches do not conform to these observations. The transport may be strong enough to be evident in the data, but not to induce a downdrift erosion effect. The large connectivity indices south of Mercury Bay are also unlikely to enable a large amount of sediment exchange. In summary, it was apparent that south of Mercury Bay that sediment exchange between beaches does occur, however it is relatively small and does not account for any alongshore volume variation on individual beaches.

5.5.2 Spectral Analysis: Lomb-Scargle Fourier Transforms

5.5.2.1 Biennial Trends and the ENSO

Lomb-Scargle spectral analysis showed the presence of a significant biennial trend oscillating on an approximate 2.5 year scale on Coromandel beaches south of the Kuaotunu Peninsula. Many authors have noted biennial trends in beach behaviour at this frequency (e.g. Eliot & Clarke, 1982; Reeve et al., 2007). Of particular interest was that no beaches located north of the Kuaotunu Peninsula showed this oscillation. It was previously hypothesised that the Kuaotunu Peninsula would provide a barrier to beach behaviour and sediment transport on a

short term scale. These results proved this hypothesis to be applicable to interannual trends. Linear trends discussed above also conform to this hypothesis. A logical explanation would relate to beach orientation differences north and south of the Kuaotunu Peninsula, however Whangapoua Beach had a similar orientation to Hahei Beach and only the latter had a significant biennial trend. In addition, Wharekaho Beach showed strong biennial oscillations along the entire beach, yet had a south-easterly orientation. Therefore, beach orientation and the direction of wave approach do not appear to be factors because of the relative similarity of the wave climate around the Coromandel Peninsula.

Approximate 2.5 year oscillations have been shown to be correlated with the ENSO on numerous occasions. Goring & Bell (1999) showed a significant correlation between MSL and the ENSO at approximately 3 years. A 2.5 year oscillation in beach profile data was observed using spectral techniques by Bittencourt et al., (1997) and was related to the ENSO. Clarke and Eliot (1988) showed that the biennial oscillation pattern involved accretion of the lower beachface with subsequent infilling of the mid-tidal zone, which was the strongest oscillation at their study site. The strongest spectral peak was 27 months for wind data, and they concluded that atmospheric processes affecting storm surge, sea level variations, and groundwater effects were associated with the beach responses. Ranasinghe et al. (2004) showed significant lagged correlations between beach rotation and the SOI, and therefore confirmed the impact of resulting wave climate variations on subaerial beach systems. Lomb-Scargle analysis of the ENSO index only showed one significant oscillation of approximately 10 years. However, the prominence of literature relating beach oscillations on an approximate biennial scale to the ENSO conclude that Coromandel beaches are also likely to be affected by the same ENSO mechanisms (e.g. Clarke and Eliot, 1988, Bittencourt et al., 1997; Goring and Bell, 1999; de Lange, 2000; Ranasinghe et al., 2004). ENSO impacts on the northeast coast of New Zealand were summarised in Table 5-3.

Table 5-3: Observed ENSO extremes on the northeast coast of New Zealand. From “Interdecadal Pacific Oscillation (IPO): a mechanism for forcing decadal scale coastal change on the northeast coast of New Zealand” by W. de Lange, 2000, *Journal of Coastal Research*, SI 34, p. 660.

	El Niño	La Niña
Air temperature	Decreased	Increased
Atmospheric pressure	SE to NW pressure gradient	NW to SE pressure gradient
Wind direction	More south-westerly winds (offshore)	More northwest- northerly winds (onshore)
Storm frequency	Reduced extratropical cyclone activity	More extratropical cyclone activity
SST	Decreased	Increased
Sea level	Drops	Rises
Wave climate	Reduced sea component	Increased sea component
Wave steepness	Reduced	Increased
Near bed flow	More onshore	More offshore
Coastal response	Tendency to accrete	Tendency to erode.

5.5.2.2 IPO Impacts on Beach Volume Variations

Qualitative analysis suggested an apparent correlation between Coromandel Beach volumes and the recent IPO index. Spectral analysis showed that a total of 20 profiles (34 %) on the Coromandel Peninsula had a long term oscillation on a similar scale to the recent IPO trend of approximately 12 years. Further, all beaches north of the Kuaotunu Peninsula had an oscillation similar to the IPO. The biennial oscillation was prominent south of the Peninsula whereas the longer term oscillation was prominent north of the Peninsula. The higher frequency ENSO variations were not as prominent in the data due to the shorter term variation. However, ENSO had a similar spectral peak and is therefore deemed significant and should impact northeast coast beaches over cycles of approximately 2 to 8 years (Goring & Bell, 1999; de Lange, 2000). The IPO trend for the last 15 to 20 years showed an apparent correlation to beach volumes which was confirmed by similar spectral frequencies. The most recent IPO peak was in the late 1980's to early 1990's and has been declining since. This conforms to the linear trend results above. Therefore, it was apparent that the IPO trend and absolute index affected beach response.

Northeast coast beaches have been identified as being sensitive to small changes in the wave climate, nearshore current regime, and sea level (de Lange, 2000). The IPO modulates ENSO behaviour therefore it was expected that long term decadal scale trends would be coupled with the IPO, and shorter interannual trends to be coupled with ENSO variations, for example, the biennial trend (e.g. Clarke & Eliot, 1988; Bittencourt et al., 1997). Therefore, it would be expected that Coromandel beaches would be linked with long term IPO trends and shorter term ENSO variations. This corresponded with findings from Bryan et al. (2008) of spit evolution on the northeast and northwest coasts of New Zealand. Beach volume trends at Hawke Bay on the east coast of New Zealand's North Island have also shown apparent relationships with the IPO phase from the early 1920's, with increasing volumes during positive phases and decreasing volumes during negative phases (Oldman et al., 2003). The analyses presented here showed that oscillations in beach volumes at different timescales conform to the hypotheses of de Lange (2000), and the findings of Oldman et al. (2003) and Bryan et al. (2008).

Decadal scale impacts of beach response to IPO extremes was summarised by de Lange (2000) in Figure 5.7. The IPO appeared to shift to a negative phase in approximately 2008 therefore suggesting a period of La Niña dominant conditions for the next 20 to 35 years. This shift was hypothesised by de Lange (2000) and Minobe (1999). This would result in erosion dominated conditions for eastern Coromandel beaches for the next 20 to 35 years. It is anticipated that the ENSO will impact beach response on an approximate biennial trend and the IPO will continue to impact beach response on an interdecadal scale.

Lomb-Scargle spectral analysis used in this thesis has been identified as containing two limitations. The first, as discussed by Larson et al. (2003) is that Fourier transforms assume a sinusoidal shape of the applied functions which restricts the functions in time and space. The IPO and ENSO functions compared here exhibited sinusoidal behaviour therefore the method is considered suitable. This was confirmed by the number of significant results obtained. For example, Minobe (1999) extrapolated the cyclic behaviour of the IPO and predicted the

next climatic regime shift would occur between 2000 and 2007. It was apparent this shift may have occurred around 2007 to 2008. Secondly, the analysis does not account for the phase difference of the spectral peaks, therefore qualitative observations of the timing of peak periods were used in this thesis. The high resolution data from 1995 onward provided sufficient detail to be able to identify the locations of peak oscillations given that they were approximately 12 years and were often evident in the data. Possible phase differences in the trends identified were therefore not considered to affect the results.

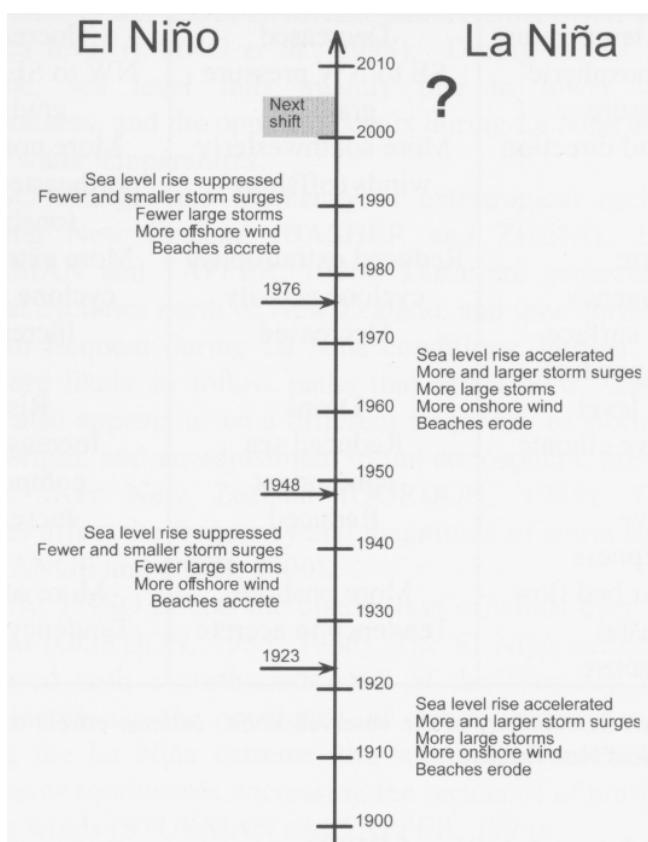


Figure 5.7: IPO phase shifts indicating the respective extreme conditions. From “Interdecadal Pacific Oscillation (IPO): a mechanism for forcing decadal scale coastal change on the northeast coast of New Zealand” by W. de Lange, 2000, *Journal of Coastal Research*, SI 34, p. 660.

5.5.3 Coromandel Beaches – Coastal Hazards (Dahm & Gibberd, 2009)

5.5.3.1 Background and Introduction to the Report

This section will discuss the findings of this thesis compared to results of Dahm and Gibberd (2009). The report was prepared for the local territorial authority, Thames Coromandel District Council (TCDC), to review primary development setbacks (PDS) for certain Coromandel beaches. The review focussed on the following beaches where the PDS impacted on the use of private property:

Whangapoua; Matarangi; Rings; Kuaotunu East; Opito; Wharekaho; Buffalo; Maramaratotara; Hahei; Tairua; Whangamata North; and, Whangamata South. The northern profile on Buffalo Beach (CCS24) was considered a separate beach system, Ohuka Beach, by Dahm and Gibberd (2009). They were considered as one beach system in this thesis as they comprise one continuous sand system. Whangamata South was typically referred to as Otahu Beach after the adjacent estuary. The report is discussed in this chapter because the objective was to review development setbacks for erosion with a 1 % annual exceedance probability (AEP) previously identified in Dahm and Munro (2002) and to determine potential long term impacts from coastal erosion. The report used a collection of beach profile data, historical aerial photos, field work, and related all results to the location of the dune toe. The beach profile data used was from the same database used in this thesis, however, only the EW data was available to Dahm and Gibberd (2009) because the remaining data were from a private dataset. The study used approximately 20 to 25 profile surveys at each site from 1979 to 2004, with some additional surveying in late 2008 following the July 2008 storm event. Approximately one quarter of the profile data available in this thesis was used by Dahm and Gibberd (2009). Overall, the report concluded that Coromandel beaches were in a state of dynamic equilibrium with no long term trend for erosion or accretion.

5.5.3.2 *General Findings and Discussion*

Significant erosion events occur following large storm events on the Coromandel Peninsula with the largest in 1978 (Hume et al., 1992) and 2008. These two events were the largest erosion events on many Coromandel Beaches in surveyed history. Severe erosion on the Coromandel was deemed more common following a number of consecutive storms (Dahm & Gibberd, 2009), typical of uniform winter erosion as identified in Chapter 4. The results presented in this thesis suggest that these individual events coupled with long term trends provide the most severe erosion, which was prominent in the demeaned beach volume timeseries (Appendix VII). The 1978 and 2008 events were the largest in recent history, therefore large events coupled with already low beach volumes are most likely to affect development and infrastructure.

The significance of such large storm events also depended on the long term state of the beach. Multi-decadal scale erosion and accretion trends have been shown to occur on many Coromandel Beaches which contribute to individual erosion events. The findings from Dahm and Gibberd (2009) largely conform to IPO variations identified within this chapter, as well as Bryan et al. (2008), Oldman et al. (2003), and as suggested by de Lange (2000). Decadal scale persistence of La Niña events and the ensuing storms are likely to induce a greater amount of erosion compared to the equivalent El Niño events during a positive IPO phase. As a result, Dahm and Gibberd (2009) suggested two periods of widespread erosion on eastern Coromandel beaches since the 1960's:

- The period from the late 1960s (about 1967 / 1968) to 1978, with maximum dune erosion following the July 1978 storm event (Dahm and Munro, 2002). In subsequent years, most (not all) eastern Coromandel beaches went through a period dominated by beach and dune recovery, extending through to at least the early-mid 1990s at most sites; and,
- The period from the mid-late 1990s (typically 1995/96) to the early 2000s (approximately 2003). Severe dune erosion cumulated at a number of beaches during this period (e.g. Buffalo, Ohuka, Otahu and Whangapoua Beaches).

The first bullet point accords to IPO trends discussed in Section 5.4.2 above. Regarding the second bullet point, the results presented in Chapter 3, this Chapter, and Appendix VII showed that severe erosion during the mid to late 1990's to approximately 2003 were very site specific trends as most beaches showed accretion from approximately 1999 until 2005 in accordance with positive / increasing IPO and decreasing / negative ENSO indices (Appendix VII). Erosion during this period was most evident on beaches in Mercury Bay. Erosion was prevalent in the mid to late 1990's, however not into the 2000's at most sites. Beach specific comparisons are discussed in the proceeding sections below.

5.5.3.3 Summary: Whangapoua Beach

The July 2008 storm event was the largest erosion event recorded at Whangapoua Beach. The report states that the most severe long term dune erosion at Whangapoua Beach occurred in the late 1990's and early 2000's. Results presented in this thesis showed that the beach volumes were low / eroding from 1993 until 1999. The standard deviation of beach volume for Whangapoua Beach was 14 % (Figure 5.8). Figure 5.8 showed that most surveyed volumes were within one standard deviation of the mean and therefore not considered severe. Several storm events in the late 1990's and early 2000's caused erosion which was greater than one standard deviation below the mean in 1996, 1999, and 2000. The latter two events were superimposed on an accretion trend from 1996 to 2007 in which beach volumes increased by approximately 30 %. Of the data used by Dahm and Gibberd (2009), only the 1996 event was more than one standard deviation below the mean. Whangapoua Beach volumes from 2003 to 2007 were near the highest in surveyed history across the entire beach and were more than one standard deviation from the mean on several occasions.

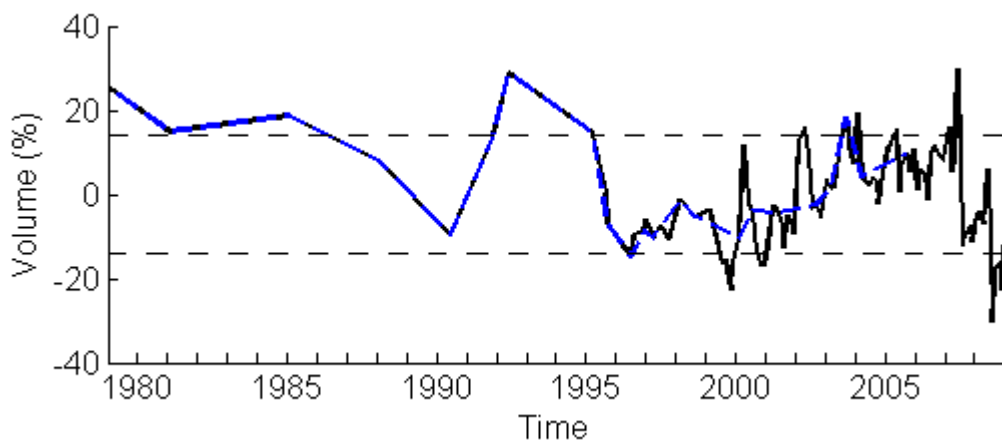


Figure 5.8: Comparison of Whangapoua Beach volumes using the data in this thesis (solid black line) compared to the data used in Dahm and Gibberd (2009; dashed blue line). The horizontal dashed black lines represent one standard deviation above and below the mean. Three surveys exceeded two standard deviations from the mean, they were accretion events in 1992 and 2007, and the July 2008 erosion event.

5.5.3.4 *Summary: Matarangi Beach*

Dahm and Gibberd (2009) used the southernmost (eastern) profile because it was deemed representative of the entire beach. Their erosion estimates determined for each site exceeded the worst measured erosion at each site. The July 2008 event was observed as causing slightly less erosion than the July 1978 event (Dahm & Gibberd, 2009). Analysis of these two profiles showed that the July 2008 event caused further landward retreat at all elevations except for a small region between RL 1.9 m and RL 2.2 m, when compared to the July 1978 event. In particular, the MSL contour was located approximately 15 m further landward in 2008, MHWS was located approximately 10 m further landward in 2008, and the dune region above RL 3.5 m was approximately 1 m to 3 m further landward in 2008. Matarangi Beach has been very stable overall with the greatest amount of variation occurring at the western end of the spit. All profiles are deemed stable in the long term.

5.5.3.5 *Summary: Rings Beach*

The PDS for Rings Beach was small compared to all other sites (Dahm & Gibberd, 2009) which acknowledged the stability of the beach system. Rings Beach was an outlier throughout this thesis due to the very small variation of the subaerial beach. This conformed to Dahm and Gibberd (2009) who state that the field observation of the PDS was very precautionary.

5.5.3.6 *Summary: Kuaotunu East Beach*

Data from the eastern profile site was not used by Dahm and Gibberd (2009) due to the proximity to the stream at the eastern end of the beach and because the central profile was considered representative of the beach. The July 2008 storm event caused the largest measured erosion across the entire beach. Prior to this event, the central profile had a long term trend of accretion from 1979. In contrast, the data from the western end of the beach had a decreasing linear trend from 2000 to 2009 indicating that the central profile was not representative of the entire beach. The beach volume data for Kuaotunu East also showed that the central profile had the smallest degree of short term variation (Figure VII.5) which

showed that the beach was more variable at each end, indicative of rotation which was evident, but not strong (Figure 4.6).

5.5.3.7 *Summary: Opito Beach*

Overall, the beach was very stable except for the northernmost profile. A majority of the beach has shallow Pleistocene sediment which is erosion resistant at the timescales of analysis considered. In contrast, the profile at the northern end had significant fluctuations of approximately 100 m attributed to realignment of an adjacent stream several decades ago (Dahm & Gibberd, 2009). The subsequent variations at the northern site were very small in comparison, which was applicable for a majority of the dataset. The significant fluctuation in the late 1970's would have significantly reduced the mean. The results from Dahm and Gibberd (2009) conform to observations within this thesis, with the observation of erosion resistant sediment confirming the primary reason for the stability of the beach.

5.5.3.8 *Summary: Wharekaho Beach*

The results presented by Dahm and Gibberd (2009) conform to those presented in this thesis for Wharekaho Beach. The northern regions of the beach showed very little variation and have a largely erosion resistant substrate. The southern site had more erodible sediment, and therefore a larger degree of variation.

5.5.3.9 *Summary: Buffalo Beach*

The results presented by Dahm and Gibberd (2009) conform to those presented in this thesis for Buffalo Beach. Although not all sites were reviewed, the data showed a large degree of variation between sites due to various natural, artificial, and human influenced factors. The only inconsistency was the timing of the identified period of most severe erosion, being in mid 2001 at the southern site (Dahm & Gibberd, 2009) compared to mid 2000 shown in Figure VII.9.

5.5.3.10 *Summary: Maramaratotara Beach*

Maramaratotara Beach was identified as an outlier beach in this thesis due to the very small degree of variation exhibited at all time scales. This compared well with the findings of Dahm and Gibberd (2009) who hypothesised that the limited beach erosion was due to the presence of erosion resistant material. The beach was described as having a thin veneer of sediment overlaying the erosion resistant material, a pre-Holocene shore platform resulting from cliff erosion.

5.5.3.11 *Summary: Hahei Beach*

The northern site at Hahei had relatively small dune toe fluctuations and the most severe erosion occurred during the 1980's and 2003 (Dahm & Gibberd, 2009). The availability of more recent data in this thesis showed that a slightly greater erosion event occurred in 2005, although the dune toe remained stable with a large amount of sediment eroded from the lower beach. The southern site was similar, except the largest dune erosion occurred following an event in 2007. The relative stability was attributed to most of the beach having an erosion resistant sub layer of pre-Holocene sediment (Dahm & Gibberd, 2009).

5.5.3.12 *Summary: Tairua Beach*

All observations made by Dahm and Gibberd (2009) were verified in this thesis. However, a justification for the different behaviour and the significant erosion at the southern end in 2003 was not given by Dahm and Gibberd (2009). Beach rotation analysis in Chapter 4 proved that a large clockwise rotation event occurred with relative erosion at the southern end of the beach and accretion at the northern end. The beach volume behaviour at each end showed opposing trends for most of the timeseries indicating the significance beach rotation has at Tairua Beach. This phenomenon was considered significant and needs to be included in any future erosion trend analysis at Tairua Beach. Further, beach behaviour at the centre of the beach cannot be described by the northern or southern profile behaviour.

5.5.3.13 *Summary: Whangamata North Beach*

Only the southern site at Whangamata North was analysed by Dahm and Gibberd (2009). The PDS determined was deemed conservative because the largest erosion event, the July 1978 storm, was located at least 5 m seaward of their erosion estimates. The southern site at Whangamata North showed no severe erosion events which occurred on most Coromandel beaches which is attributed to the embayed morphology of the beach. Similarly, the northern profile showed a large degree of short term variation, but relative stability in the long term with no apparent severe erosion events.

5.5.3.14 *Summary: Whangamata South Beach*

Dahm and Gibberd (2009) showed that the worst erosion at the northern end of the beach occurred in 1979, compared to the rest of the beach which occurred in 2003. The latter conforms to findings presented in this thesis as profile data was not available from 1979 except at the southern end of the beach. Overall, Whangamata South was relatively stable as identified at Whangamata North. The sheltering effect from adjacent and nearby islands may have a significant impact on beach behaviour as evidenced by the apparent lack of large erosion events.

5.5.4 Interannual Variation in Wave Conditions

Lomb-Scargle spectral analysis was performed on the wave data because it is also applicable to evenly spaced data (Lomb, 1976; Scargle, 1982). However, there was one month of missing data during 1997 therefore the Lomb-Scargle method was ideal. The similarity between the Lomb-Scargle results for the IPO and wave data suggest that the IPO also affected wave climate on an approximate 9.5 year scale. The 40.2 year cycle identified was similar to the IPO oscillation commonly accepted to be 40 – 70 years (Mantua et al., 1997; Minobe, 1999; de Lange, 2000; Mantua & Hare, 2002). This oscillation was likely to be related to the IPO, but due to the 30 year wave data available the timing of the previous peak may not be exact, similar to the IPO peaks identified in the volume data. The oscillation appeared to be directly linked with the overall IPO trend whereas the beach volume data was only long enough to show a relationship with the recent IPO

trend. The IPO has been linked with wave climate variations which further confirm the relationship (Goring & Bell, 1999; de Lange & Gibb, 2000; Salinger et al., 2001).

The similarity between the low frequency wave climate variations, the IPO, and recent beach volume trends suggest a relationship between the IPO mechanisms on wave climate and subsequent beach response. Of interest however, was that the number of storm wave events showed no apparent correlation with the IPO or ENSO index. Approximately half of all storm wave events occurred during positive ENSO and IPO indices, and similarly for negative indices. This contrasts to many published results which state that La Niña events are coupled with a larger number of storm wave events in the south west Pacific Ocean (e.g. Storlazzi & Griggs, 1998a; 1998b; de Lange, 2000; Harley, 2009b). The reasons for this are unknown, however may be attributed to the parameters used in the wave model hindcast.

5.6 SUMMARY

Analysis of interannual beach behaviour showed that the beach state classification was not a determining factor, however spatial variation, beach orientation, and large scale littoral drift systems were important. The following conclusions can be drawn from the interannual analyses:

- Many Coromandel beaches had linear erosion trends from 1995 to 2009 which accords to a decreasing IPO trend. The 30 year trends were also erosion dominated, however provided worst case erosion rates due to the uneven temporal sampling resolution of the data, with early surveys undertaken during periods of high beach volumes. Beach volumes during the late 1980's and early 1990's were the highest since the late 1970's, and likely to have been the highest since the early 1940's.
- Beaches north of the Kuaotunu Peninsula appeared to be part of a nearshore littoral drift system from Otama to Whangapoua. The eastern ends of these beaches were typical of downdrift erosion from headland bypassing (Rings Beach was excluded as it consisted of one profile only).

- Most beaches south of the Kuaotunu Peninsula had an increasing erosion trend toward the southern end of the beach. It is hypothesised that the southern ends of Coromandel beaches are more prone to north-easterly storm wave events in which the northern end of these beaches are partially sheltered.
- A significant biennial oscillation was evident at most beaches south of the Kuaotunu Peninsula, and none to the north. This appeared to be related to ENSO oscillations prevalent in the south Pacific.
- An approximate 12 year oscillation accorded to the IPO oscillation was evident in all beaches north of the Kuaotunu Peninsula, as well as several to the south.

Overall, beaches with an easterly orientation appear to be more affected by ENSO oscillations on a timescale of approximately 2.5 years. Beaches with a more northerly orientation were more affected by the IPO, although it was evident across the entire Peninsula.

A comparison of the results presented in this thesis compared to the report prepared by Dahm and Gibberd (2009) resulted in the following conclusions:

- The July 2008 storm event was the largest in surveyed history across most Coromandel beaches. The July 2008 and 1978 events had the most widespread and significant erosion at most Coromandel beaches therefore individual storm events are deemed to have a greater impact than cumulative storm events as suggested by Dahm and Gibberd (2009).
- The results presented by Dahm and Gibberd (2009) for Whangapoua Beach differ to those presented identified in this chapter. The results in this thesis are considered more representative due to the higher resolution timeseries used. This was most evident in Figure 5.8 in which the severe erosion period reported by Dahm and Gibberd (2009) was generally within one standard deviation of the mean volume.
- Their analysis of Kuaotunu East Beach stated that the central profile was representative of the entire beach. Results in this chapter showed the

central profile was the most stable, therefore not representative of the entire beach.

- Beach rotation events were significant at Tairua Beach and not accounted for in the PDS at Tairua Beach.

CHAPTER SIX

CONCLUSIONS AND RECOMMENDATIONS

6.1 INTRODUCTION

This research aimed to quantify the temporal and spatial variation of beach behaviour on the eastern Coromandel Peninsula. A large beach profile dataset of approximately 5500 surveys across 61 profile sites from 1979 to 2009 was used. Analysis of the data was undertaken at four timescales; 6-weekly, seasonal, interannual, and the long term trends. The conclusions presented in this chapter relate directly to the expected outcomes and hypotheses identified within each chapter, and address the 4 research aims of the thesis identified in Section 1.2.

A summary classification table and map (Figure 6.1 and Table 6-1), based on the data presented in Table 2-1 and the subsequent beach state classifications identified in this thesis, are presented below. Figure 6.1 showed the beach locations and the corresponding behavioural responses identified at all timescales in this thesis. The map information is contained in Table 6-1. The summary relates to overall average beach behaviour as opposed to individual profile behaviour and provides a summary of Coromandel beach behaviour. The 3 character reference on the map corresponds to the 3 right hand columns of the table, those being: episodic class; seasonal class; and, interannual class. A key for the alpha-numeric reference is also located in Table 6-1. For example, Hahei Beach (BB3) is deciphered as follows: Episodic class B, therefore being an intermediate beach with had a low magnitude of large volume change events; Seasonal class B, therefore being an intermediate beach which had a moderate seasonal amplitude; and, Interannual class 3, therefore it is located south of the Kuaotunu Peninsula in which ENSO and IPO were typically evident.

6.2 BEACH CLASSIFICATION

Chapter 2 described the geomorphologic variation between the 19 beaches. The initial classification showed the difference in beach orientations north and south of the Kuaotunu Peninsula (Figure 2.4). The data in Chapter 2 provided base information for the resulting classification using the Wright and Short (1984) beach state model. The average intertidal beach slope and dimensionless fall parameter calculations suggested two overall beach groups, intermediate and reflective sloped beaches. Analysis of the behaviour in subsequent chapters identified a total of four classifications using the data presented: intermediate beaches; reflective beaches; harbour adjacent beaches; and, outliers. The latter two classifications were anomalies to the Wright and Short (1984) model in which harbour adjacent beaches were intermediate beaches but had behavioural characteristics similar to reflective beaches, a consequence of being located immediately adjacent to harbour / estuary mouths. Rings Beach (an outlier) had similar geomorphologic characteristics to other sandy beaches, however the behaviour was significantly different. Maramaratotara Beach (the other outlier) had coarse calcite sediment which was deemed to affect beach behaviour.

6.3 SHORT TERM BEACH VARIATION

The beach classification was applied to short term beach morphology changes on Coromandel beaches. The analysis showed that short term behaviour was dependent on the intertidal slope and grain size, and thus followed the beach state classification of Wright and Short (1984). In particular, short term beach variation accorded to their model by exhibiting the following behaviour:

- Intermediate beaches have more small volume changes and rare large volume change events. Within all intermediate beaches studies there was more variability in behaviour than all reflective beaches. The smaller volume changes were illustrated by lower standard deviations of beach volume and a higher frequency of low magnitude of change events. The variation of beach states was attributed to the greater range of beach slopes, the different grain size between profiles, and exponential decay constants, which ultimately governed the behaviour. Cross-shore variation

of intermediate beaches showed increasing variation with decreasing elevation on the beach face, in particular, the intertidal area varied the most. The standard deviation of beach volume increased from the dune to upper beach to intertidal region.

- Reflective beaches had the greatest volume variations which was particularly evident in the magnitude of change analysis. Also of significance was the reflective beaches had more variable upper beach regions than intertidal regions which were in direct contrast to intermediate beaches. The reflective beaches all had very similar short term behaviours as identified by the higher standard deviations, higher magnitudes of change, and similar decay constants. The behaviour was attributed to the coarse grains and steep beach faces impacting nearshore wave processes such as wave run-up.
- Harbour adjacent beaches were intermediate sloped beaches but had a high frequency of large magnitude of change events and larger standard deviations of volume. This behaviour was similar to reflective beaches. The intertidal region was the most variable on harbour adjacent beaches. Harbour adjacent beaches also had a narrow range of sediment sizes, intertidal beach slopes, and similar behaviour between the four sites.
- Outlier beaches had a very large frequency of low magnitude of change events and had very little short term beach variation. These two beaches had the smallest standard deviations of beach volume at all cross-shore regions analysed.

Analysis showed that dune regions on all Coromandel beaches were very stable and seldom subjected to erosion events. The two largest storm events which had the greatest spatial impact occurred following the July 1978 event and July 2008 event. With regard to forcing mechanisms, analysis showed that beach volume change was poorly correlated to the time-averaged wave height between surveys. It is hypothesised that analysis of beach volume change needs to incorporate shorter term wave climate variations as well as the timing of storm events to better understand individual beach response to storms. The only conclusion drawn from the short term analysis at Ngarunui Beach was that most of the variation occurred

within the intertidal region which was also typical of east coast intermediate beaches. The intertidal area had a significantly greater elevation range and cross shore extent due to the greater tidal range and low beach slope. Therefore, it would be expected that greater intertidal volume variations could occur, even though dissipative beaches typically represent eroded systems.

6.4 SEASONAL VARIATION AND OSCILLATION

The beach state classifications also applied to Coromandel beach behaviour on the seasonal scale. Reflective beaches had a stronger seasonal oscillation than intermediate beaches, and also reached their peak seasonal volume earlier in the year. Reflective beaches had a seasonal volume variation of approximately 15 % whereas intermediate beaches were approximately 10 %. Outlier beaches had a seasonal signal although it was very small (<5 %). All beaches had uniform erosion in winter however it only occurred for 6 weeks during July and the first half of August. The anomalies to this behaviour were profiles located adjacent to harbour entrances which showed irregular behaviour through the year, often with increased volumes during winter, attributed to sediment inputs from the adjacent harbour / estuary during storm and heavy precipitation events. Spectral analyses of raw volume data showed significant seasonal oscillations at several beaches which was not anticipated given the sampling frequency of the data. Therefore, the beaches that showed spectral peaks of 1 year were considered to have strong seasonal signals. Only 1 profile site south of the Kuaotunu Peninsula showed this spectral peak.

Beach rotation was prominent on embayed beaches on the Coromandel Peninsula. Of interest however, were the strong alongshore variations evident at Pauanui and Whangamata South Beaches. It was hypothesised that sediment pulses from the adjacent harbours caused the alongshore variations of up to 10°. Beach rotation versus the time-averaged wave energy flux between profiles yielded low correlations. Short term wave energy flux variations were subsequently deemed more significant and longer term rotation events appeared to be related to ENSO events. Seasonal variations in the wave data showed a typical winter spike in

wave height, as well as a spike in February and March. The summer increase only affected reflective beaches which showed erosion in the following 1.5 month interval.

6.5 INTERANNUAL BEACH VARIATIONS

Linear trend analysis showed that 15 year trends encasing the high resolution data overall showed greater change rates compared to 30 year trends. The 15 year trend was impacted by positive ENSO and IPO events in the early to mid 1990's, followed by a decreasing trend and subsequent impacts in the late 1990's and early 2000's. The 30 year trends were considered more representative of long term behaviour. However, most surveys prior to 1990 were sampled in summer, therefore were highly likely to have had high beach volumes, which were compounded by a positive IPO phase, and are therefore considered to be exaggerated erosion trends. The onset of a negative IPO phase from approximately 2008 does present an interesting anomaly, because decadal scale persistence of La Niña trends for the next 20 to 35 years are likely to cause long term erosion of eastern Coromandel beaches. The linear trend analysis showed strong evidence for a nearshore littoral drift system on beaches north of the Kuaotunu Peninsula. Increasing beach volume trends from east to west, as well as erosion at all beaches (excluding Rings which had insufficient data) at the eastern or downdrift side of the headlands were used to determine this hypothesis.

ENSO and IPO impacts on subaerial beach volume trends were initially identified by qualitative observations of beach volume data and quantified using spectral analysis. ENSO was dominant at a 2.5 year scale on beaches south of the Kuaotunu Peninsula, or alternatively, beaches with an easterly orientation. IPO variations were evident on beaches across the Coromandel Peninsula, and were most prominent north of the Kuaotunu Peninsula. The IPO oscillation was also stronger than the ENSO impacts as identified by the respective spectral powers. The trends evident in the volume data were affected by climatic variations in wave height and direction (e.g. Ranasinghe et al. 2004). Beach classification showed no apparent significance when analysing Coromandel Beaches on an interannual

scale. An approximate 40 year oscillation in the wave data suggest beaches will oscillate on a similar scale which is near the largest IPO scale.

6.5.1 Conclusions: Dahm and Gibberd (2009)

The following conclusions are suggested because some results presented in this thesis differ from the findings of Dahm and Gibberd (2009) which is the most recent and widespread study applicable to Coromandel beaches. The primary reason for the different results obtained was attributed to the different data used for analysis. Whilst the same beach profile dataset was used, Dahm and Gibberd (2009) had approximately one quarter of the data used in this thesis, and not all profile sites were analysed by Dahm and Gibberd (2009).

Overall, their report stated that cumulative storm events were most significant for determining primary development setbacks (PDS). This contrasts to evidence presented in their report and this thesis, that the individual storm events of July 1978 and July 2008 were the two largest erosion events that affected most eastern Coromandel beaches. This showed that the greatest erosion in surveyed history was caused by individual storm wave events. Results produced by Yates et al. (2009) also showed that when a beach is in an eroded state, higher equilibrium wave energy is required to continue eroding a beach, therefore a continual increase in wave energy is required to continually erode beaches, which is not likely. Further, sufficient data has not been available for an entire negative IPO phase, which has been hypothesised to continue for the next 20 to 35 years (Minobe, 1999; de Lange, 2000). Therefore, ensuing decadal scale persistence of La Niña conditions are likely to negatively affect beach volumes on the Coromandel Peninsula.

Regarding individual beaches, Whangapoua was stated as being in a severe erosion trend from the mid 1990's to approximately 2003. Analysis showed this cyclic behaviour to be insignificant, with only one profile survey during this period being more than one standard deviation below the mean beach volume. The beach also had an overall accretion trend from 1996 to 2007. At Kuaotunu

East Beach, the central profile was deemed representative of the beach behaviour by Dahm and Gibberd (2009). It was shown that this profile was the most stable of the three on Kuaotunu East Beach, therefore was not likely to be representative of the entire beach behaviour which also showed varying degrees of rotation. Lastly, Tairua Beach rotated which contributed to beach variations at the short term, medium term, and interannual scale therefore needs to be accounted for. Alongshore variations at Tairua were not identified by Dahm and Gibberd (2009).

6.6 RECOMMENDATIONS FOR FURTHER RESEARCH

Results presented in this thesis showed that Coromandel beaches showed a large degree of variation. Recommendations and suggestions for further analysis and monitoring efforts are as follows:

- Ideally, profiling at the current frequency should be retained where possible as the dataset is largely unprecedented due to its temporal and spatial variation, unless other monitoring methods are implemented. At a minimum, all profile sites should be maintained on a biannual sampling regime. For the intermediate beaches, the first should occur around April and May, and the second in September to encase maximum annual variations. For reflective beaches, the first survey should be in February or March. This will still enable interannual trends to be identified.
- Intermediate beaches north of the Kuaotunu Peninsula all had similar short term beach volume changes, seasonal oscillations (excluding Otama), and showed strong IPO signals. Results suggest that further analysis may identify a potential indicator beach between these systems as they showed similar behaviour at all timescales of analysis.
- Reflective beaches showed similar trends at all scales which also suggest that a potential indicator beach scenario may exist.
- Further detailed analysis of harbour adjacent beaches, including Buffalo Beach and Cooks Beach, is unlikely to yield predictive mechanisms. Therefore, the high frequency monitoring should be maintained at these sites so ongoing analyses of the behaviours can be determined. This is also significant given that most of these beaches have some of the most

seaward located development on the Peninsula, and they did not show typical responses to short or long term trends, which highlights the unpredictability of these systems.

- Rings Beach and Maramaratotara Beach are not likely to be subject to any significant variation in the foreseeable future, therefore biannual surveying is considered suitable.
- Further large spatial scale research should focus on the 3 apparent sediment transport / behaviour cells identified, being: northerly orientated beaches located north of the Kuaotunu Peninsula from Whangapoua to Otama; Mercury Bay beaches including Opito Bay; and, easterly orientated beaches from Hahei to Whiritoa.
- Detailed analysis at no greater than 5 year intervals should be undertaken in order to continue sufficient analysis of cumulative impacts from ENSO events, rotation (where applicable), and IPO driven changes.
 - Erosion dominant conditions are likely to persist for the next 20 to 35 years on the Coromandel Peninsula. Analysis of the spectral power of the IPO coupled with storm erosion monitoring and modelling may provide vital information on potential risks to development and infrastructure.

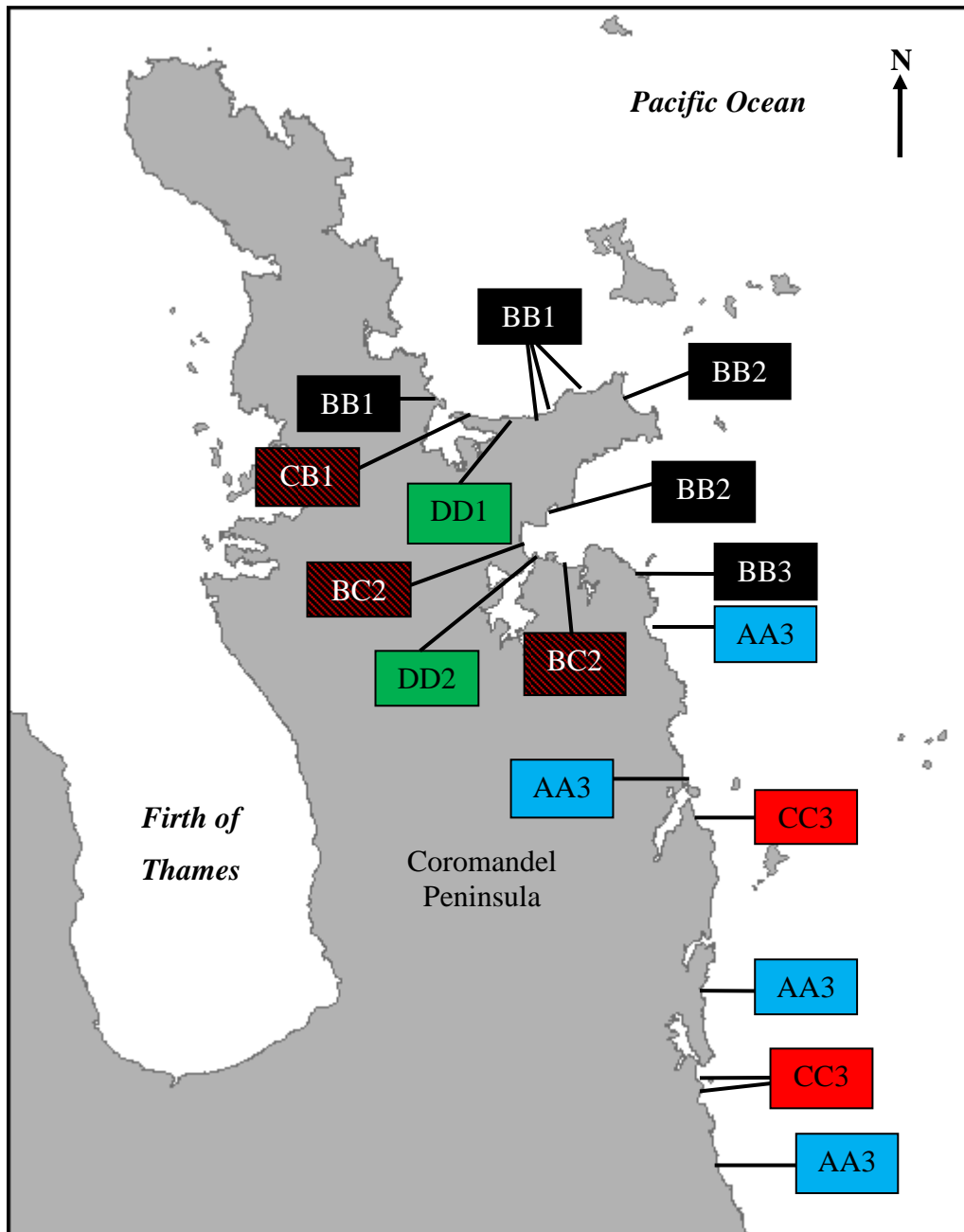


Figure 1: Site map with summary classifications. Refer Table 6-1 and in text for definitions.

Table 6-1: Summary beach classification data and beach state classifications for the episodic, seasonal, and interannual behaviour for Whangapoua to Maramaratotara Beaches.

Beach	Grain Size (μm)	Slope	Orientation ($^{\circ}$)	Episodic Class	Seasonal Class	Interannual Class
Whangapoua	322	0.05	41	B	B	1
Matarangi	275	0.02	12	C	B	1
Rings	402	0.10	5	D	D	1
Kuaotunu West	346	0.06	348	B	B	1
Kuaotunu East	427	0.05	343	B	B	1
Otama	395	0.07	356	B	B*	1
Opito Bay	252	0.03	59	B	B	2
Wharekaho	306	0.05	120	B	B	2
Buffalo	197	0.02	83	B	C	2
Maramaratotara	1072	0.11	39	D	D	2
Classification Definitions:						
Episodic: A= High magnitude of large volume change events B= Low magnitude of large volume change events C= High magnitude of large volume change events D= Very little variation. Few large magnitude of change events		Seasonal: A= Strong seasonal cycle B= Moderate seasonal cycle C= Weak seasonal cycle D= Irregular behaviour and no seasonal cycle		Interannual: 1 = North of Kuaotunu Peninsula, IPO dominant 2 = Mercury Bay, ENSO dominant 3 = South of Mercury Bay, IPO and ENSO evident		

Table 6-1: continued for Cooks Beach to Whiritoa Beach.

Beach	Grain Size (µm)	Slope	Orientation (°)	Episodic Class	Seasonal Class	Interannual Class
Cooks	204	0.05	56	B	C*	2
Hahei	302	0.07	37	B	B	3
Hot Water	430	0.11	77	A	A	3
Tairua	427	0.12	53	A	A	3
Pauanui	246	0.04	71	C	C	3
Onemana	429	0.13	89	A	A	3
Whangamata North	247	0.04	74	C	C	3
Whangamata South	225	0.03	110	C	C	3
Whiritoa	395	0.13	66	A	A	3
Classification Definitions:						
Episodic: A= High magnitude of large volume change events B= Low magnitude of large volume change events C= High magnitude of large volume change events D= Very little variation. Few large magnitude of change events		Seasonal: A= Strong seasonal cycle B= Moderate seasonal cycle C= Weak seasonal cycle D= Irregular behaviour and no seasonal cycle		Interannual: 1 = North of Kuaotunu Peninsula, IPO dominant 2 = Mercury Bay, ENSO dominant 3 = South of Mercury Bay, IPO and ENSO evident		

Table 6-1: continued

Class	Sub-class			
BB	1	2	3	Intermediate beaches located across the entire Peninsula
CB	1			Harbour adjacent beach with intermediate behaviour on a seasonal scale located north of the Kuaotunu Peninsula
DD	1	2		Outlier beach located north of the Kuaotunu Peninsula and within Mercury Bay
BC		2		Harbour adjacent beach with intermediate behaviour on an episodic scale in Mercury Bay
AA			3	Reflective beaches located south of the Kuaotunu Peninsula
CC			3	Harbour adjacent beaches located south of the Kuaotunu Peninsula

*Otama Beach B** – the behaviour at Otama was identified as intermediate due to its initial classification, timing of the peak seasonal volume, and location being north of the Kuaotunu Peninsula. The seasonal behaviour was significantly higher at Otama than all other Coromandel beaches.

*Cooks Beach C** – the behaviour at Cooks Beach was identified as harbour adjacent at the seasonal scale. The three profiles located nearest the harbour entrance all showed harbour adjacent behaviour, that being irregular with no seasonal scale. The two northern profiles on Cooks Beach showed strong seasonal cycles similar to the intermediate beaches with a peak seasonal volume in April to May, and an overall variation of approximately 10 %.

REFERENCES

- Aagaard, T., Davidson-Arnott, R., Greenwood, B., & Nielsen, J. (2004). Sediment supply from shoreface to dunes: linking sediment transport measurements and long-term morphological evolution. *Geomorphology*, *60*, 205–224.
- Anthony, E.J. (1998). Sediment-wave parametric characterization of beaches. *Journal of Coastal Research*, *14*(1), 347-352.
- Aubrey, D.G., & Ross, R.M. (1985). The quantitative description of beach cycles. *Marine Geology*, *69*, 155-170.
- Bittencourt, A.C.S.P., Sampaio, E.E.S., & Farias, F.F. (1997). Beach imaging through the time evolution of topographical profiles. *Journal of Coastal Research*, *13*(4), 1141-1149.
- Bogle, J.A., Bryan, K.R., Black, K.P., Hume, T.M., & Healy, T.R. (2001). Video observations of rip formation and evolution. *Journal of Coastal Research*, *SI 34*, 117-127.
- Bowman, D., Guillen, J., Lopez, L., & Pellegrino, V. (2009). Planview geometry and morphological characteristics of pocket beaches on the Catalan coast (Spain). *Geomorphology*, *108*, 191-199.
- Bradshaw, B.E. (1991). *Nearshore and inner shelf sedimentation on the east Coromandel Coast, New Zealand* (Unpublished PhD thesis). University of Waikato, Hamilton, New Zealand.
- Bryan, K.R., Gallop, S.L., van de Lageweg, W.I., & Coco, G. (2009). Observations of rip channels, sandbar-shoreline coupling and beach rotation at Tairua Beach, New Zealand. In I. Dawe (Ed.), *Proceedings of Australasian Coasts and Ports Conference 2009*. Wellington, New Zealand: New Zealand Coastal Society.
- Bryan, K.R., Kench, P.S., & Hart, D.E. (2008). Multi-decadal coastal change in New Zealand: Evidence, mechanisms and implications. *New Zealand Geographer*, *64*, 117-128.
- Bryan, K.R., Robinson, A., & Briggs, R.M. (2007). Spatial and temporal-variability of titanomagnetite placer deposits on a predominantly black sand beach. *Marine Geology*, *236*(1-2), 45-59.
- Capobianco, M., de Vriend, H.J., Nicholls, R.J., & Stive, M.J.F. (1999). Coastal area impact and vulnerability assessment: the point of view of a morphodynamic modeller. *Journal of Coastal Research*, *15*, 701-716.
- Carter, R.W.G., & Balsillie, J.H. (1983). A note on the amount of wave energy transmitted over nearshore sand bars. *Earth Surface Processes and Landforms*, *8*(3), 213-222.
- Clarke, D.J., & Eliot, I.G. (1988). Low-frequency changes of sediment volume on the beachface at Warilla Beach, New South Wales, 1975-1985. *Marine Geology*, *79*, 189-211.
- Crowell, M., Leatherman, S.P., & Buckley, M.K. (1991). Historical Shoreline Change: Error Analysis and Mapping Accuracy. *Journal of Coastal Research*, *7*(3), 839-852.
- Dahm, J., & Gibberd, B. (2009). *Coromandel beaches – coastal hazards: Review of primary development setback at selected beaches* (Thames Coromandel District Council). Hamilton, New Zealand: Focus Resource Management Group.

- Dahm, J., & Munro, A. (2002). *Coromandel beaches: Coastal hazards and development setback recommendations* (Environment Waikato Technical Report 02/06). Hamilton, New Zealand.
- Dail, H.J., Merrifield, M.A., & Bevis, M. (2000). Steep beach morphology changes due to energetic wave forcing. *Marine Geology*, 162, 443-458.
- Dalrymple, R.A., & Thompson, W.W. (1977). Study of equilibrium beach profiles. *Proceedings Fifteenth Coastal Engineering Conference, 1976, Honolulu: Hawaii*. (pp. 1277—1296). New York, USA: American Society of Civil Engineers.
- Davidson, M.A., & Turner, I.L. (2009). A behavioural template beach profile model for predicting seasonal to interannual shoreline evolution. *Journal of Geophysical Research*, 114, F01020.
- de Lange, W.P. (2000). Interdecadal Pacific Oscillation (IPO): a mechanism for forcing decadal scale coastal change on the Northeast coast of NZ? *Journal of Coastal Research*, SI 34, 657-664.
- de Lange, W.P., & Gibb, J.G. (2000). Seasonal, interannual, and decadal variability of storm surges at Tauranga, New Zealand. *New Zealand Journal of Marine and Freshwater Research*, 34(3), 419-434.
- de Lange, W.P., Healy, T.R., & Darlan, Y. (1997). Reproducibility of sieve and settling tube textural determinations for sand-sized beach sediment. *Journal of Coastal Research*, 13(1), 73-80.
- Dolan, R., Fenster, M.S., & Holme, S.J. (1991). Temporal analysis of shoreline recession and accretion. *Journal of Coastal Research*, 7(3), 723-744.
- Dubois, R.N. (1988). Seasonal changes in beach topography and beach volume in Delaware. *Marine Geology*, 8, 79-96.
- Eliot, I.G., & Clarke, D.J. (1982). Seasonal and biennial fluctuation in subaerial beach sediment volume on Warilla beach, New South Wales. *Marine Geology*, 48, 89-103.
- Eliot, I., & Clarke, D. (1989). Temporal and spatial bias in the estimation of shoreline rate-of-change statistics from beach survey information. *Coastal Management*, 17(2), 129-156.
- Emery, K.O. (1961). A simple method of measuring beach profiles. *Limnology and Oceanography*, 6(1), 90-93.
- Environment Waikato (2002). *Coastal hazards & development setback recommendations summary report May 2002*. Environment Waikato, 39pp.
- Fenster, M.S., & Dolan, R. (1993). Historical shoreline trends along the outer banks, North Carolina: Processes and responses. *Journal of Coastal Research*, 9(1), 172-188.
- Fenster, M.S., Dolan, R., & Eleder, J.F. (1993). A new method for predicting shoreline positions from historical data. *Journal of Coastal Research*, 9(1), 147-171.
- Gallop, S.L., Bryan, K.R., & Coco, G., (2009). Video observations of rip currents on an embayed beach. *Journal of Coastal Research*, SI 56, 49-53.
- Goikoetxea, N., Borja, A., Fontan, A., Gonzalez, M., & Valencia, V. (2009). Trends and anomalies in sea-surface temperature, observed over the last 60 years, within the southeastern Bay of Biscay. *Continental Shelf Research*, 29, 1060-1069.

- Goring, D.G. & Bell, R.G. (1999). El Niño and decadal effects on sea-level variability in northern New Zealand, a wavelet analysis. *New Zealand Journal of Marine and Freshwater Research*, 33(4), 587-598.
- Gorman, R.M., Bryan, K.R., & Laing, A.K. (2003a). Wave hindcast for the New Zealand region: deep-water wave climate. *New Zealand Journal of Marine and Freshwater Research*, 37, 589-612.
- Gorman, R.M., Bryan, K.R., & Laing, A.K. (2003b). Wave hindcast for the New Zealand region: nearshore validation and coastal wave climate. *New Zealand Journal of Marine and Freshwater Research*, 37, 567-588.
- Gourlay, M.R. (1992). Wave set-up, wave run-up and beach water-table - interaction between surf zone hydraulics and groundwater hydraulics. *Coastal Engineering*, 17(1-2), 93-144.
- Gunawardena, Y., Ilic, S., Southgate, H.N., & Pinkerton, H. (2008). Analysis of the spatio-temporal behaviour of beach morphology at Duck using fractal methods. *Marine Geology*, 252, 38-49.
- Harley, M.D., Turner, I.L., Short, A.D., & Ranasinghe, R. (2009a). Rotation and oscillation of an embayed beach. *Coastal Engineering 2008, 1-5*, 865-875.
- Harley, M.D. (2009b). *Daily to decadal embayed beach response to wave and climate forcing* (Unpublished PhD thesis). University of New South Wales, Sydney, Australia.
- Harley, M.D., Turner, I.L., Short, A.D., & Ranasinghe, R. (2009c). An empirical model of beach response to storms – SE Australia. In I. Dawe (Ed.), *Proceedings of Australasian Coasts and Ports Conference 2009*. Wellington, New Zealand: New Zealand Coastal Society.
- Hart, D.E., & Bryan, K.R. (2008). New Zealand coastal system boundaries, connections and management. *New Zealand Geographer*, 64, 129-143.
- Healy, T.R., & Dell, P.M. (1987). Baseline data beach surveys for management of an embayed coastline, east Coromandel, New Zealand. *Journal of Shoreline Management*, 3, 1-29.
- Healy, T.R., Dell, P.M., & Willoughby, A.J. (1981). *Coromandel coastal survey volume 1 basic survey data*. Hauraki Catchment Board. Report No. 114, 233pp.
- Holman, R.A., Symonds, G., Thornton, E.B., & Ranasinghe, R. (2006). Rip spacing and persistence on an embayed beach. *Journal of Geophysical Research*, 111, C01006.
- Hume, T.M. (1979). *Factors contributing to coastal erosion on the east coast of Northland during July 1978*. (Water and Soil Division Report). Auckland, New Zealand: Ministry of Works and Development.
- Hume, T.M., Bell, R.G., de Lange, W., Healy, T.R., Hicks, D.M., & Kirk, R.M. (1992). Coastal oceanography and sedimentology in New Zealand, 1967-91. *New Zealand Journal of Marine and Freshwater Research*, 26, 1-36.
- Hume, T.M. & Dahm, J. (1991). *An investigation of the effects of Polynesian and European land use on sedimentation in Coromandel estuaries*. Department of Conservation Consultancy Report, No. 7106:3, 47p.
- Inman, I.J. (1953). Aerial and seasonal variations in beach and near-shore sediments at La Jolla, California. *Beach Erosion Board Technical Memo. No. 39*.
- Jimenez, J.A., Guillen, J., & Falques, A. (2008). Comment on the article “Morphodynamic classification of sandy beaches in low energetic marine environment” by Gomez-Pujol, L., Orfilla, A., Canellas, B., Alvarez-

- Ellacuria, A., Mendez, F.J., Medina, R., & Tintore, J. *Marine Geology*, 242, pp. 235-246. *Marine Geology*, 255, 96-101.
- Klein, A.H.F., Benedet Filho, L., & Schumacher, D.H. (2002). Short-term beach rotation processes in distinct headland bay beach systems. *Journal of Coastal Research*, 18(3), 442-458.
- Komar, P.D. (1998). *Beach processes and sedimentation*. Upper Saddle River, New Jersey: Prentice Hall.
- Labitzke, K. (1982). On the interannual variability of the middle stratosphere during the northern winters. *Journal of the Meteorological Society of Japan*, 60, 124-138.
- Lacey, E.M., & Peck, J.A. (1998). Long-term beach profile variations along the south shore of Rhode Island, U.S.A. *Journal of Coastal Research*, 14(4), 1255-1264.
- Land Information New Zealand, (2009). *NZ202 Chart Catalogue*. Retrieved from www.linz.govt.nz/hydro/charts
- Larson, M., Capobianco, M., Jansen, H., Rozynski, G., Southgate, H., Stive, M., Wijnberg, K., & Hulscher, S. (2003). Analysis and modeling of field data on coastal morphological evolution over yearly and decadal time scales. Part 1: background and linear techniques. *Journal of Coastal Research*, 19(4), 760-775.
- Larson, M., & Kraus, N.C. (1994). Temporal and spatial scales of beach profile change, Duck, North Carolina. *Marine Geology*, 117, 75-94.
- Latif, M., & Barnett, T.P. (1996). Decadal climate variability over the North Pacific and North America: dynamics and predictability. *Journal of Climate*, 9, 2407-2423.
- Lee, G., Nicholls, R., & Birkemeier, W.A. (1998). Storm-driven variability of the beach-nearshore profile at Duck North Carolina, USA, 1981-1991. *Marine Geology*, 148, 163-177.
- List, J.H., & Farris, A.S. (1999). Large-scale shoreline response to storms and fair weather. In N.C. Kraus & W. G. McDougal (Ed.), *Coastal Sediments '99* (pp. 1324-1338). Reston, Va., U.S.A: American Society of Civil Engineers.
- Lizarraga-Arciniega, R., Martinez-Diaz de Leon, A., Delgado-Gonzalez, O., Torres, C.R., & Galindo-Bect, L. (2007). Alternation of beach erosion/accretion cycles related to wave action off Rosarito, Baja California, Mexico. *Ciencias Marinas*, 33(3), 259-269.
- Lomb, N.R. (1976). Least-squares frequency analysis of unequally spaced data. *Astrophysics and Space Science*, 39, 447-462.
- McLean, R.F. (1979). *Dimensions of the Whiritoa sand system and implications for sand mining and shore erosion*. Unpublished Report to the Hauraki Catchment Board, Te Aroha, New Zealand.
- Mantua, N.J., Hare, S.R., Zhang, Y., Wallace, J.M., & Francis, R.C. (1997). A Pacific interdecadal climate oscillation with impacts on salmon production. *Bulletin of the American Meteorological Society*, 78, 1069-1079.
- Mantua, N.J., & Hare, S.R. (2002). The Pacific decadal oscillation. *Journal of Oceanography*, 58, 35-44.
- Masselink, G., & Pattiaratchi, C.B. (2001). Seasonal changes in beach morphology along the sheltered coastline of Perth, Western Australia. *Marine Geology*, 172, 243-263.

- Mead, S., & Moores, A. (2005). *Estuary sedimentation: a review of estuarine sedimentation in the Waikato region* (Environment Waikato Technical Report Series 2005/13). Hamilton, New Zealand: Environment Waikato.
- Medina, R., Losada, M.A., Losada, I.J., & Vidal, C. (1994). Temporal and spatial relationship between sediment grain size and beach profile. *Marine Geology*, *118*, 195-206.
- Miller, J.K., & Dean, R.G. (2007a). Shoreline variability via empirical orthogonal function analysis: Part I temporal and spatial characteristics. *Coastal Engineering* *54*, 111-131.
- Miller, J.K., & Dean, R.G. (2007b). Shoreline variability via empirical orthogonal function analysis: Part II relationship to nearshore conditions. *Coastal Engineering* *54*, 133-150.
- Minobe, S. (1997). A 50-70 year climatic oscillation over the North Pacific and North America. *Geophysical Research Letters*, *24*, 683-686.
- Minobe, S. (1999). Resonance in bidecadal and pentadecadal climate oscillations over the North Pacific: Role in climatic regime shifts. *Geophysical Research Letters*, *26*, 855-858.
- Morton, R.A., Gibeaut, J.C., & Paine, J.G. (1995). Meso-scale transfer of sand during and after storms: implications for prediction of shoreline movement. *Marine Geology*, *126*, 161-179.
- Munoz-Perez, J.J., & Medina, R. (In press). Comparison of long-, medium- and short-term variations of beach profiles with and without submerged geological control. *Coastal Engineering*.
- Ojeda, E., & Guillen, J. (2008). Shoreline dynamics and beach rotation of artificial embayed beaches. *Marine Geology*, *253*, 51-62.
- Oldman, J.W., Smith, R.K., & Ovenden, R. (2003). *Coastal erosion hazard assessment of the Foreworld sites between Gill Rd and Franklin Rd, Bayview, Hawke Bay* (NIWA Client Report, FWL03202). Hamilton, New Zealand.
- Ozolcer, I.H. (2008). An experimental study on geometric characteristics of beach erosion profiles. *Ocean Engineering*, *35*, 17-27.
- Plant, N.G., Holman, R.A., Freilich, M.H., & Birkemeier, W.A. (1999). A simple model for interannual sandbar behavior. *Journal of Geophysical Research-Oceans*, *104*(C7), 15,755-15,776.
- Quartel, S., Kroon, A., & Ruessink, B.G. (2008). Seasonal accretion and erosion patterns of a microtidal sandy beach. *Marine Geology*, *250*, 19-33.
- Quiroz, R.S., 1981. Periodic modulation of the stratospheric quasi-biennial oscillation. *Monthly Weather Review*, *109*, 665-675.
- Ranasinghe, R., McLoughlin, R., Short, A., & Symonds, G. (2004). The southern oscillation index, wave climate, and beach rotation. *Marine Geology*, *204*, 273-287.
- Reeve, D., Li, Y., Lark, M., & Simmonds, D. (2007). An investigation of the multi-scale temporal variability of beach profiles at Duck using wavelet packet transforms. *Coastal Engineering*, *54*, 401-415.
- Rooney, J.J.B., & Fletcher, C.H. III. (2005). Shoreline change and Pacific climatic oscillations in Kihei, Maui, Hawaii. *Journal of Coastal Research*, *21*(3), 535-547.
- Ross, D.J., McQueen, D.J., & Kettles, H.A. (1994). Land rehabilitation under pasture on volcanic parent materials: changes in soil microbial biomass and C and N metabolism. *Australian Journal of Soil Research*, *32*, 1321-

- 1327.
- Ruf, T. (1999). The lomb-scargle periodical in biological rhythm research: analysis of incomplete and unequally spaced time-series. *Biological Rhythm Research*, 30(2), 178-201.
- Salinger, M.J., Renwick, J.A., & Mullan, A.B. (2001). Interdecadal pacific oscillation and south pacific climate. *International Journal of Climatology*, 21(14), 1705-1721.
- Scarfe, B.E. (2008). *Oceanographic considerations for the management and prediction of surfing breaks* (Unpublished PhD thesis). University of Waikato, Hamilton, New Zealand.
- Scargle, J. (1982). Studies in astronomical time-series analysis. II-Statistical aspects of spectral analysis of unevenly spaced data. *The Astrophysical Journal* 263, 835–853.
- Shepard, F.P. (1950). *Beach cycles in Southern California*. U.S. army corps of engineers, beach erosion board. Technical Memo. 20, Beach Erosion Board, U.S. Army Corps of Engineers, Washington D.C.
- Shoelson, B. (1999). *Lomb-Scargle*. Retrieved from Mathworks, Mathworks website: <http://www.mathworks.com/matlabcentral/fileexchange/993-lombscargle-m>
- Short, A.D. (1979a). Wave power and beach stages: A global model. *Proceedings Sixteenth International Conference: August 27 to September 3, 1978, Hamburg, Germany*. (pp.1145-1162). New York, U.S.A: American Society of Civil Engineers.
- Short, A.D. (1979b). Three dimensional beach stage model. *Journal of Geology*, 87, 553--571.
- Short, A.D. (1981). Beach response to variations in breaker height. *Proceedings Seventeenth Coastal Engineering Conference, March 23 to 28, 1980, Sydney: Australia*. (pp. 1016—1035) New York, USA: American Society of Civil Engineers.
- Short, A.D. (1999). Wave-dominated beaches. In A.D. Short, (Ed.), *Handbook of Beach and shoreface morphodynamics*, (pp. 173-203). Chichester, England: John Wiley & Sons Ltd.
- Short, A.D., Cowell, P.J., Cadee, M., Hall, W., & Van Dijke, B. (1995). Beach rotation and possible relation to the southern oscillation. *In Proceedings of Ocean and Atmosphere Pacific International Conference Adelaide*. (pp. 329-334). Adelaide, Australia: National Tidal Facility.
- Short, A.D., & Masselink, G. (1999). Embayed and structurally controlled beaches. In A.D. Short, (Ed.), *Handbook of Beach and shoreface morphodynamics*, (pp. 142-161). Chichester, England: John Wiley & Sons Ltd.
- Short, A.D., & Trembanis, A.C. (2004). Decadal scale patterns in beach oscillation and rotation Narrabeen Beach, Australia: Time series, PCA and wavelet analysis. *Journal of Coastal Research*, 20(2), 523-532.
- Short, A.D. & Wright, L.D. (1981). Beach systems of the Sydney region. *Australian Geographer*, 15, 8-16.
- Smith, R.K., & Bryan, K.R., (2007). Monitoring beach face volume with a combination of intermittent profiling and video imagery. *Journal of Coastal Research*, 23(4), 892-898.

- Smith, G.L. & Zarillo, G.A. (1990). Calculating long-term shoreline recession rates using aerial photographic and beach profiling techniques. *Journal of Coastal Research*, 6 (1), 111-120.
- Steeghs, L. (2007). *Morphodynamics of the Whitianga tidal inlet and Buffalo Bay, New Zealand*. (Unpublished MSc thesis). University of Waikato, Hamilton, New Zealand.
- Stewart, D. (2002). *Coromandel coastal survey historical data summary* (Environment Waikato Technical Report Series 2002/07). Hamilton, New Zealand: Environment Waikato.
- Stewart, D. (2006). *Coromandel coastal survey: establishing a common datum for surveys of Coromandel beach profiles* (Environment Waikato Technical Report Series 2006/01). Hamilton, New Zealand: Environment Waikato.
- Stive, M.J.F., Aarninkhof, S.G.J., Hamm, L., Hanson, H., Larson, M., Wijnberg, K.M., Nicholls, R.J., & Capobianco, M. (2002). Variability of shore and shoreline evolution. *Coastal Engineering*, 47, 211-235.
- Storlazzi, C.D., & Griggs, G.B. (1998a). The 1997-98 El Niño and erosion processes along the central coast of California. *Shore & Beach*, 66, 12-17.
- Storlazzi, C.D., & Griggs, G.B. (1998b). Influence of El Niño Southern Oscillation (ENSO) events on the coastline of central California. *Journal of Coastal Research*, SI 26, 146-153.
- Thom, B.G., & Hall, W. (1991). Behaviour of beach profiles during accretion and erosion dominated periods. *Earth Surface Processes and Landforms*, 16, 113-127.
- Van Loon, H., Zerefos, C.S. & Repapis, C.C. (1982). The southern oscillation in the stratosphere. *Monthly Weather Review*, 110, 225-229.
- Wijnberg, K.M. (2002). Environmental controls on decadal morphologic behaviour of the Holland coast. *Marine Geology*, 189, 227-247.
- Winant, C.D., Inman, D.L., & Nordstrom, C.E. (1975). Description of seasonal beach changes using empirical eigenfunctions. *Journal of Geophysical Research*, 80(15), 1979-1986.
- Wood, A., Bryan, K.R., Smith, R.K., Coco, G., & Pickett, V. (2009). Indicator beaches on the Coromandel Peninsular, New Zealand. In I. Dawe (Ed.), *Proceedings of Australasian Coasts and Ports Conference 2009*. Wellington., New Zealand: New Zealand Coastal Society.
- Wright, L.D., & Short A.D. (1983). Morphodynamics of beaches and surf zones in Australia. In P.D. Komar (Ed.), *Handbook of Coastal Processes and Erosion*, (pp. 35-64). Boca Raton, FL: CRC Press.
- Wright, L.D. (1981). Beach cut in relation to surfzone morphodynamics. *Proceedings Seventeenth Coastal Engineering Conference, March 23 to 28, 1980, Sydney: Australia*. (pp. 978-996) New York, USA: American Society of Civil Engineers.
- Wright, L.D., Nielsen, P., Short, A.D., & Green, M.O. (1982b). Morphodynamics of a macrotidal beach. *Marine Geology*, 50, 97-128.
- Wright, L.D., & Short, A.D. (1984). Morphodynamic variability of surf zones and beaches: a synthesis. *Marine Geology*, 56, 93-118.
- Yates, M.L., Guza, R.T., & O'Reilly, W.C. (2009). Equilibrium shoreline response: observations and modelling. *Journal of Geophysical Research*, 114, C09014.
- Zhang, Y., Wallace, J.M., & Battisti, D.S. (1997). ENSO-like interdecadal variability: 1900-93. *Journal of Climate*, 10(5), 1004- 1020.

Indicator beaches on the Coromandel Peninsula, New Zealand

Andrew Wood¹, Karin R. Bryan¹, R. Keith Smith², Giovanni Coco³ and Vernon Pickett⁴

¹University of Waikato, Hamilton, New Zealand

²Coastal Consultant, 178 Collins Road, RD2 Hamilton 3282

³National Institute of Water and Atmospheric Research, Hamilton, New Zealand

⁴Environment Waikato, Hamilton, New Zealand

Abstract

Analysis of the spatial and temporal variation of 18 beaches along the eastern Coromandel Peninsula (New Zealand) from Whangapoua in the north to Whiritoa in the south shows preliminary evidence of indicator beaches. These are beaches whose behaviour represents that of a similar group of beaches. Beach similarity was classified by measuring beach length, beach connectivity to neighbouring beaches, and aspect. Five beaches were selected for further analysis. The analysis of variability in beachface volumes was undertaken using an extensive beach profile database established in 1978. The database has a higher-resolution sampling interval from 1996 until present (a maximum sampling period of approximately bimonthly). Preliminary results show that the 5 selected beaches are in phase with the Interdecadal Pacific Oscillation (IPO). Superimposed on this trend were episodic events that were evident at most sites, whilst some displayed annual and/or inter-annual cycles of erosion and accretion. Variability associated with these events was different between beach sites, with shorter embayed beaches showing more stability than longer beaches. Moreover single storm events appear to have different impacts on different regions of the coast. As a result, a number of smaller sub-cells of behaviour can be identified along the Coromandel Peninsula.

1 Introduction

The eastern Coromandel Peninsula (New Zealand) beaches sustained considerable amounts of subdivision and land development during the 1960's (Healy et al. 1981; Environment Waikato 2002). Development was typically located close to the top of the frontal dune, and in many cases the dunes were levelled to provide views of the ocean from private dwellings (Environment Waikato 2002). As a result, erosion of the subaerial beach profile is a primary concern as many beaches are thought to be closed sedimentary systems (Healy et al. 1981), meaning that sediment supply is very limited and can lead to loss of recreation areas or private land.

Beach profiling via the Emery method (Emery 1961) is labour intensive and

thus widespread sampling at reasonable frequencies (i.e. the 6 weekly periods of the dataset analysed in this paper) can be very expensive. Identifying indicator beaches on the eastern Coromandel Peninsula would reduce the cost of beach monitoring while still providing suitable datasets whose outcomes are not solely related to one site. Timeseries data, statistical analysis, and the identification of erosion and accretion trends are necessary to understand the temporal and spatial variation of beach systems and are vital to coastal management. The rationale behind the development of a beach profile dataset is to identify and quantify the effect of wave climate on beachface spatial and temporal variability. This will in turn allow us to recognise indicator beaches for the Coromandel Peninsula where monitoring would generate data that could be

applied to other beaches that demonstrate similar behaviour. This will reduce the time, money and effort placed to sample numerous beaches. This paper provides interim results on the analysis undertaken to detect the presence of indicator beaches and sediment transport sub-cells on the eastern Coromandel Peninsula.

2 Methods

2.1 Study Sites and Data Classification

The eastern Coromandel Peninsula is a storm dominated coast (Bradshaw et al. 1990) with the predominant wave direction from the north east (Gorman et al. 2003) and an average spring tidal range of 1.8m. Five beaches were selected to encompass a range of behaviours represented in the 18-beach dataset (Fig. 1). Sediment samples to determine grain size characteristics were collected during a field excursion on the 25th and 26th May 2009. Sediment samples were obtained from the middle regions of the intertidal zone at each of the 61 profiles sites on the Coromandel Peninsula. Samples varied in size but were approximately 150 grams and comprised of sediment from the top 50-80mm of the beach.

Because of the possible effect on wave propagation, offshore islands were given a yes/no value depending on whether islands were present within 10 kilometres of the beach or within the 50m depth contour (whichever was smallest). Beach lengths were calculated from the ArcGIS 1:50,000 topographic database and were defined as the length of shoreline along the region containing sand and inlet (e.g. Hart and Bryan 2008). Beach orientation was calculated as the vector average of the orientation of the shoreline at both ends of the beach (e.g. Hart and Bryan 2008). Connection distance to the left and right (looking seaward) was calculated as the approximate distance of coastline between two beaches (e.g. Hart and Bryan 2008). The average intertidal beach slope was calculated using an average of the lowest 3 surveyed points (above MLWS) for the entire timeseries. Mean grain size characteristics were measured using the Rapid Sediment Analyser.

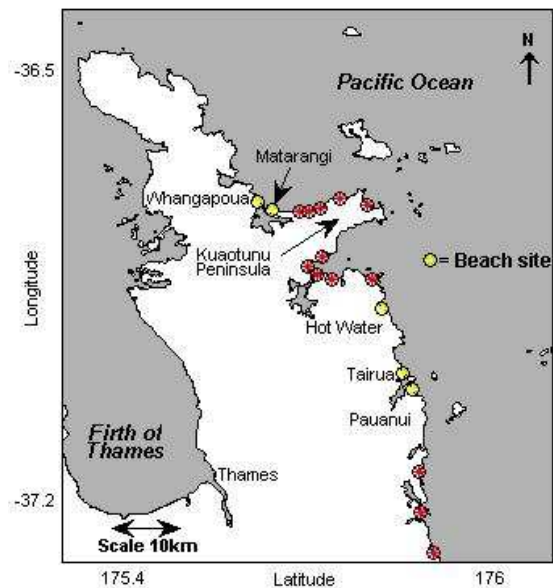


Figure 1: Coromandel Peninsula location map detailing the eighteen study sites comprised in the project along the east coast. Yellow markers denote beaches studied in this paper. Auckland is 75km west from Matarangi.

The northern most beach selected, Whangapoua, is a short (1804m, see Table 1) pocket beach with headland barriers at each end and a very small estuary at the northern end. Whangapoua Beach is an intermediate sloped beach (Table 1) with a median grain size of 250 μ m (fine sand). Pungapunga Island is a small island (2590m², taken from cadastral maps available in the Quickmap software) located toward the northern end of Whangapoua Beach approximately 150m seaward of mean high water springs.

Matarangi Beach is a dune barrier beach system, located immediately east of Whangapoua. Matarangi Beach is the longest (4618m, Table 1) and lowest-sloped beach analysed in this study (Table 1), and is characterised by a median grain size of 270 μ m (medium sand). Matarangi Beach abuts a headland at the eastern end of the beach and the spit extends to the west where it terminates at the entrance to Whangapoua Harbour.

Tairua and Pauanui are the southernmost beaches considered in this study and are separated by a headland and the entrance to Tairua Harbour. Tairua is a short (1511m), steep pocket beach (Table 1) with a

median grain size of 390µm (medium sand). Tairua Beach abuts headlands at each end. Pauanui is a relatively long (2899m) dune barrier beach with a low gradient (Table 1) and fine grained sediment (230µm fine sand). Pauanui Beach abuts a rocky headland to the south and terminates at Royal Billy Point in the entrance to Tairua Harbour in the north. Both Tairua and Pauanui beaches have offshore islands located landward of the 20m depth contour. Shoe Island is located 3km east of the Tairua Harbour entrance and Slipper Island is located 7km south east of the entrance. Hot Water Beach is centrally located between the four aforementioned beaches (Fig. 1). It is a short (1865m), steep beach (Table 1) with relatively coarse sediment (380µm medium sand) and three streams entering the coast at the northern, central, and southern sections of the beach. Hot Water Beach abuts headlands at each end.

Table 1: Beach classification parameters (see text for more details).

Beach Name	Beach Length (m)	Average Orientation (°)	Connection Distance (m)	Average Slope
Whangapoua	1804	41	L: 1230 R: 990	0.05
Matarangi	4618	12	L: 990 R: 735	0.02
Hot Water	1865	77	L: 1156 R: 5890	0.11
Tairua	1511	53	L: 2571 R: 1389	0.12
Pauanui	2899	71	L: 1389 R: 5201	0.03

The profile sites were established in 1979 after the renowned storms in winter 1978 (Hume 1979; cited in Hume et al 1992) and sporadically sampled by Environment Waikato. In addition, Keith Smith (Private Consultant) and Ron Ovenden (National Institute of Water and Atmospheric Research, NIWA) have been undertaking regular beach profile surveys of the Coromandel beaches since 1990 and have gathered an extensive database across 61 profile sites (5 of which are selected here). These have been profiled every 2

months since 1996 and 6-weekly more recently. All beach profiles were undertaken using the Emery method (Emery, 1961). Each survey begins from a known benchmark typically located landward of the dune crest. During each survey points of interest such as the edge of vegetation line, storm high water line, high water mark, and saturated surfaces were measured as often as possible (Smith and Bryan, 2007).

2.2 Data Analysis

Raw beach profile data were input into the Beach Profile Analysis Toolbox (BPAT) software. Upon verification in BPAT, profile surveys were analysed by a variety of different methods. The raw profile data were then extracted in ASCII format for analysis with Matlab Software. Computer algorithms were written to calculate various parameters of interest and to extract timeseries data consisting of: profile elevations; beach volumes; beach slope; summary statistics; and, seasonal trends. The beach volumes were divided into three regions comprising the dune region, the upper beach region, and the intertidal region. Statistical analysis was performed on each volume region. Seasonal trends were analysed by time-averaging and grouping the intertidal beach volumes into 6 week blocks over the entire 30-year dataset.

Intertidal beach volumes were evaluated by calculating the area under each individual beach profile from mean high water springs (MHWS) to mean low water springs (MLWS, relative level 0.9 to relative level -0.9). The average spring tidal range for the eastern Coromandel Peninsula is 1.8m (LINZ). The NIWA tide forecaster indicates the flood and ebb tides have approximately equal amplitudes hence the values of 0.9m and -0.9m above sea level (ASL) were used for upper and lower limits. The resulting "triangle" area under each beach profile was evaluated as part of the intertidal volume. The horizontal area from the intertidal zone landward to a common datum was then added to the triangle to quantify the advance or retreat of the profile. The upper beach area was calculated using the same method, with the elevation limits set from MHWS to 3.5m ASL. Visual observations indicate this is an average

elevation to which dune vegetation and storm debris are commonly located. This was then considered to be an accurate limit for the upper extent of regular wave action. In some cases, beach profiles did not extend as far as MLWS. These profiles were extrapolated by taking the last 3 surveyed points, averaging the slope between them and extending the data at the average gradient to MLWS.

3 Results

3.1 Intertidal Beach Volumes

Intertidal beach volumes from each of the five beach sites are shown in Figure 2. The beaches are plotted (top to bottom) from north to south and have been demeaned to give an indication of cut and fill rates. Relatively long term trends of erosion or accretion (e.g. greater than a seasonal cycle) occur at similar timeframes throughout the Peninsula. Each of the beach sites in Figure 2 displays a trend of accretion from the beginning of 2002 until early 2007. An erosion trend prior to this accretion event from 1998-2002 is also apparent in the data. These trends are less evident at Hot Water Beach. There are numerous occasions where relatively large erosion/accretion events are prominent. Some events or trends occur across more than one beach, but very seldom through all of them. For example, a period of accretion at the beginning of 2000 was observed in all the profiles except Pauanui Beach. An example where uniform accretion occurred for all the profiles is at the beginning of 2007 (Fig. 2). There is a gap in the data at Tairua Beach and Matarangi Beach where no profile

surveys were undertaken for a period of more than 12 months. At Matarangi there are no data prior to July 1996. At Tairua Beach there are no data from August 1996 to July 1999 and the Pauanui Beach data begins in July 1996.

Figure 3 illustrates timeseries of intertidal, upper beach, and dune volumes for Whangapoua Beach. The profiles are plotted against the Interdecadal Pacific Oscillation (IPO) for the same time period. Timeseries analysis of the three horizontal volume regions on Whangapoua Beach (Fig. 3) shows that intertidal and upper beach volumes follow long term trends of erosion/accretion similar to the temporal variations in the IPO index. A comparison with Figure 2 shows that intertidal beach volumes across the eastern Coromandel beaches analysed follow a similar long term trend of erosion and accretion. The derived beach volume timeseries shows a long term signal that is in phase with the IPO.

Figure 3 illustrates a marked similarity between the intertidal and upper beach volumes for Whangapoua Beach. Standard deviations of the three volume regions are plotted in Figure 4 for each site. The timeseries in Figure 3 does not illustrate a seasonal cycle because it is much smaller relative to the interannual variations. A storm event in July 2008 which caused significant intertidal erosion across the Peninsula (Fig. 2, but predominantly north of the Kuaotunu Peninsula) is evident in Figure 3 across the entire beach profile.

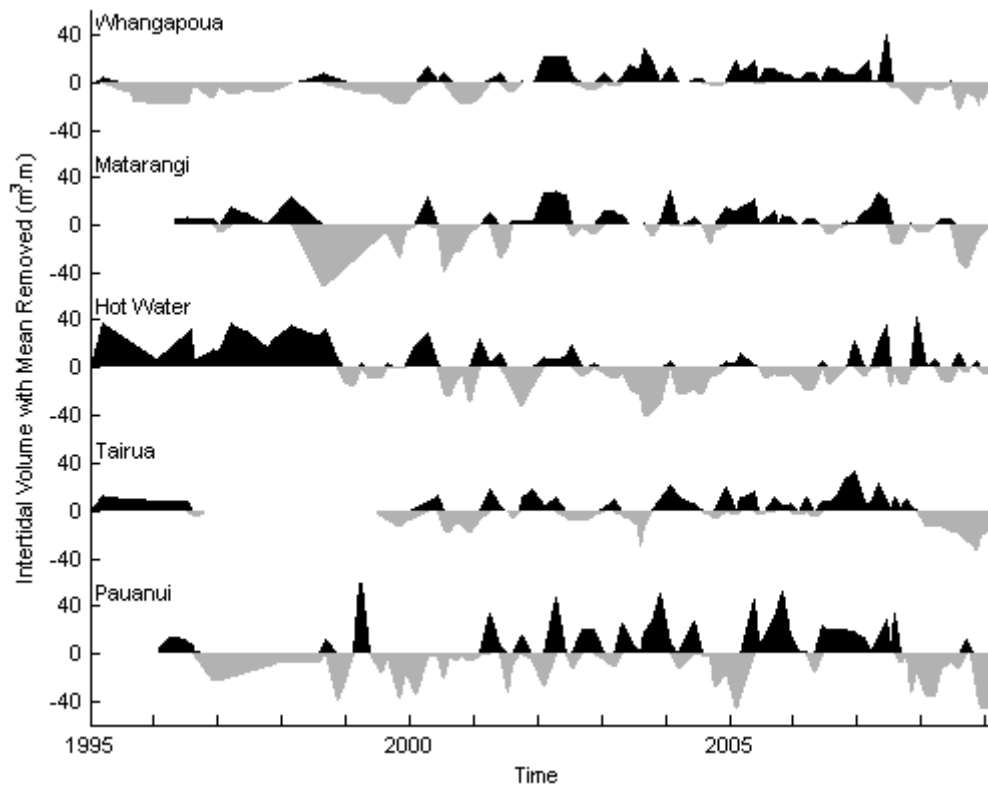


Figure 2: Intertidal beach volume trends for the five selected sites from north to south. All timeseries have been demeaned. The shaded areas above and below zero represent periods of erosion or accretion about the mean volume.

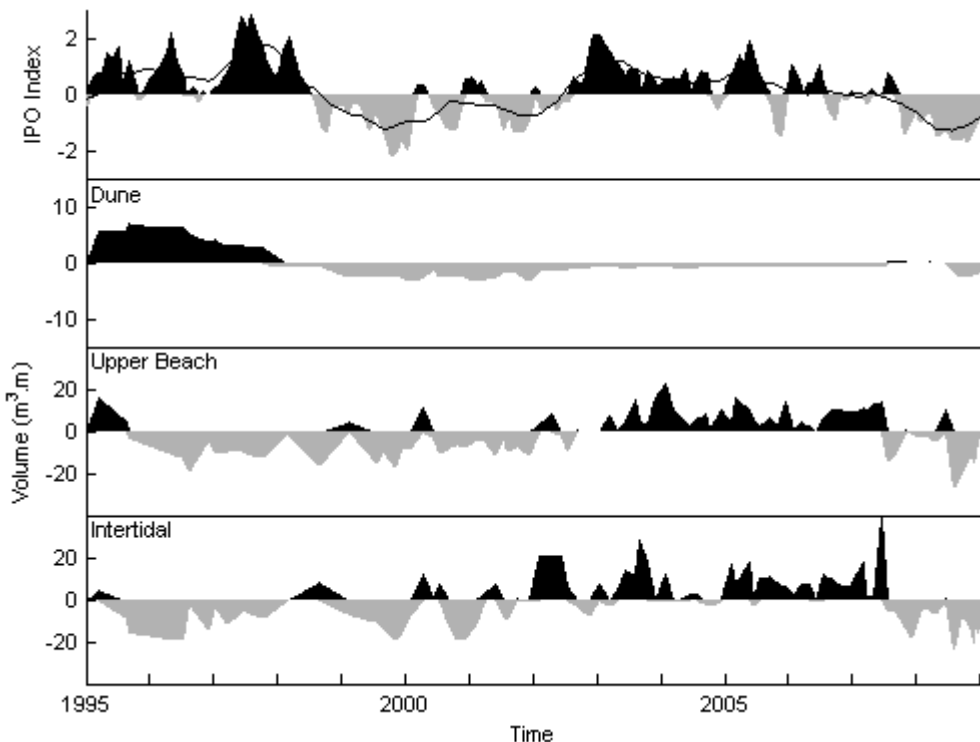


Figure 3: Whangapoua Beach volumes over time for the intertidal region, upper beach region, and dune region. The IPO for the same period is shown in the top panel.

In the last 15 years there have been shifts in the IPO index which can be observed in the beach data. However, sharp changes in the magnitude of the IPO index are not coupled with sharp changes in erosion or accretion events in the beach sediment volume (Fig. 3). This might indicate that there is a finite response time between the IPO phase and the beach volume change.

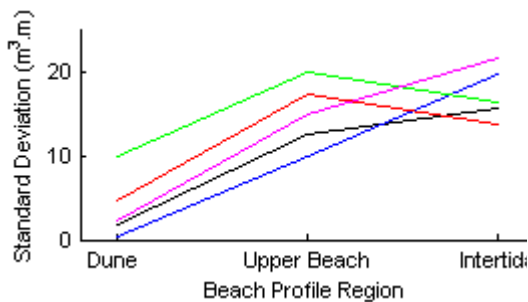


Figure 4: The standard deviation of beach volumes for each horizontal region at Whangapoua Beach (black line), Matarangi Beach (blue line), Hot Water Beach (green line), Tairua Beach (red line), and Pauanui Beach (pink line).

Pauanui and Matarangi beaches have the lowest gradients, fine sediment and highest standard deviation for intertidal beach volumes (Fig. 4). The dune regions have the least variability of the

beach profile (Fig. 4) for all beaches. The highest standard deviations for the steepest two beaches (Tairua and Hot Water) are for the upper beach region, thus being more variable than the respective intertidal areas. Longshore sediment transport is not analysed in this study as only one profile site per beach is used.

The raw timeseries data did not indicate the presence of an obvious seasonal trend in either the intertidal beach volumes for each profile (Fig. 2), or the total beach volume in the case of Whangapoua Beach (Fig. 3). However, when the volumes were time-averaged in 6 week blocks and the seasons grouped for the entire dataset (1979-present), a seasonal trend was evident. Figure 5 displays time-averaged intertidal volumes for each profile site. The maximum accretion period occurs in the April to mid-May bracket for three of the five beaches. These three beaches also have the finest grain sediment and lowest average intertidal beach slope (Whangapoua, Matarangi and Pauanui). The two steep, coarse sand beaches (Hot Water and Tairua) have peak seasonal volumes in the mid-February to March bracket, and both have significant average erosion during the April to mid-May bracket.

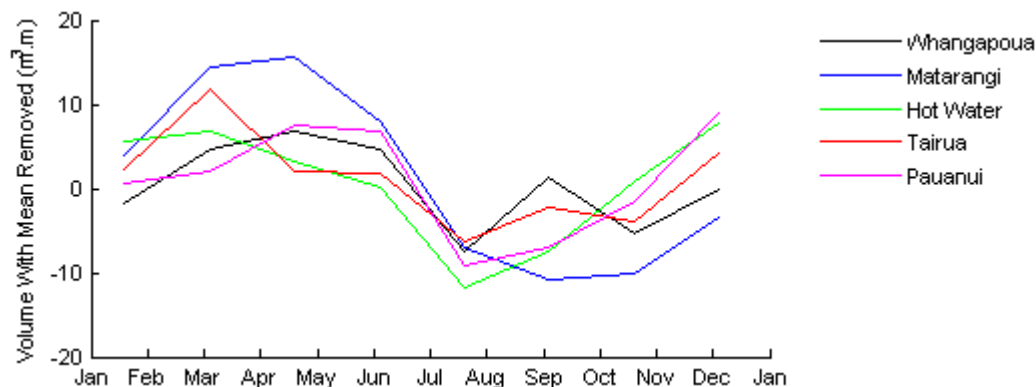


Figure 5: Seasonal variability along the eastern Coromandel Peninsula through the calendar year using time-averaged intertidal volumes for each profile site. Intertidal beach volume data from 1979 to present was averaged over 6 weekly blocks beginning from January 1 for the calendar year.

4 Discussion

4.1 Data/Sampling Error

The beach profile dataset is unique due to its large spatial and temporal extent, with relatively high sampling frequency since 1995. The Emery method used to

collect the data has been the most widely applied method of beach surveying since its inception in the 1960's (Smith and Bryan 2007) but is limited by site specific conditions at the time of surveying. Original testing of the

Emery method (Emery, 1961) showed the average error in elevation between two points as 0.035ft (~10.6mm) with a maximum of 0.18ft (~55mm). These low values are not large enough to add significant error to the data presented.

4.2 Short Term Trends

The Kuaotunu Peninsula defines a boundary between two cells (north and south) where localised erosion/accretion events show a remarkable difference in behaviour. Events occurring at Whangapoua Beach and Matarangi Beach typically have little to no similarity to the observations collected at Hot Water, Tairua, or Pauanui Beaches. However, individual events are still important as there are numerous examples in Figure 2 where relatively large erosion and/or accretion events are the dominant feature in each timeseries. Short term trends often occur at more than one beach, but seldom through all the profiles. This provides preliminary evidence that no beach can be an indicator for the entire eastern Coromandel Peninsula for short term erosion/accretion trends. For example, a large north easterly storm event in July 2008 eroded large volumes from the profiles at Whangapoua Beach and Matarangi Beach (45% and 38% of the pre-event volume respectively), but significantly lower amounts south of the Kuaotunu Peninsula (less than 25%). A second example is the erosion event at the beginning of 2000 at Pauanui Beach when other timeseries showed periods of accretion (Fig. 2, Section 3.1). It is unknown why Pauanui Beach behaved differently during a period of average accretion (Fig. 5). Future analysis of other profiles on Pauanui Beach will identify whether this was a localised event or occurred along the entire beach.

4.3 Seasonal Trends

The seasonally-averaged data show a strong seasonal trend through the year with accretion occurring from spring to autumn, and erosion during the winter period. The accretion cycle begins at approximately the same time for all profiles (over a 6 week bracket from July to mid-August). Matarangi Beach was the only profile not to show an average increase from this point onward. In this case the increase was delayed until the

following 6 week bracket (mid-August to September). This accretion continued until the end of April for all profiles except Hot Water Beach and Tairua Beach. These latter two beaches began to retreat during the mid-February to March bracket. As with the standard deviations of beach volumes in horizontal regions (Fig. 4), the steep, coarse sand beaches behaved differently than the finer grained, low gradient beaches.

Figure 5 illustrates that the duration of winter erosion of the beach profiles was much shorter compared to the time required for the profiles to accrete the same amount in summer. This implies that erosion of the beachface is relatively fast and uniform compared to the accretion period. This is a result of more energetic winter storms eroding sediment in winter faster than it can accumulate on the beachface in summer (Medina et al. 1994). During the winter months, the reduction in beach volume was surprisingly similar between beaches, considering the different nature of the beaches studied. The erosion period from mid-June to July is almost identical at each of the five beaches. This implies that regardless of the peak seasonal volume, the profiles typically retreat during a uniform period to a seasonal volume minimum.

Evaluating the standard deviation of the volume variation within each of the beach horizontal regions (Fig. 4) is a common method of analysis for beach profile timeseries (e.g. Larson et al. 2003). The two beaches with the lowest gradient and fine sediment (Matarangi and Pauanui) have the highest standard deviation of volume for the intertidal area. This confirms that the finer grained sediments in the intertidal zone are the most active and easily transported for the beaches in the study. Conversely, the two steep, coarse sand beaches (Hot Water and Tairua) have more variable upper beach regions than intertidal regions. It is apparent that the stability of the intertidal region might be governed by the grain size and/or steepness of the intertidal area, with tidal effects and inundation not being as relevant as on fine grained beaches. With the timeseries data available, the expected outcome would have been

increasing standard deviations from the dune to upper beach to intertidal region (e.g. Whangapoua, Matarangi, and Pauanui Fig. 4). This was only the case for beaches with low gradients and fine sediment. This suggests that the beaches do not behave in a uniform manner independently of slope and grain size.

4.4 Long Term Trends and the Interdecadal Pacific Oscillation

The timeseries data in Figure 2 indicates that the five beaches follow similar trends of erosion and accretion within the intertidal area across a large spatial scale (e.g. the Coromandel Peninsula). As previously mentioned, the Kuaotunu Peninsula was hypothesised to be a boundary for sediment movement. However, beaches north and south of the Kuaotunu Peninsula appear to have similar long term trends which suggest a large scale cycle is a dominant feature of sediment movement and intertidal beach volumes. All the profiles analysed in Figure 2 display similar erosion trends from 1998 until 2002, followed by net accretion until 2007, then erosion until the end of the timeseries.

For the Whangapoua Beach profile, the IPO appears to have limited impact on short term variability in sediment budgets, but evidence exists for a correlation with long term trends (Fig. 3). This comparison provides evidence that climate oscillations of sea surface temperatures, sea level pressures, and wind stresses experienced under warm and cool periods of the IPO (Mantua and Hare, 2002) are impacting beach sediment budgets on the eastern Coromandel Peninsula. Mantua and Hare (2002) also state that the impacts of the IPO are broadly similar to those connected with lesser extremes of El Nino Southern Oscillation variations.

Matarangi Beach and Pauanui Beach are unique in that they are relatively long, flat, barrier beaches with fine beach sediment and adjacent harbour entrances. Climatic variations due to the IPO may explain why Matarangi and Pauanui beaches appear to have a stronger relationship with the IPO phase. Precipitation and groundwater effects could be a significant factor and thus

impact the seasonal trend of the intertidal volumes.

5 Conclusions

Analysis of intertidal beach volumes for the five beaches indicates that long term trends of erosion and accretion are coupled with the IPO. Further analysis of the upper beach area of one site identified that long term erosion and accretion in the upper beach region was also coupled with the IPO. Time-averaged seasonal cycles indicated an overall oscillatory pattern for erosion and accretion at all sites of the Coromandel. The time-averaged data showed that the seasonal rate and periods of erosion at all sites were fairly uniform. The data will enable reasonably accurate forecasting of minimum time-averaged erosion volumes on a seasonal basis at each site. Long term trends of erosion and accretion are evident in the data whereas single events appear to be sporadic and determined by local conditions. Further work will apply these methods to the entire indicator beach project across all 61 profile sites. Expanding the work to all profile sites will enable detailed analysis of spatial variability on individual beaches and across beaches (e.g. beach rotation and longshore sediment transport trends). The role of wave characteristics on beach change will also be addressed in future work.

Acknowledgements

The authors wish to thank Environment Waikato and FRST Contract WRHC092 for financial support. Many thanks to Ron Ovenden for his ongoing assistance with data collection. AW supported by University of Waikato Masters Fees Scholarship, the University of Waikato Masters Research Scholarship, EW and the Department of Conservation (Dr Stella Frances Scholarship).

References

- Bradshaw, B.E. Healy, T.R. Dell, P.M. and Bolstad, W.M. (1990). Inner shelf dynamics on a storm-dominated coast, east Coromandel, New Zealand. *Journal of Coastal Research*, Vol. 7 No. 1, 11-30.
- Emery, K.O. (1961). A simple method for measuring beach profiles. *Limnology and Oceanography*, 6, 90-93.

- Environment Waikato, (2002). Coastal hazards and development setback recommendations summary report May 2002. Environment Waikato, Hamilton, 39 pp.
- Gorman, R.M. Bryan, K.R. and Laing, A.K. (2003). Wave hindcast for the New Zealand region: nearshore validation and coastal wave climate. *New Zealand Journal of Marine and Freshwater Research*, Vol. 37 No.3, 567-588.
- Hart, D.E. and Bryan, K.R. (2008). New Zealand coastal system boundaries, connections and management. *New Zealand Geographer*, 64, 129-143.
- Healy, T.R. Dell, P.M. and Willoughby, A.J. (1981). Coromandel Coastal Survey Vol. 1 Basic Survey Data. Hauraki Catchment Board. Report No. 114, 233 pp.
- Hume, T. M. (1979). Factors contributing to coastal erosion on the east coast of Northland during July 1978. Water and Soil Division report. Ministry of Works and Development, Auckland, 25 pp.
- Hume, T.M. Bell, R.G. de Lange, W.P. Healy, T.R. Hicks, D.M. and Kirk, R.M. (1992). Coastal oceanography and sedimentology in New Zealand, 1967-91. *New Zealand Journal of Marine and Freshwater Research*, Vol. 26, 1-36.
- Larson, M. Capobianco, M. Jansen, H. Rozynski, G. Southgate, H. Stive, M. Wijnberg, K. and Hulscher, S. (2003). Analysis and modeling of field data on coastal morphological evolution over yearly and decadal time scales. Part 1: background and linear techniques. *Journal of Coastal Research*, Vol. 19 No.4, 760-775.
- Mantua, N.J. and Hare, S.R. (2002). The Pacific decadal oscillation. *Journal of Oceanography*, Vol. 58, 35-44.
- Medina, R. Losada, M.A. Losada, I.J. and Vidal, C. (1994). Temporal and spatial relationship between sediment grain-size and beach profile. *Marine Geology*, Vol. 18 No. 3-4, 195-206.
- Smith, R.K. and Bryan, K.R. (2007). Monitoring beach face volume with a combination intermittent profiling and video imagery. *Journal of Coastal Research*, Vol. 23 No. 4, 892-898.

APPENDIX II

AERIAL PHOTOS AND PROFILE INFORMATION

Aerial photos from each beach site with markers illustrating the primary benchmark location are displayed in this appendix. All images were obtained from Google Earth and orientated to the north if not stated. Table VII-1 illustrates the date of establishments for each profile. The beaches and profile sites were all listed from north to south, or in some cases left to right looking seaward. Some of the northerly orientated beaches use this latter definition due to their orientations. All profile sites are still in use. Note that Pauanui CCS38 was established in 1981, however there were 5 profiles from this date until 1990, then the profile was disestablished until 2004. This lack of data was not considered for a majority of the thesis.

Table II-1: List of all profiles used in the study at each beach from north to south.

Beach / Profile Name	Date established	Beach / Profile Name	Date established
Whangapoua CCS12	16-1-1979	Hot Water CCS35-1	12-1-1981
Whangapoua CCS11	16-1-1979	Hot Water CCS35	13-1-1979
Whangapoua CCS11-1	27-1-1981	Hot Water CCS34	13-1-1979
Matarangi CCS16	15-1-1979	Tairua CCS37	13-1-1979
Matarangi CCS15	15-1-1979	Tairua CCS36-1	25-5-1992
Matarangi CCS14	14-1-1979	Tairua CCS36-2	29-7-2003
Matarangi CCS13	14-1-1979	Tairua CCS36	13-1-1979
Rings CCS18	14-1-1979	Pauanui CCS38	5-1-1981
Kuaotunu West CCS19-4	29-4-1981	Pauanui CCS38-1	4-8-1993
Kuaotunu West CCS19-1	15-1-1981	Pauanui CCS39-1	27-7-1995
Kuaotunu West CCS19-5	28-11-1996	Pauanui CCS39-2	5-1-1981

Kuaotunu East CCS20	16-2-1988	Pauanui CCS40-1	10-1-1979
Kuaotunu East CCS20-2	15-1-1981	Otama CCS45	14-1-1979
Kuaotunu East CCS21	16-1-1981	Otama CCS46	14-1-1979
Wharekaho CCS22-1	15-2-1991	Opito CCS49	14-1-1979
Wharekaho CCS22	12-1-1981	Opito CCS49-1	4-7-1996
Wharekaho CCS23	13-1-1979	Opito CCS47-1	4-7-1996
Buffalo CCS24	13-1-1979	Opito CCS48	14-1-1979
Buffalo CCS25	13-1-1979	Opito CCS48-1	14-1-1981
Buffalo CCS25-1	31-1-1991	Onemana CCS54	9-2-1981
Buffalo CCS26	13-1-1979	Onemana CCS53	9-2-1981
Buffalo CCS27	13-1-1979	Whangamata North CCS55-1	27-7-1995
Maramaratotara CCS28	13-1-1979	Whangamata North CCS56	19-7-1990
Cooks CCS29	13-1-1979	Whangamata South CCS57	19-7-1990
Cooks CCS30	13-1-1979	Whangamata South CCS57-3	1-12-1991
Cooks CCS31	13-1-1979	Whangamata South CCS57-2	8-9-2002
Cooks CCS31-1	31-1-1991	Whangamata South CCS58	20-12-1978
Cooks CCS31-2	31-1-1991	Whiritoa CCS59	19-7-1990
Hahei CCS32	13-1-1979	Whiritoa CCS61	29-3-1995
Hahei CCS33	13-1-1979	Whiritoa CCS62	1-12-1990
		Whiritoa CCS63	19-7-1990

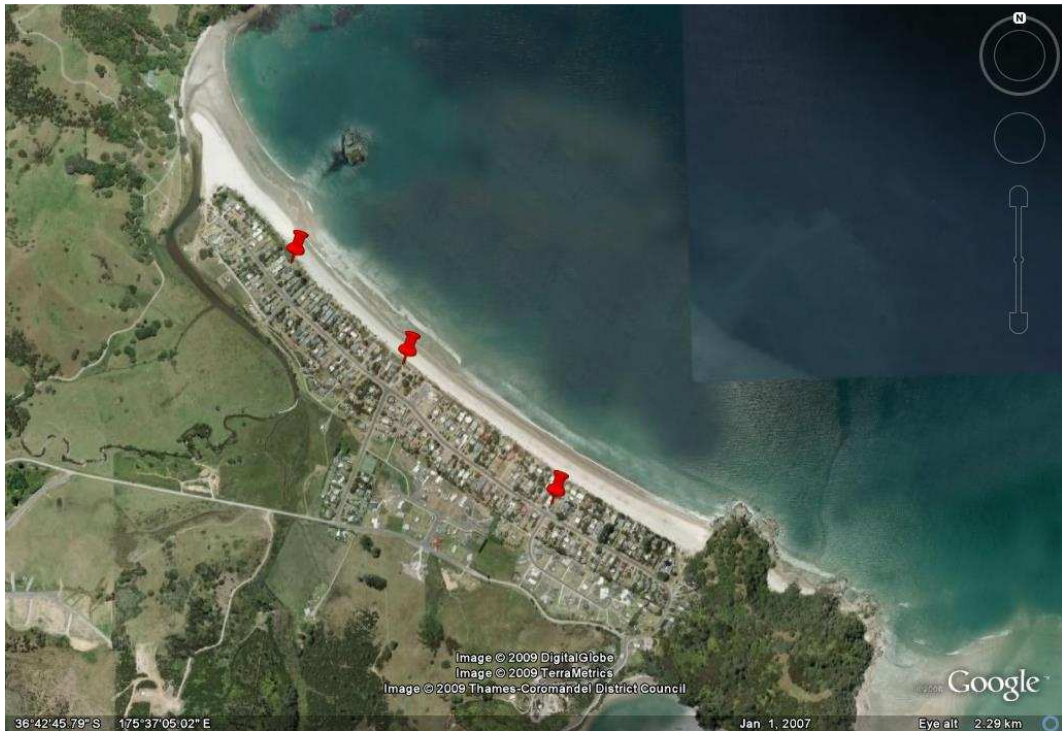


Figure II.1: Whangapoua Beach and profile sites. The entrance to Whangapoua Harbour is in the lower right hand corner.

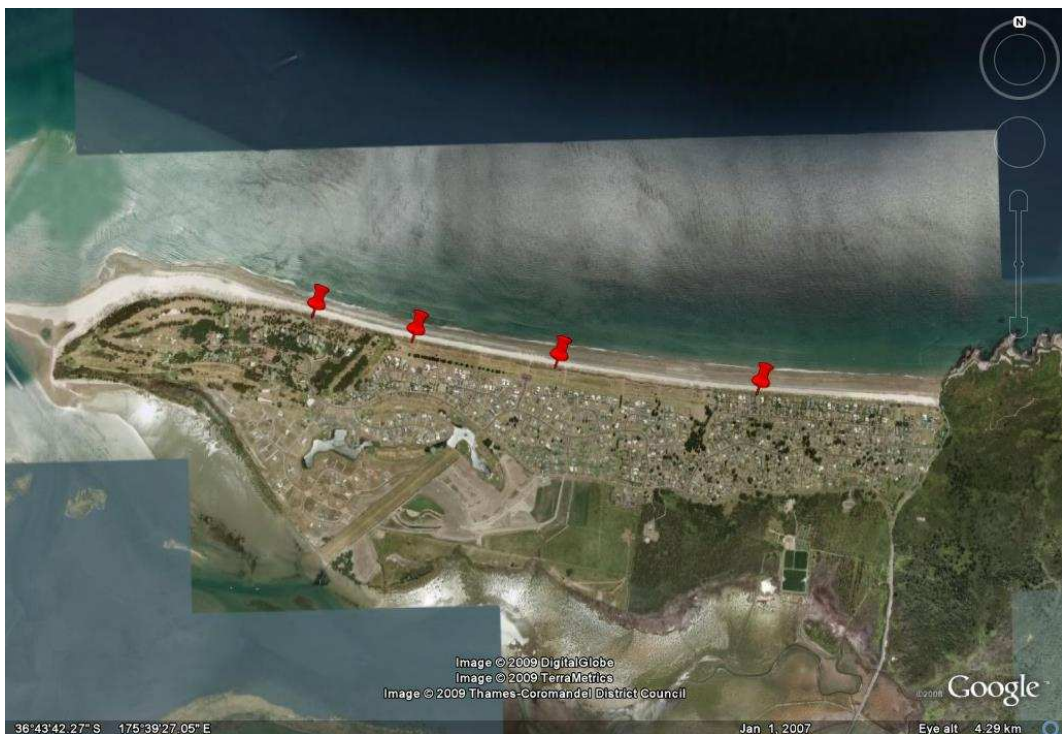


Figure II.2: Matarangi Beach and profile sites. The entrance to Whangapoua Harbour is to the left of the distal end of the spit.

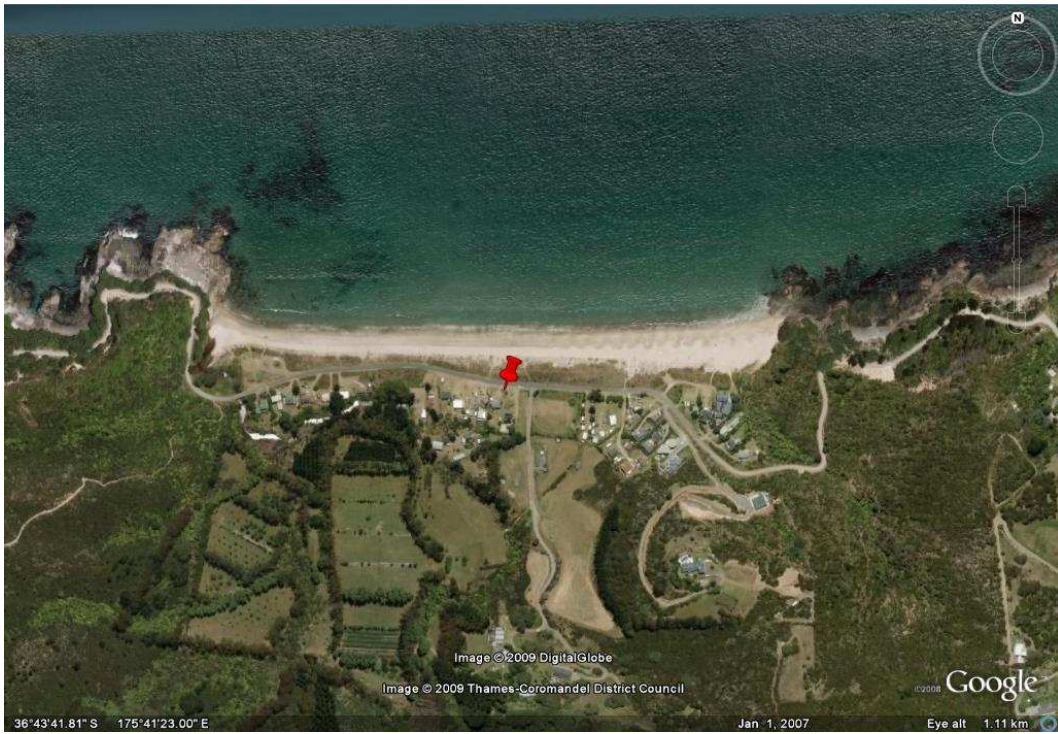


Figure II.3: Rings Beach showing the central profile location. Cusp formations are evident on the eastern half of the beach.



Figure II.4: Kuaotunu West Beach showing the profile sites. The large rock outcrop to the east represents the headland barrier to Kuaotunu East Beach.

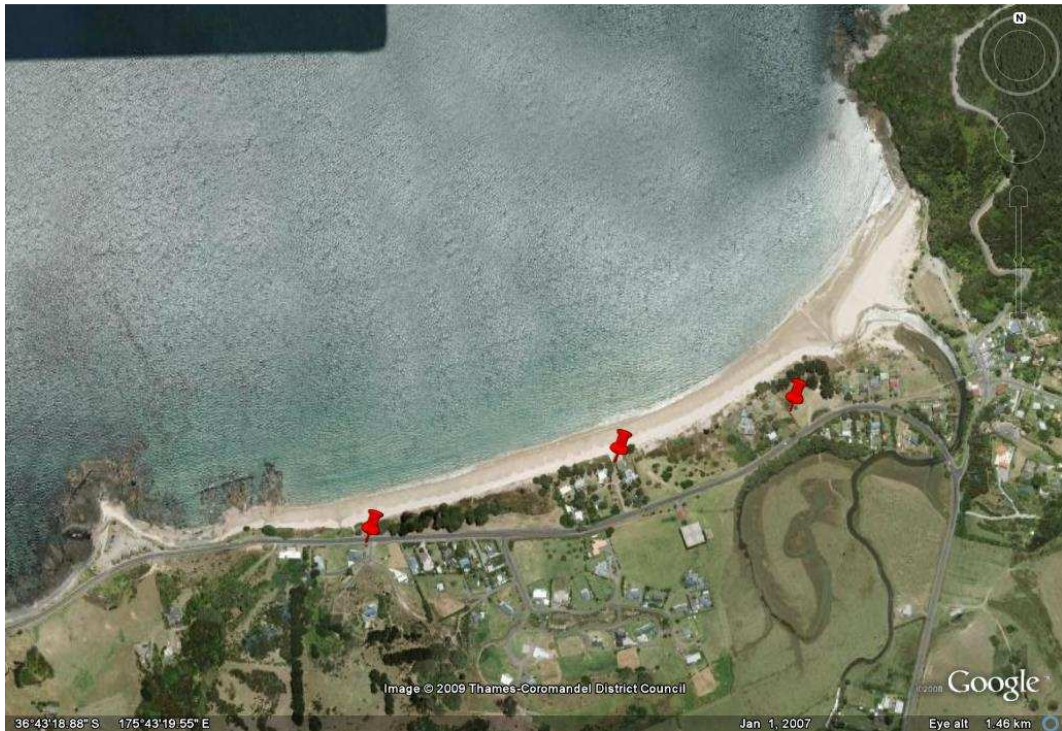


Figure II.5: Kuaotunu East Beach showing the profile sites. The large rock outcrop to the west represents the headland barrier to Kuaotunu West Beach.



Figure II.6: Otama Beach showing the two profile sites.



Figure II.7: Opito Beach showing the five profile sites. The northern end of the beach has restricted access. The large orientation change from north to south is evident.

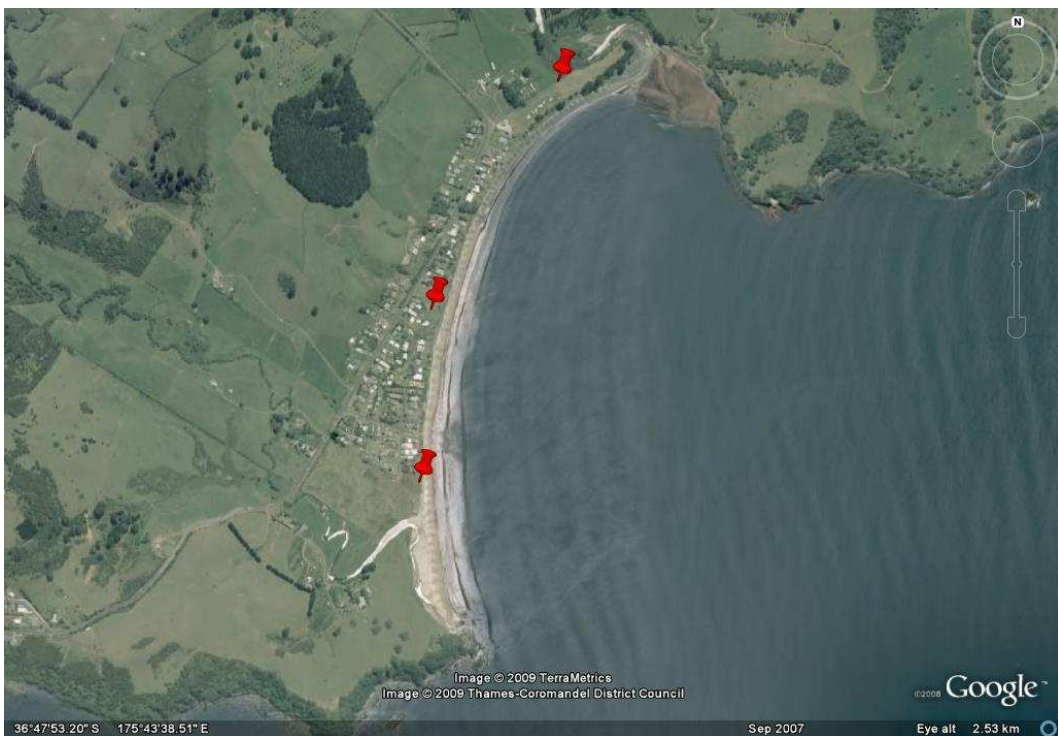


Figure II.8: Wharekaho Beach showing the 3 profile sites. In particular, the sheltered location of the northern profile site and the overall orientation of the beach.



Figure II.9: Buffalo Beach showing the five profile sites from north to south. The short embayed beach with one profile site is Maramaratotara Beach. The western end of Cooks Beach is shown in the bottom left corner.

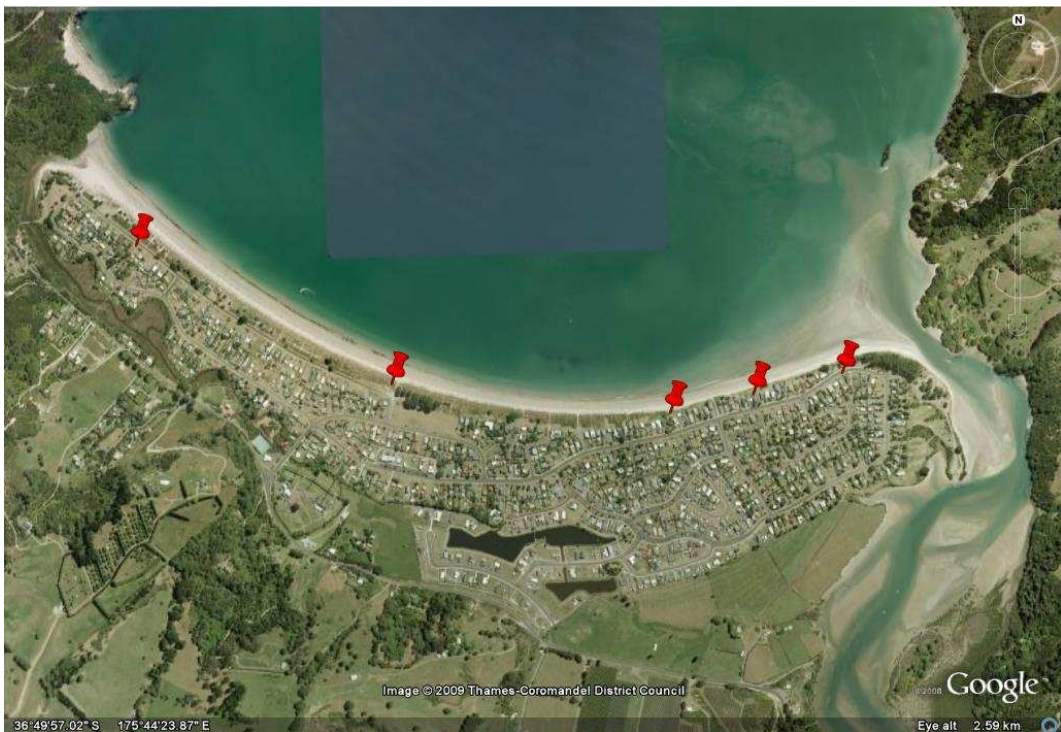


Figure II.10: Cooks Beach showing the five profile sites and the relatively close spacing between the eastern three profiles in proximity to the entrance to Purangi estuary.

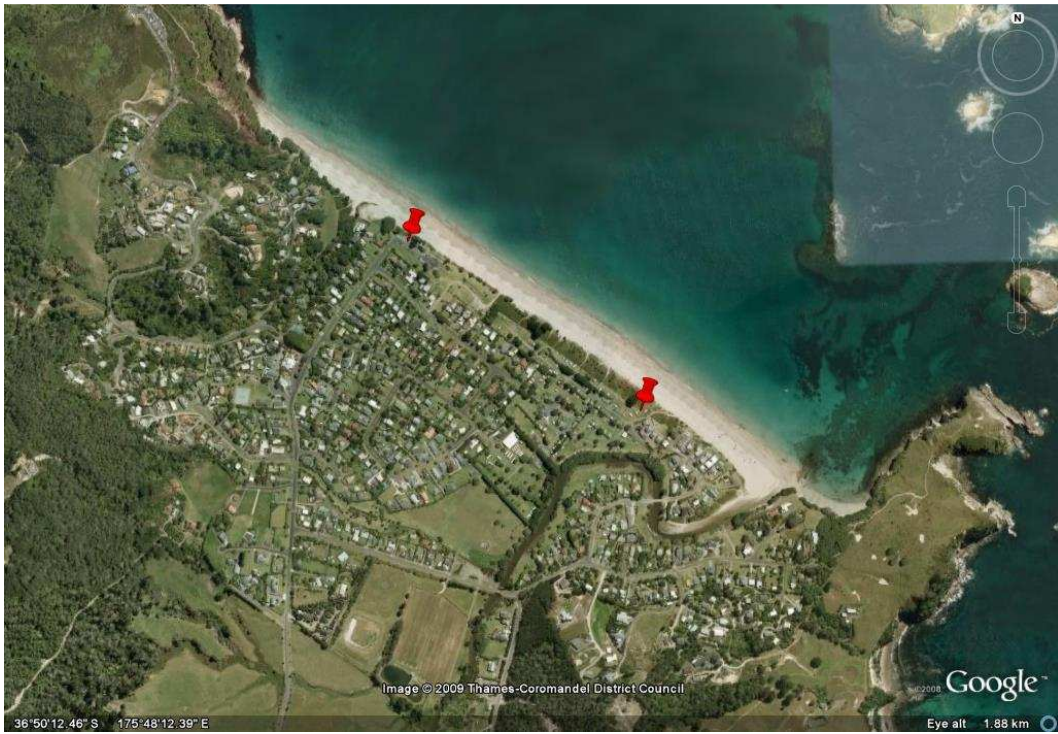


Figure II.11: Hahei Beach showing the location of the two profile sites. Cusp formations are evident across the beach face.



Figure II.12: Hot Water Beach showing the three profile sites.

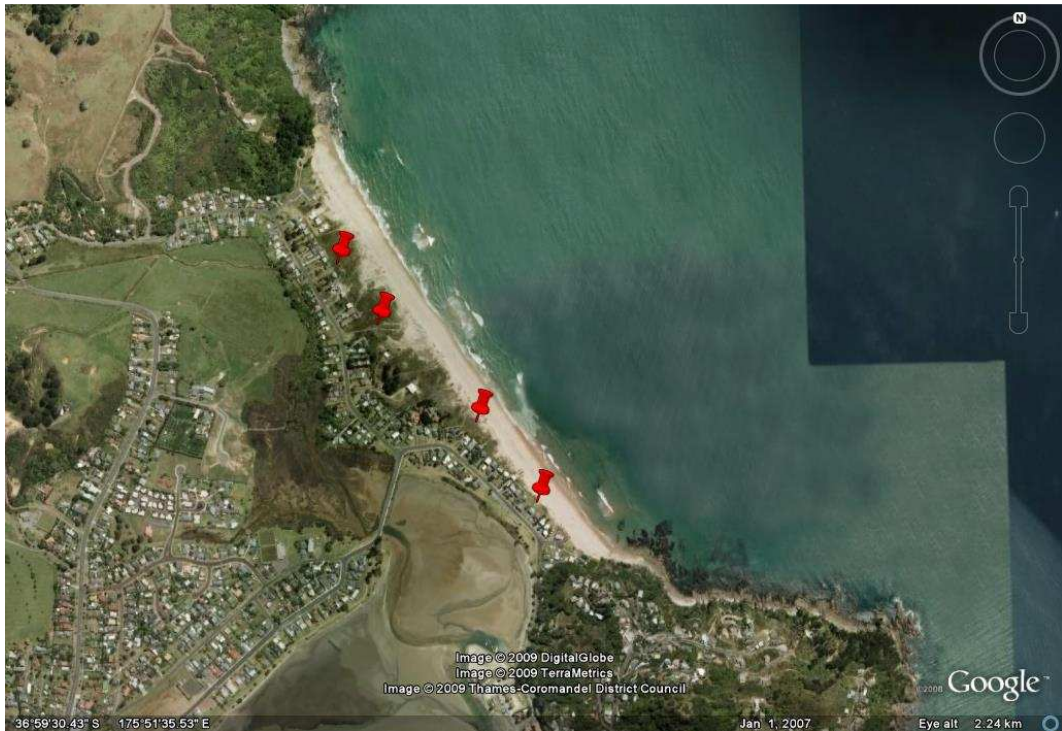


Figure II.13: Tairua Beach showing the four profile sites. Paku hill in the bottom part of the image separates Tairua Beach from the entrance to Tairua Harbour and adjacent Pauanui Beach. The harbour is evident immediately behind the housing at the southern end of the beach.



Figure II.14: Pauanui Beach showing the five profile sites. Paku hill is evident at the top of the image as well as the entrance to Tairua Harbour.

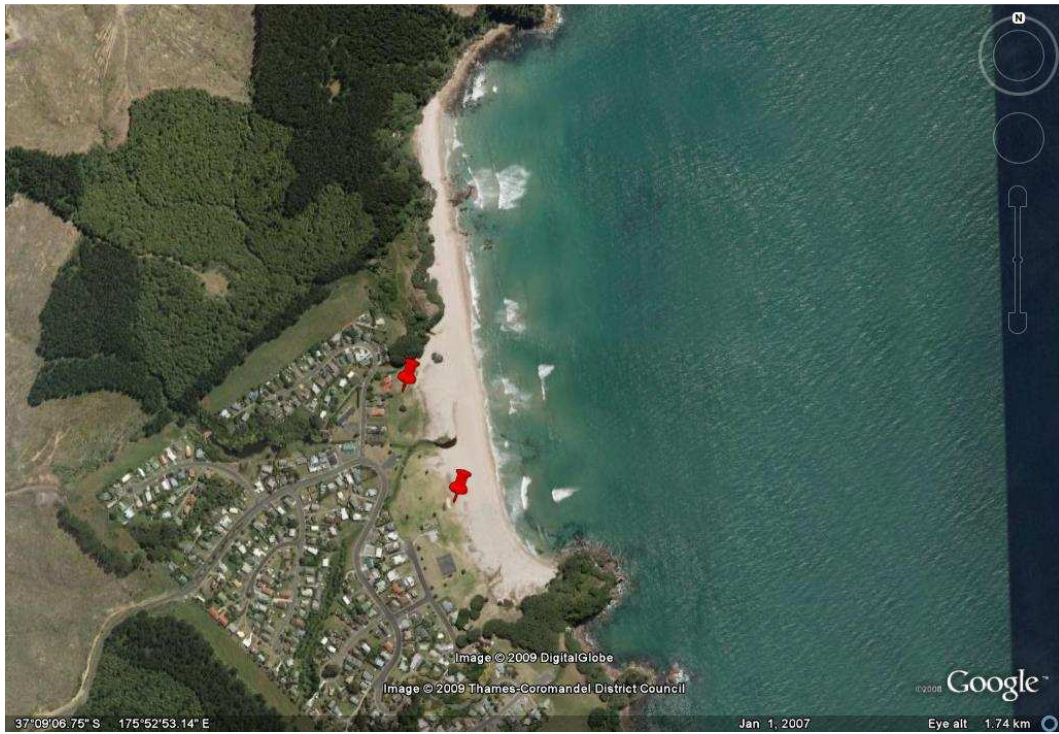


Figure II.15: Onemana Beach and the two profile locations.

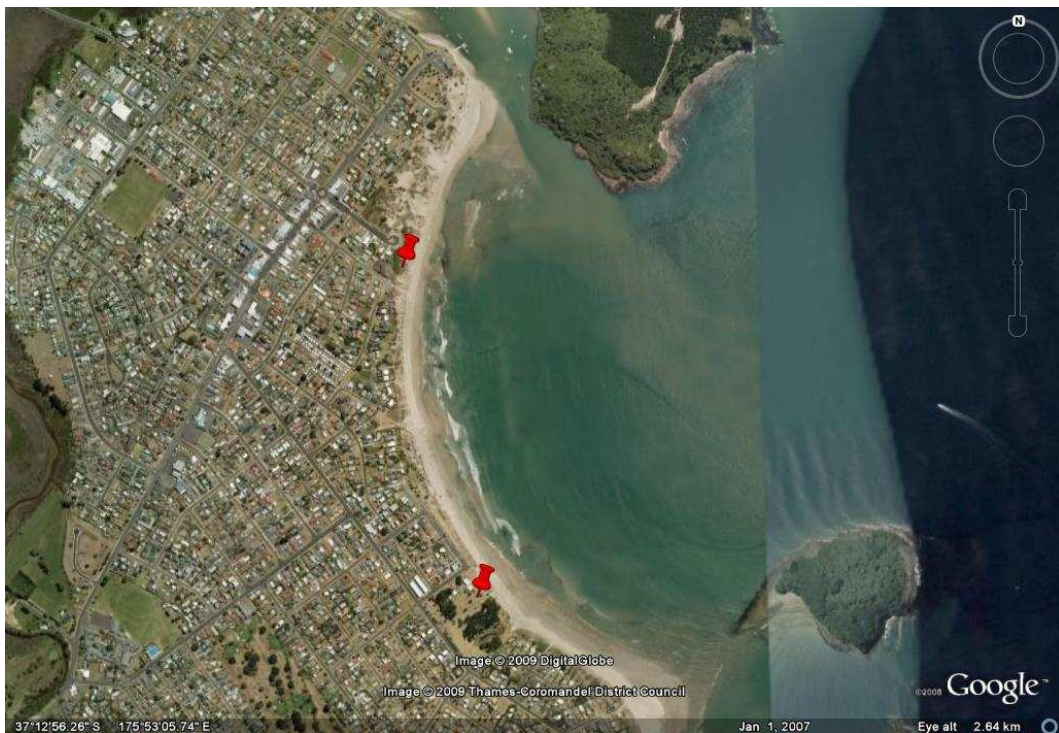


Figure II.16: Whangamata North Beach showing the two profile sites. The entrance to Whangamata Harbour is evident at the top of the image. Hauturu Island at the southern end of the beach has caused a large salient in the lee side of the island.

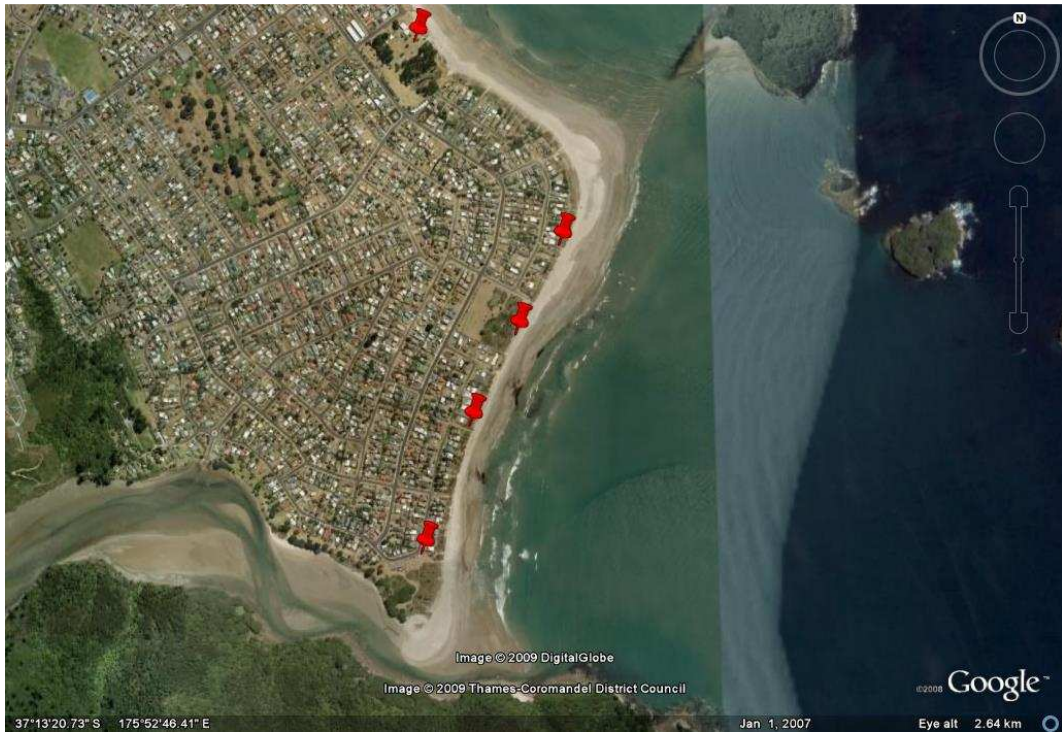


Figure II.17: Whangamata South Beach showing the four profile sites. The entrance to Otahu estuary is evident at the southern end of the beach. Hauturu Island and the salient in behind is evident at the top of the image.



Figure II.18: Whiritoa Beach showing the four profile sites.



Figure II.19: Ngarunui Beach, Raglan showing the four beach profile sites and location of wave data from Scarfe (2008).

APPENDIX III

INTERTIDAL BEACH SLOPE TIMESERIES

Contained within this appendix are each individual profile intertidal beach slope data. The data represent raw timeseries from 1990 to 2009. Data prior to 1990 were considered insignificant due to the large spacing between surveys. These data were included in the average intertidal beach slope calculations because the date of survey was not important. The average intertidal slope used for the beach classification according to Wright and Short (1984) were shown in each figure caption for the respective profile from north to south, top to bottom. The method of calculation was discussed in Section 3.3.1. The benchmark labels are illustrated on each figure panel. All beaches and profiles are shown from north to south and on equal x- and y-axes.

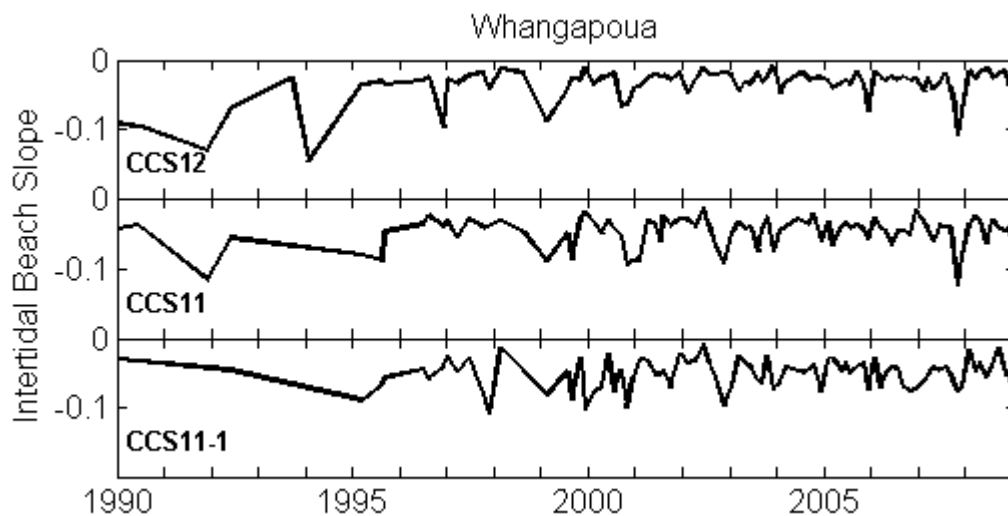


Figure III.1: Whangapoua Beach intertidal beach slope timeseries. The average slopes were 0.035, 0.049, and 0.050.

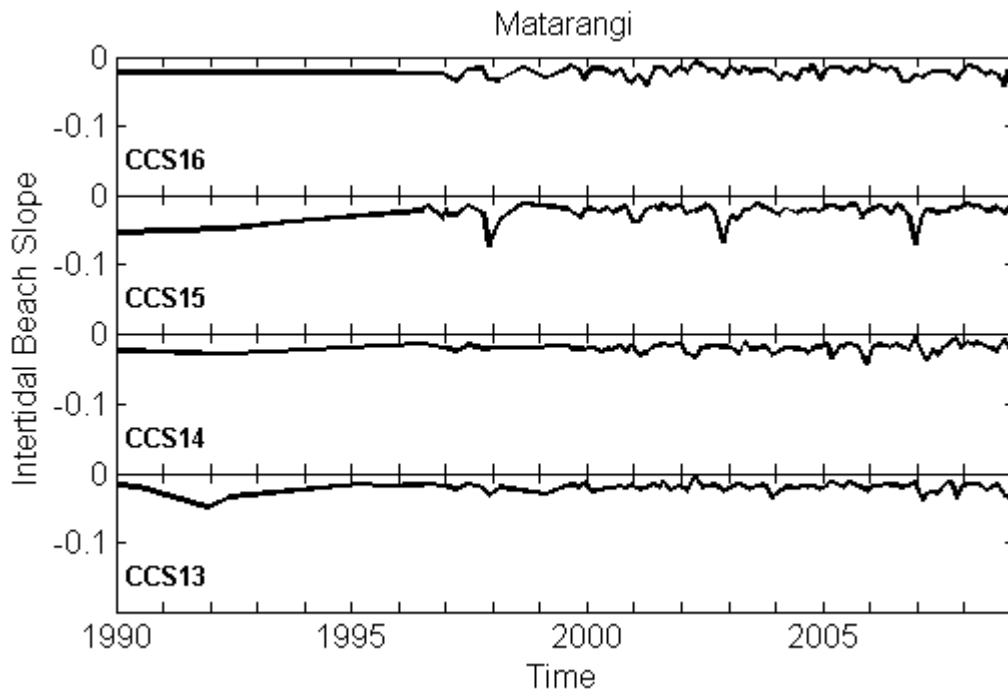


Figure III.2: Matarangi Beach intertidal beach slope timeseries. The average slopes were 0.023, 0.024, 0.022, and 0.020.

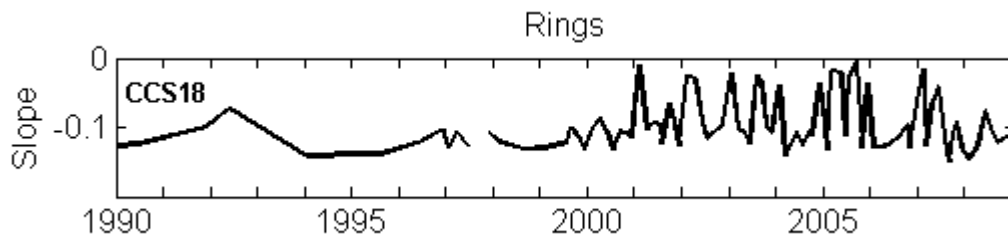


Figure III.3: Rings Beach intertidal beach slope timeseries. The average slope was 0.98. The gap in the data was due to there being insufficient survey data within the intertidal area to determine the average slope. The profile survey had a very straight intertidal beach slope.

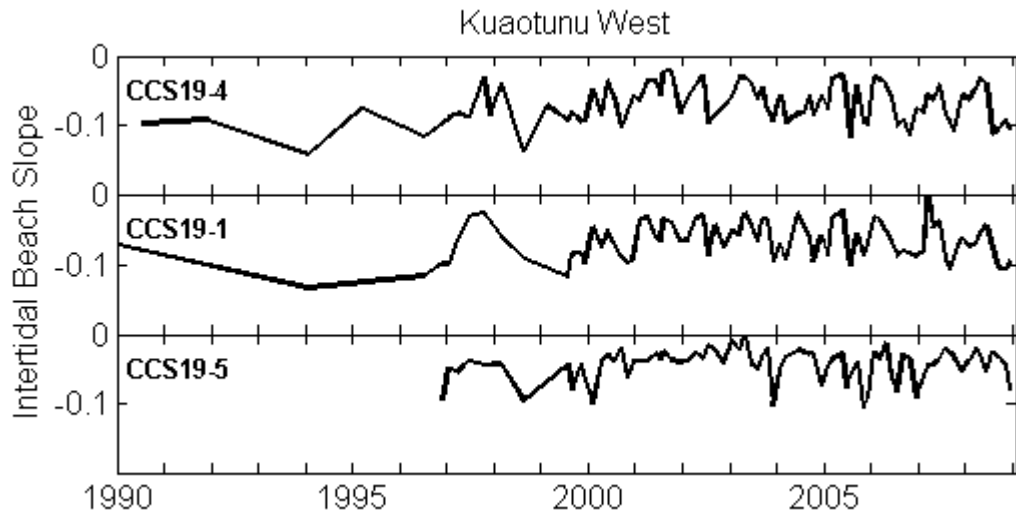


Figure III.4: Kuaotunu West Beach intertidal beach slope timeseries. The average slopes were 0.071, 0.066, and 0.044.

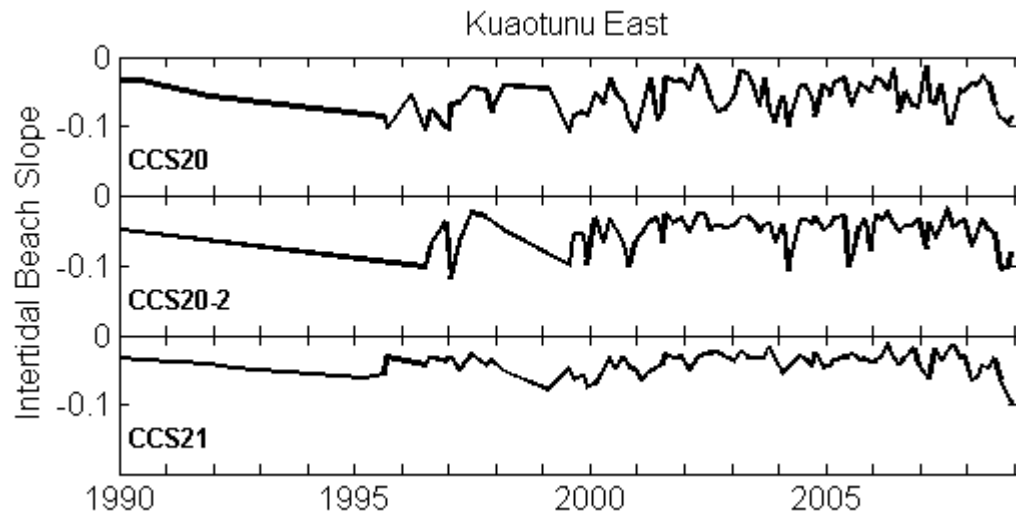


Figure III.5: Kuaotunu East Beach intertidal beach slope timeseries. The average slopes were 0.058, 0.052, and 0.040.

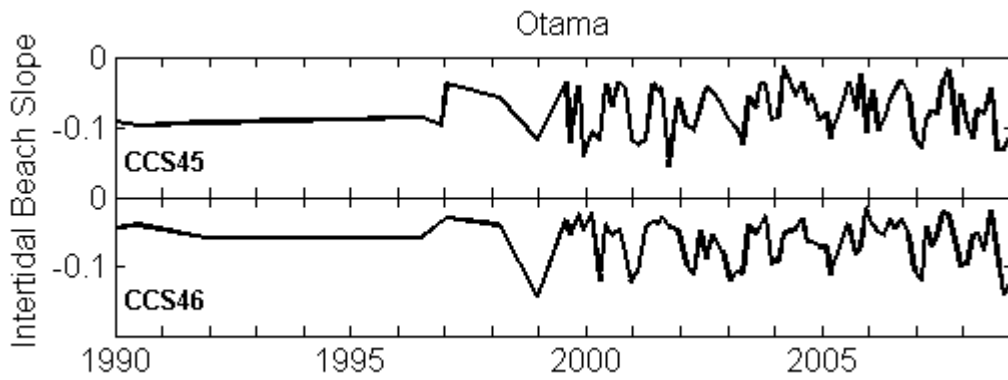


Figure III.6: Otama Beach intertidal beach slope timeseries. The average slopes were 0.076 and 0.064.

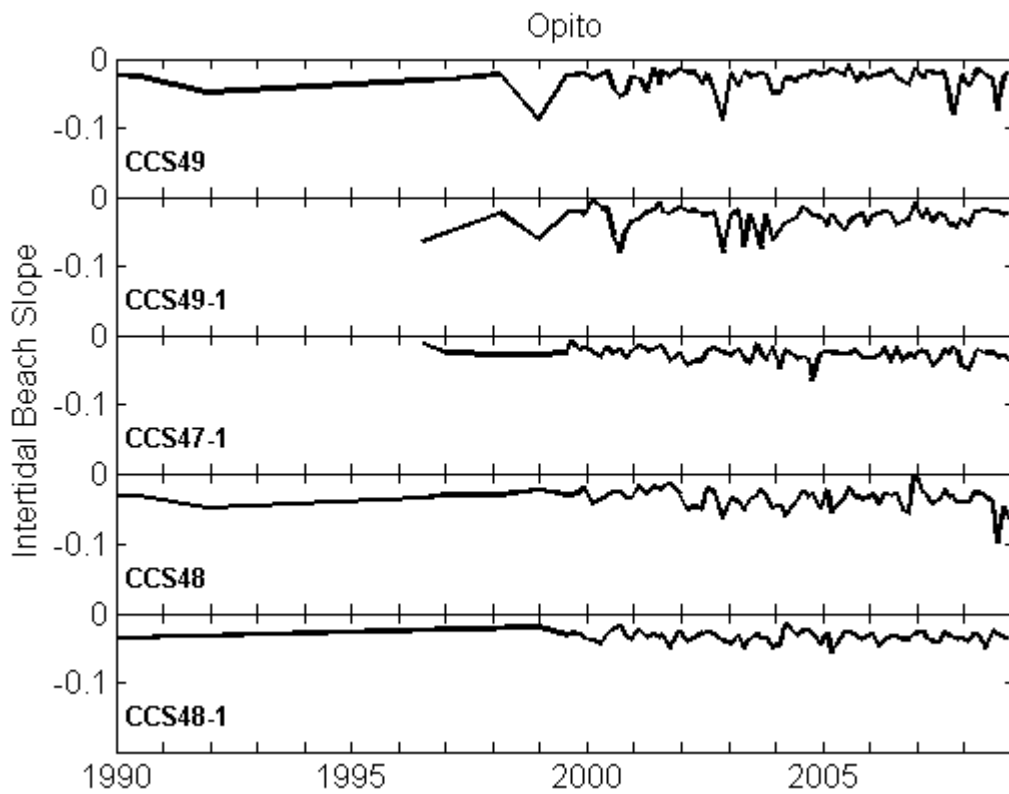


Figure III.7: Opito Beach intertidal beach slope timeseries. The average slopes were 0.30, 0.031, 0.028, 0.036, and 0.034.

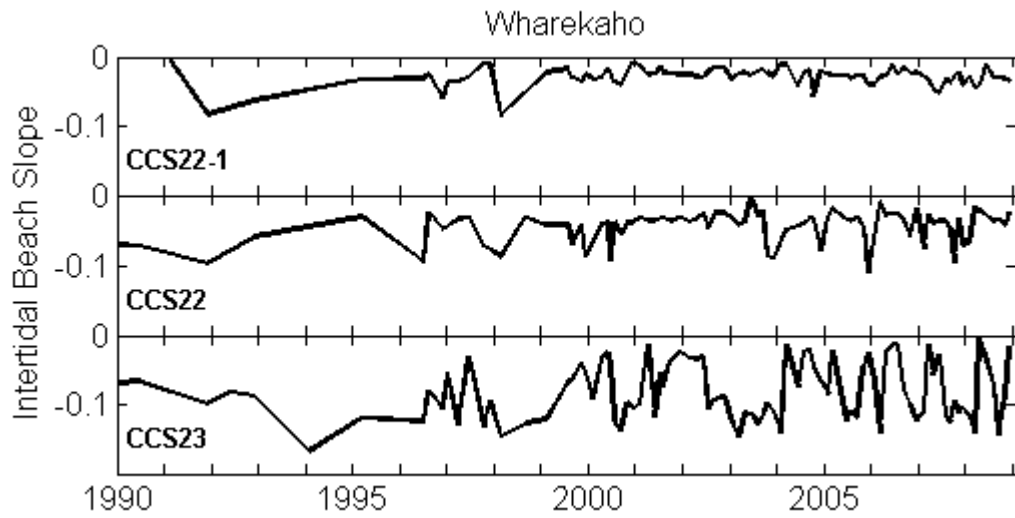


Figure III.8: Wharekaho Beach intertidal beach slope timeseries. The average slopes were 0.027, 0.042, and 0.078.

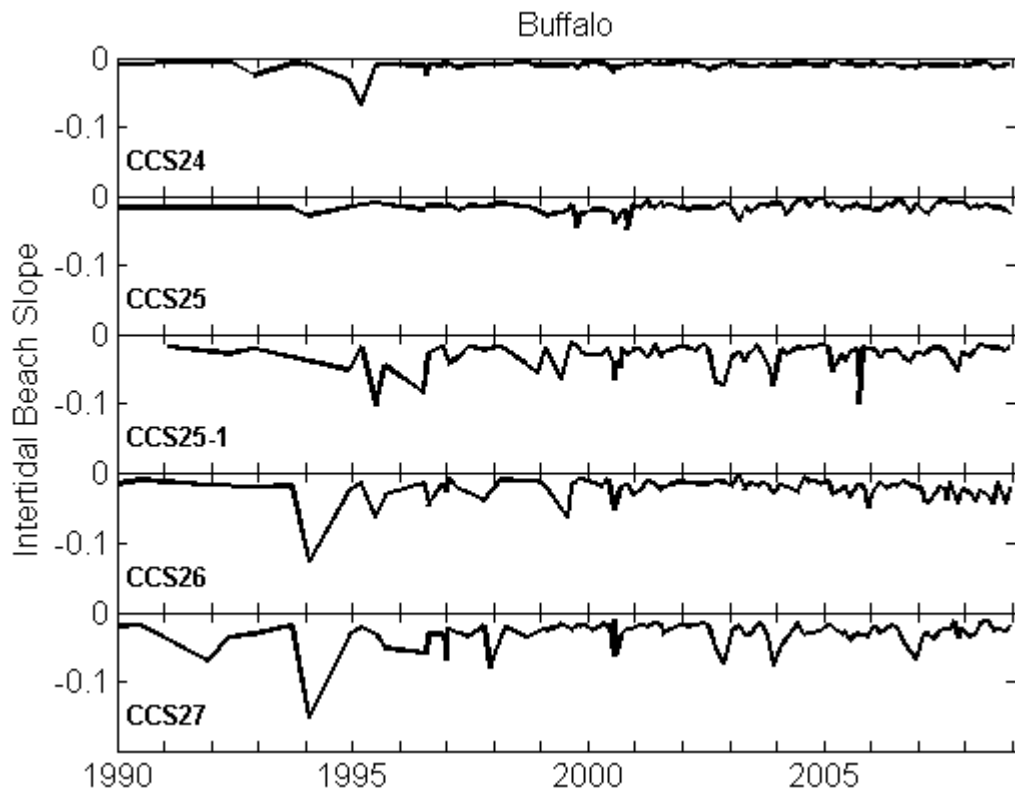


Figure III.9: Buffalo Beach intertidal beach slope timeseries. The average slopes were 0.012, 0.017, 0.031, 0.034, and 0.031.

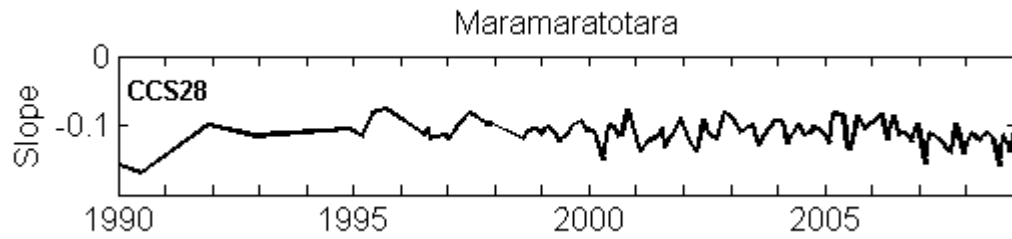


Figure III.10: Maramaratotara Beach intertidal beach slope timeseries. The average slope was 0.11.

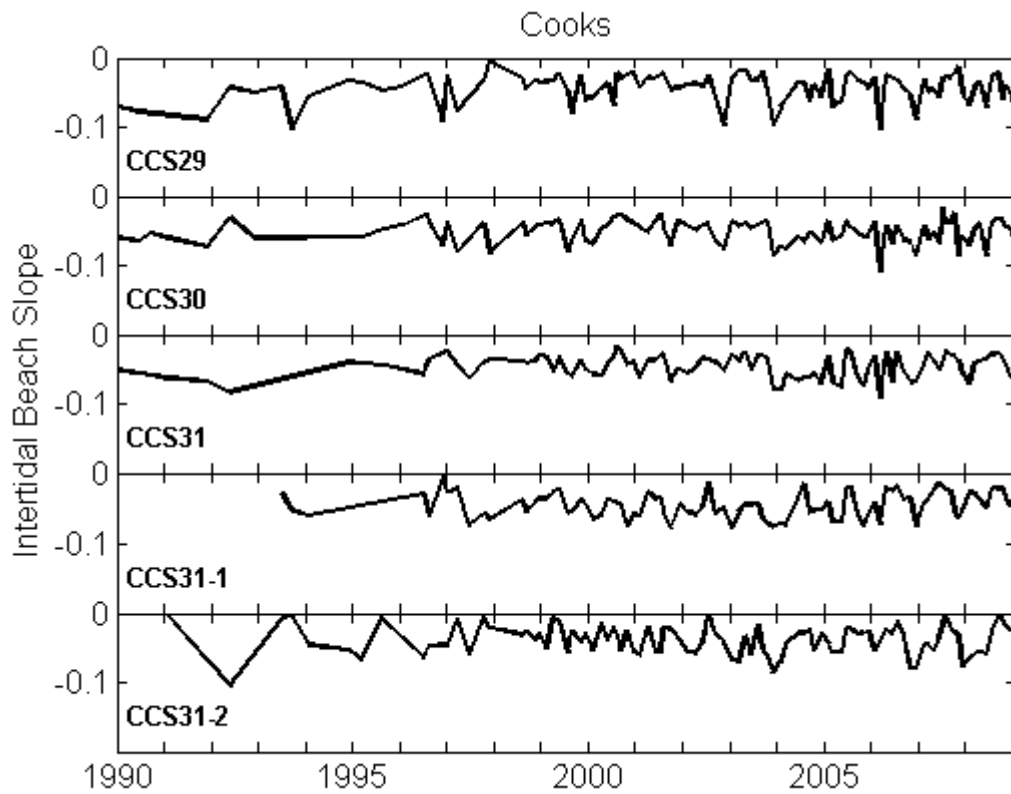


Figure III.11: Cooks Beach intertidal beach slope timeseries. The average slopes were 0.044, 0.051, 0.046, 0.045, and 0.040.

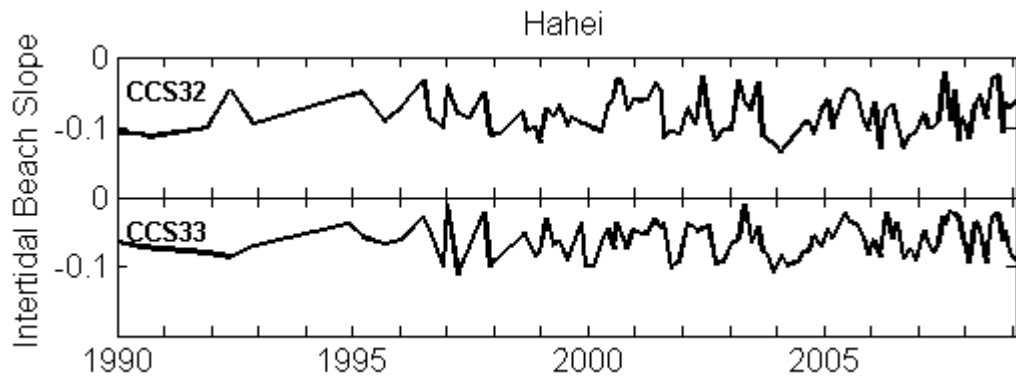


Figure III.12: Hahei Beach intertidal beach slope timeseries. The average slopes were 0.082 and 0.062.

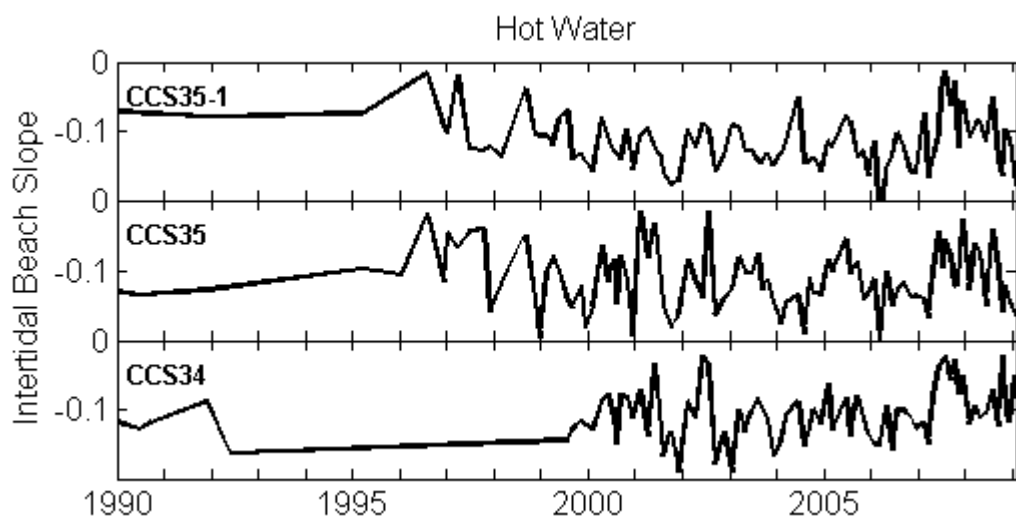


Figure III.13: Hot Water Beach intertidal beach slope timeseries. The average slopes were 0.11, 0.11, and 0.11.

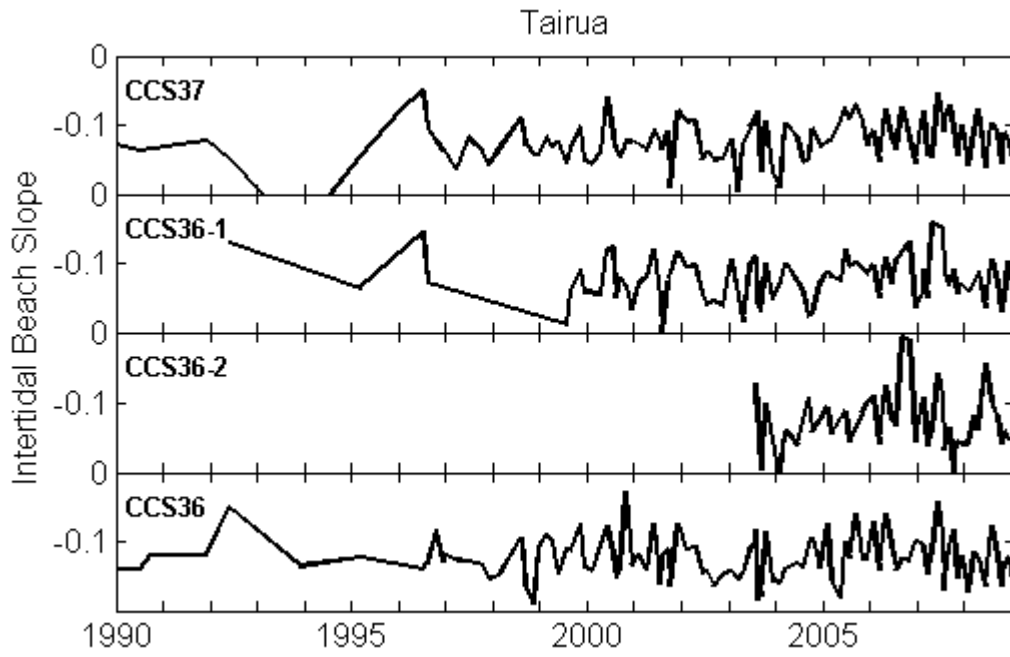


Figure III.14: Tairua Beach intertidal beach slope timeseries. The average slopes were 0.12, 0.12, 0.12, and 0.12.

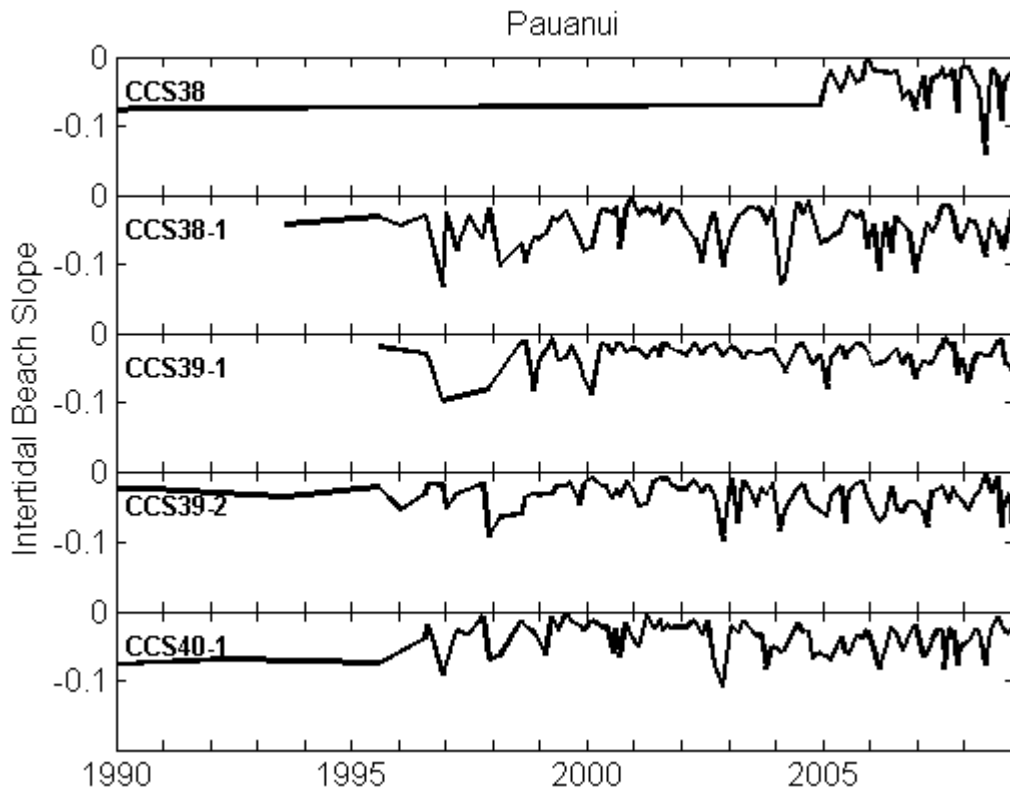


Figure III.15: Pauanui Beach intertidal beach slope timeseries. The average slopes were 0.039, 0.048, 0.033, 0.036, and 0.039.

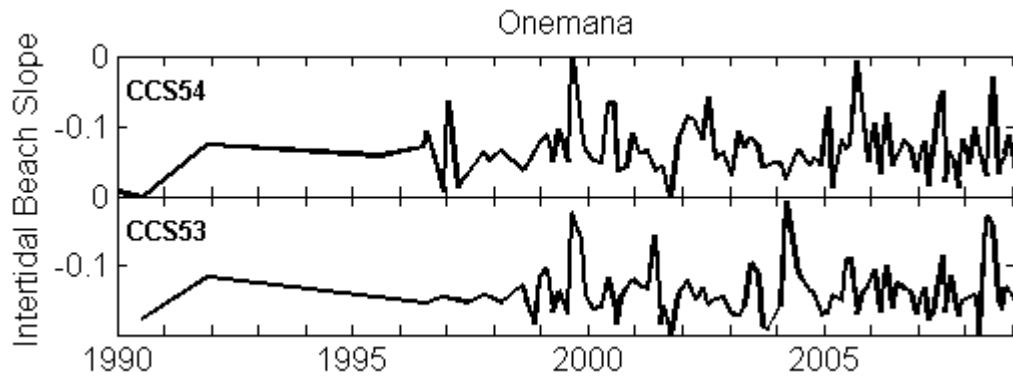


Figure III.16: Onemana Beach intertidal beach slope timeseries. The average slopes were 0.13 and 0.14.

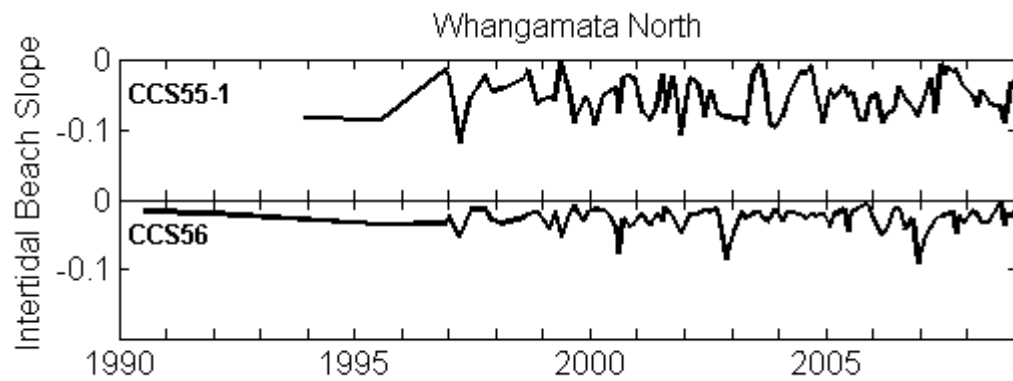


Figure III.17: Whangamata North Beach intertidal beach slope timeseries. The average slopes were 0.054 and 0.028.

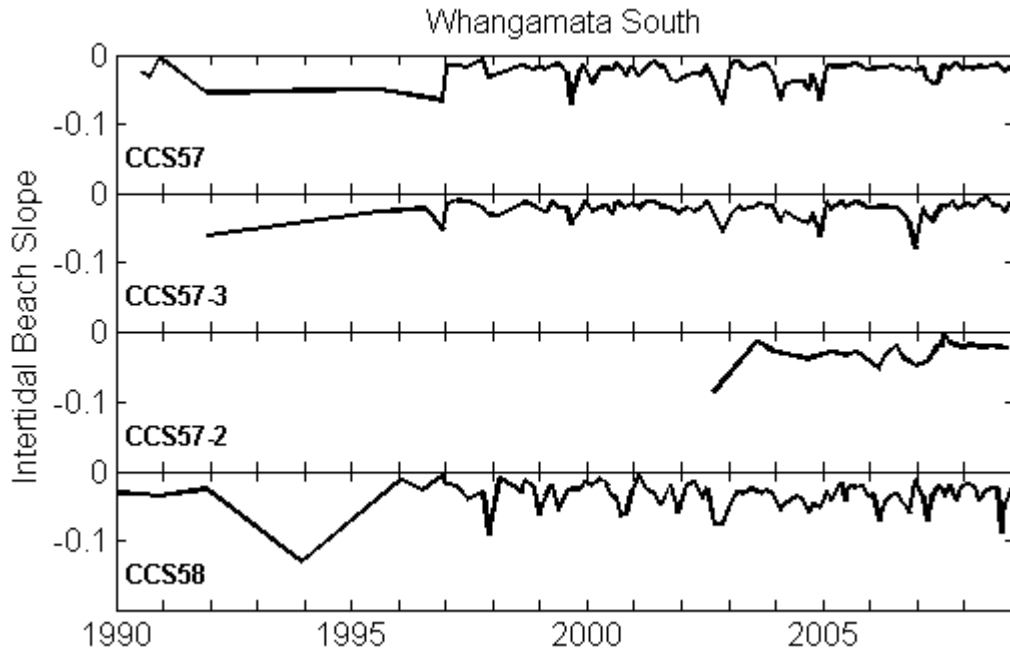


Figure III.18: Whangamata South Beach intertidal beach slope timeseries. The average slopes were 0.024, 0.024, 0.029, and 0.035.

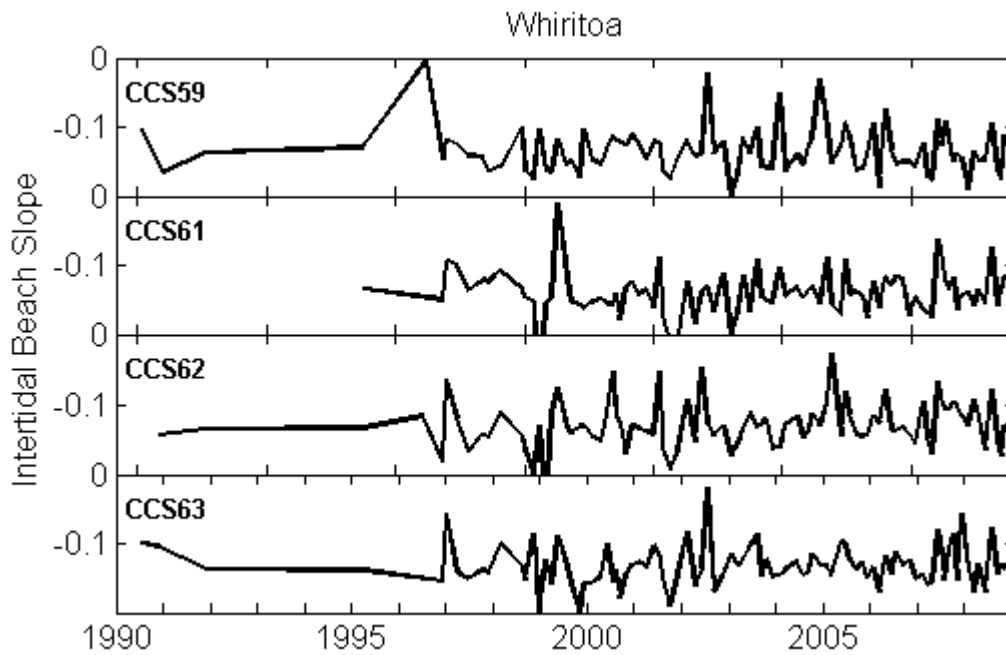


Figure III.19: Whiritoa Beach intertidal beach slope timeseries. The average slopes were 0.13, 0.14, 0.13, and 0.13.

APPENDIX IV

BEACH ELEVATION TIMESERIES

This appendix contains graphs of beach elevation through time for the entire subaerial beach. The data were used to observe beach profile variation through time at all cross-shore locations where an example timeseries was shown in Figure 3.2. All beaches and profiles are shown from north to south and the benchmark labels are illustrated on each figure panel. (refer Table II-1). The y-axis represents the cross-shore distance with 0 being the landward-most surveyed benchmark. Time is uniform along all x-axes from 1990 to January 2009. The colour bar on the right hand side represents the elevation relative to MSL. The horizontal black line in each figure panel is the location of the MSL contour. All profiles were plotted to MWLS which is RL -0.9 m.

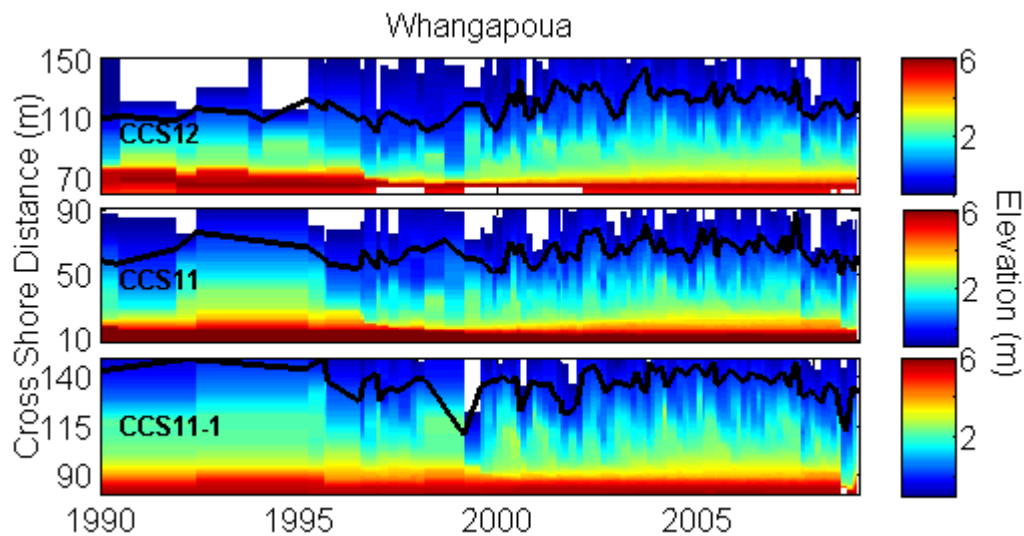


Figure IV.1: Whangapoua Beach elevation timeseries.

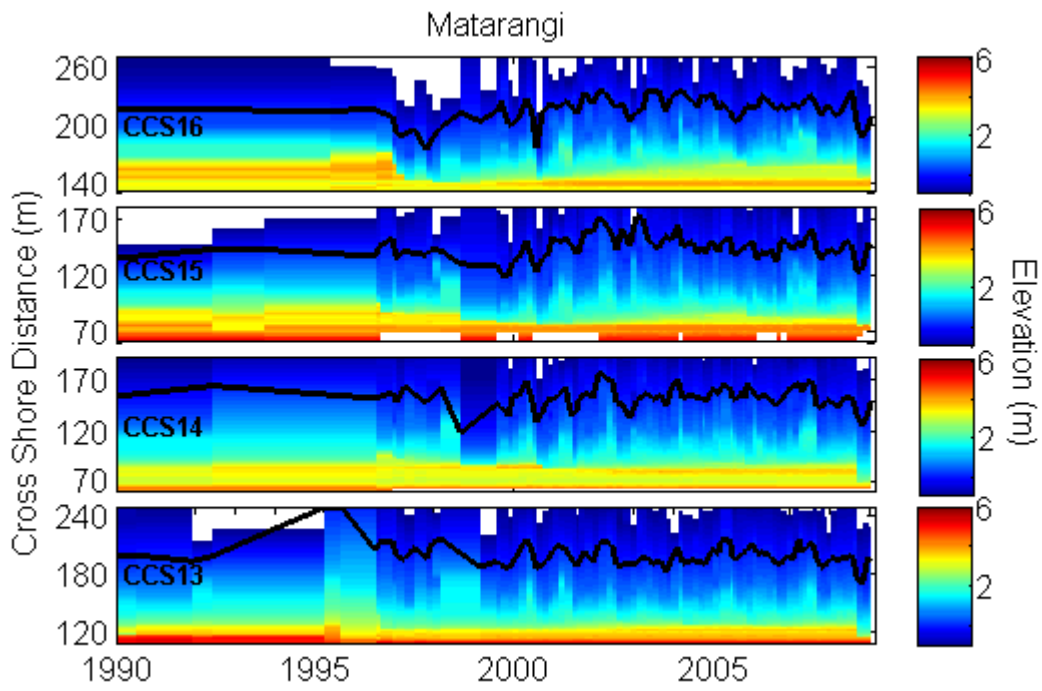


Figure IV.2: Matarangi Beach elevation timeseries.

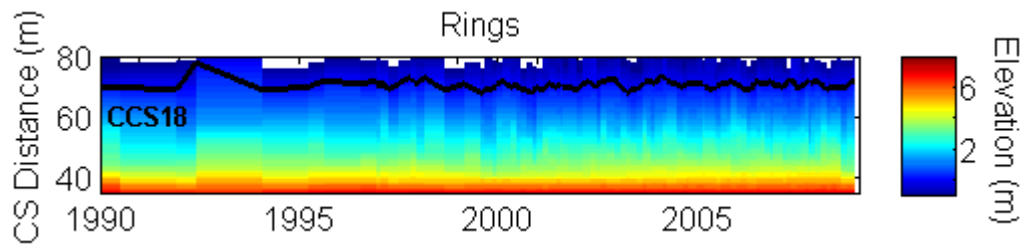


Figure IV.3: Rings Beach elevation timeseries. CS distance is the cross-shore distance.

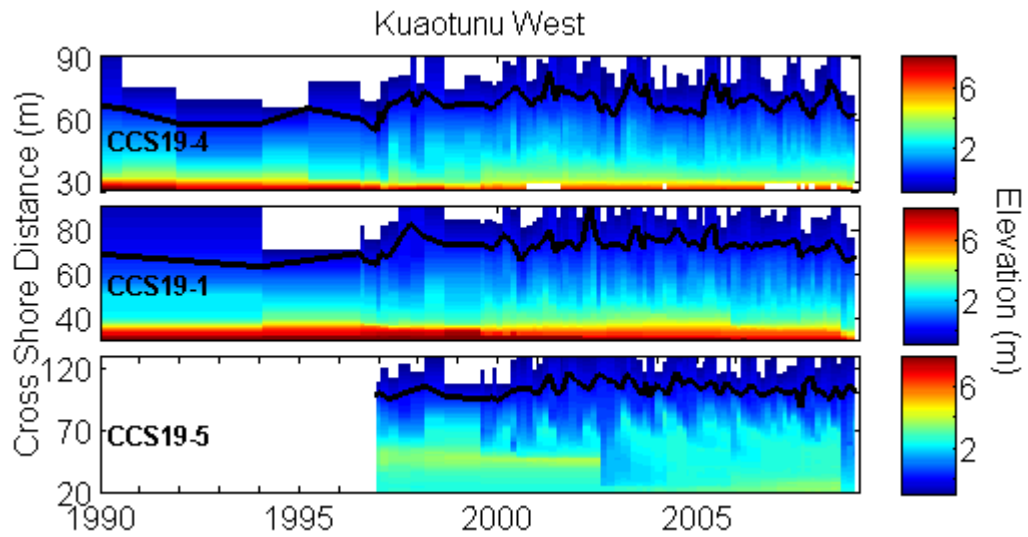


Figure IV.4: Kuaotunu West Beach elevation timeseries.

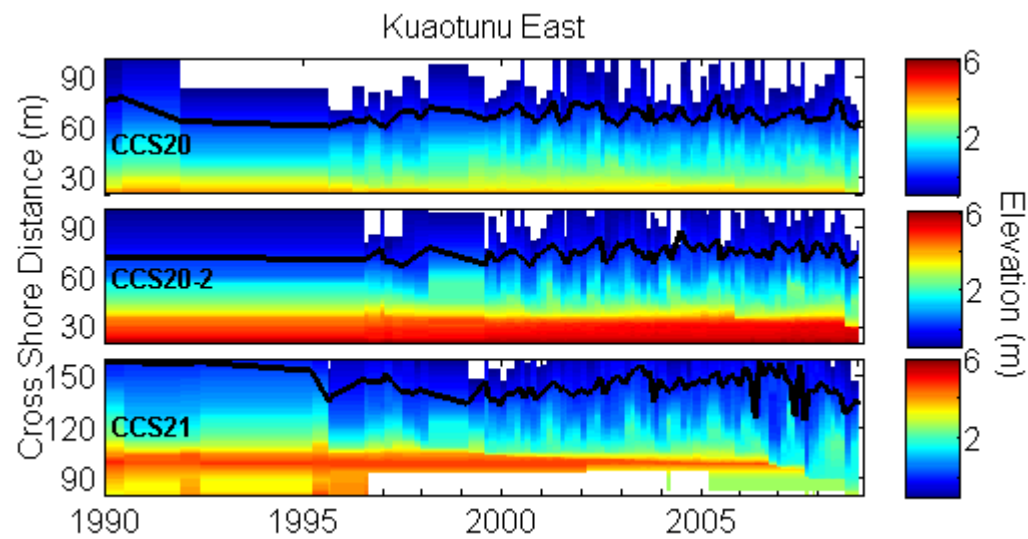


Figure IV.5: Kuaotunu East Beach elevation timeseries.

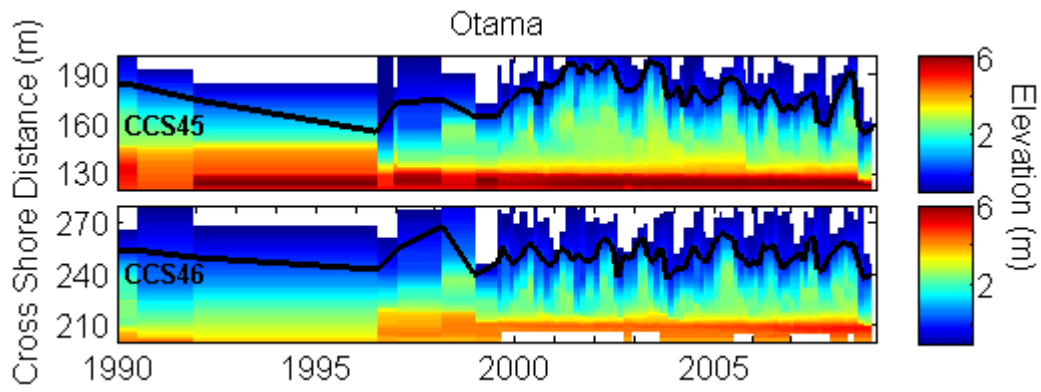


Figure IV.6: Otama Beach elevation timeseries.

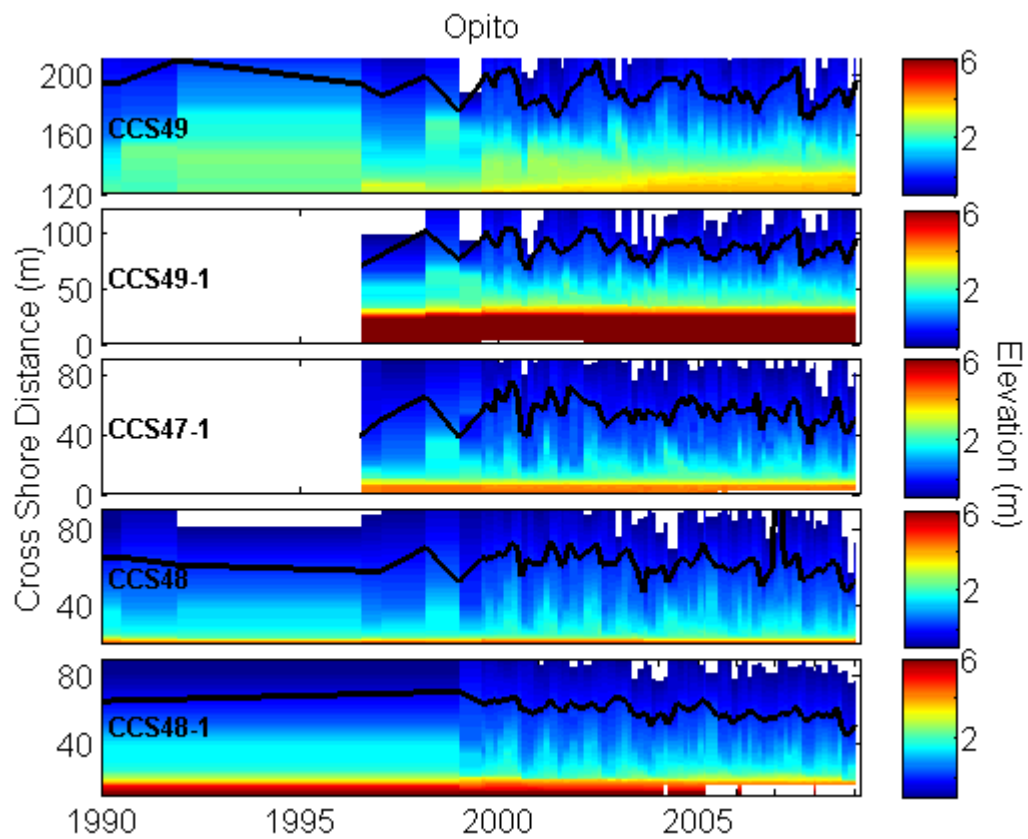


Figure IV.7: Opito Beach elevation timeseries.

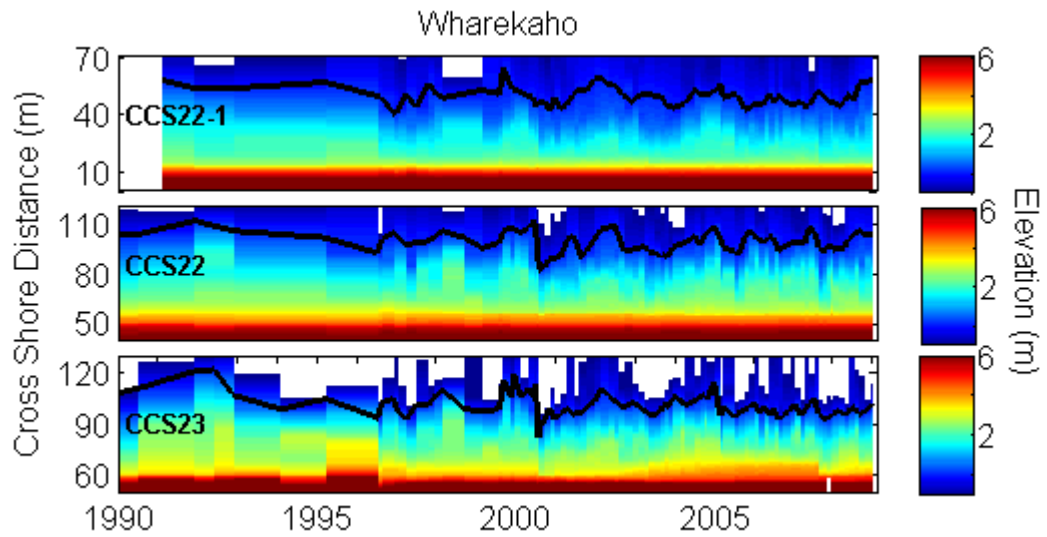


Figure IV.8: Whangapoua Beach elevation timeseries.

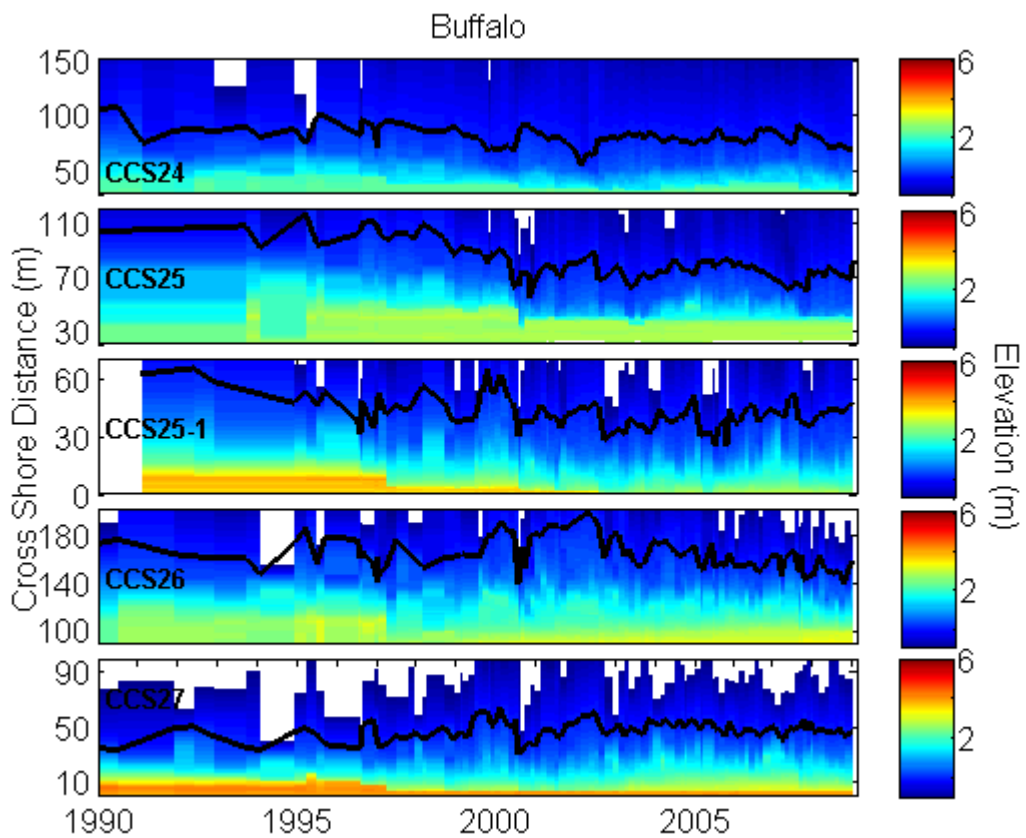


Figure IV.9: Buffalo Beach elevation timeseries.

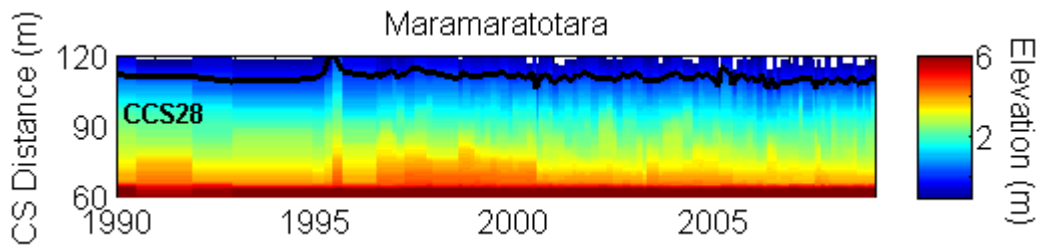


Figure IV.10: Maramaratotara Beach elevation timeseries. CS distance is the cross-shore distance.

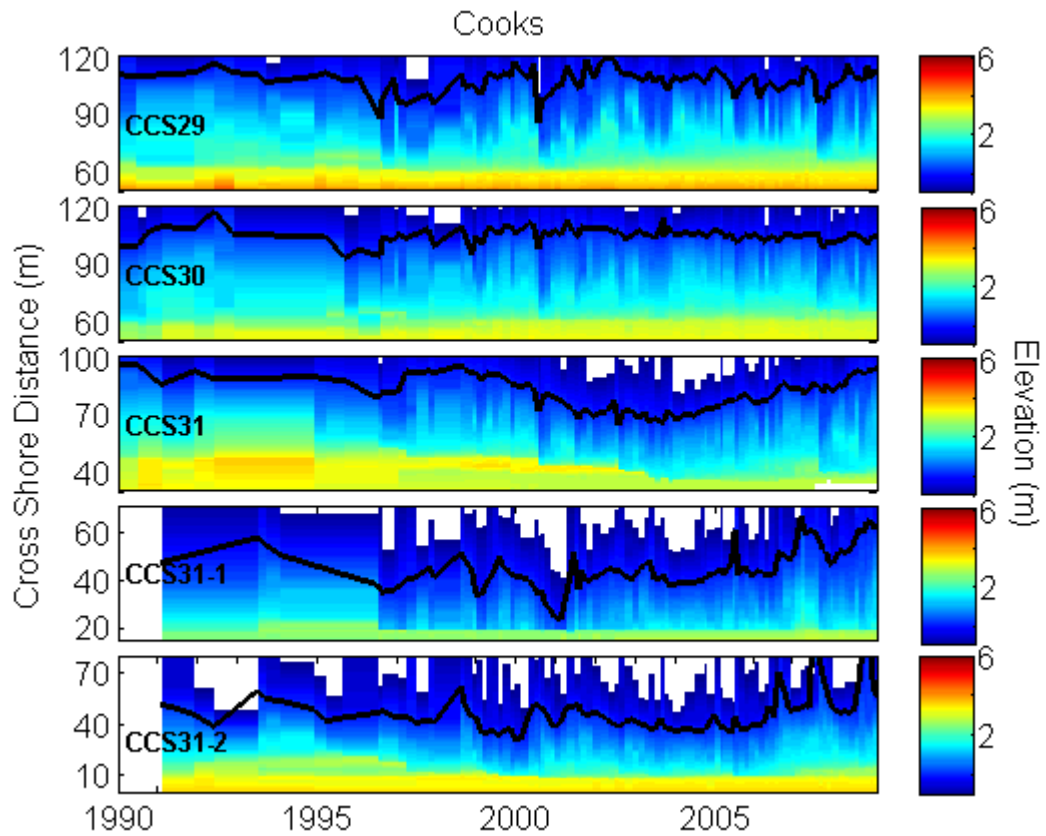


Figure IV.11: Cooks Beach elevation timeseries.

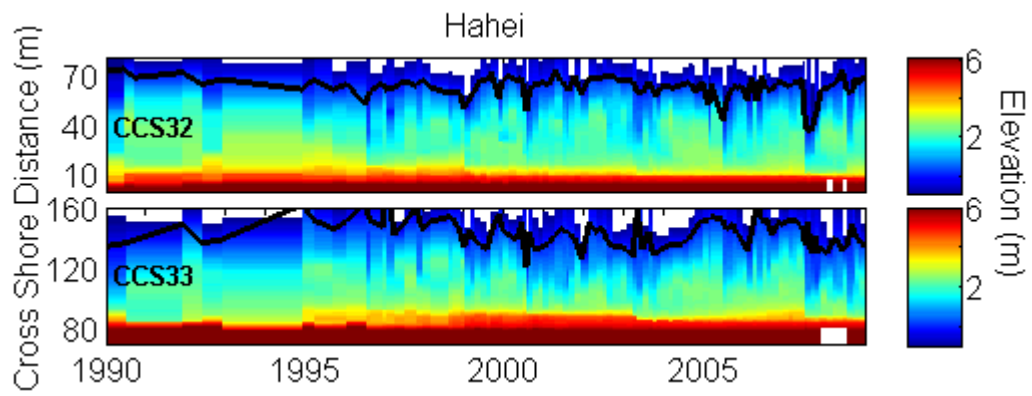


Figure IV.12: Hahei Beach elevation timeseries.

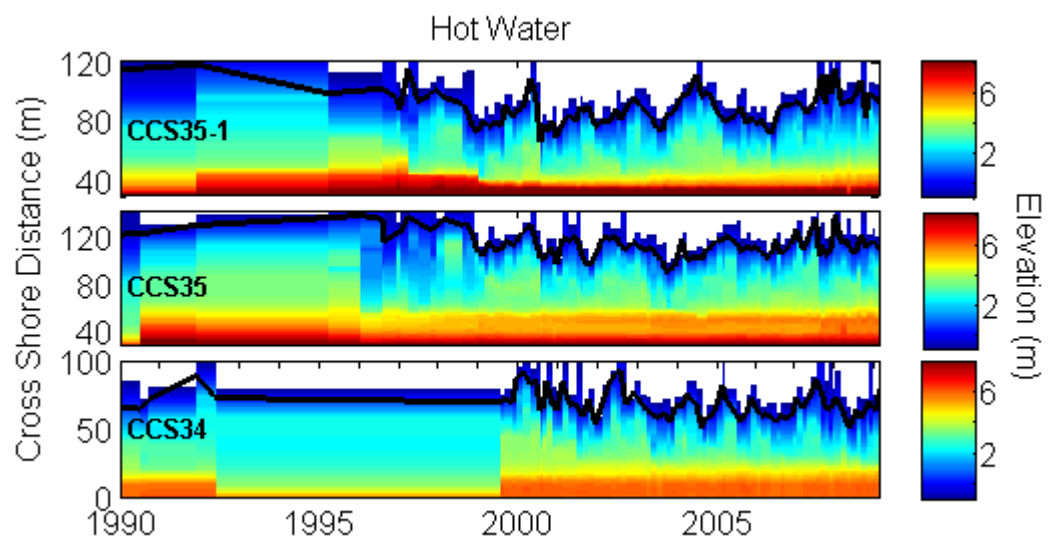


Figure IV.13: Hot Water Beach elevation timeseries.

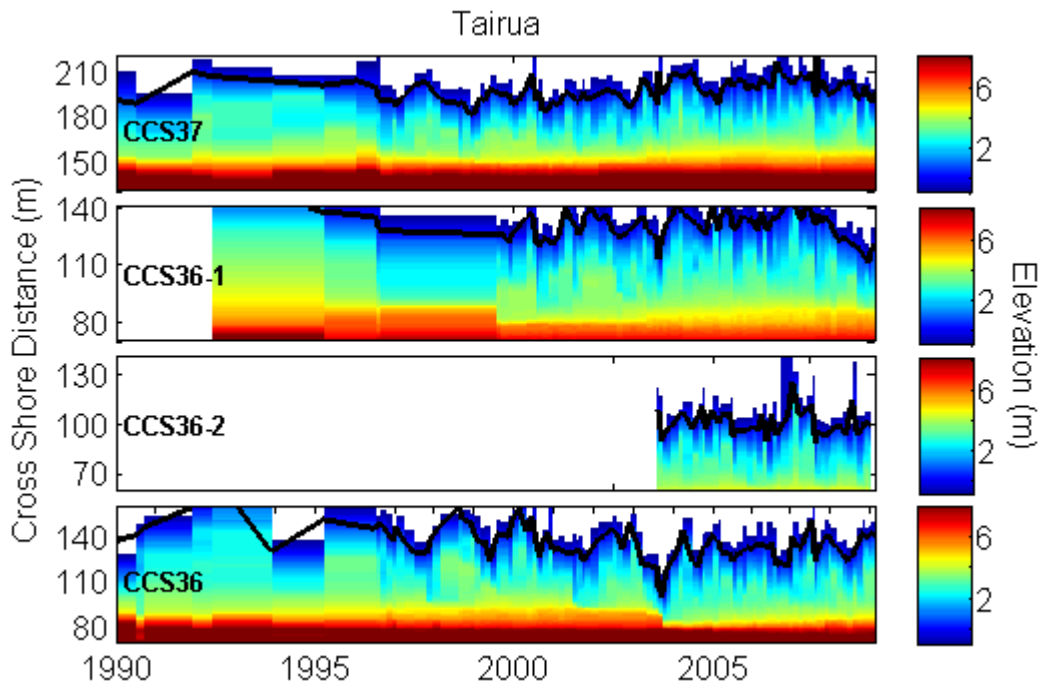


Figure IV.14: Tairua Beach elevation timeseries.

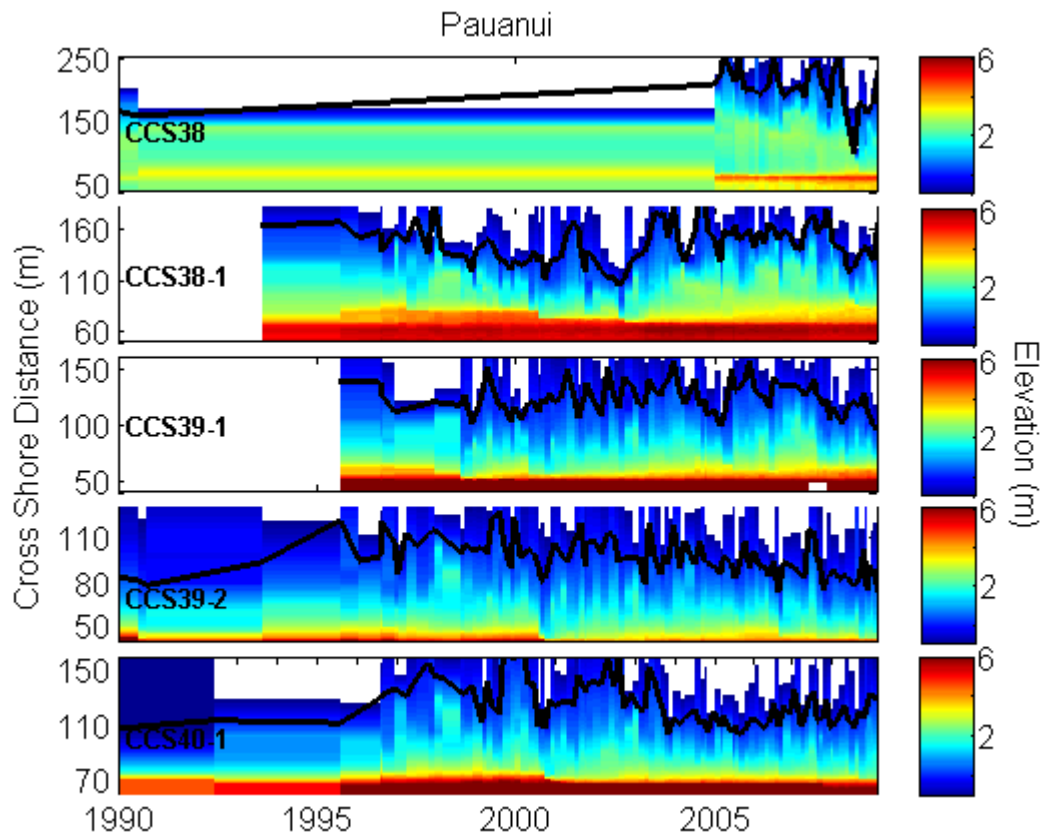


Figure IV.15: Pauanui Beach elevation timeseries.

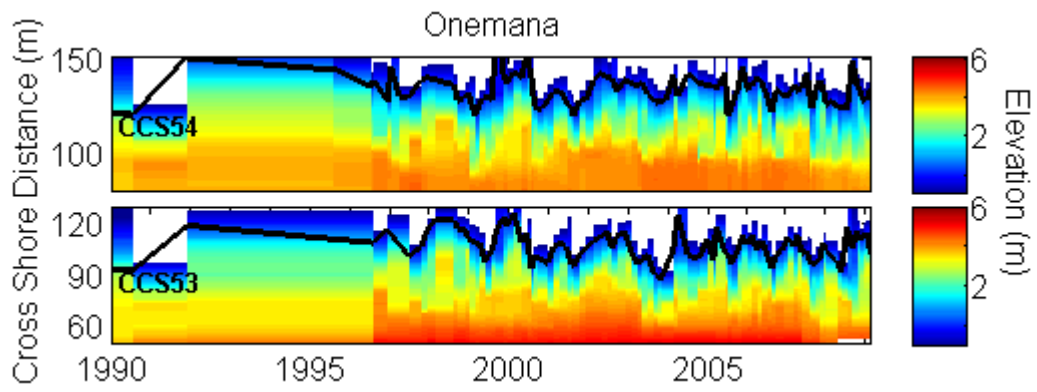


Figure IV.16: Onemana Beach elevation timeseries.

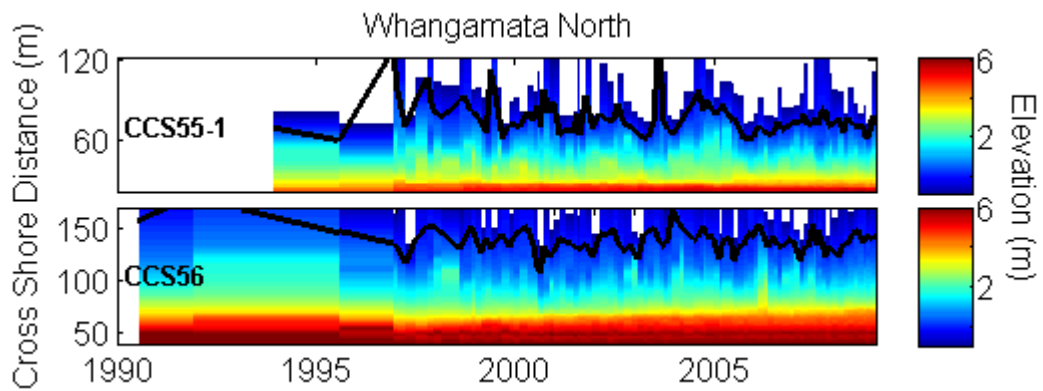


Figure IV.17: Whangamata North Beach elevation timeseries.

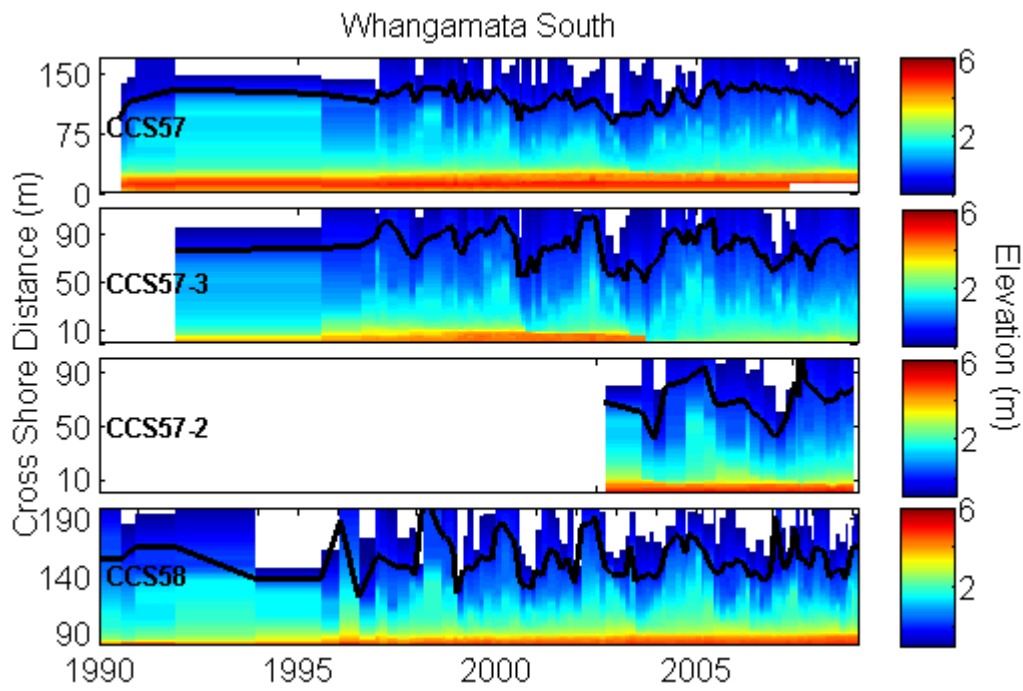


Figure IV.18: Whangamata South Beach elevation timeseries.

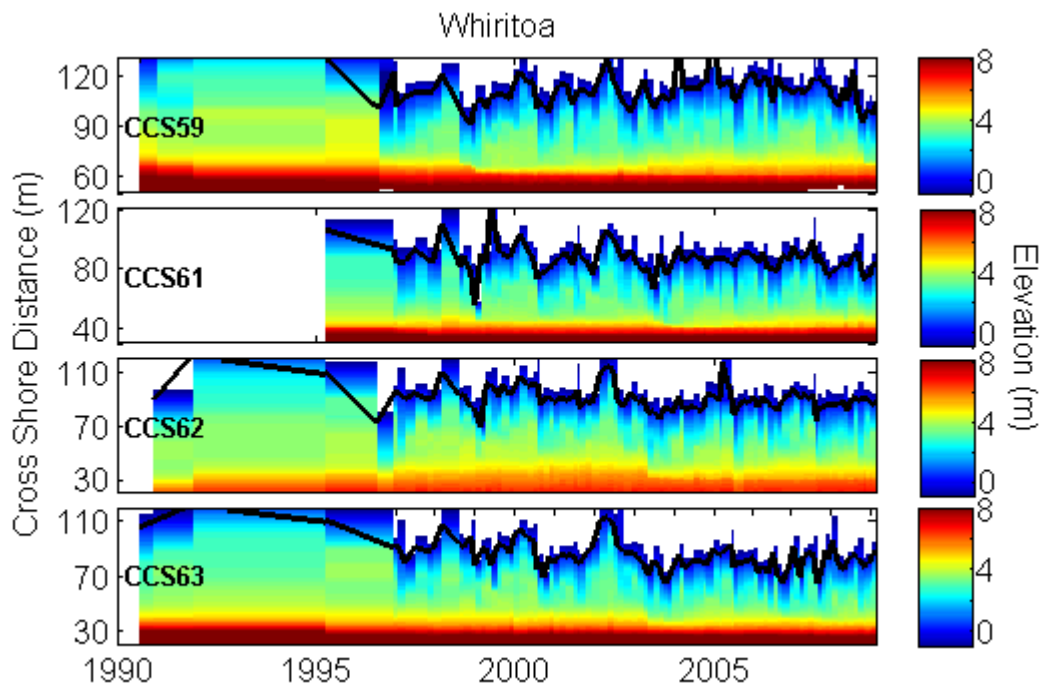


Figure IV.19: Whiritoa Beach elevation timeseries.

APPENDIX V

HORIZONTAL VOLUME SEGMENT TIMESERIES

This appendix contains graphs of the horizontal beach volume segments for each profile site. All of the figures generated are the same as the example timeseries shown in Chapter 3 (Figures 3.5 – 3.8) with regard to x- and y-axis limits, and the different unit of measure for the dune data. The beaches and profiles are displayed from north to south for the entire peninsula (refer Table II-1), with dune volume data in the top panel, upper beach volume data in the middle panel, and intertidal volume data in the bottom panel. All data have been demeaned. The dune data were measured in $\text{m}^3 \cdot \text{m}^{-1}$ and the axis limits were $\pm 20 \text{ m}^3 \cdot \text{m}^{-1}$. The upper beach and intertidal data are percentages of the mean volume with the axis limits being $\pm 50\%$. All profiles and panels are plotted from 1995 to January 2009 encasing the high resolution data available. The key findings regarding the data were the similarities between the upper beach and intertidal area, and the lack of short term variation in the dune data in most instances.

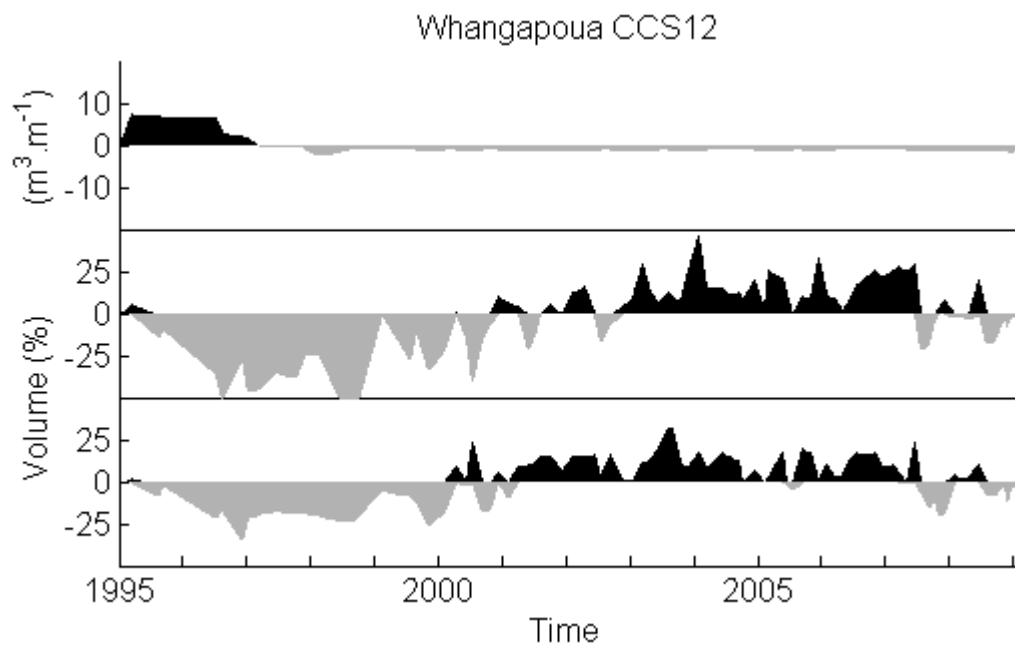


Figure V.1: Whangapoua CCS12 horizontal beach segment volume data.

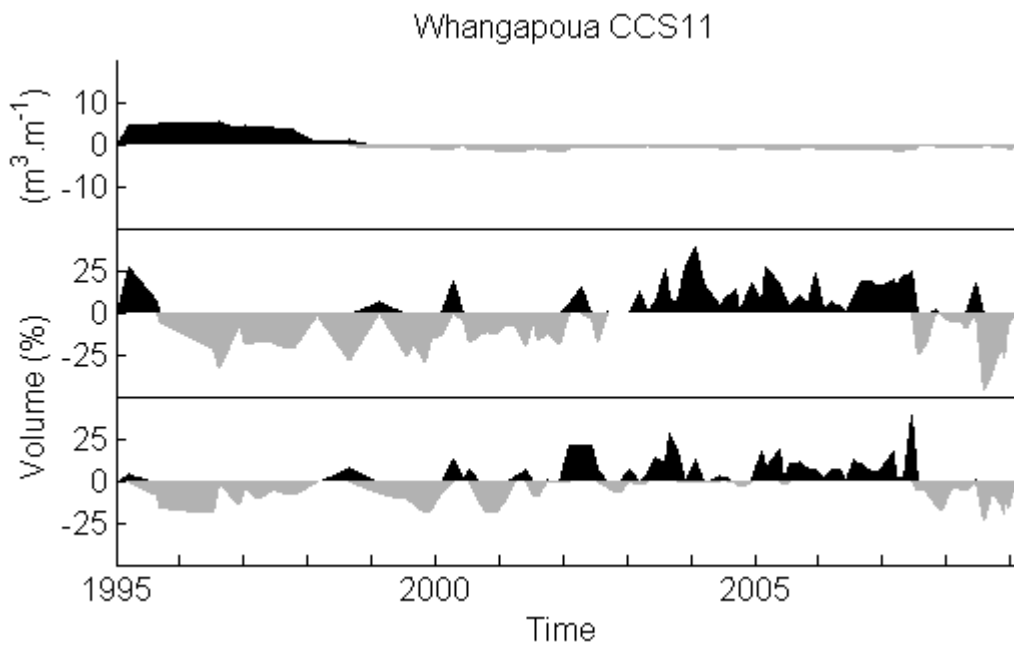


Figure V.2: Whangapoua CCS11 horizontal beach segment volume data.

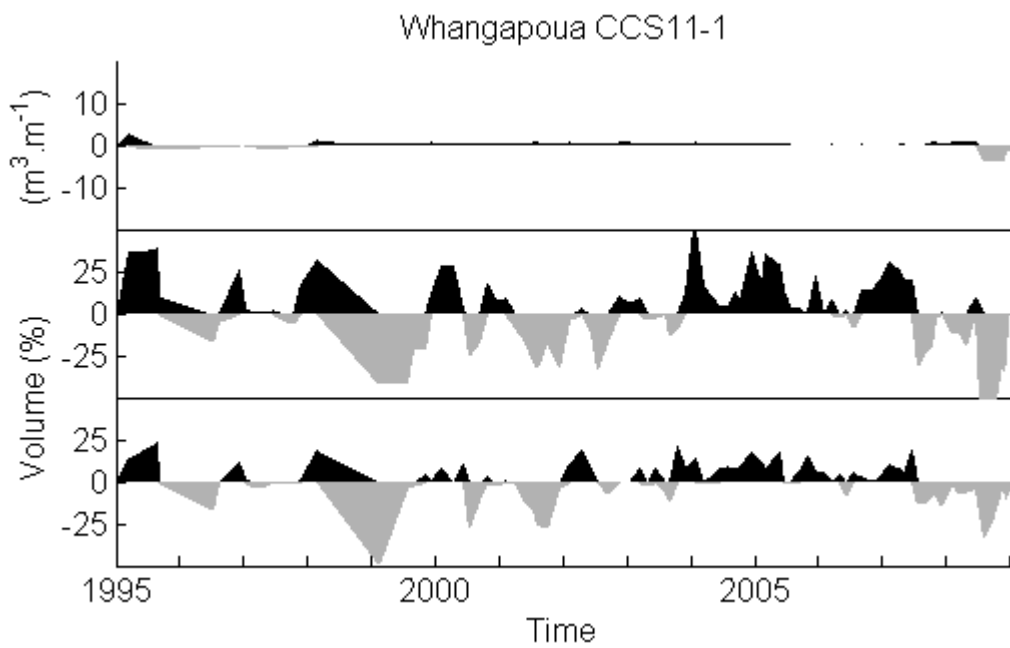


Figure V.3: Whangapoua CCS11-1 horizontal beach segment volume data.

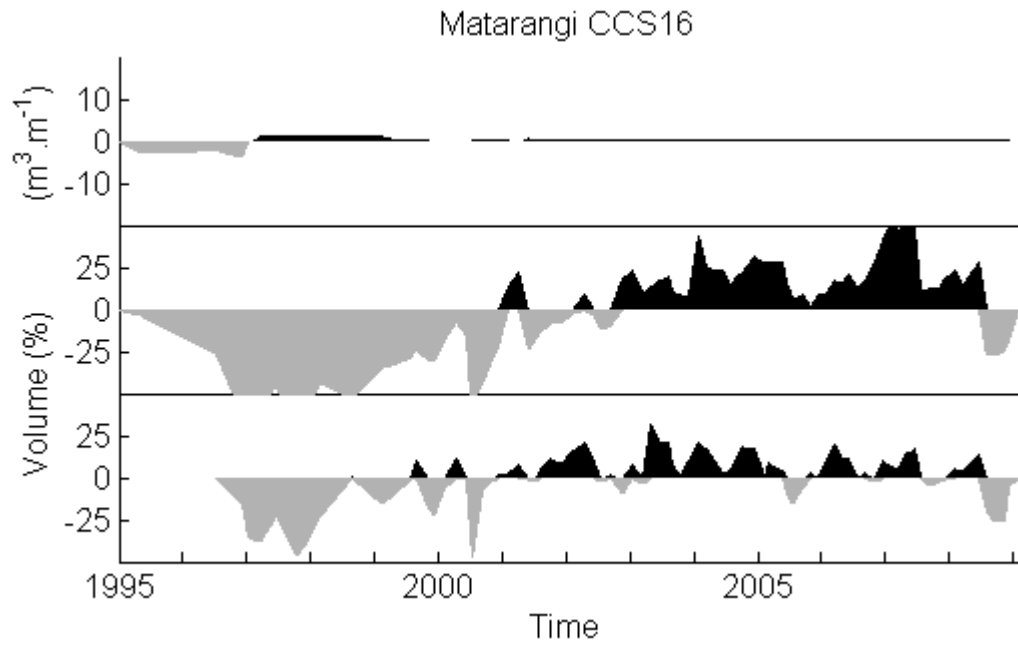


Figure V.4: Matarangi CCS16 horizontal beach segment volume data.

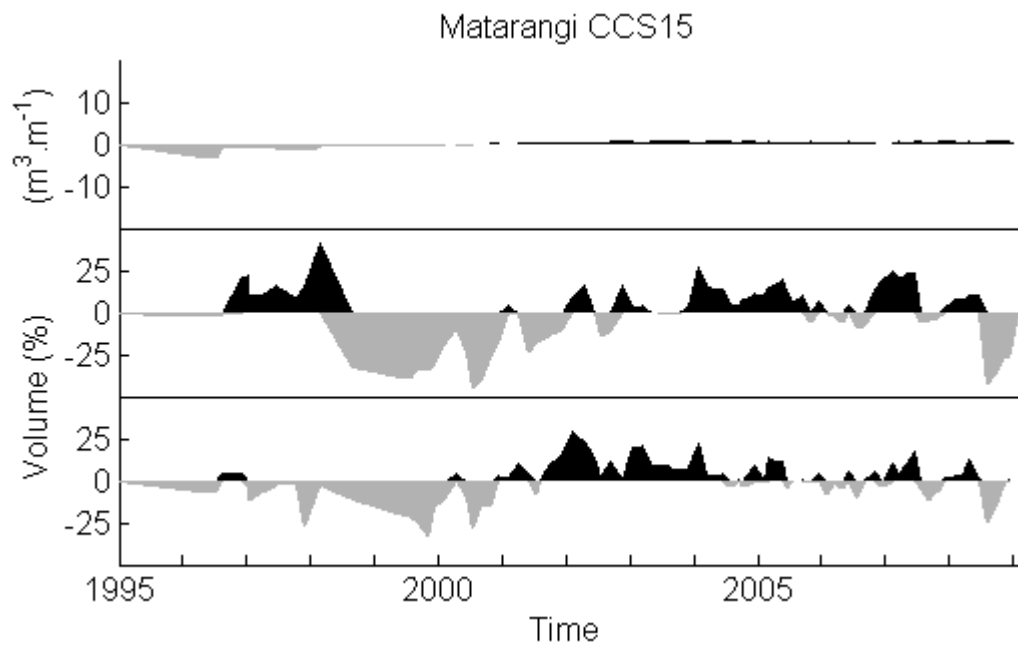


Figure V.5: Matarangi CCS15 horizontal beach segment volume data.

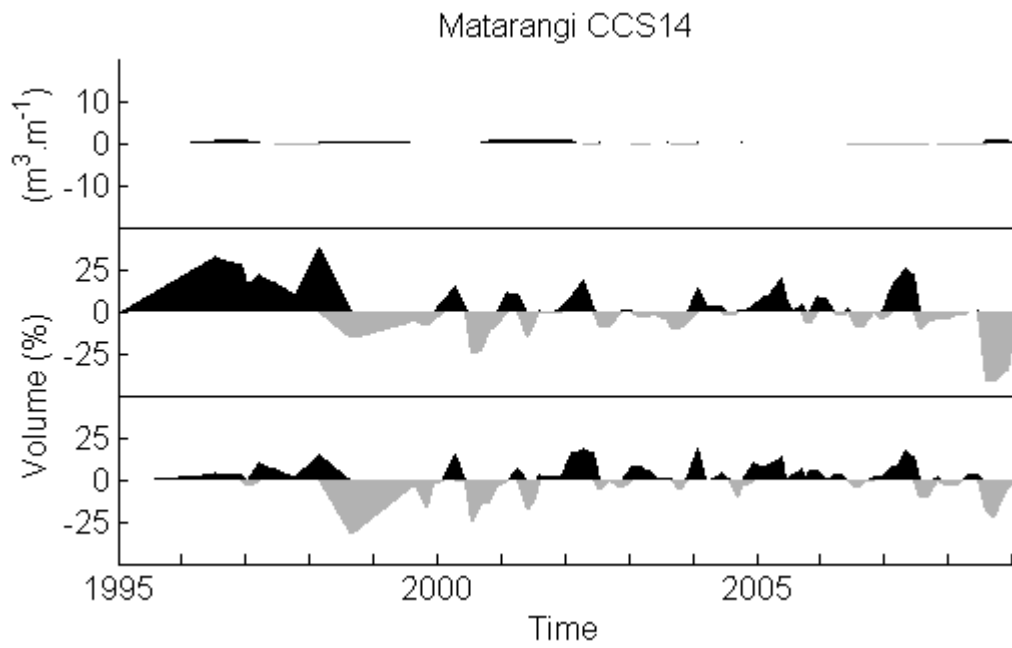


Figure V.6: Matarangi CCS14 horizontal beach segment volume data.

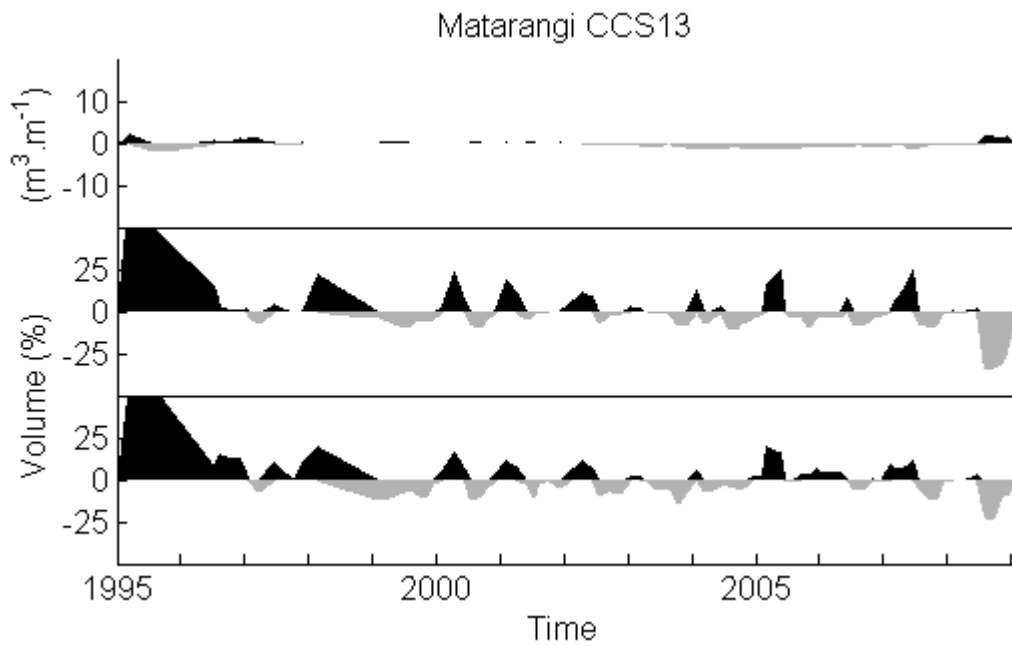


Figure V.7: Matarangi CCS13 horizontal beach segment volume data.

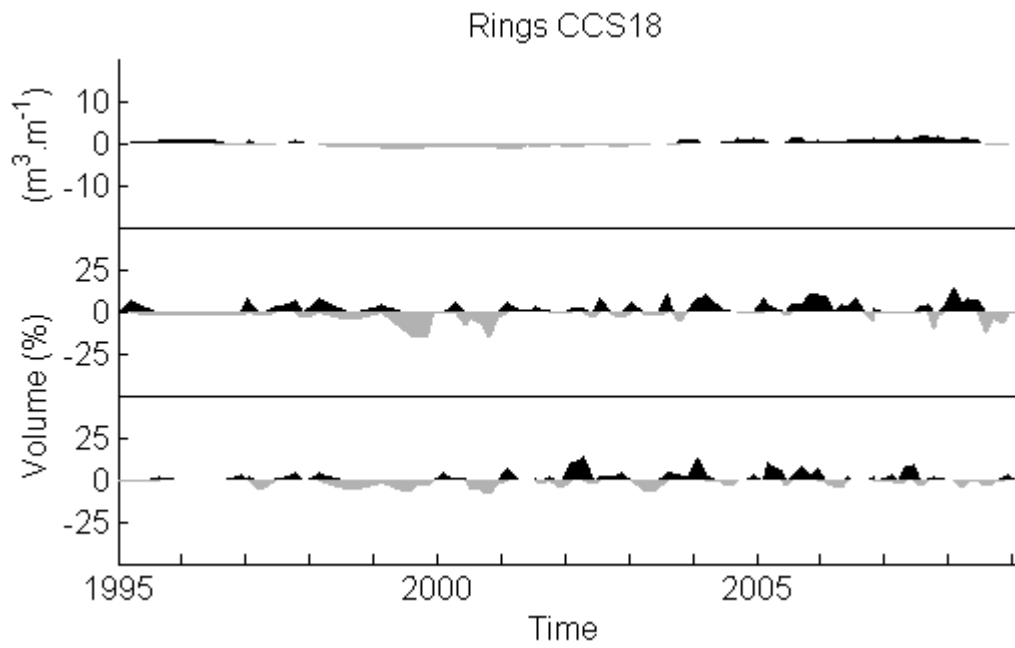


Figure V.8: Rings CCS18 horizontal beach segment volume data.

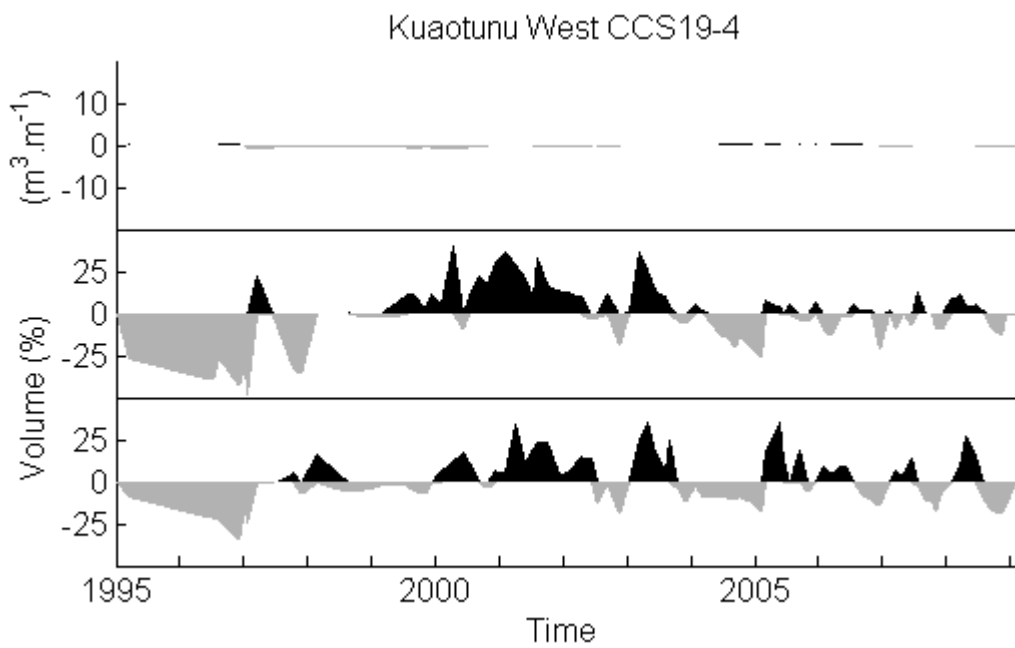


Figure V.9: Kuaotunu West CCS19-4 horizontal beach segment volume data.

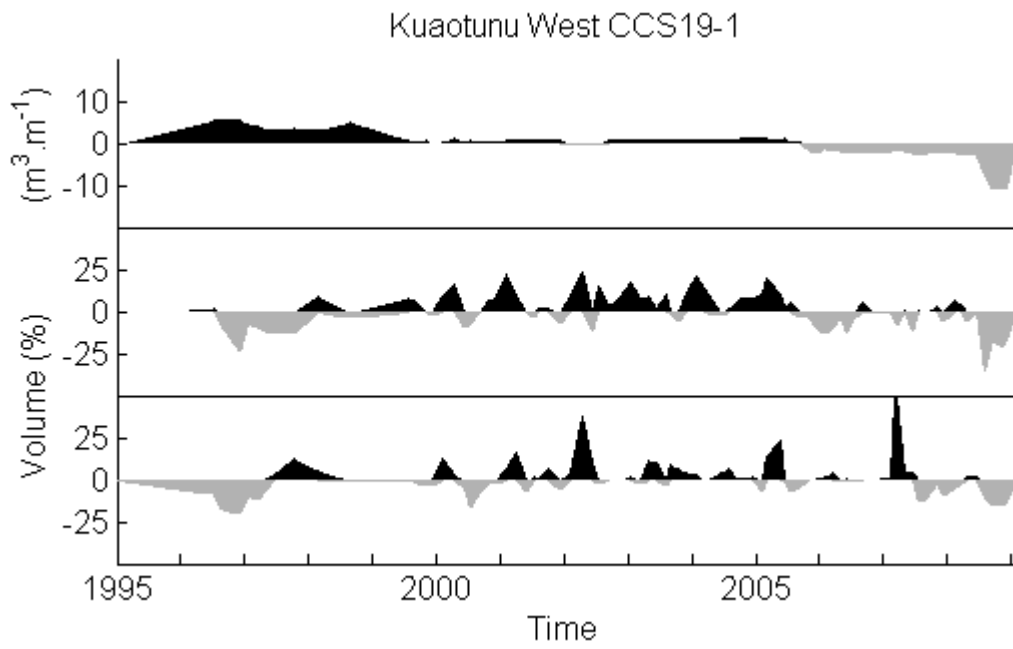


Figure V.10: Kuaotunu West CCS19-1 horizontal beach segment volume data.

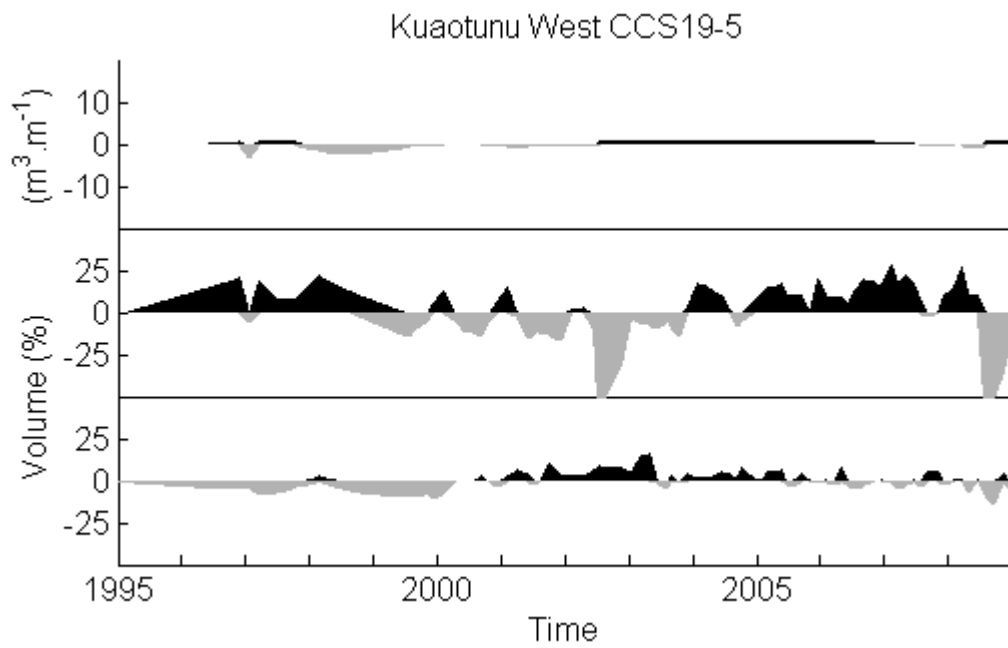


Figure V.11: Kuaotunu West CCS19-5 horizontal beach segment volume data.

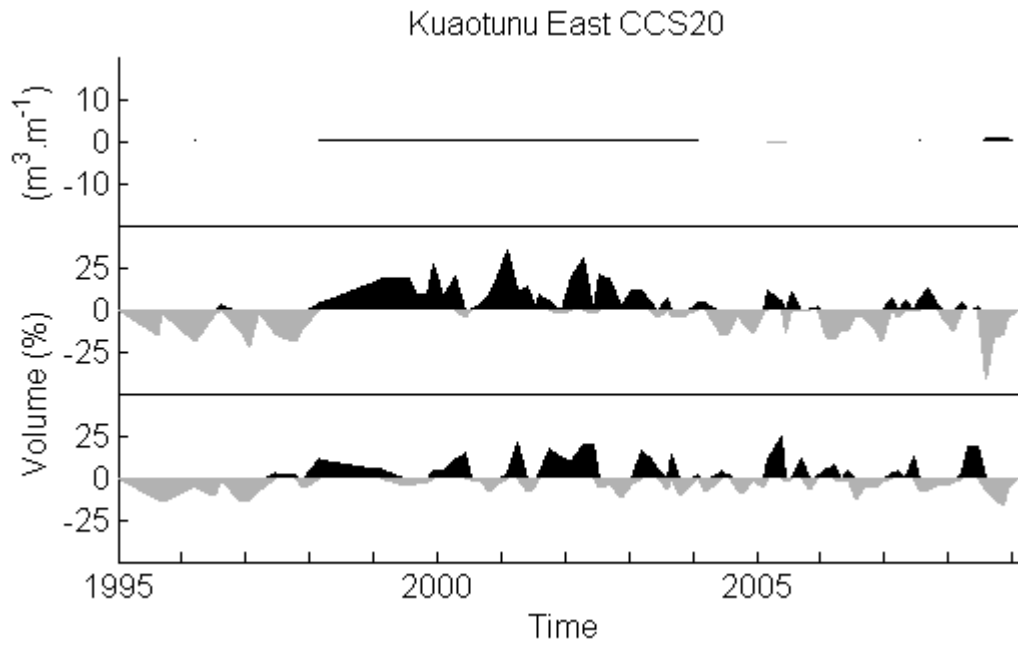


Figure V.12: Kuaotunu East CCS20 horizontal beach segment volume data.

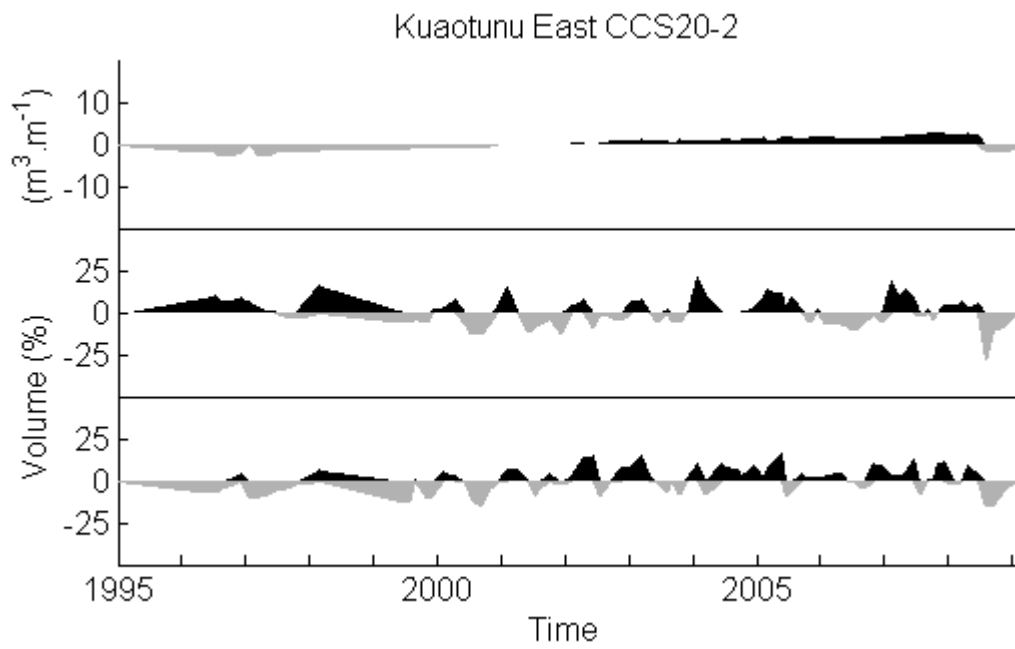


Figure V.13: Kuaotunu East CCS20-2 horizontal beach segment volume data.

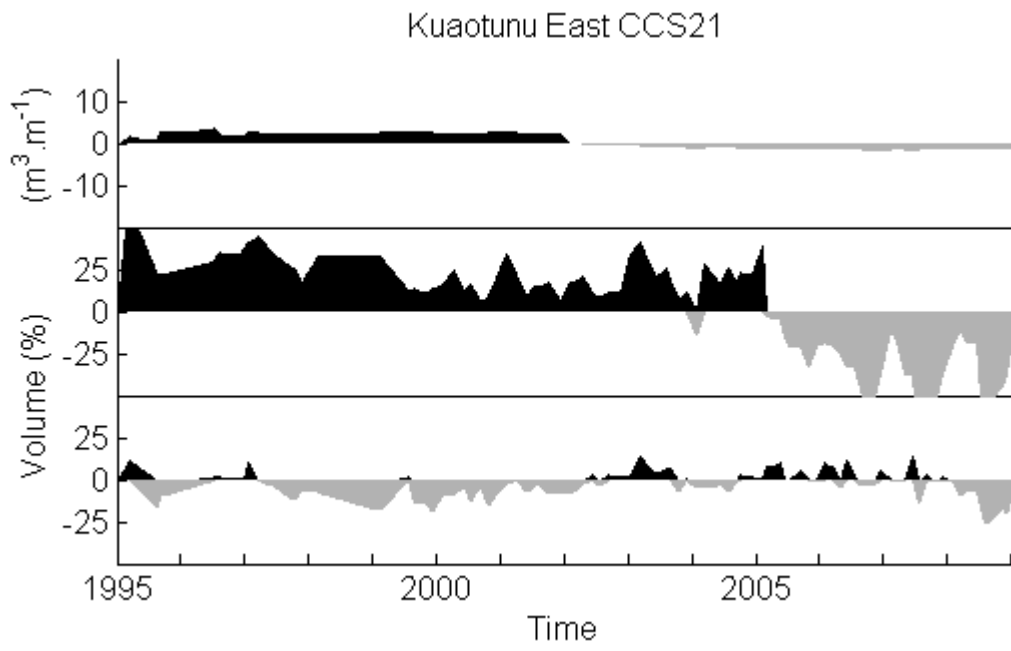


Figure V.14: Kuaotunu East CCS21 horizontal beach segment volume data.

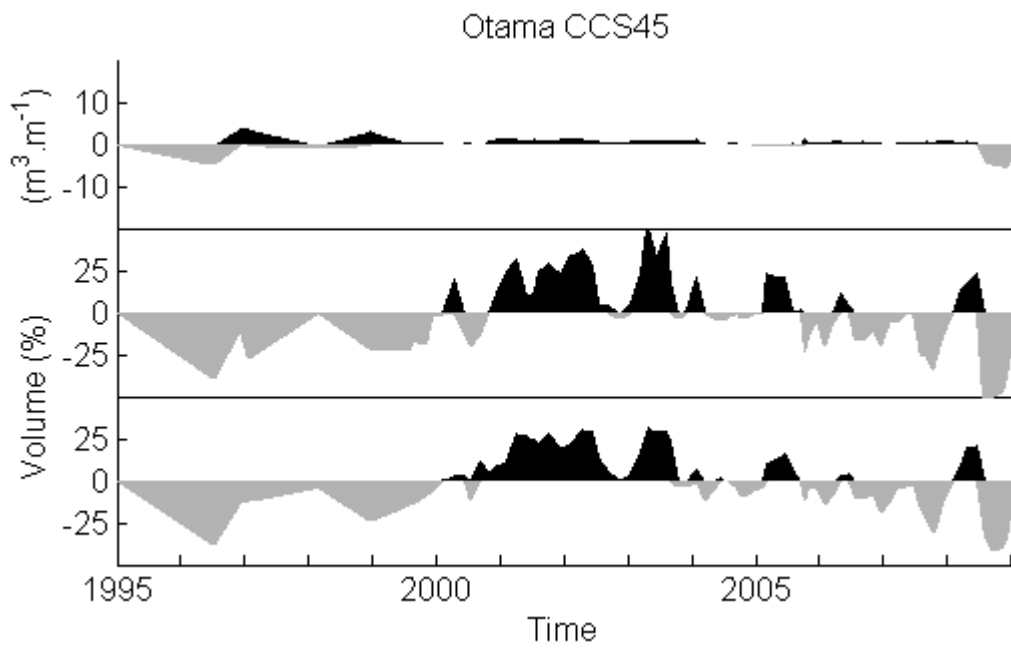


Figure V.15: Otama CCS45 horizontal beach segment volume data.

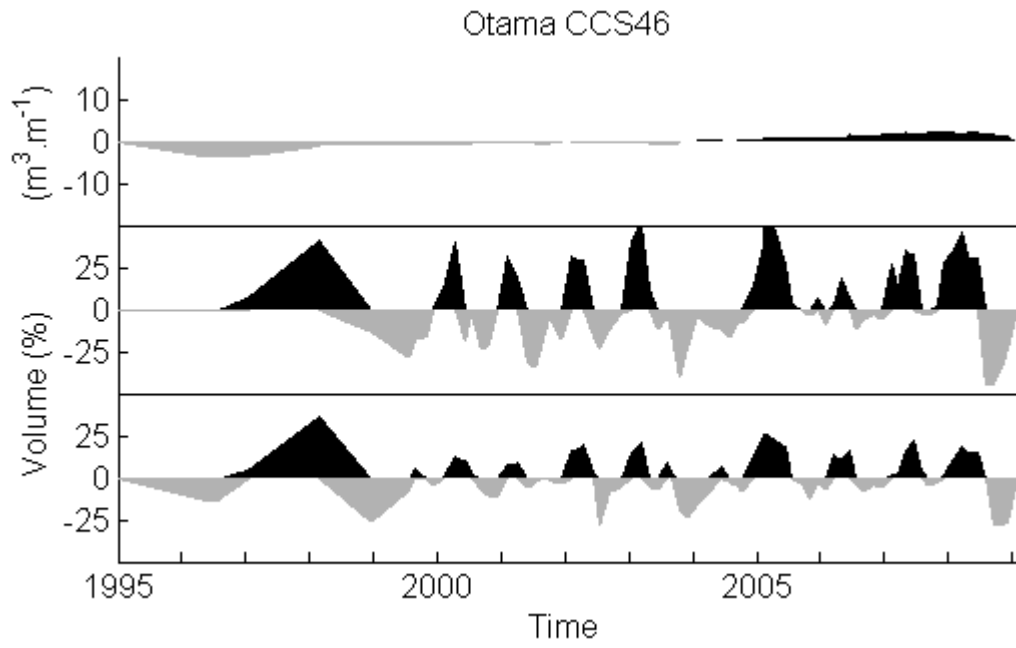


Figure V.16: Otama CCS46 horizontal beach segment volume data.

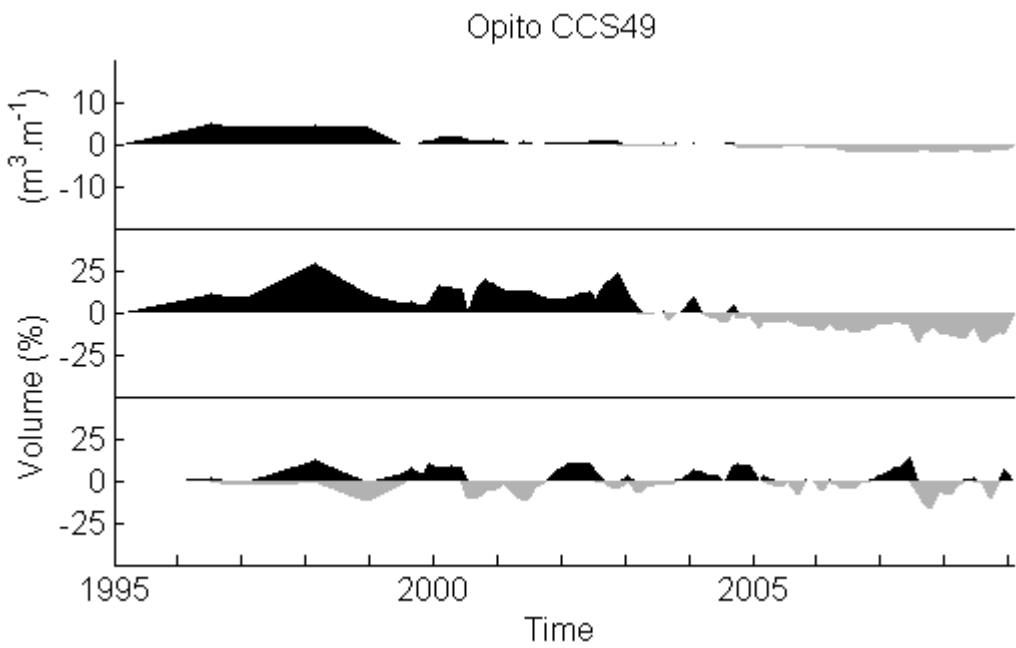


Figure V.17: Opito CCS49 horizontal beach segment volume data.

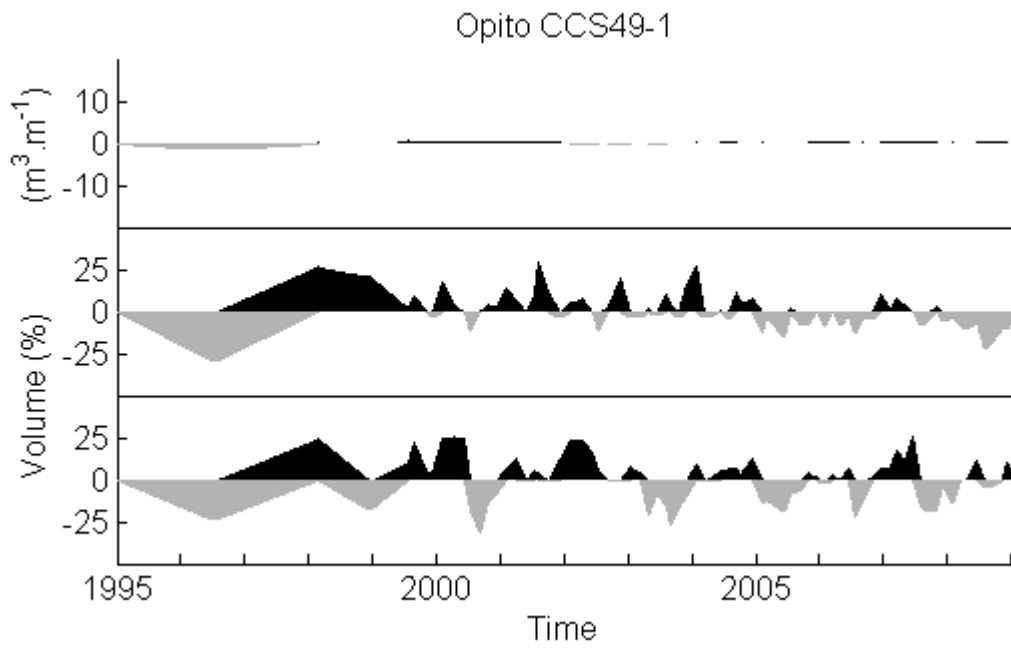


Figure V.18: Opito CCS49-1 horizontal beach segment volume data.

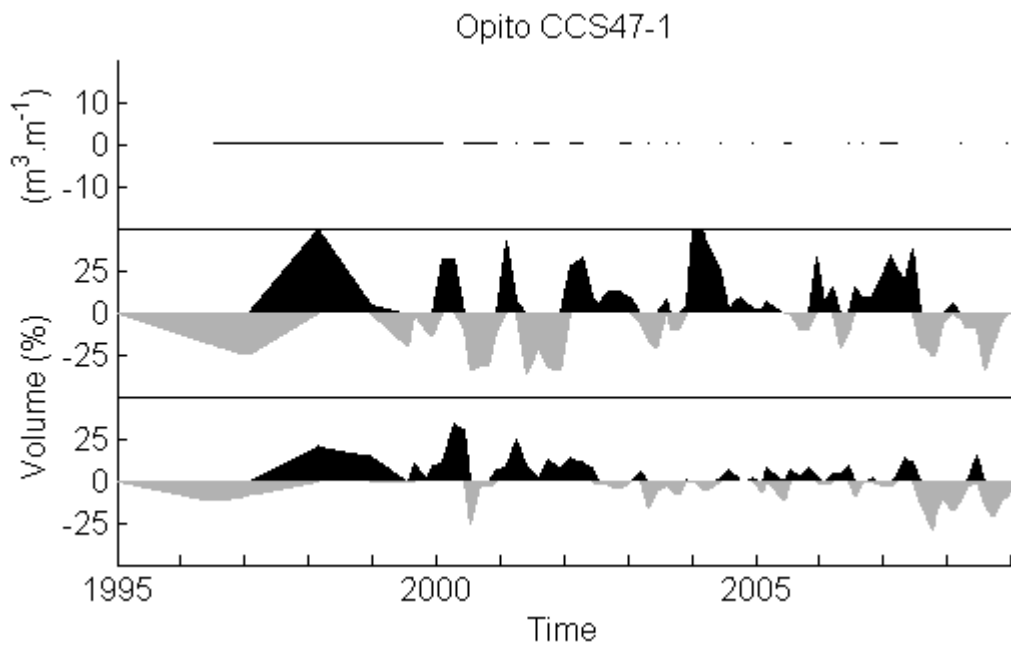


Figure V.19: Opito CCS47-1 horizontal beach segment volume data.

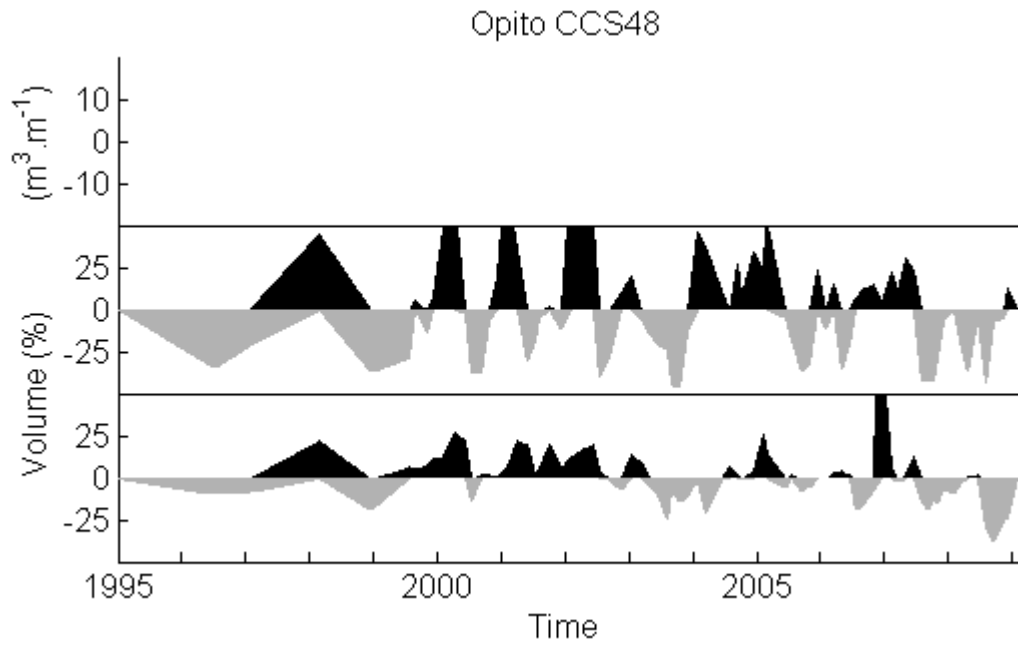


Figure V.20: Opito CCS48 horizontal beach segment volume data.

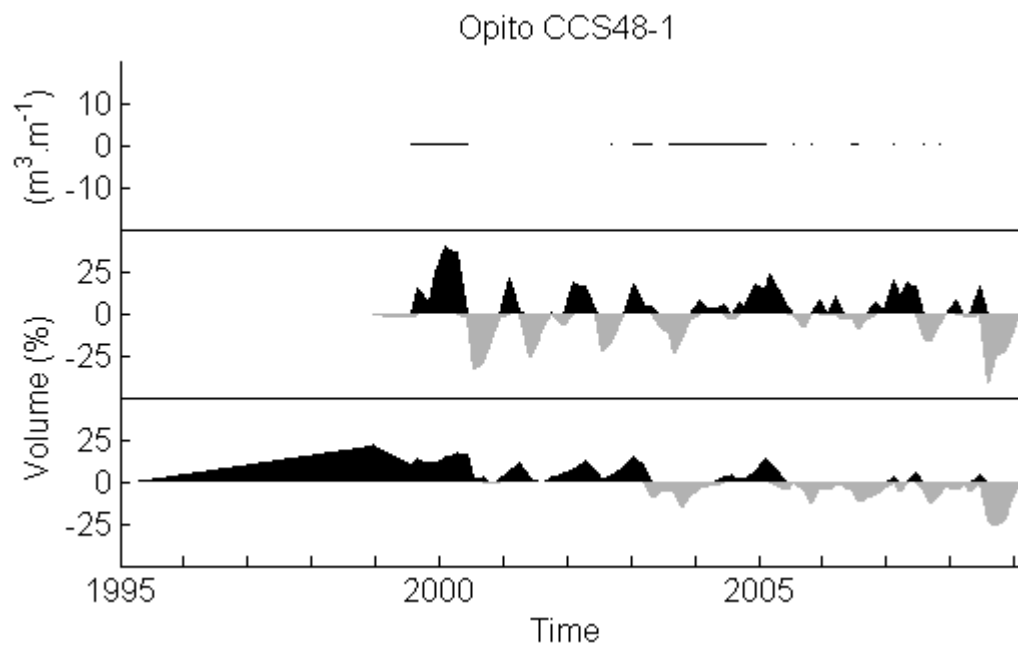


Figure V.21: Opito CCS48-1 horizontal beach segment volume data.

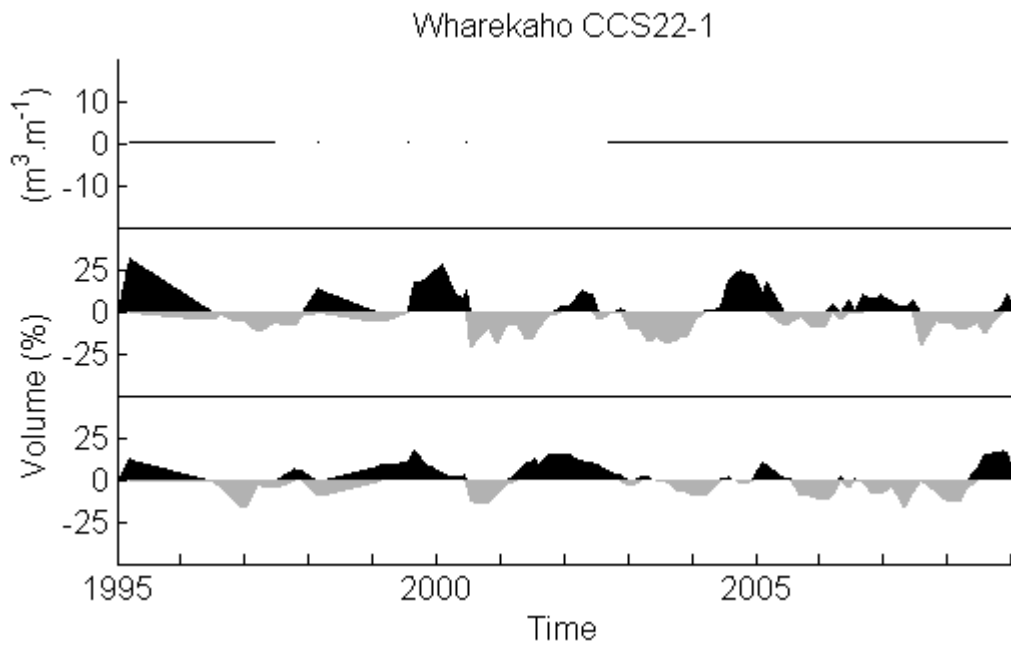


Figure V.22: Wharekaho CCS22-1 horizontal beach segment volume data.

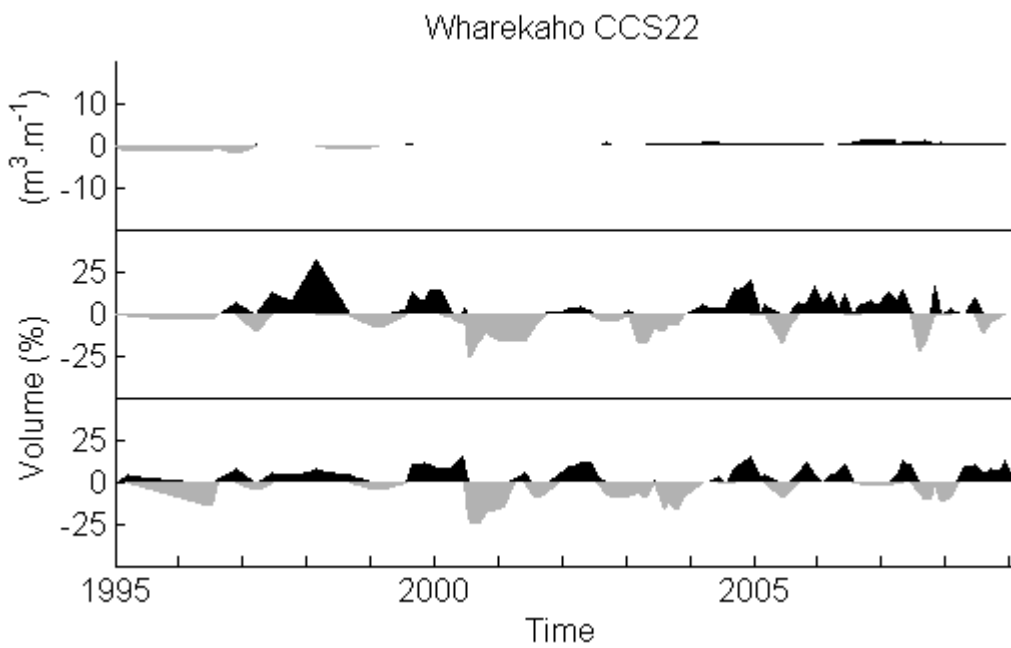


Figure V.23: Wharekaho CCS22 horizontal beach segment volume data.

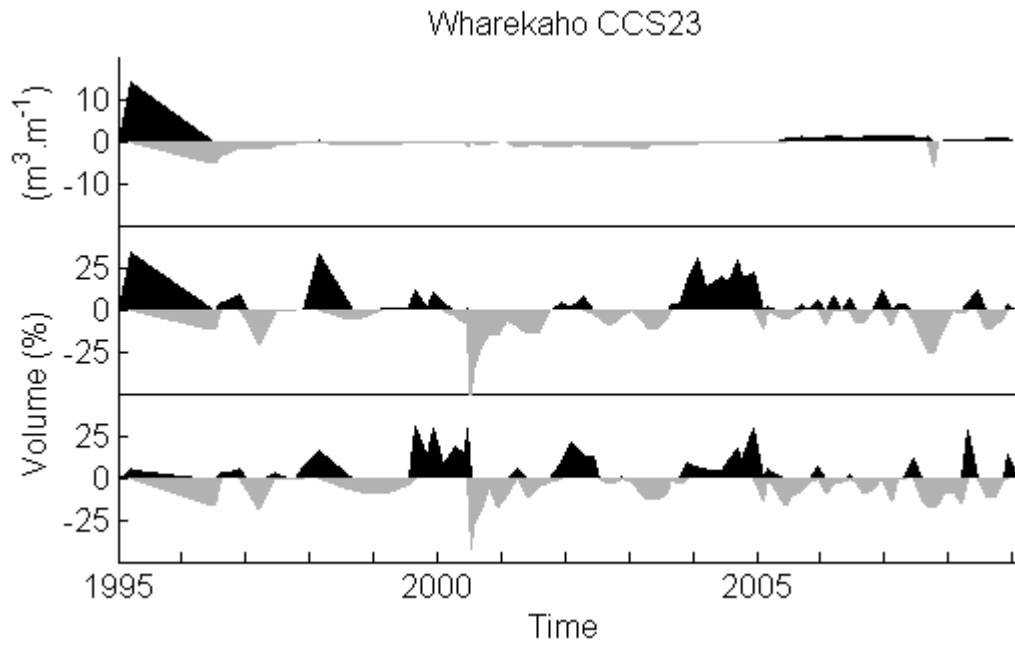


Figure V.24: Wharekaho CCS23 horizontal beach segment volume data.

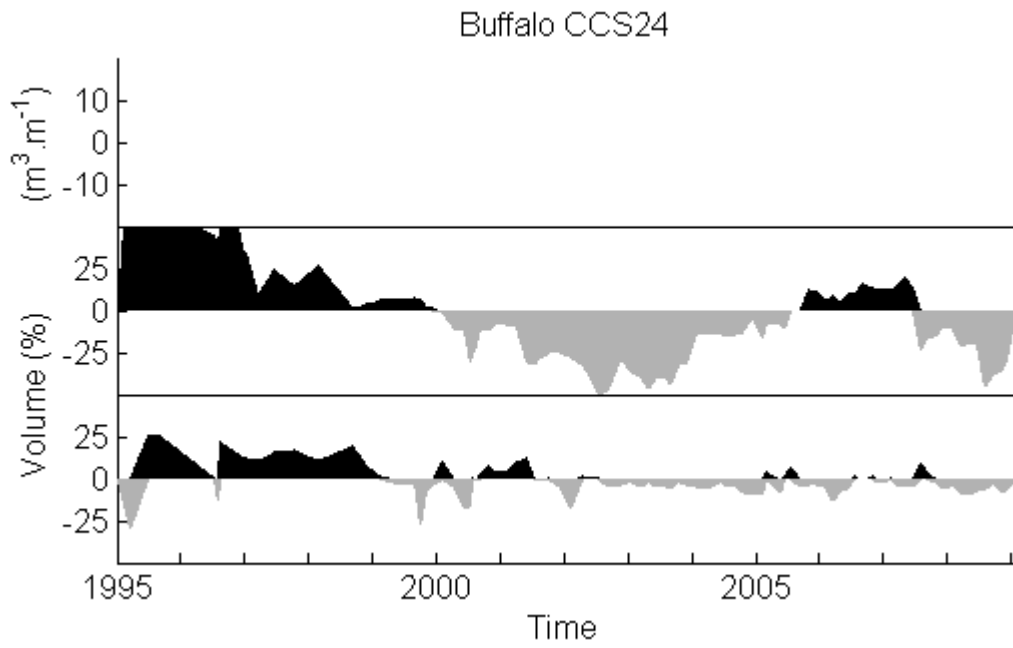


Figure V.25: Buffalo CCS24 horizontal beach segment volume data.

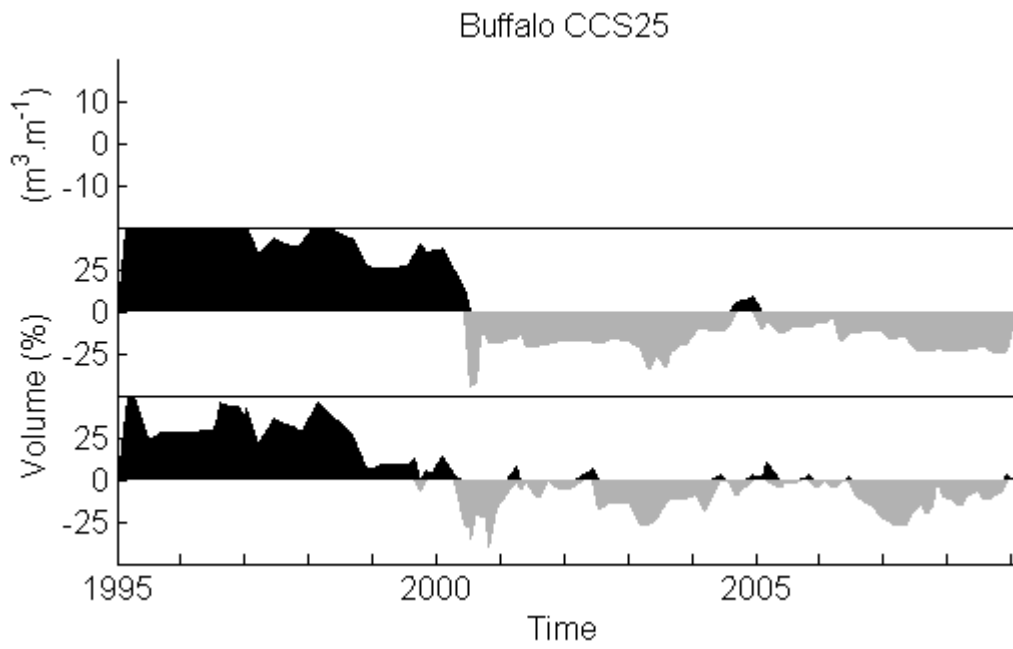


Figure V.26: Buffalo CCS25 horizontal beach segment volume data.

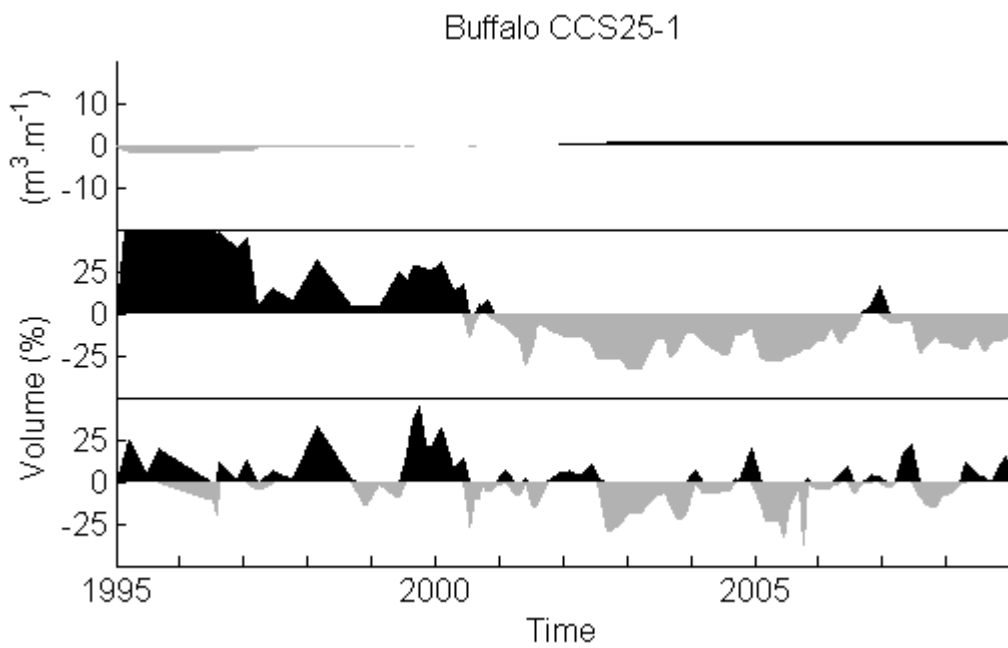


Figure V.27: Buffalo CCS25-1 horizontal beach segment volume data.

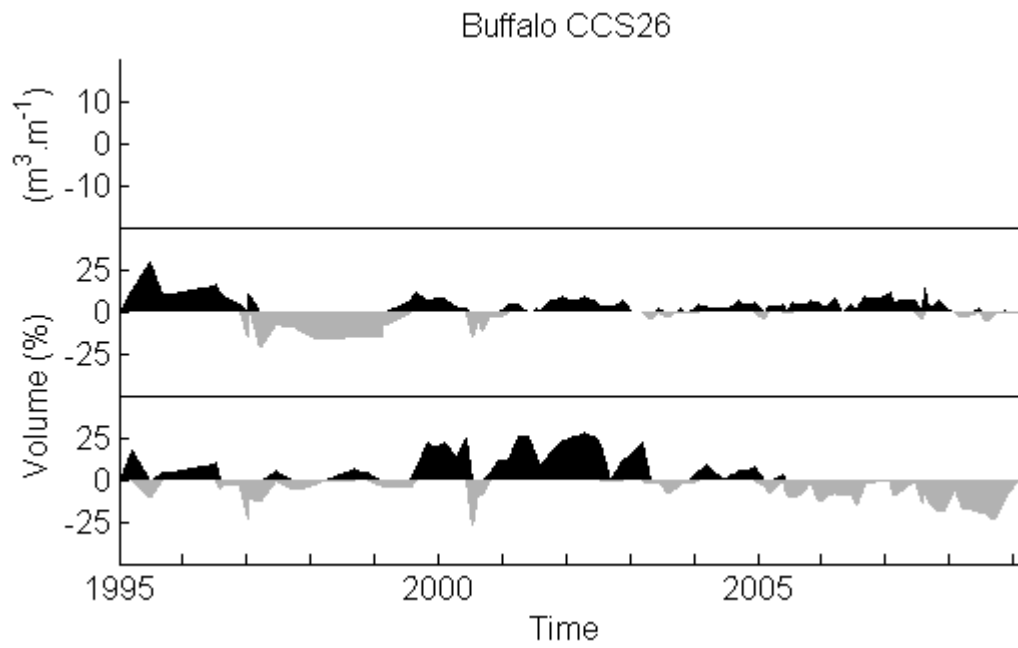


Figure V.28: Buffalo CCS26 horizontal beach segment volume data.

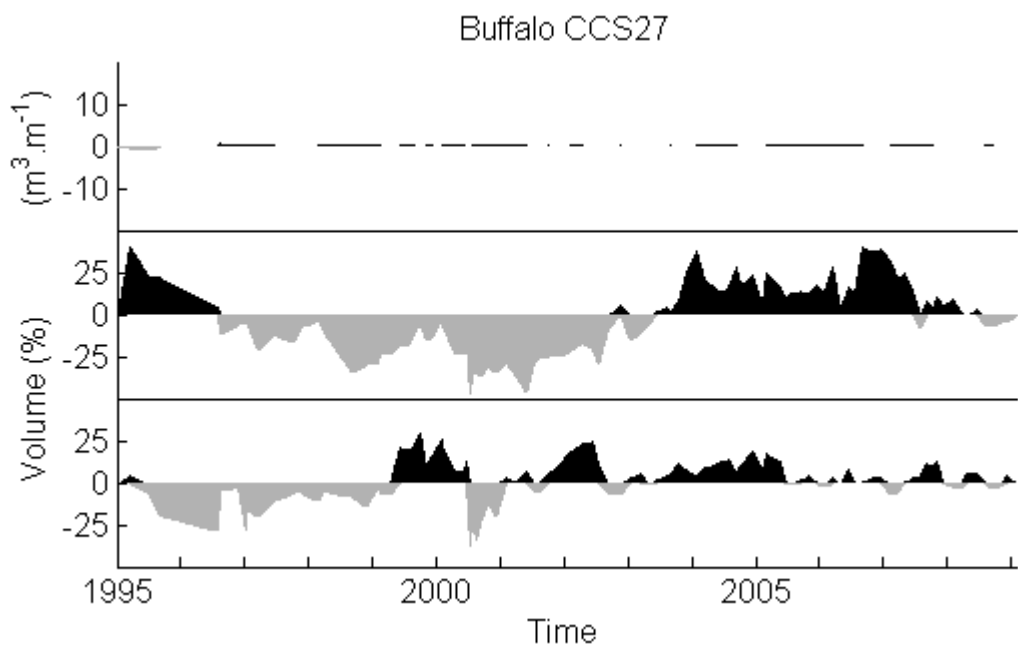


Figure V.29: Buffalo CCS27 horizontal beach segment volume data.

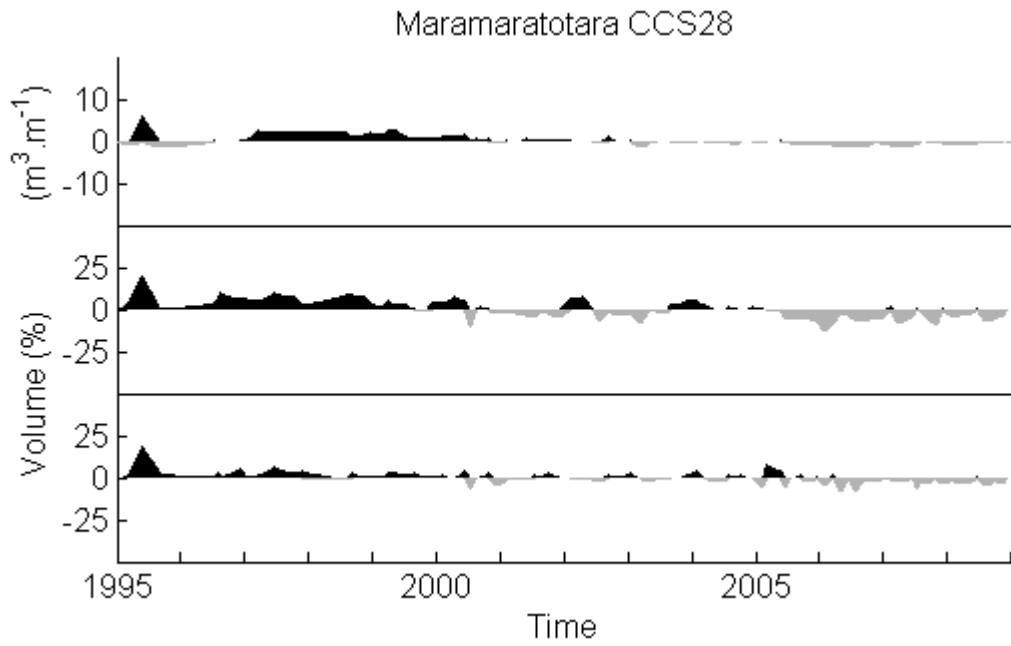


Figure V.30: Maramaratotara CCS28 horizontal beach segment volume data.

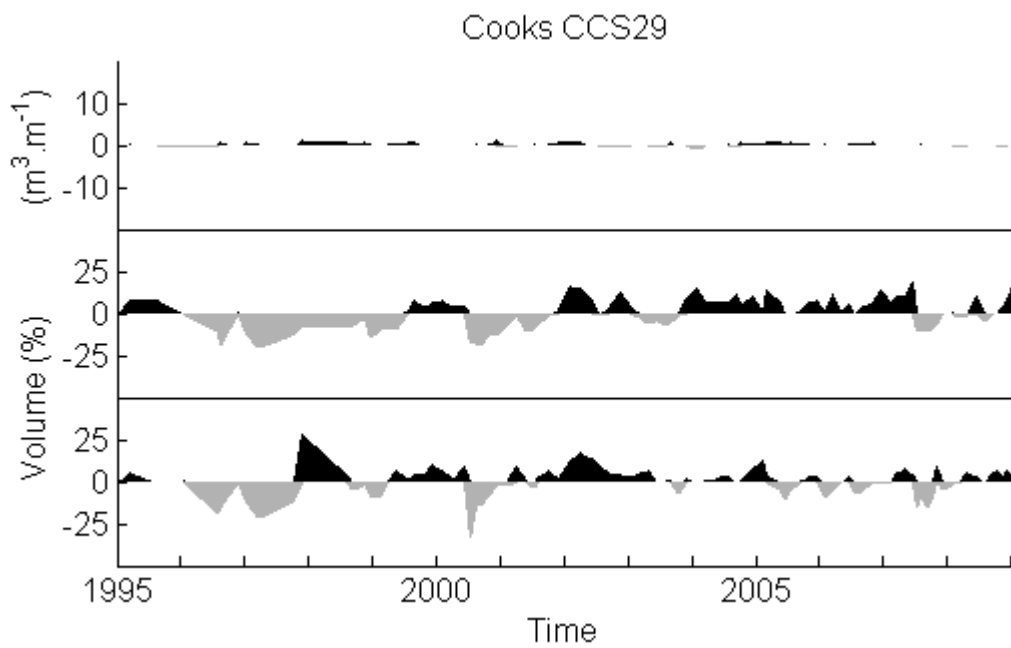


Figure V.31: Cooks CCS29 horizontal beach segment volume data.

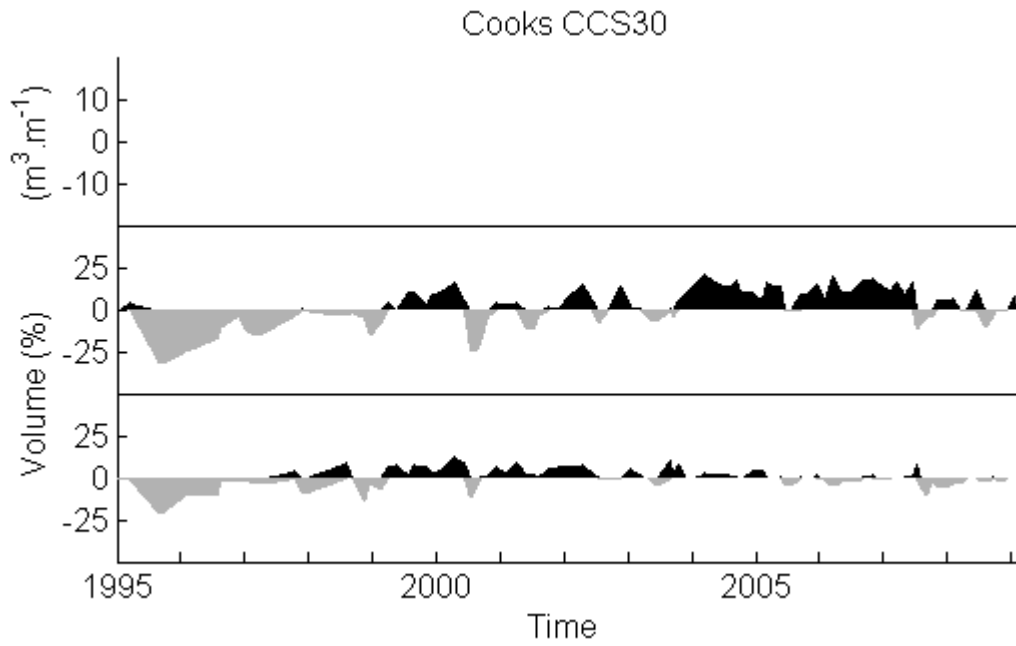


Figure V.32: Cooks CCS30 horizontal beach segment volume data.

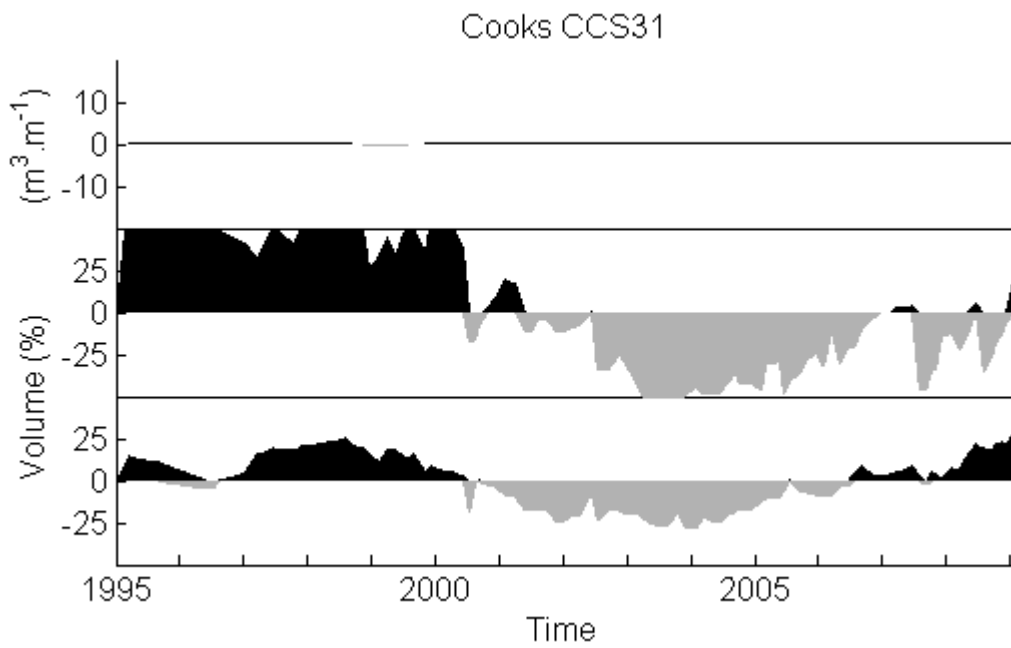


Figure V.33: Cooks CCS31 horizontal beach segment volume data.

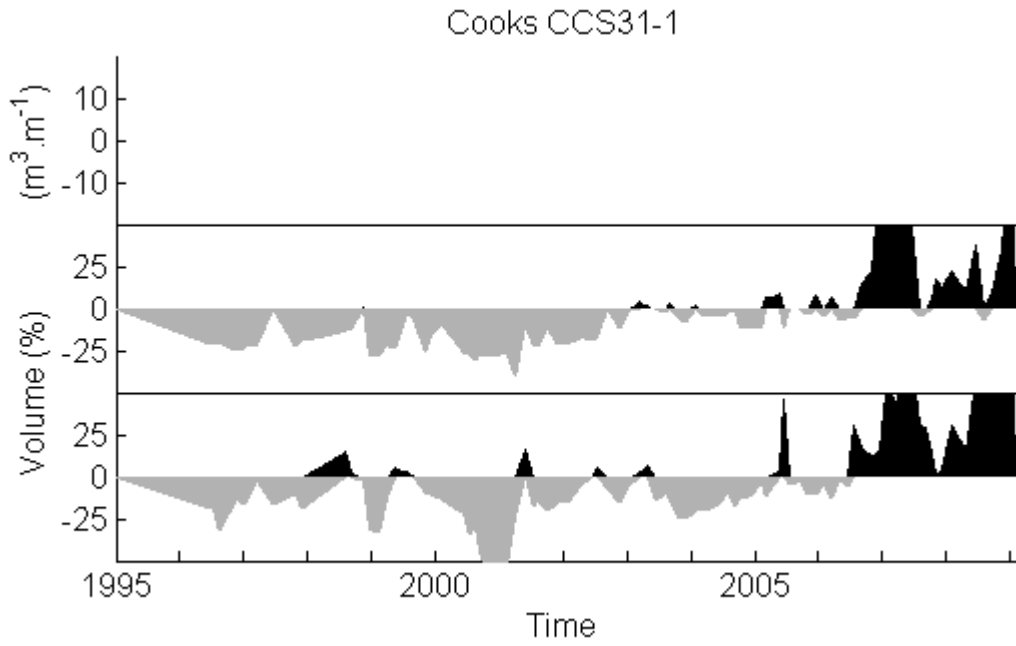


Figure V.34: Cooks CCS31-1 horizontal beach segment volume data.

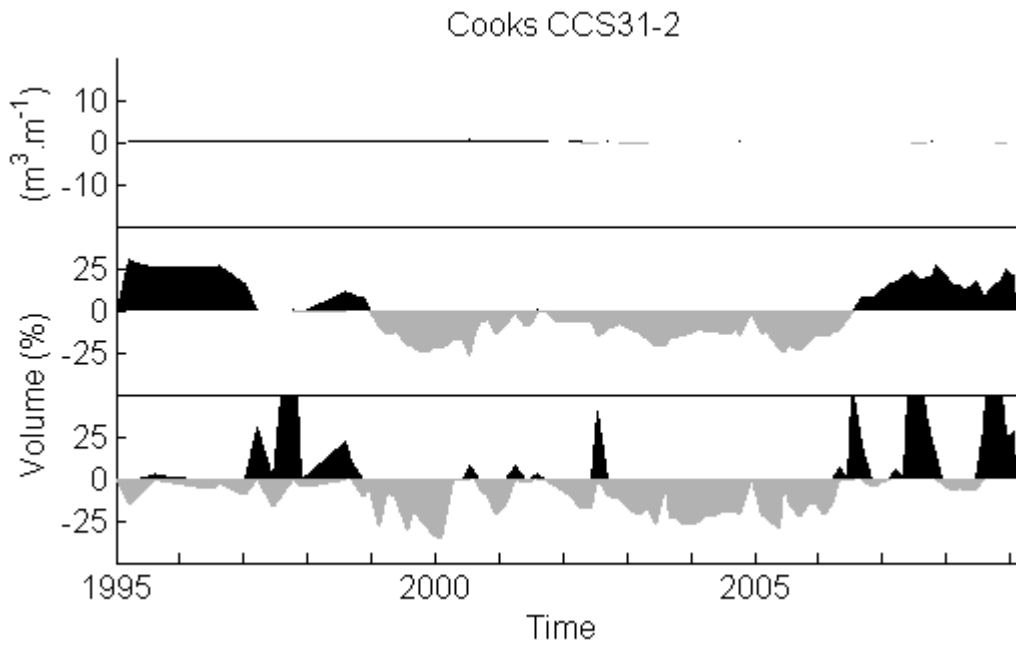


Figure V.35: Cooks CCS31-2 horizontal beach segment volume data.

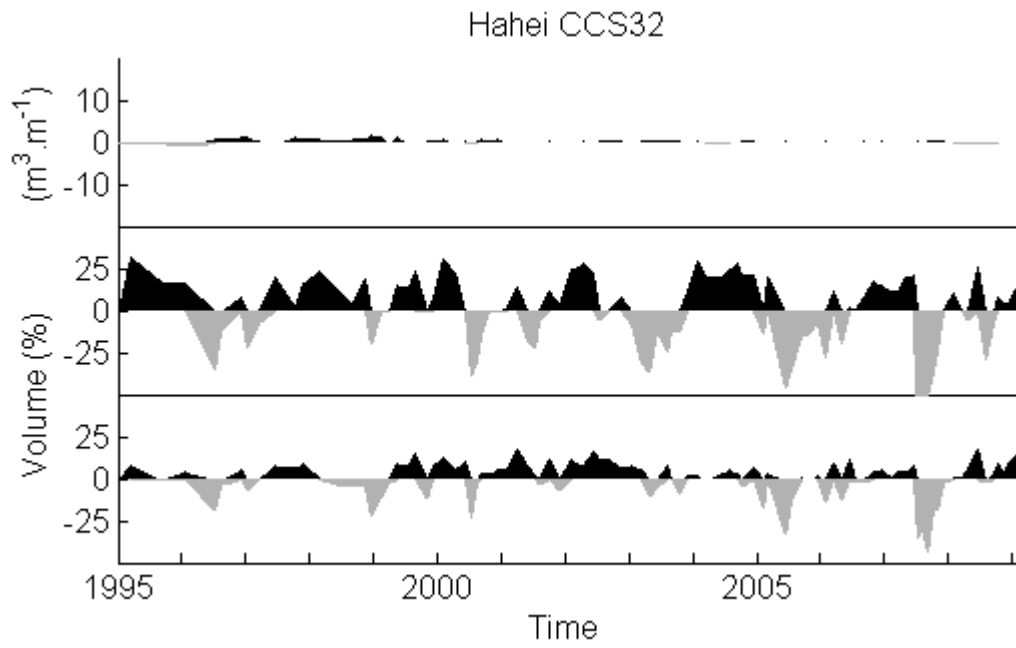


Figure V.36: Hahei CCS32 horizontal beach segment volume data.

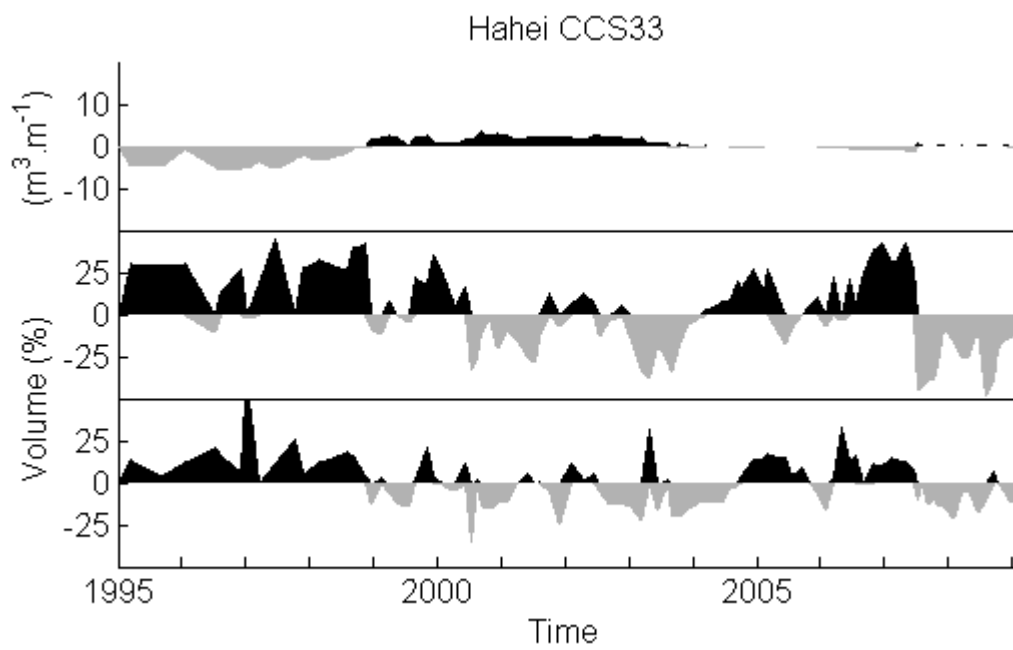


Figure V.37: Hahei CCS33 horizontal beach segment volume data.

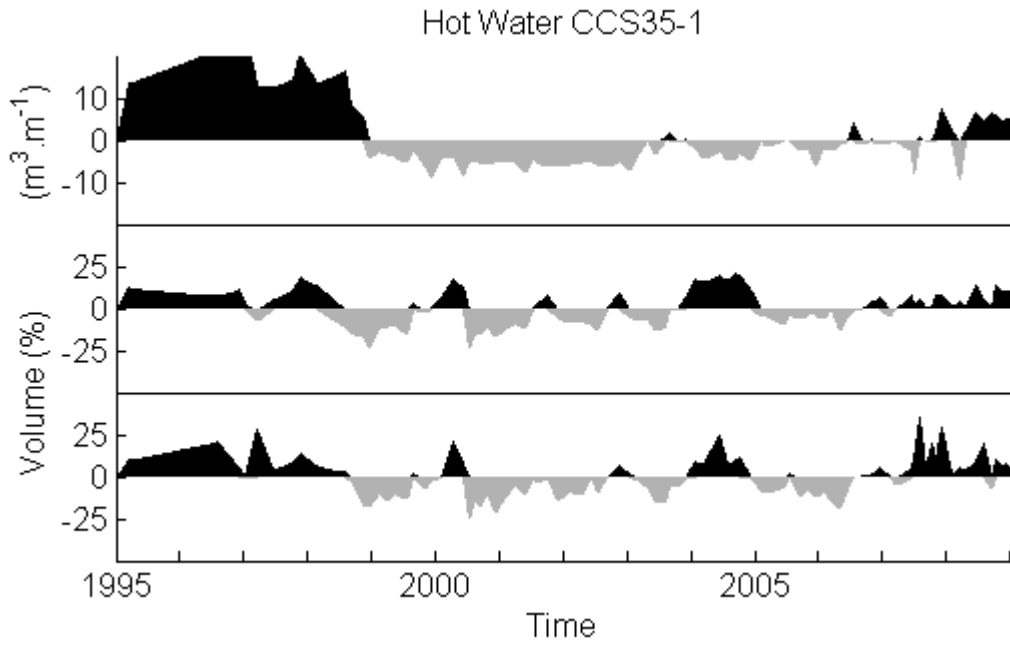


Figure V.38: Hot Water CCS35-1 horizontal beach segment volume data.

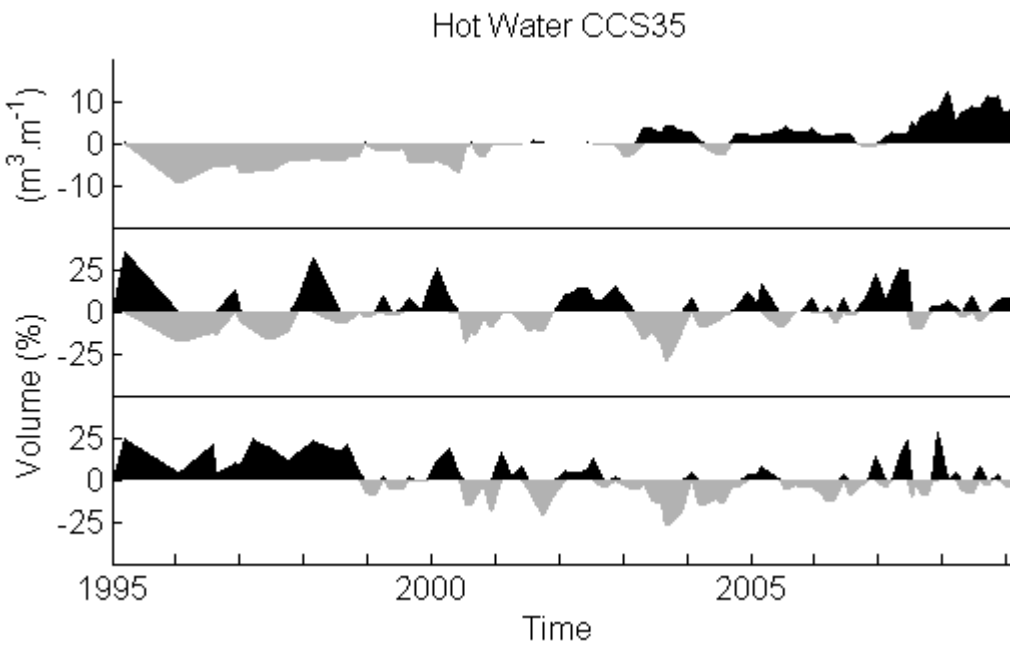


Figure V.39: Hot Water CCS35 horizontal beach segment volume data.

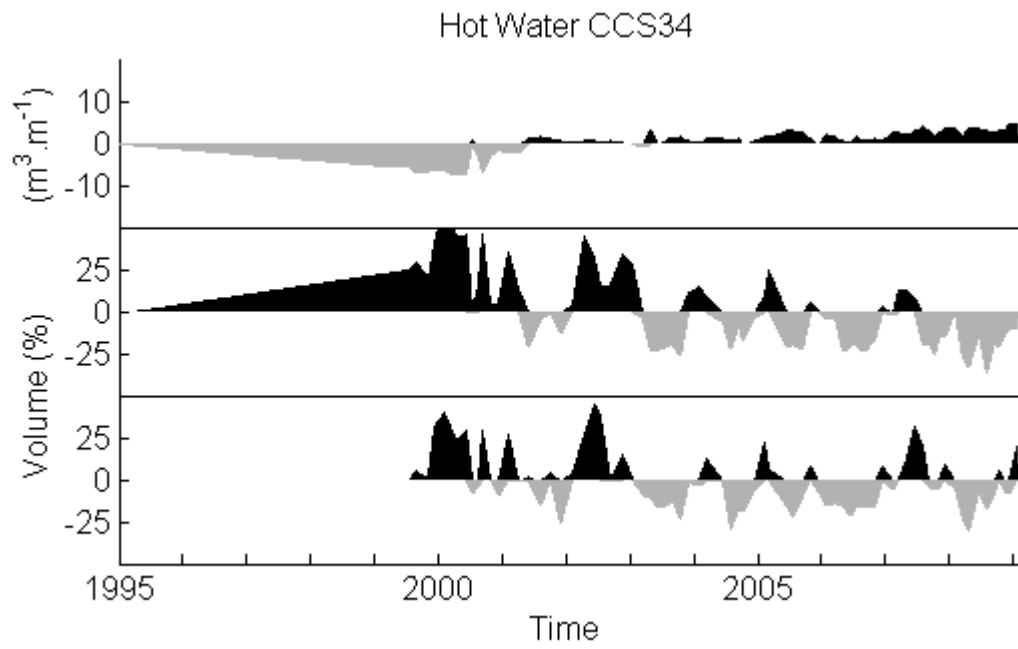


Figure V.40: Hot Water CCS34 horizontal beach segment volume data.

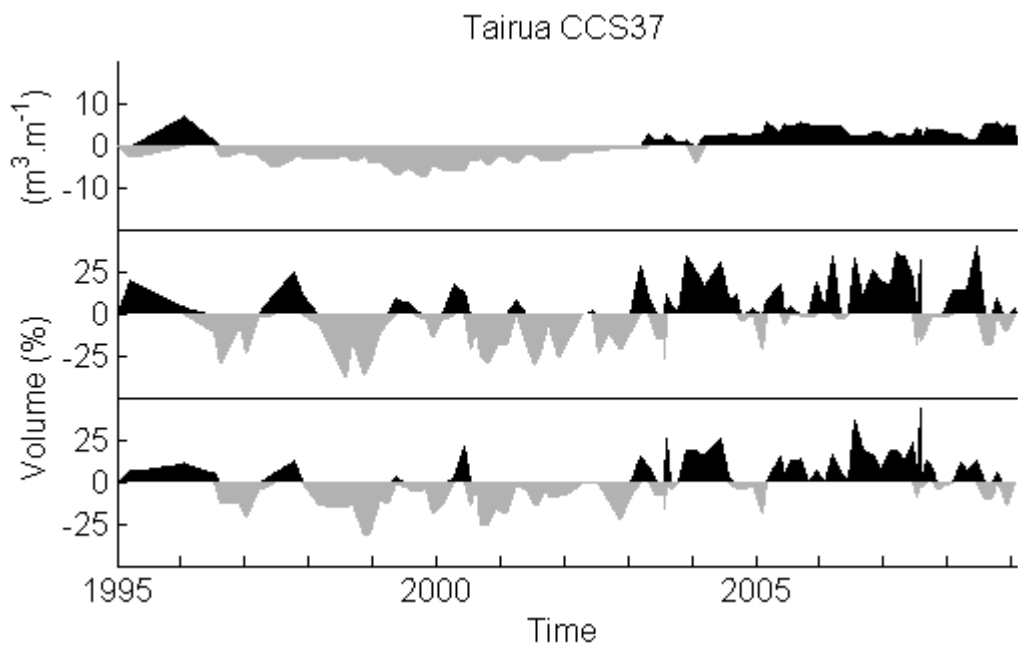


Figure V.41: Tairua CCS37 horizontal beach segment volume data.

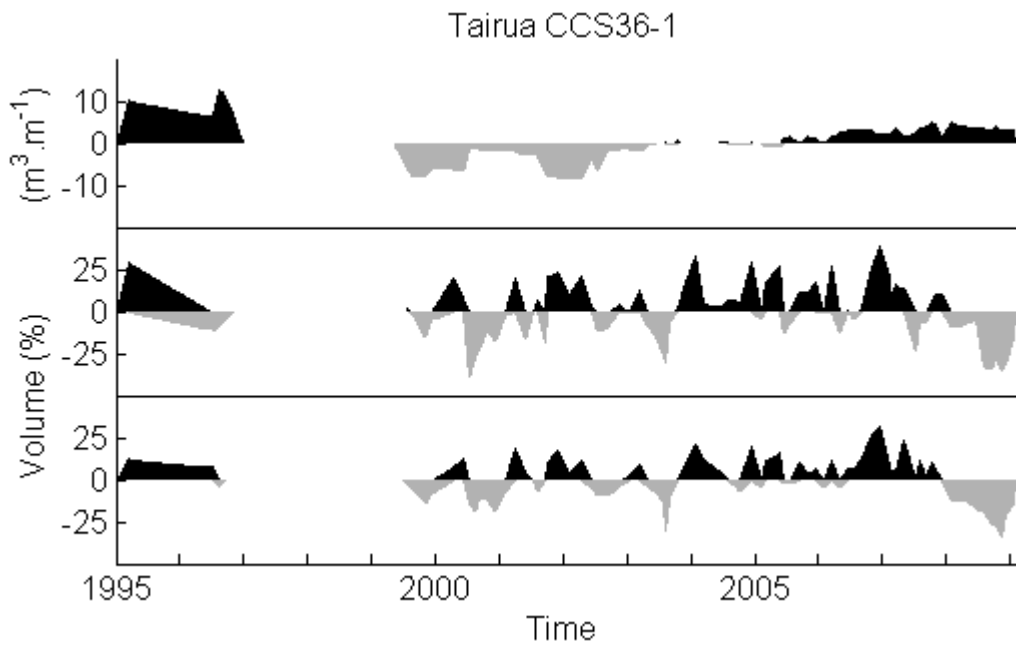


Figure V.42: Tairua CCS36-1 horizontal beach segment volume data.

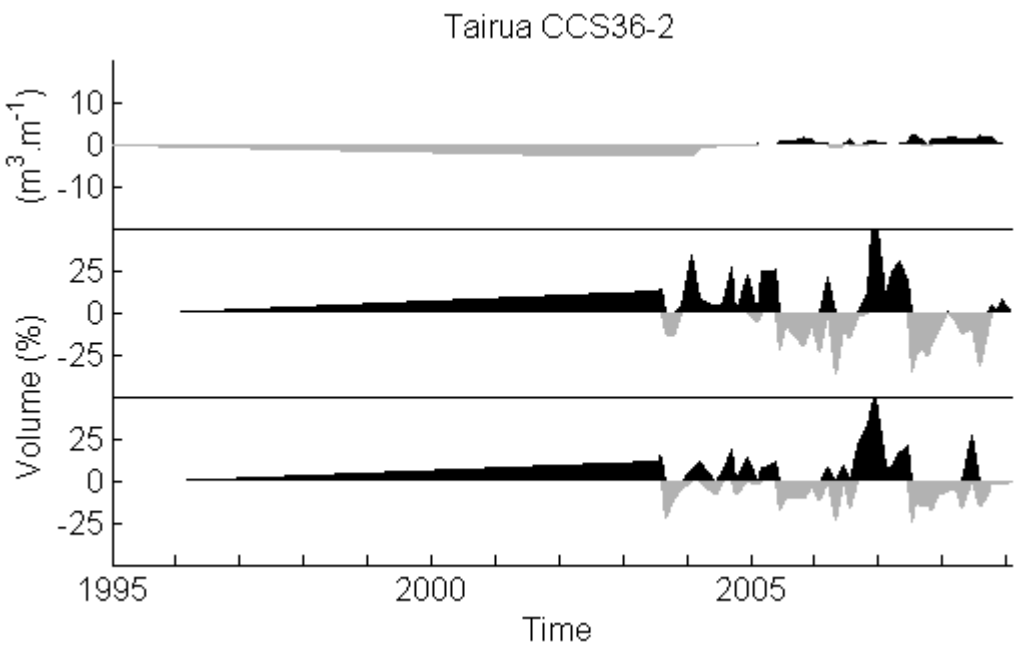


Figure V.43: Tairua CCS36-2 horizontal beach segment volume data.

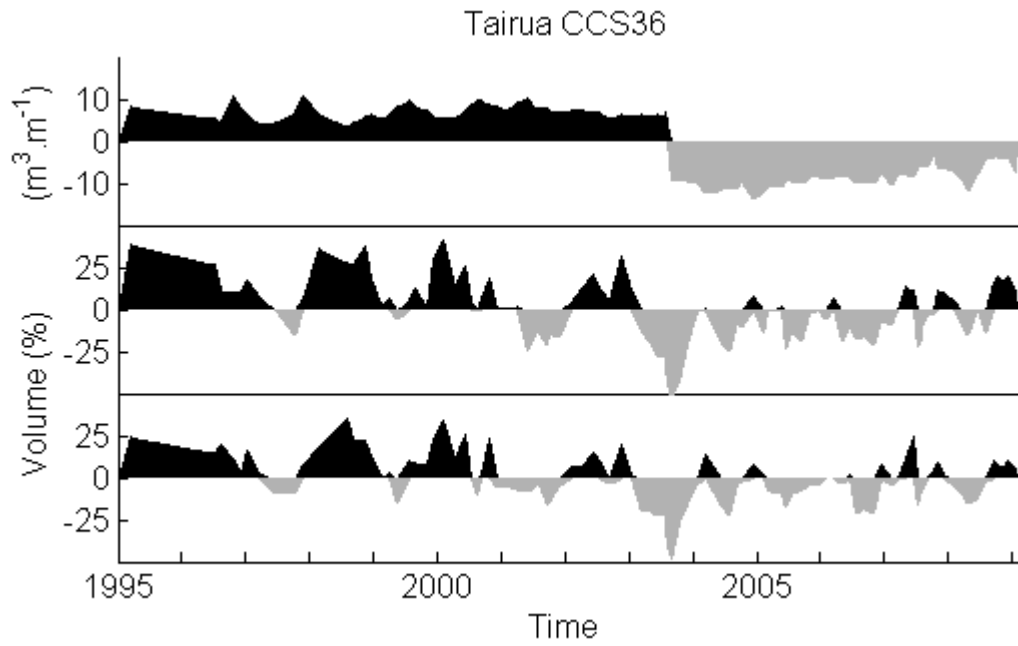


Figure V.44: Tairua CCS36 horizontal beach segment volume data.

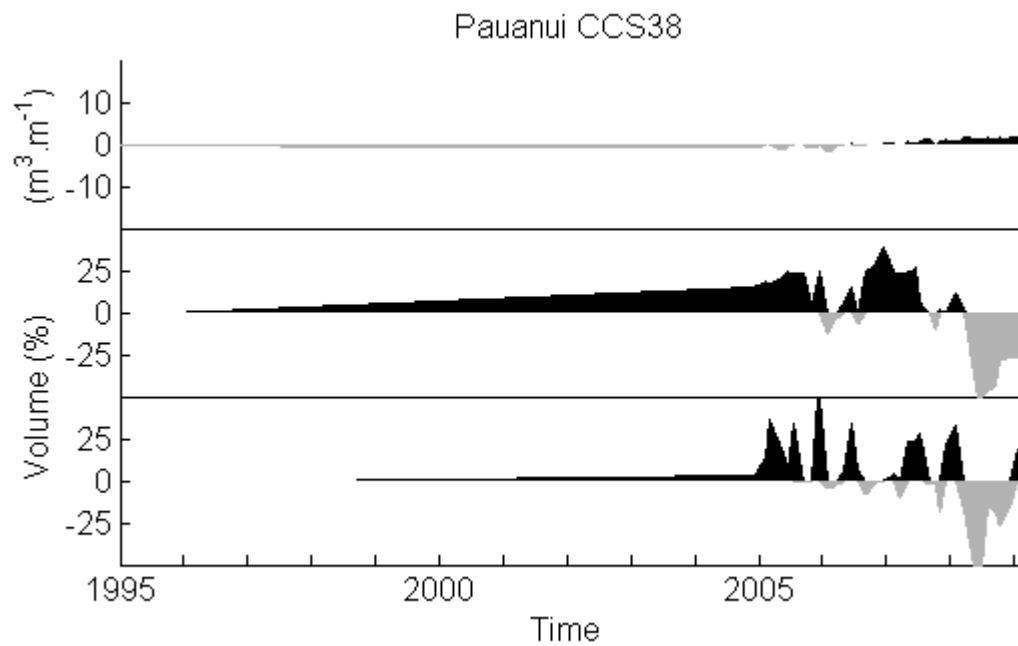


Figure V.45: Pauanui CCS38 horizontal beach segment volume data.

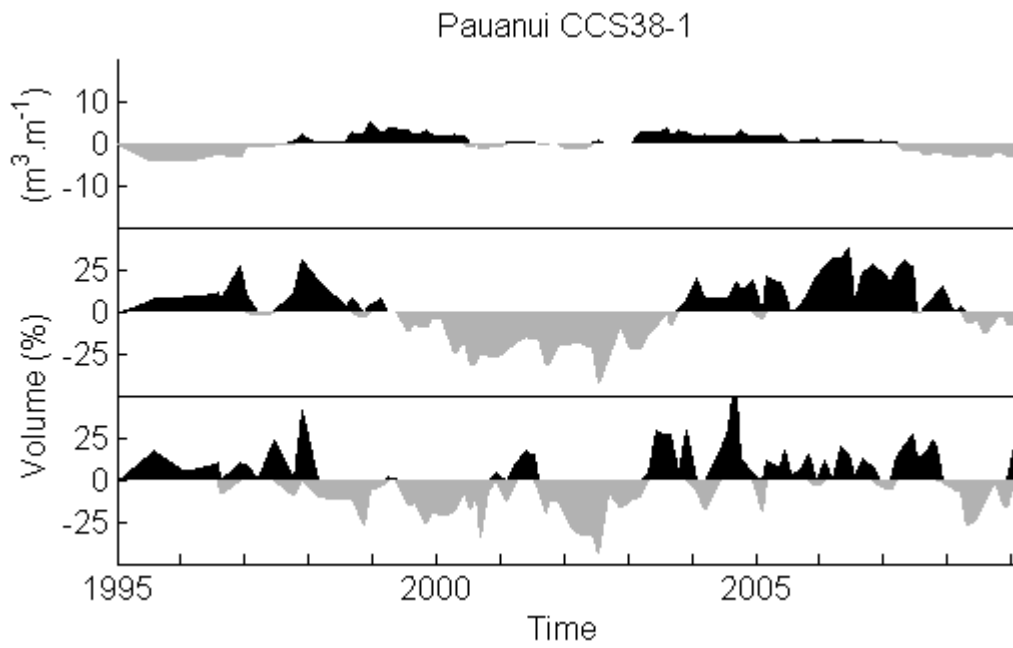


Figure V.46: Pauanui CCS38-1 horizontal beach segment volume data.

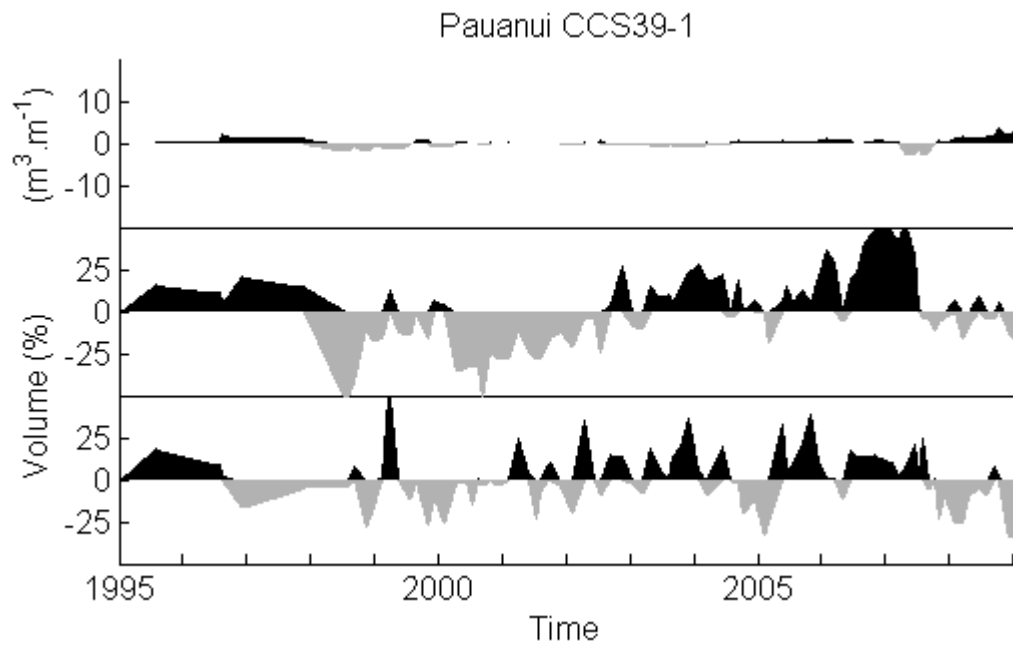


Figure V.47: Pauanui CCS39-1 horizontal beach segment volume data.

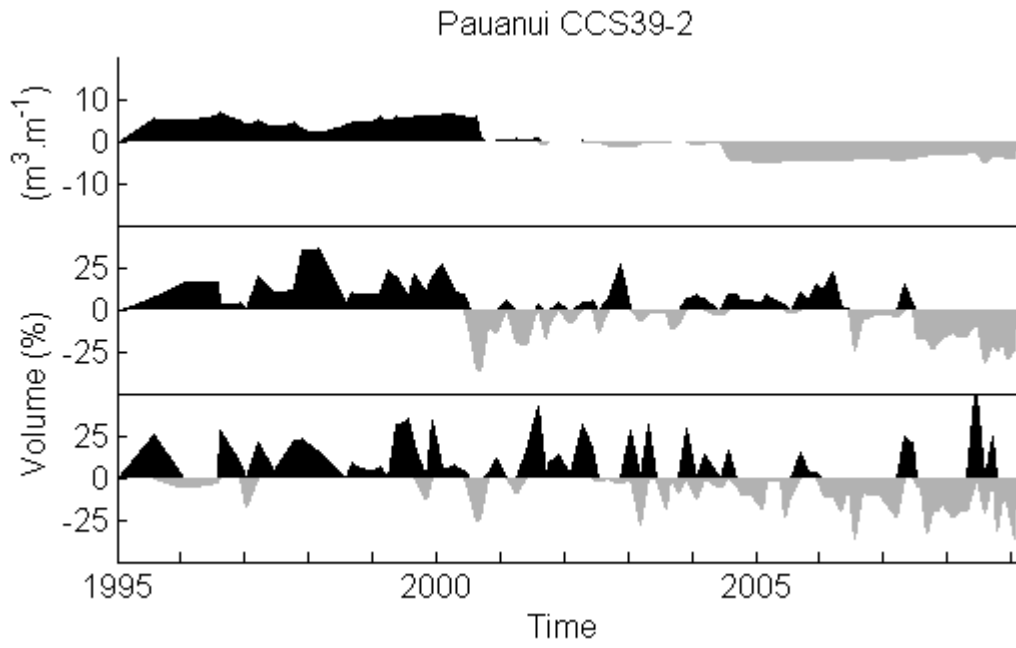


Figure V.48: Pauanui CCS39-2 horizontal beach segment volume data.

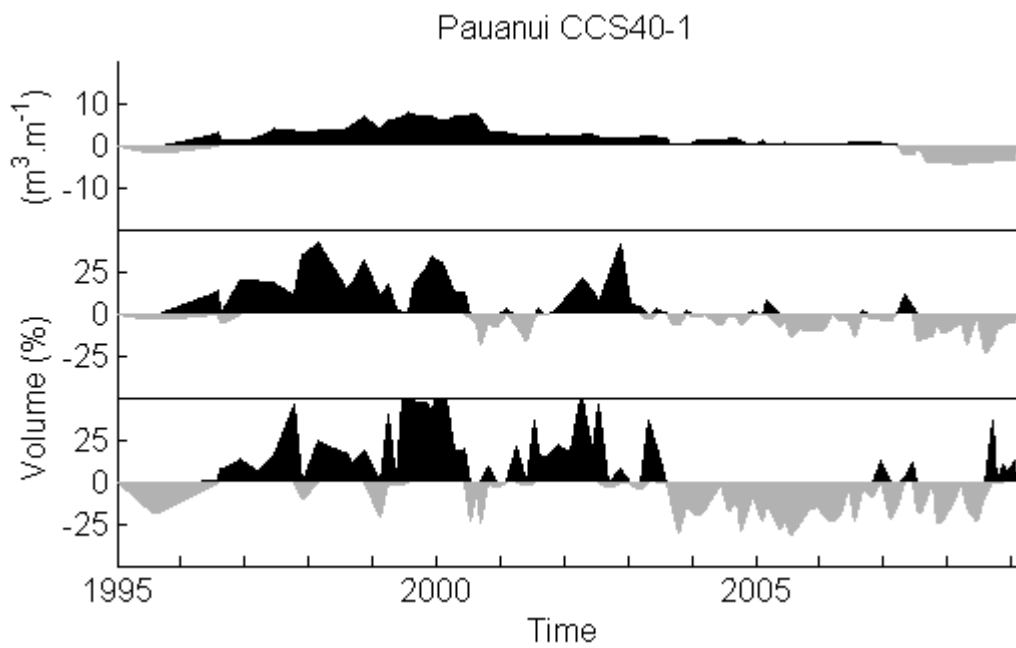


Figure V.49: Pauanui CCS40-1 horizontal beach segment volume data.

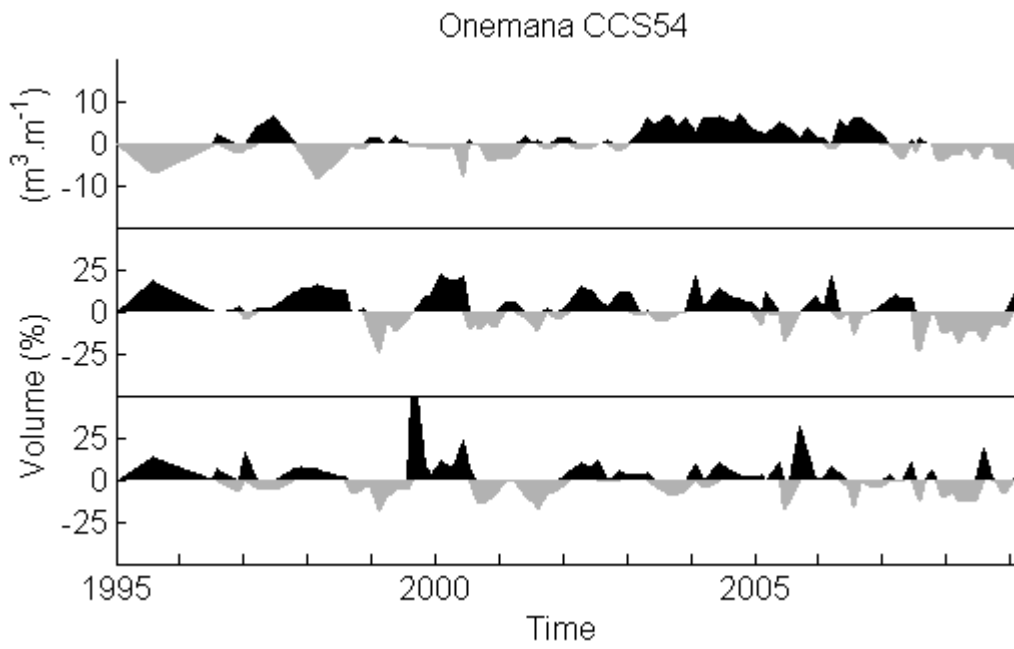


Figure V.50: Onemana CCS54 horizontal beach segment volume data.

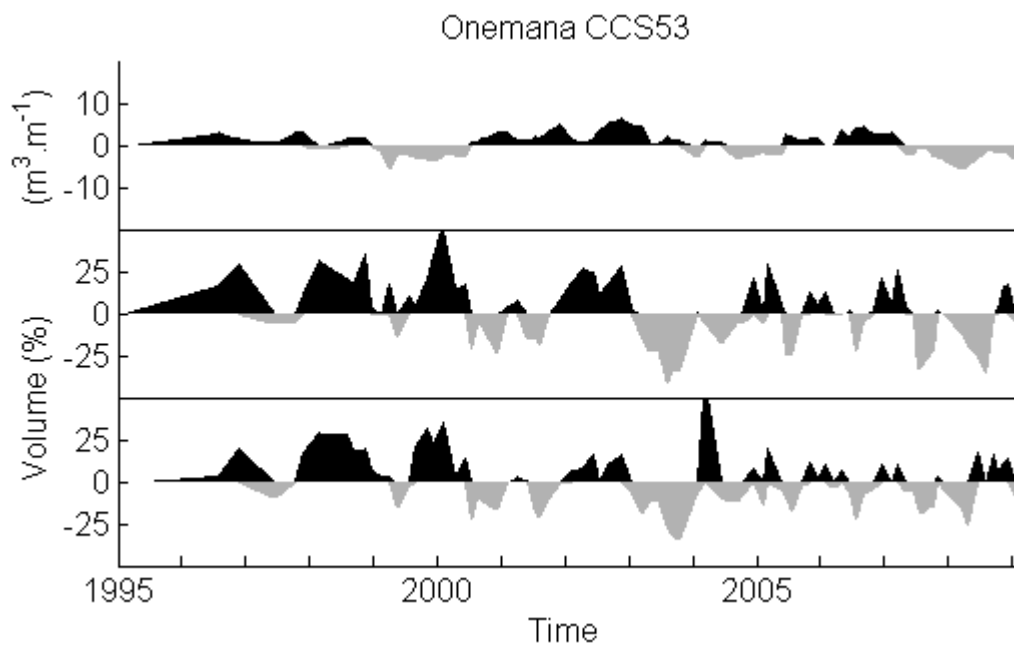


Figure V.51: Onemana CCS53 horizontal beach segment volume data.

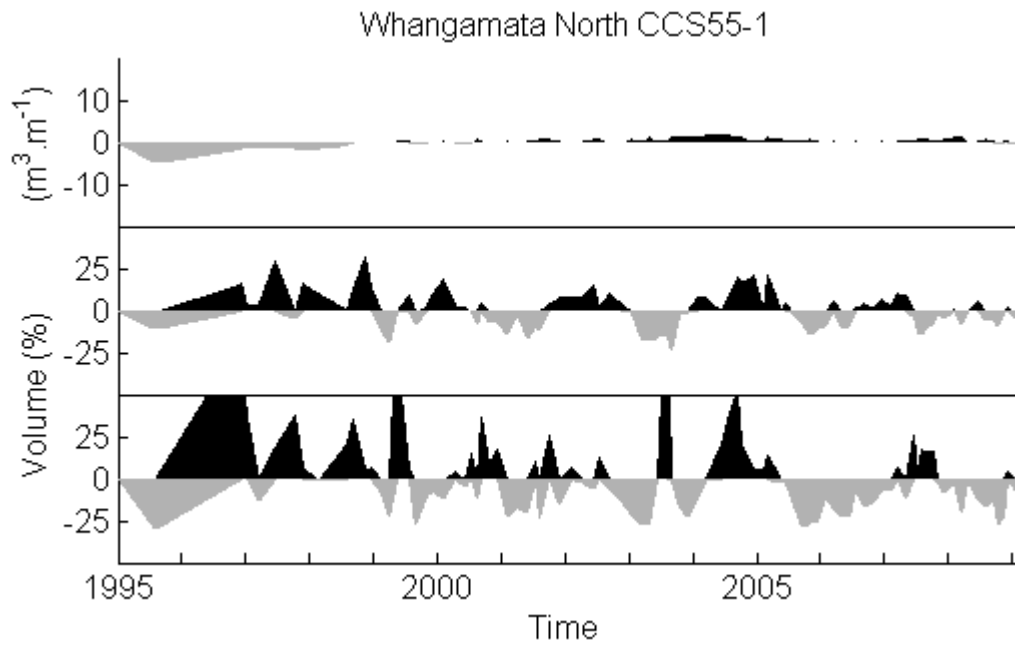


Figure V.52: Whangamata North CCS55-1 horizontal beach segment volume data.

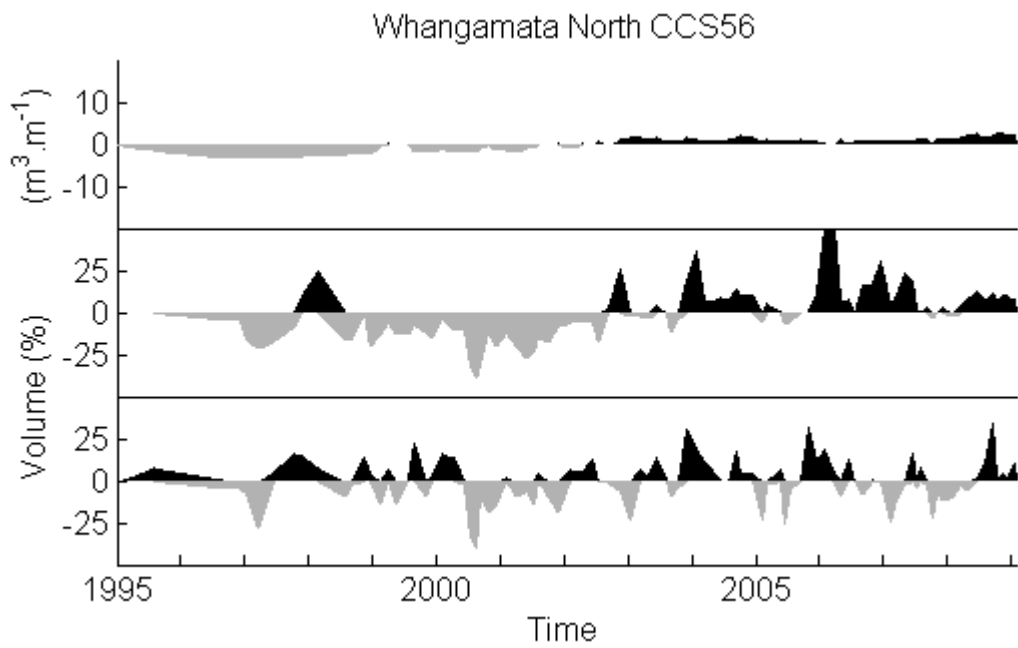


Figure V.53: Whangamata North CCS56 horizontal beach segment volume data.

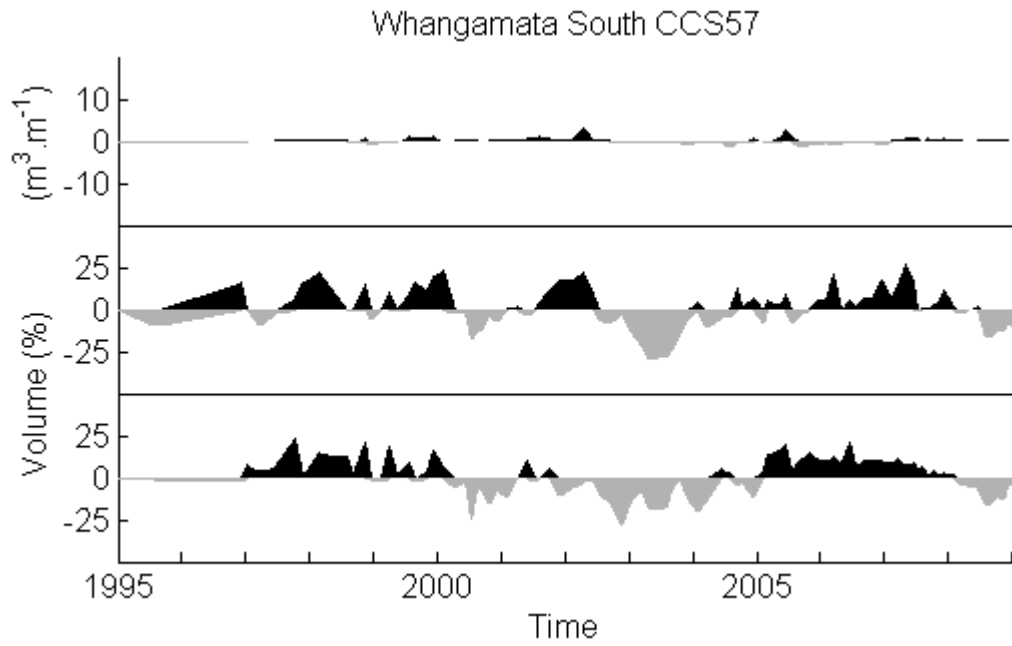


Figure V.54: Whangamata South CCS57 horizontal beach segment volume data.

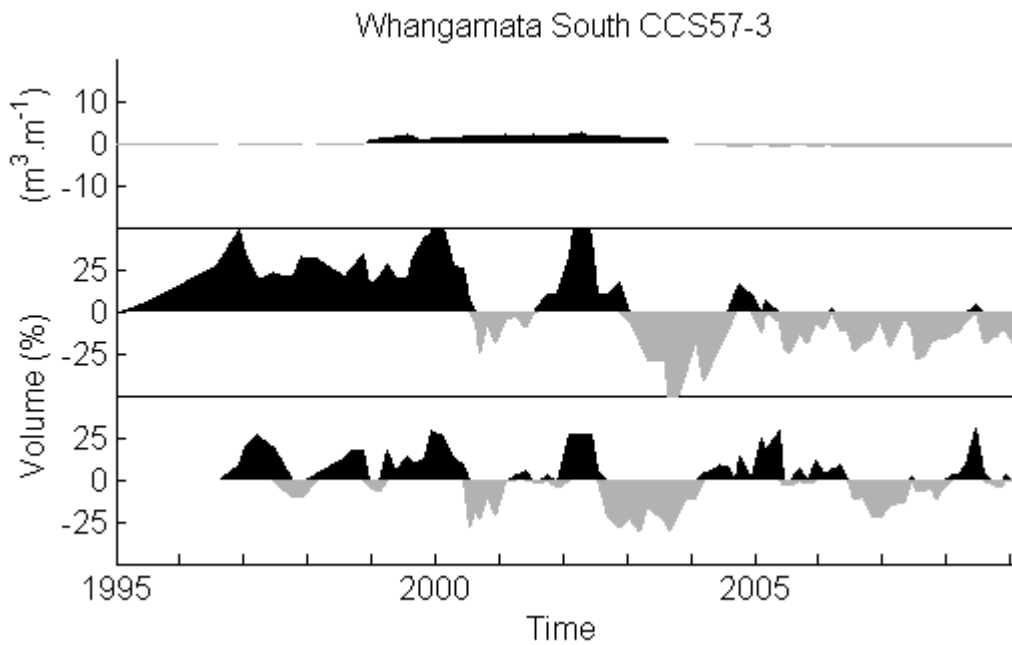


Figure V.55: Whangamata South CCS57-3 horizontal beach segment volume data.

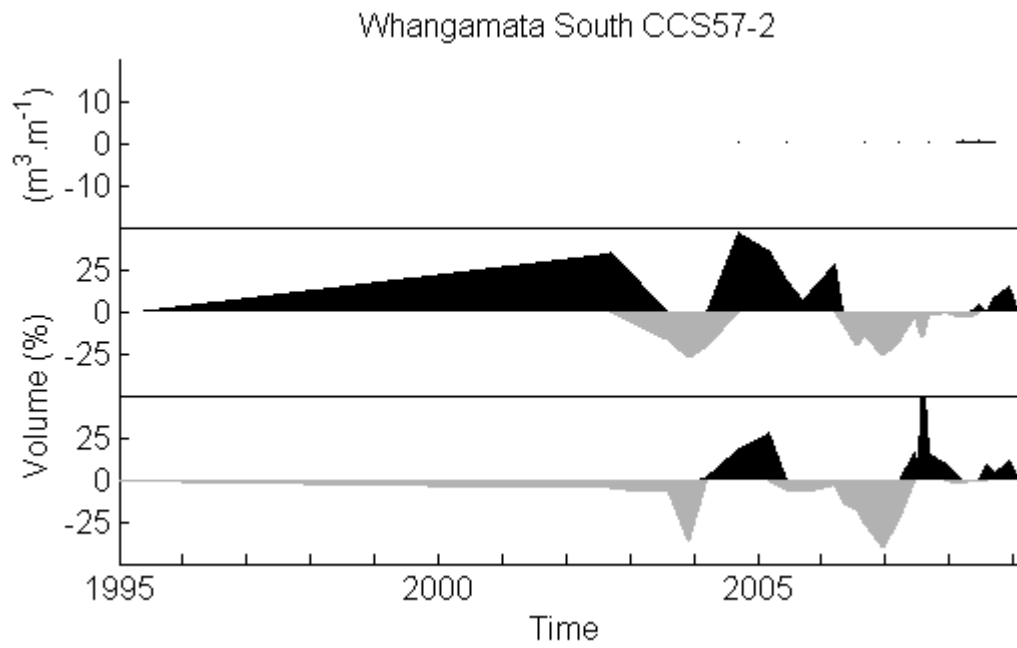


Figure V.56: Whangamata South CCS57-2 horizontal beach segment volume data.

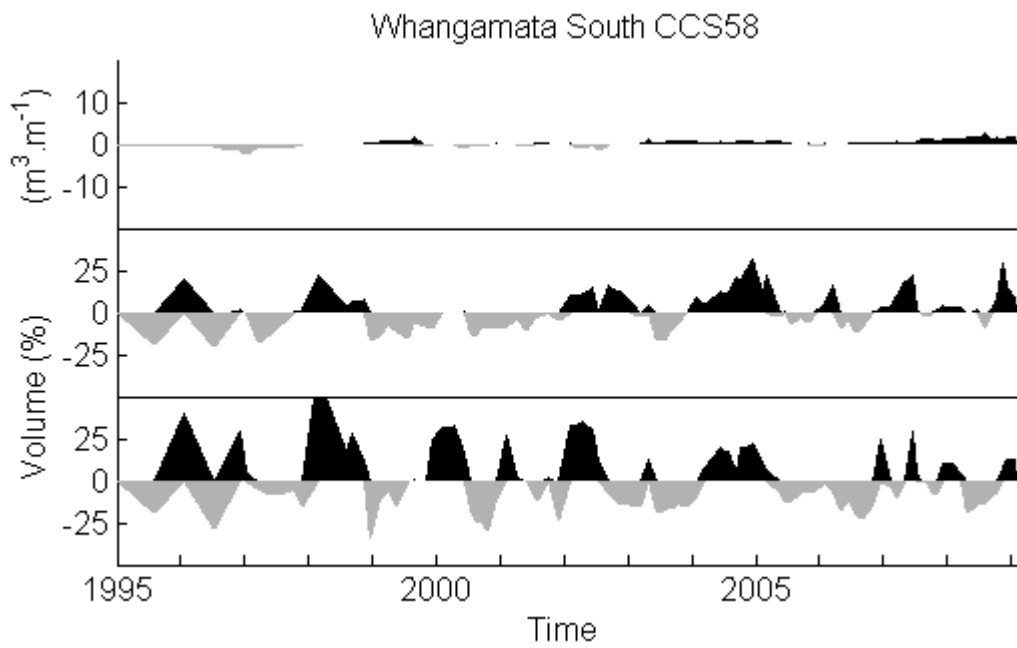


Figure V.57: Whangamata South CCS58 horizontal beach segment volume data.

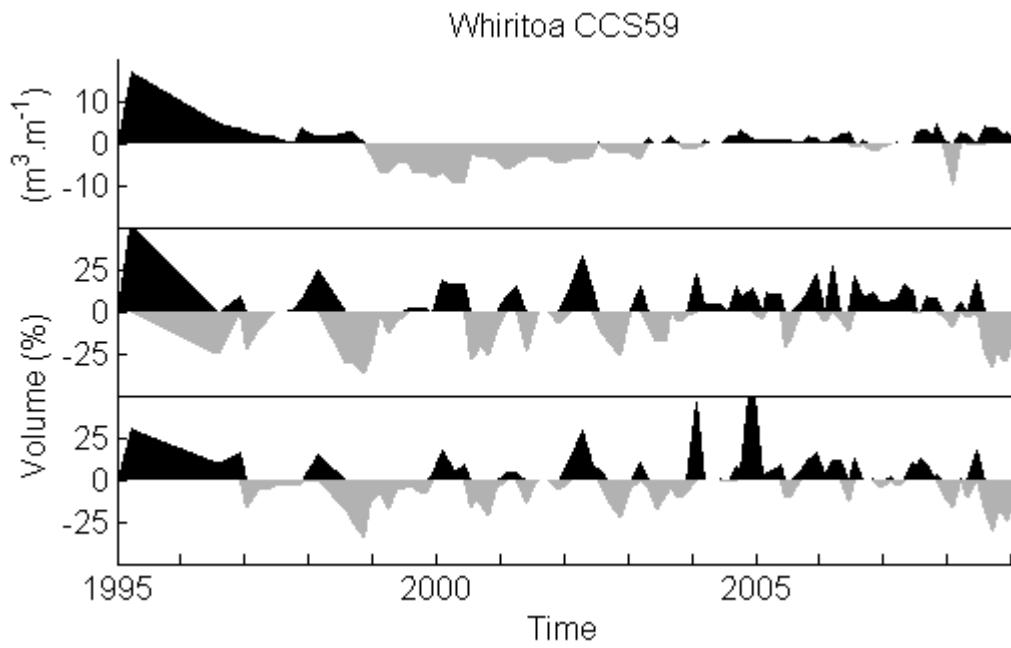


Figure V.58: Whiritoa CCS59 horizontal beach segment volume data.

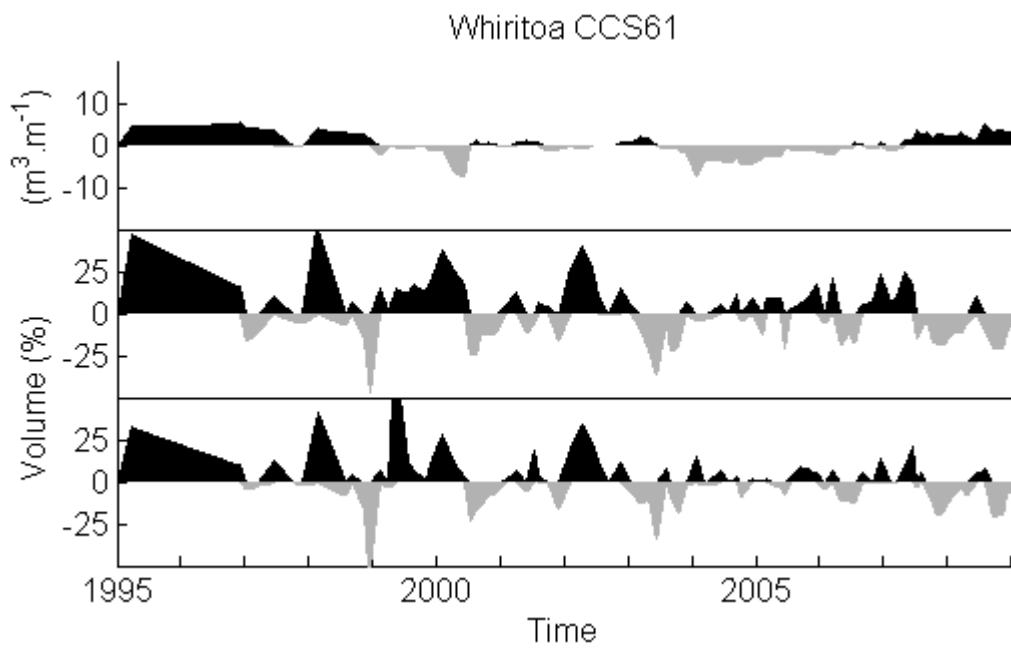


Figure V.59: Whiritoa CCS61 horizontal beach segment volume data.

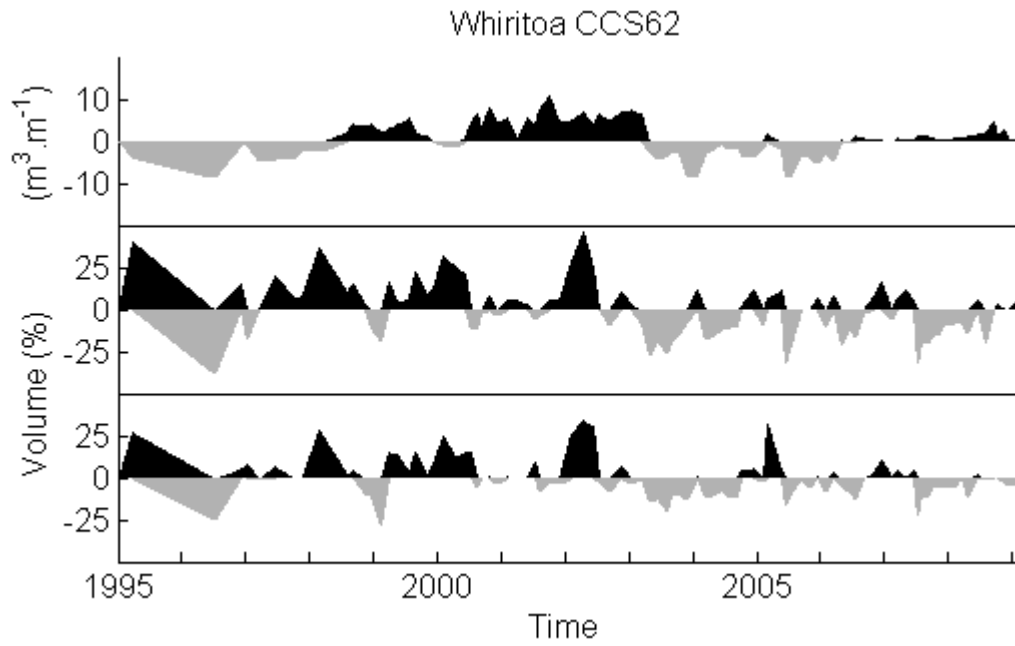


Figure V.60: Whiritoa CCS62 horizontal beach segment volume data.

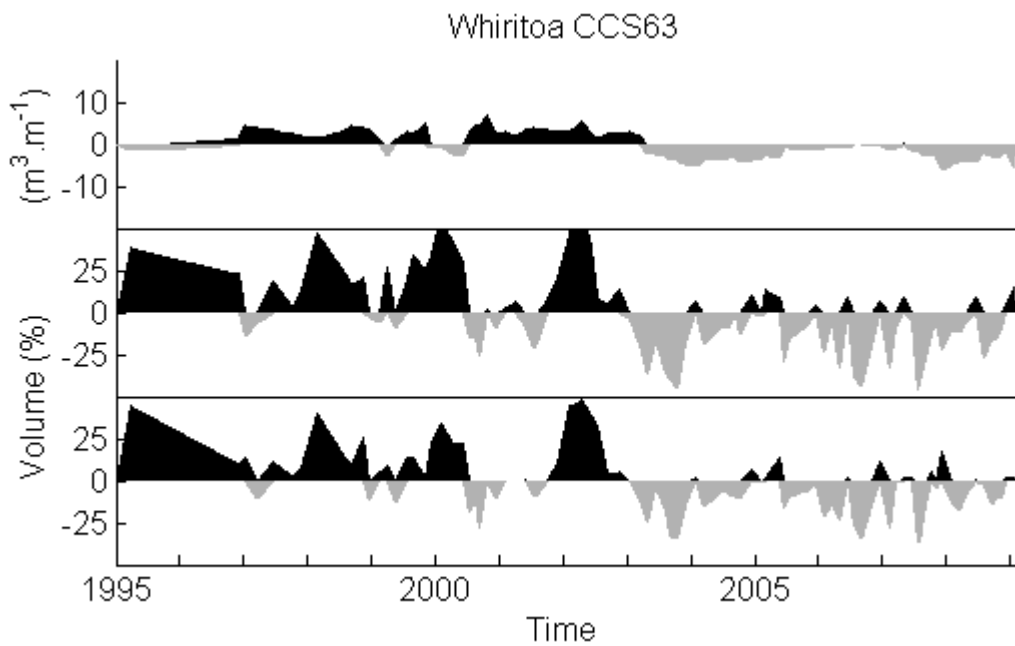


Figure V.61: Whiritoa CCS63 horizontal beach segment volume data.

APPENDIX VI

STANDARD DEVIATIONS: HORIZONTAL VOLUME SEGMENT ANALYSIS

This appendix contains all the standard deviation of beach volume segment results for each individual profile. Figure 3.9 showed the beach average data grouped according to the Wright and Short (1984) classification. Chapter 3 alluded to various aspects of the raw data, hence why they are shown. All graphs in this appendix maintain the same figure properties regarding profile locations. The beaches and profiles are plotted from north to south (refer Table II.1) with the following colour scheme in each figure: solid black line (northernmost); dotted blue line; dashed green line; dash-dot red line; and, solid magenta line with circle marker points. The y axis data are the standard deviations of beach volume and a common unit of $\text{m}^3.\text{m}^{-1}$ was used. The x axis represents the three horizontal volume segment regions (SD) as defined in Section 3.3.1. The key findings were:

- intermediate beaches had increasing standard deviations with decreasing elevation on the beach face;
- reflective beaches had more variable upper beach regions;
- the four steepest intermediate beaches each had one profile with a more variable upper beach region, those being Kuaotunu West, Kuaotunu East, Otama, and Hahei. This behaviour was evident in the eastern profiles of the former 3 beaches and the western profile at Hahei; and
- the very low results for the two outlier beaches.

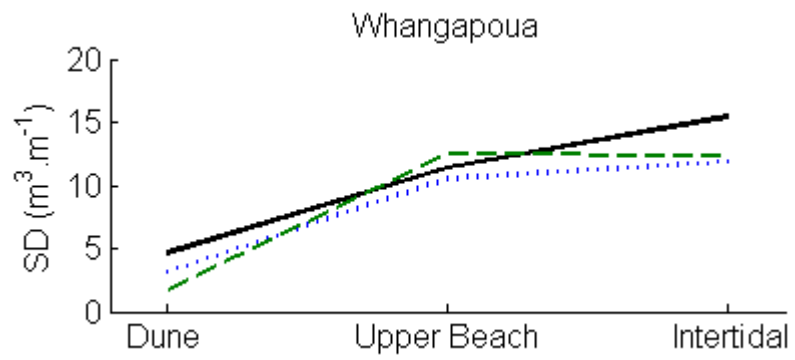


Figure VI.1: Whangapoua Beach standard deviations of the horizontal volume segment analysis.

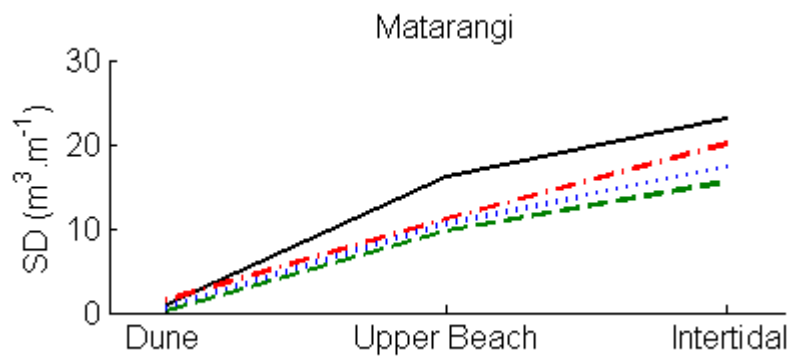


Figure VI.2: Matarangi Beach standard deviations of the horizontal volume segment analysis.

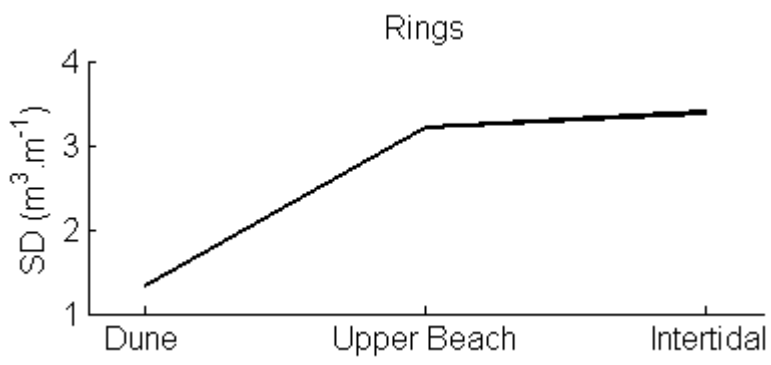


Figure VI.3: Rings Beach standard deviations of the horizontal volume segment analysis.

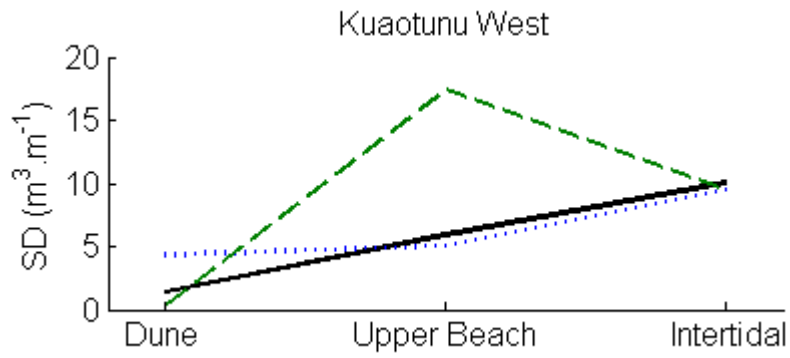


Figure VI.4: Kuaotunu West Beach standard deviations of the horizontal volume segment analysis.

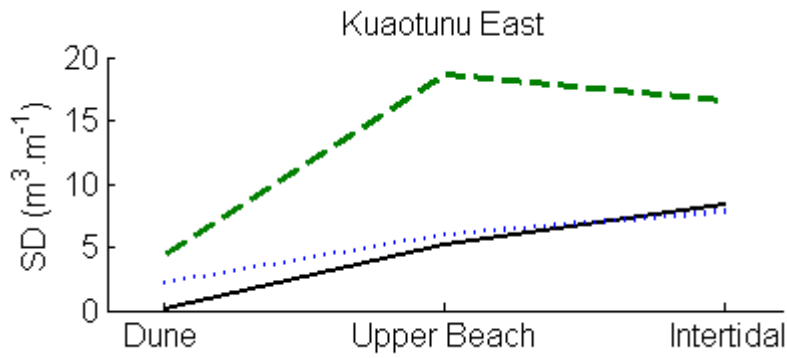


Figure VI.5: Kuaotunu East Beach standard deviations of the horizontal volume segment analysis.

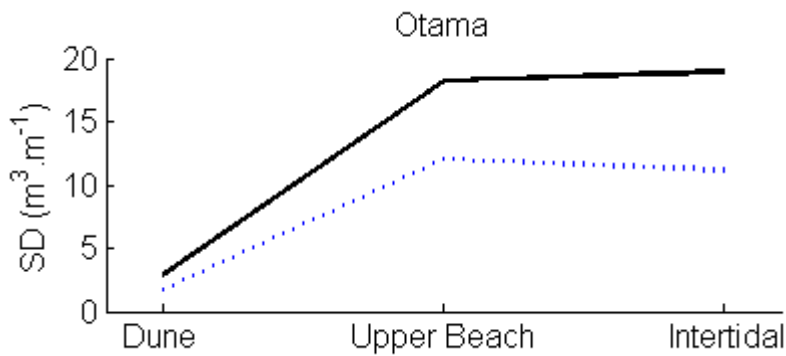


Figure VI.6: Otama Beach standard deviations of the horizontal volume segment analysis.

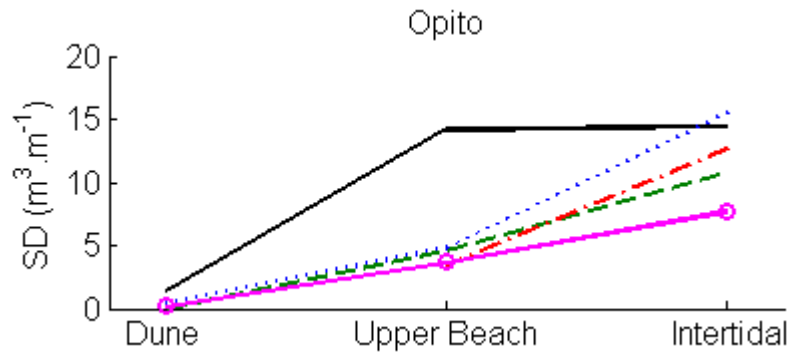


Figure VI.7: Opito Beach standard deviations of the horizontal volume segment analysis.

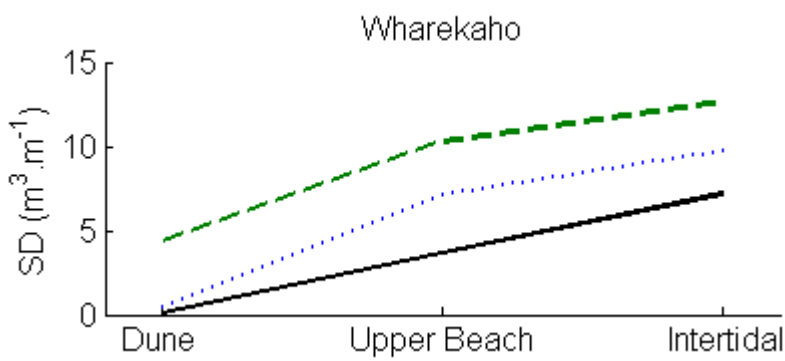


Figure VI.8: Wharekaho Beach standard deviations of the horizontal volume segment analysis.

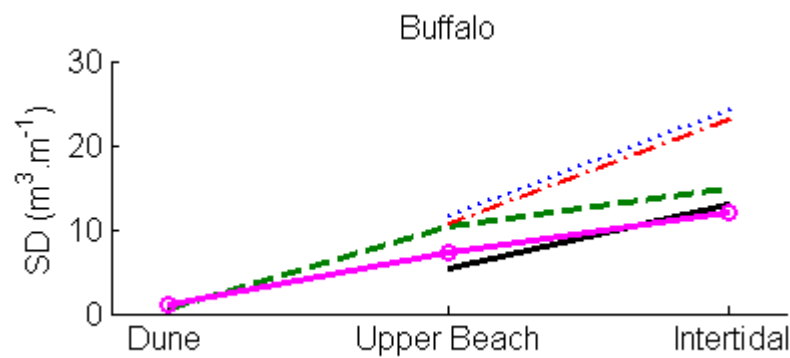


Figure VI.9: Buffalo Beach standard deviations of the horizontal volume segment analysis.

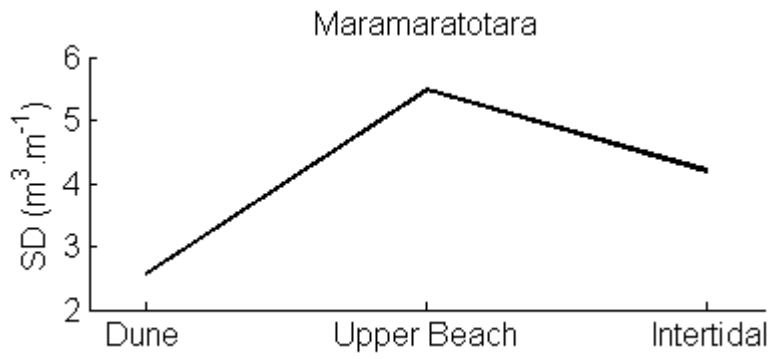


Figure VI.10: Maramaratotara Beach standard deviations of the horizontal volume segment analysis.

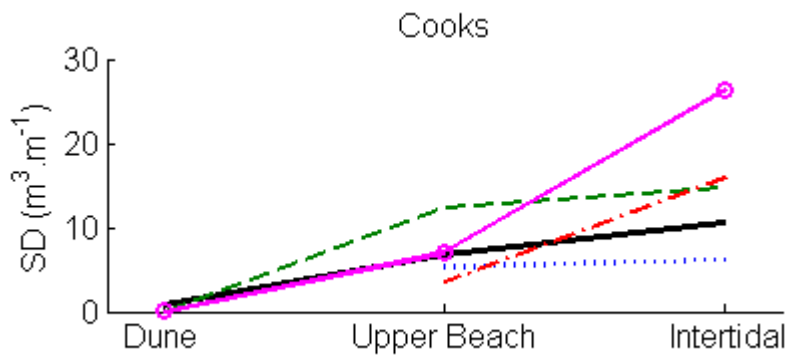


Figure VI.11: Cooks Beach standard deviations of the horizontal volume segment analysis.

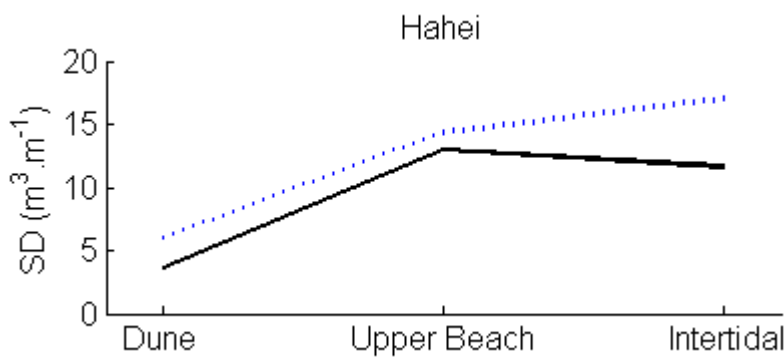


Figure VI.12: Hahei Beach standard deviations of the horizontal volume segment analysis.

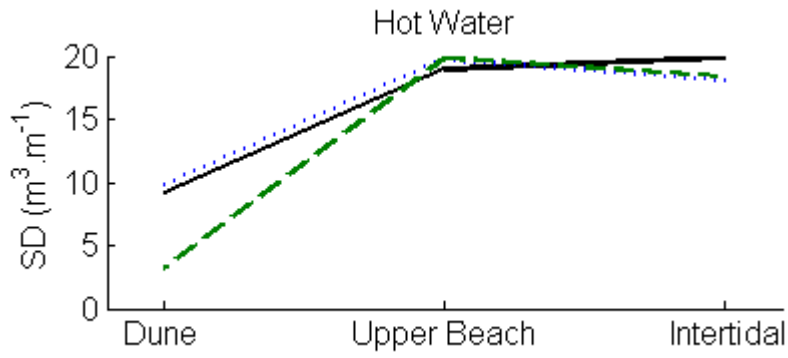


Figure VI.13: Hot Water Beach standard deviations of the horizontal volume segment analysis.

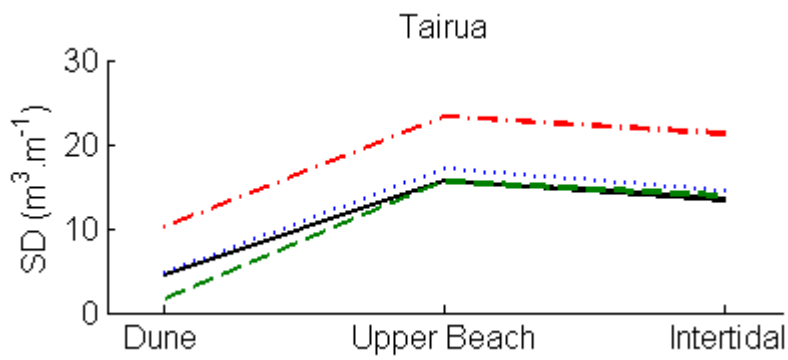


Figure VI.14: Tairua Beach standard deviations of the horizontal volume segment analysis.

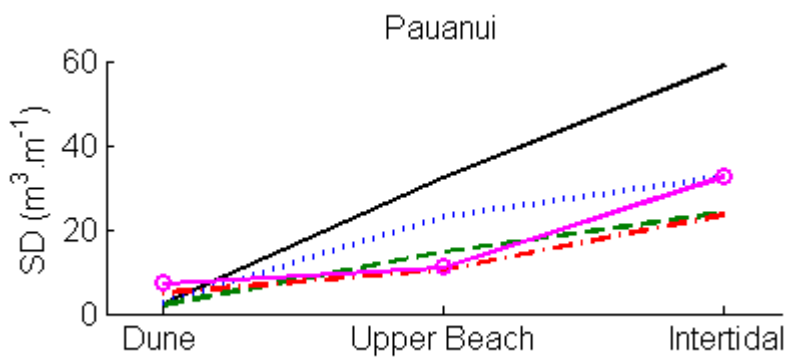


Figure VI.15: Pauanui Beach standard deviations of the horizontal volume segment analysis.

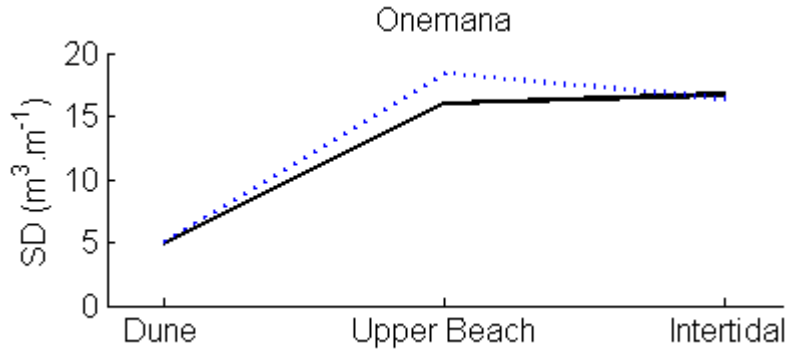


Figure VI.16: Onemana Beach standard deviations of the horizontal volume segment analysis.

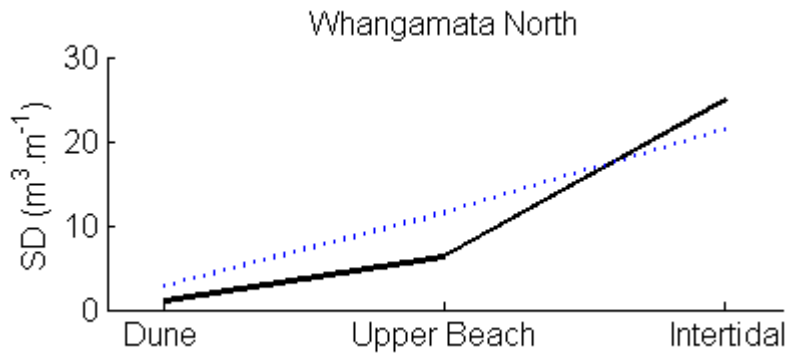


Figure VI.17: Whangamata North Beach standard deviations of the horizontal volume segment analysis.

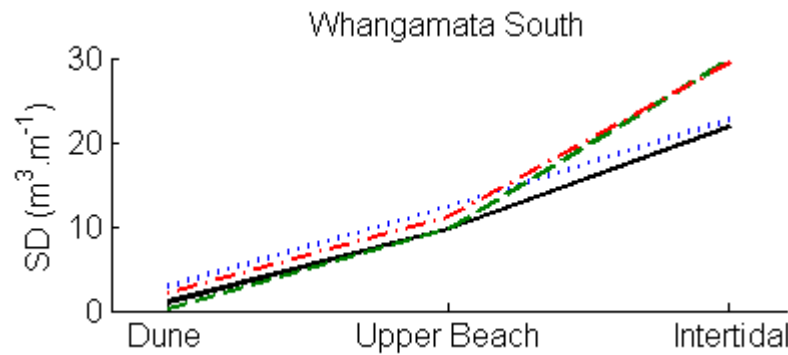


Figure VI.18: Whangamata South Beach standard deviations of the horizontal volume segment analysis.

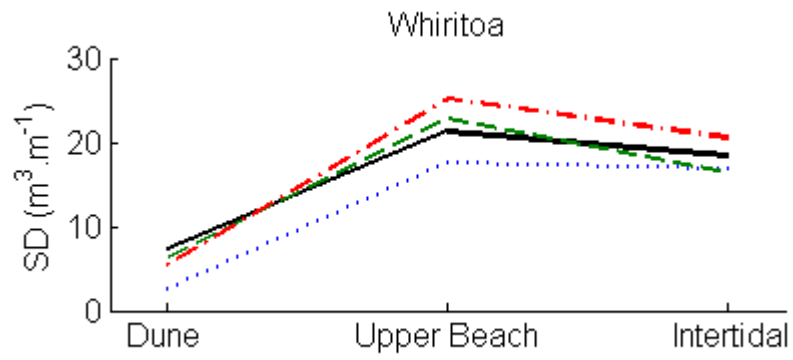


Figure VI.19: Whiritoa Beach standard deviations of the horizontal volume segment analysis.

APPENDIX VII

DEMEANED BEACH VOLUME TIMESERIES

Beach profile timeseries graphs are displayed in this appendix. The standard deviation of volume was averaged for each beach from the data presented here. The example timeseries figures in Chapter 3 illustrated several profiles, however all profiles could not be included within the Chapter due to obvious size and word limitations. As a result, the data is presented here with very brief notes on key behaviours and characteristics which were eluded at various stages during the thesis. Figure captions are not provided because all figures are self explanatory. Each figure has all available data displayed from 1979 to 2009 and has been demeaned. The horizontal dashed lines represent one standard deviation above and below the mean, or 68 % of the short term volume variation. All figures have equal x- and y-axes, with the y-axis showing demeaned beach volumes with maximum bounds of $\pm 50\%$ of the subaerial beach volume for each respective dataset. The figures are shown from Whangapoua to Whiritoa, north to south, and each individual figure shows the respective beach profiles from north to south (left to right looking seaward), top to bottom.

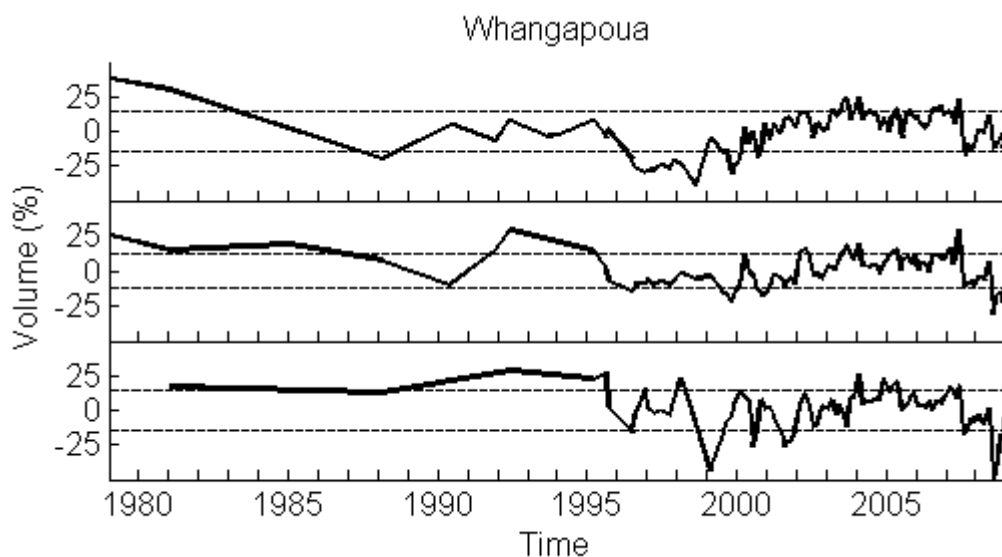


Figure VII.1: Whangapoua Beach volume timeseries. The horizontal dashed lines represent one standard deviation above and below the mean.

- The beach showed very similar behaviour in the alongshore direction. There is also an increasing amount of variation toward the southern end of the beach.
- Elevated beach volumes between 1980 and 1990 conform to IPO related behaviour of increased volumes during this period. The high resolution data from 1995 onward showed an apparent relationship.

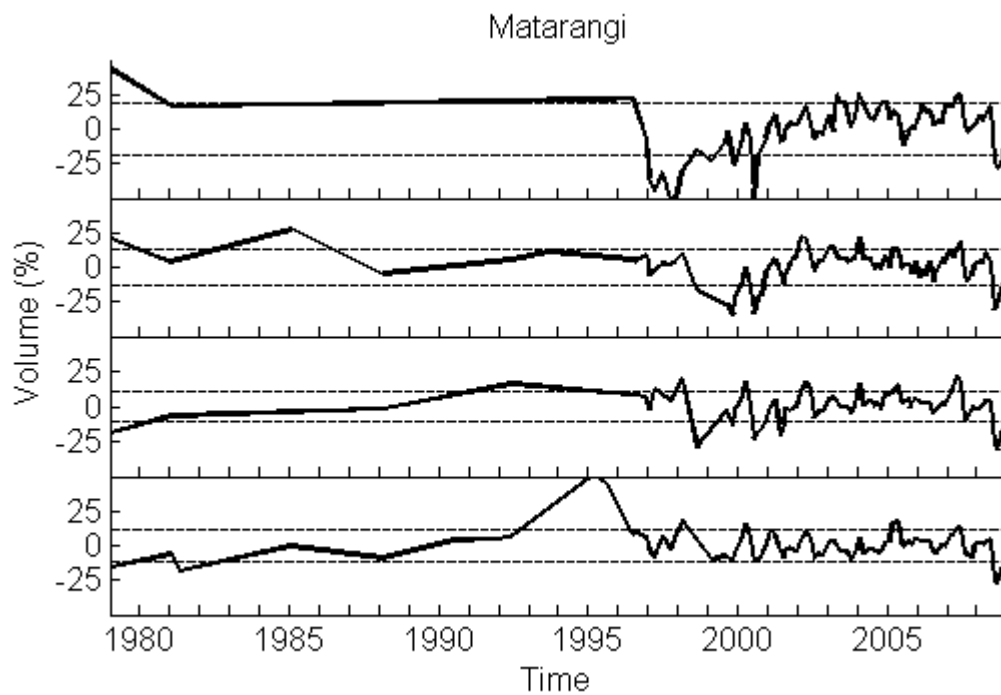


Figure VII.2: Matarangi Beach volume timeseries. The horizontal dashed lines represent one standard deviation above and below the mean.

- The beach showed a decreasing amount of cyclic behaviour in accordance with the IPO from north to south (west to east is more representative at Matarangi). The 3 northern profiles show an apparent IPO correlation. Interestingly the northern end of the beach appeared to have relatively high volumes following the July 1978 storm whereas the southern two profiles were low.
- In addition to the 1978 and 2008 storm events, low beach volumes were prevalent in the late 1990's except the southern profile.
- Seasonal erosion and accretion was evident in the raw data at the southern end of the beach.

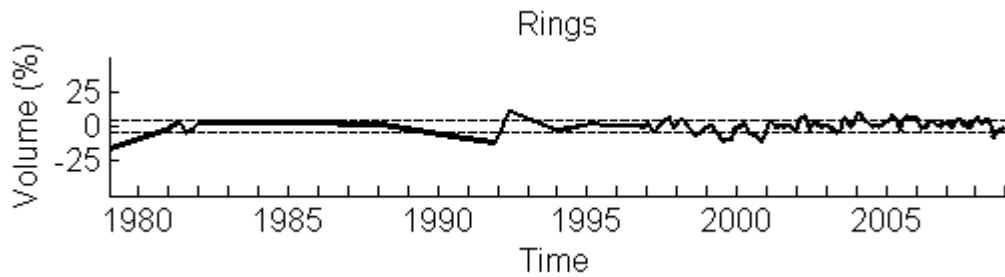


Figure VII.3: Rings Beach volume timeseries. The horizontal dashed lines represent one standard deviation above and below the mean.

- The stability of the beach at all timescales is particularly evident in all available data. Reducing the sampling frequency would not be expected to reduce the quality of the data because the beach showed no significant oscillations.

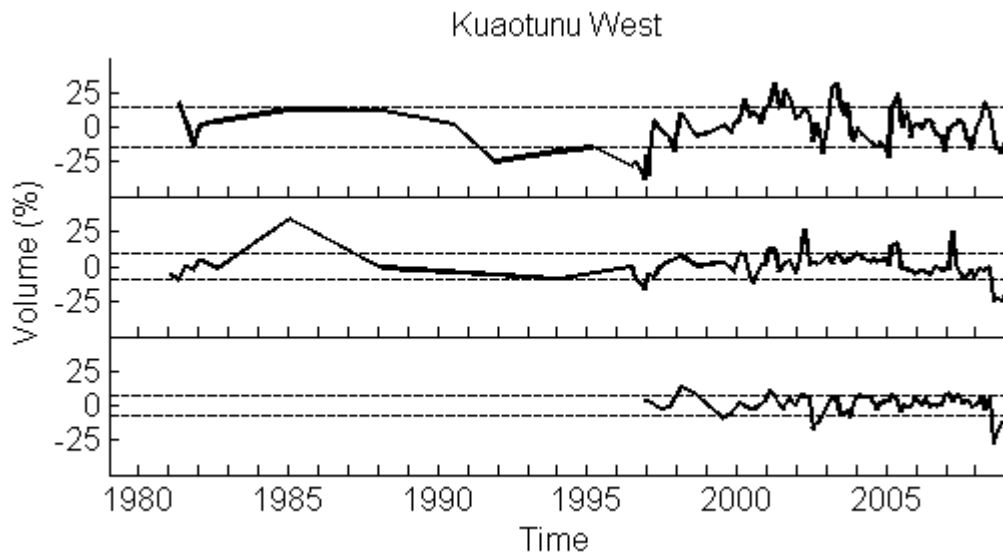


Figure VII.4: Kuaotunu West Beach volume timeseries. The horizontal dashed lines represent one standard deviation above and below the mean.

- The northern two profiles show greater variation than the southern profile. They also show the apparent IPO relationship prominent on beaches north of the Kuaotunu Peninsula. The eastern end of the beach was very stable since 1996, with the exception of the July 2008 storm event.

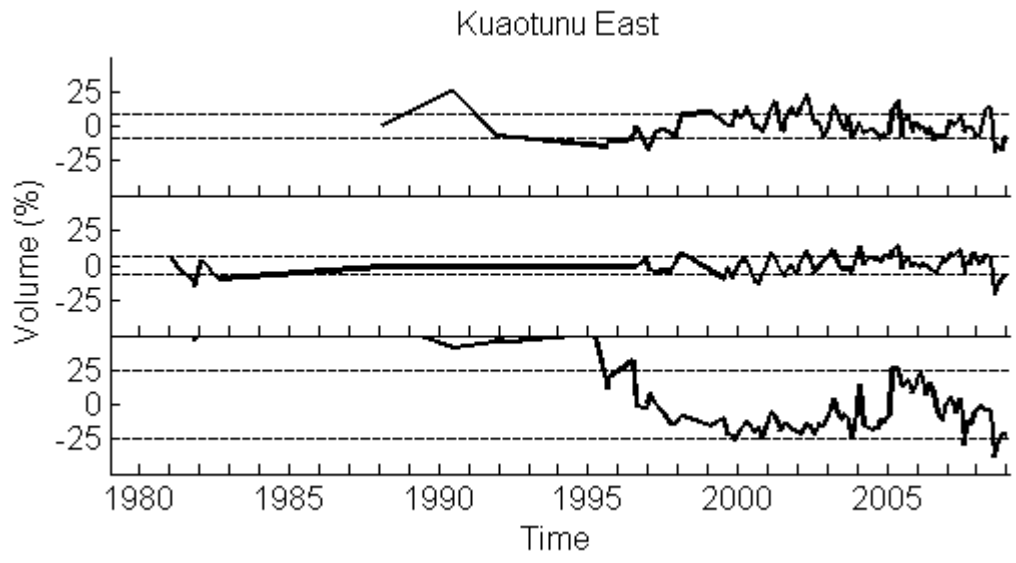


Figure VII.5: Kuaotunu East Beach volume timeseries. The horizontal dashed lines represent one standard deviation above and below the mean.

- The significant variation at the eastern end was a result of erosion of the primary dune system. The central profile showed the highest degree of stability with only one large erosion event in 2008.

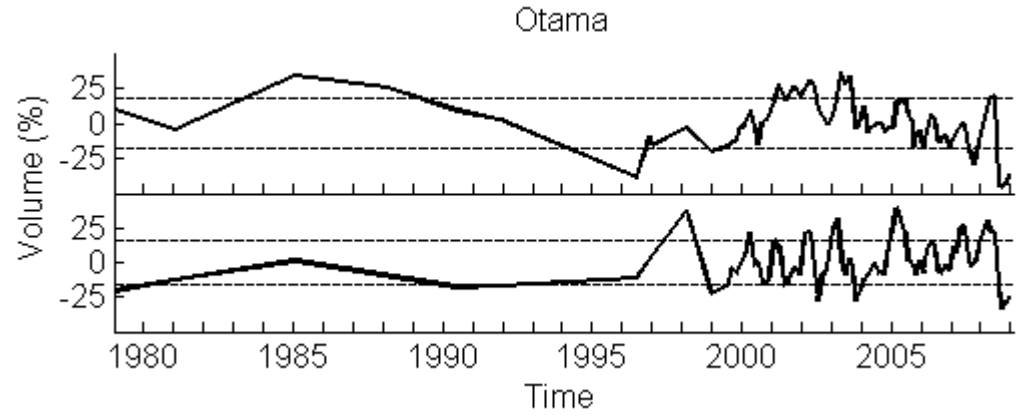


Figure VII.6: Otama Beach volume timeseries. The horizontal dashed lines represent one standard deviation above and below the mean.

- Seasonal oscillations are prominent at the southern end of the beach whilst the northern end showed an IPO relationship. The July 2008 storm event had a huge impact on the beach with both profiles being subject to variation of greater than 2 standard deviations. The foredune was more pronounced in the early data at the northern site, hence the apparent

significant erosion leading into 1997. There was very little variation in the cross-shore location of the MSL contour during this time however, which indicated the stability of the profile.

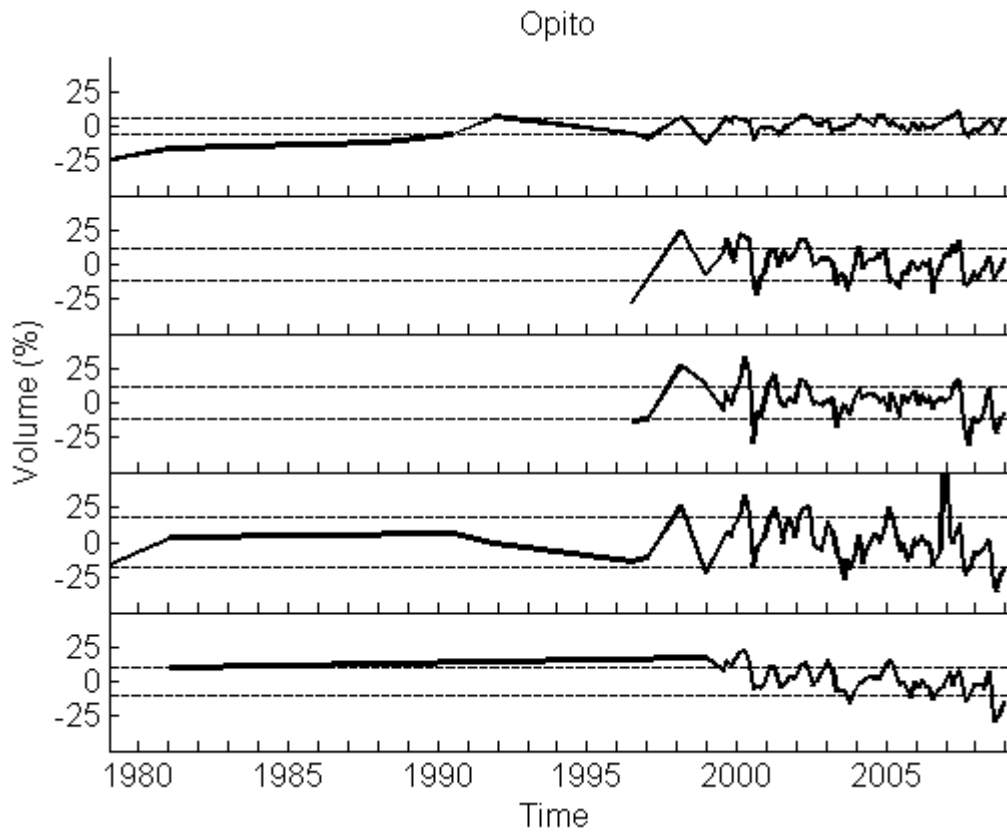


Figure VII.7: Opito Beach volume timeseries. The horizontal dashed lines represent one standard deviation above and below the mean.

- The stability at the northern site is exaggerated by the very low beach volume in the late 1970's. However the site did show a reasonable amount of long term stability regardless. The southern two profiles appeared to show slight erosion trends from 2000 to 2009. Overall the beach showed relative stability for the available data.

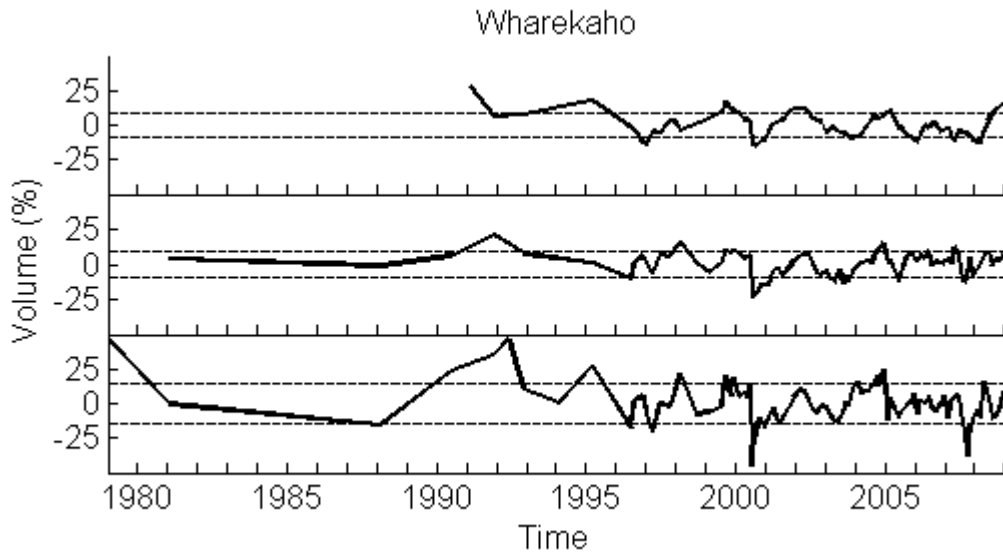


Figure VII.8: Wharekaho Beach volume timeseries. The horizontal dashed lines represent one standard deviation above and below the mean.

- Increasing variation in the beach from north to south was evident. The northern profile also showed a prominent biennial trend which was confirmed in Chapter 5. The entire beach was not eroded during the July 1978 or July 2008 storm events which highlights the sheltered nature of the beach.

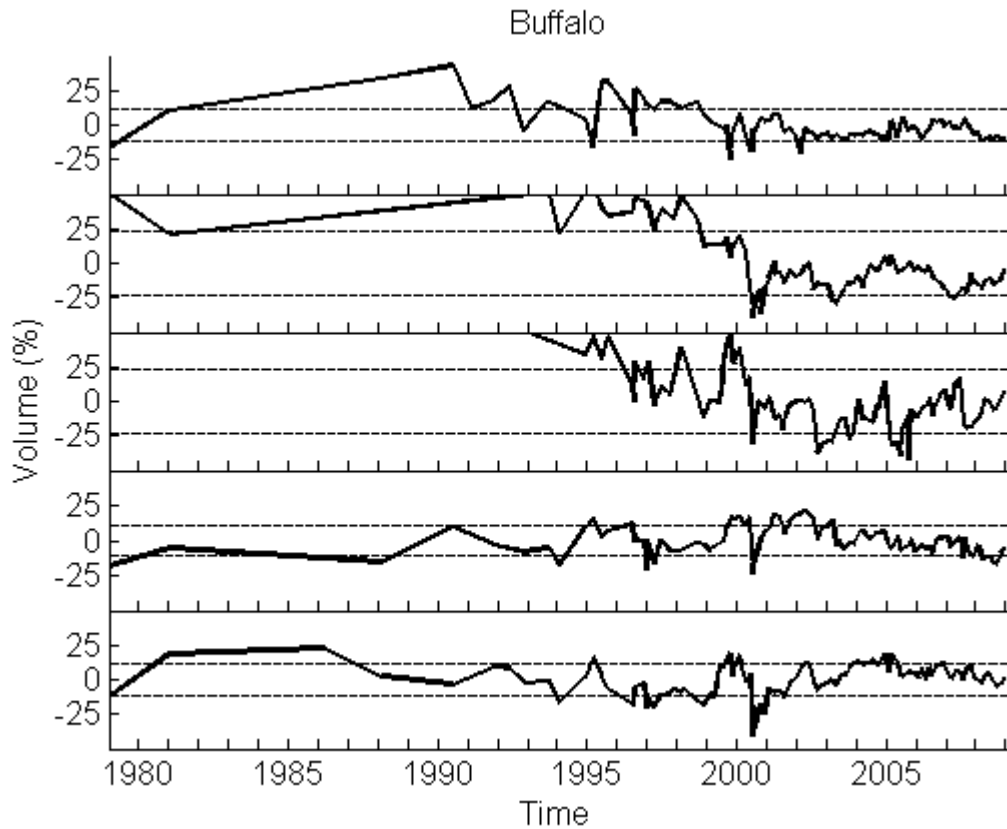


Figure VII.9: Buffalo Beach volume timeseries. The horizontal dashed lines represent one standard deviation above and below the mean.

- Significant erosion of the northern 3 profiles from the early 1990's to early 2000's was prominent. These profiles showed recovery or stability since this significant erosion however. A prominent erosion event across the entire beach occurred in mid 2000. Interestingly the two harbour adjacent profiles at the southern end of the beach showed relative stability. These two profile sites are located relatively centrally and appear most exposed to the dominant northeast and easterly wave climate.

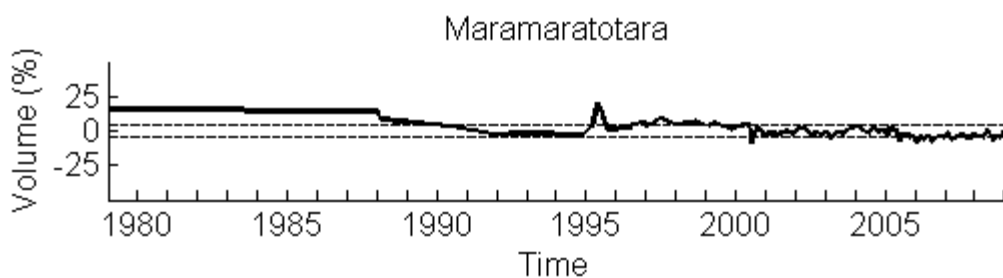


Figure VII.10: Maramaratotara Beach volume timeseries. The horizontal dashed lines represent one standard deviation above and below the mean.

- Overall the beach was subject to very minor volume change. The most prominent feature is the long term erosion trend for the entire timeseries which has shown a total variation of greater than 2 standard deviations.

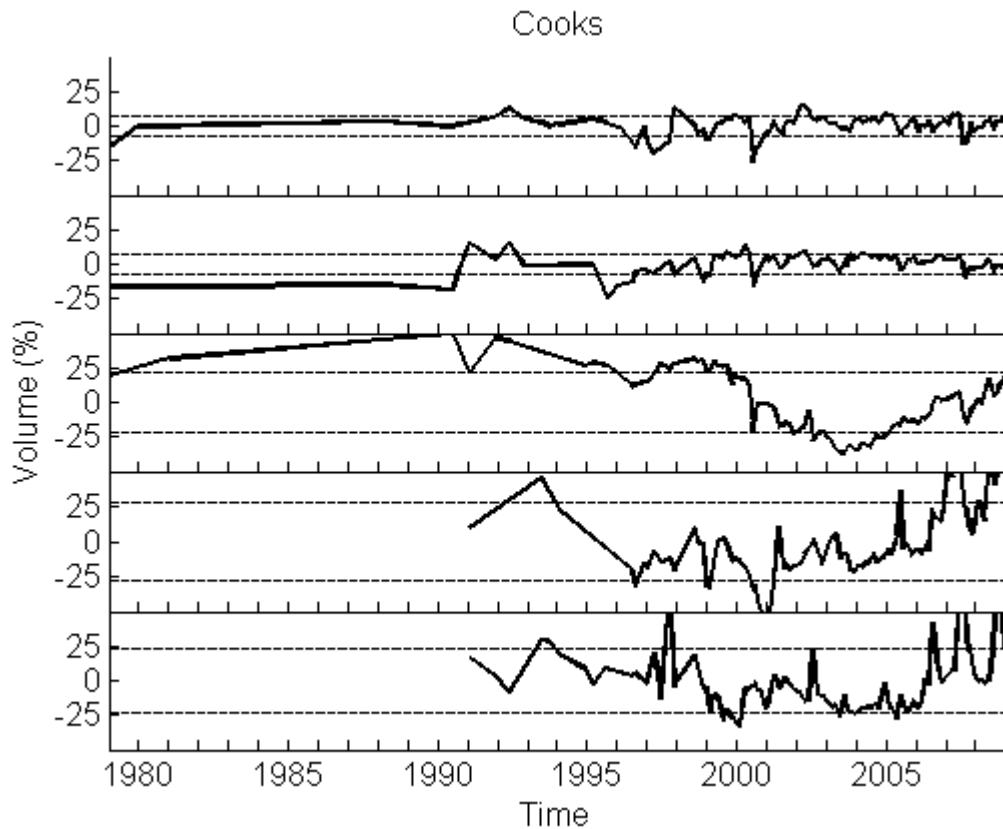


Figure VII.11: Cooks Beach volume timeseries. The horizontal dashed lines represent one standard deviation above and below the mean.

- The different behaviour alluded to in Chapter 4 is prominent. The southern 3 profiles show completely different and strong cyclic behaviour when compared to the northern 2 profiles. Overall the northern 2 profiles have been stable following erosion from the 1978 storm. Harbour adjacent impacts were particularly evident in the southern profile with large volume increases during winter in 2006, 2007, and 2008.

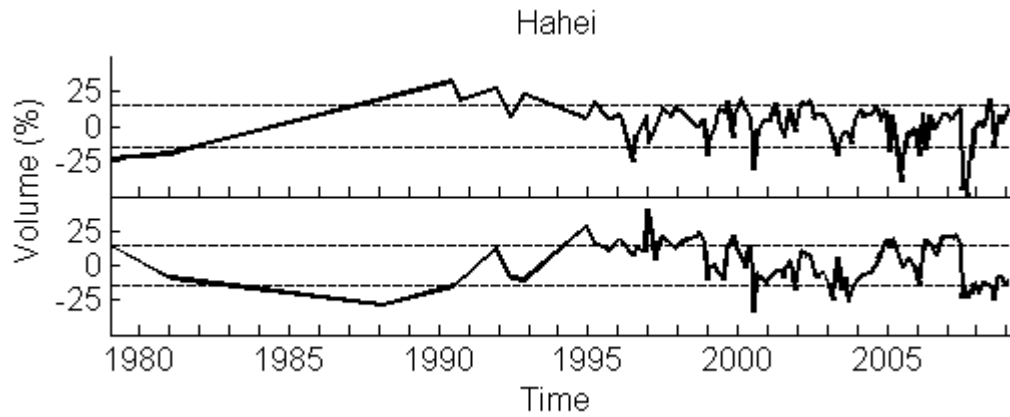


Figure VII.12: Hahei Beach volume timeseries. The horizontal dashed lines represent one standard deviation above and below the mean.

- Contrasting beach volumes were evident following the July 1978 storms. The data showed that both profiles showed a relatively large degree of variation, however both exhibit long term stability.

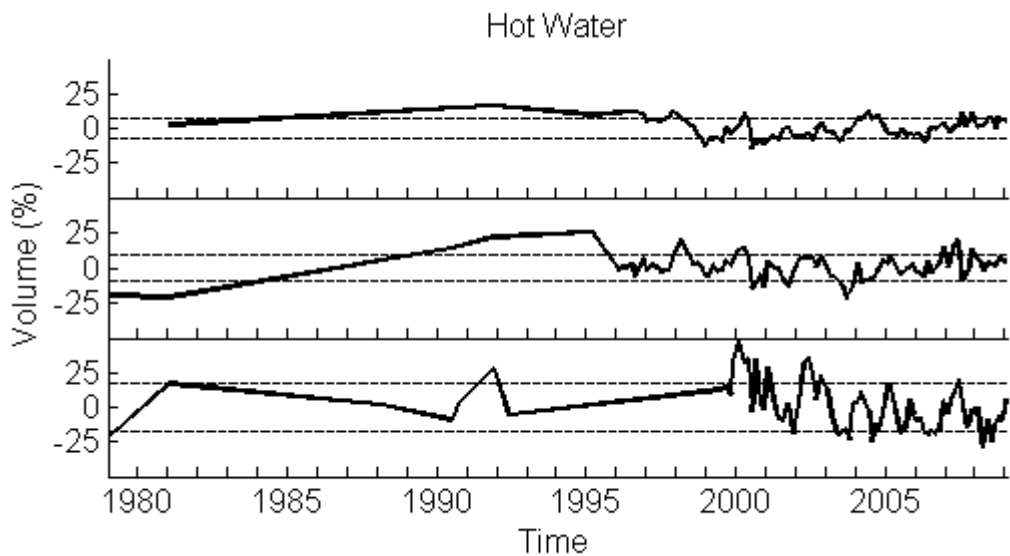


Figure VII.13: Hot Water Beach volume timeseries. The horizontal dashed lines represent one standard deviation above and below the mean.

- The large volume variations typical of reflective beaches were most prominent at the southern end of Hot Water Beach. The increasing standard deviations from north to south were also prevalent on beaches south of Mercury Bay.

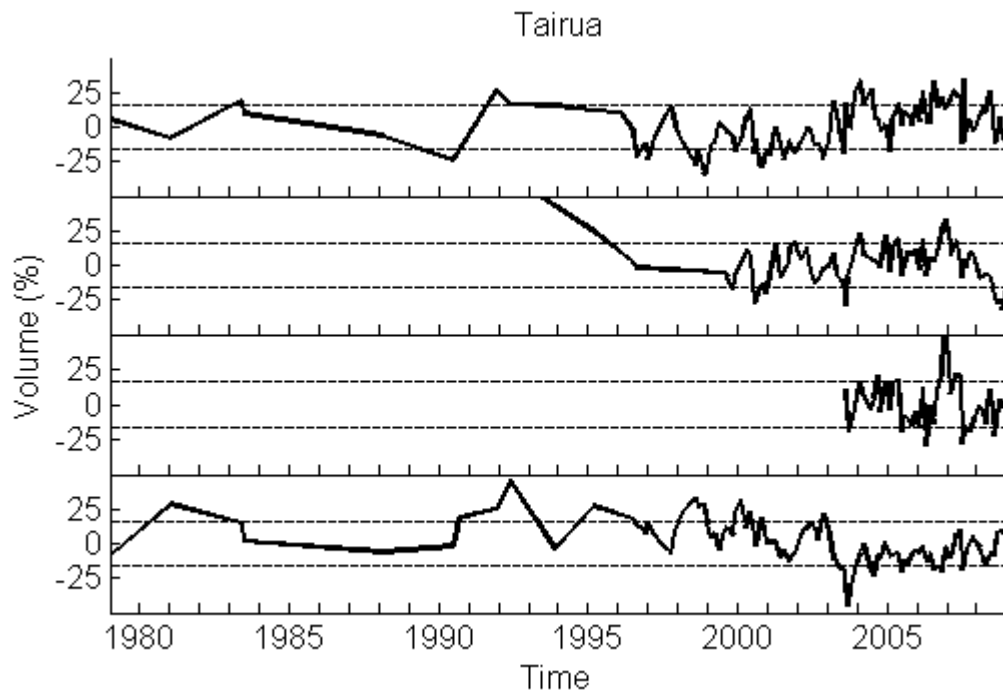


Figure VII.14: Tairua Beach volume timeseries. The horizontal dashed lines represent one standard deviation above and below the mean.

- Beach rotation was evident in the raw data with contrasting interannual trends of high and low volumes between the northern and southern ends of the beach. The large magnitudes of change for reflective beaches are particularly prevalent at Tairua. With relatively large standard deviations and short term variability.

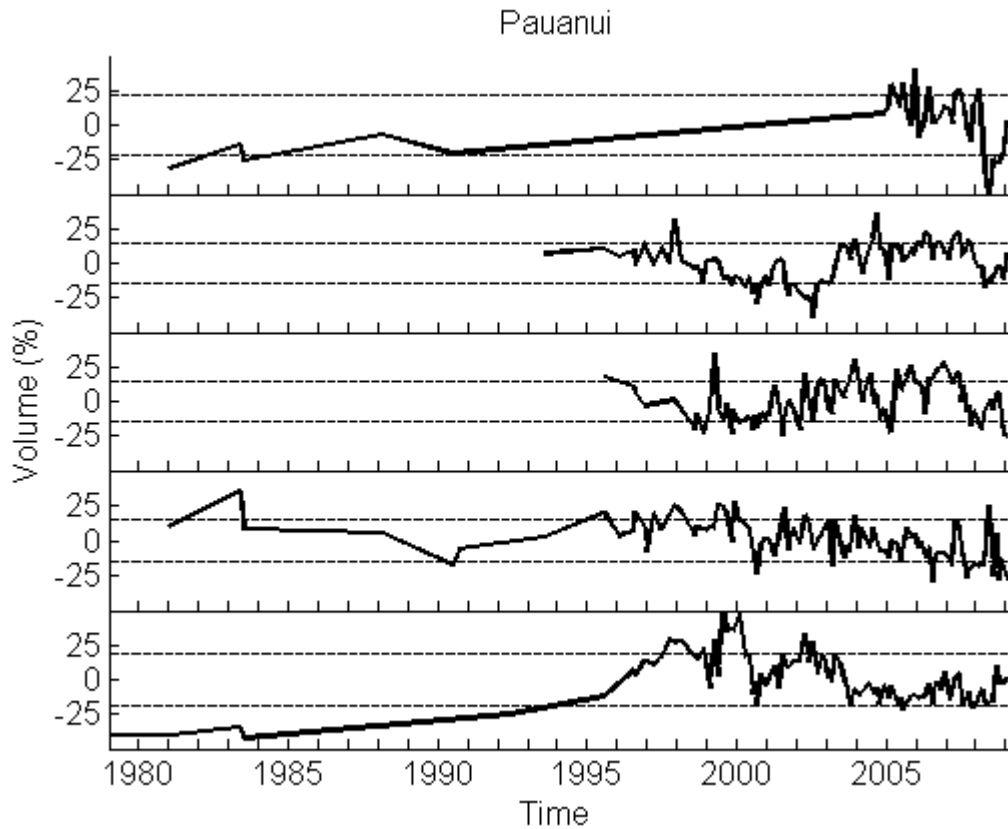


Figure VII.15: Pauanui Beach volume timeseries. The horizontal dashed lines represent one standard deviation above and below the mean.

- The short dataset not considered at the northern site is prevalent with an approximate 15 year period where no surveys were taken. When ignoring the northern most profile, the two southern profiles and the next two profiles from the north show similar behaviour between the adjacent profiles, but was not uniform across the beach.

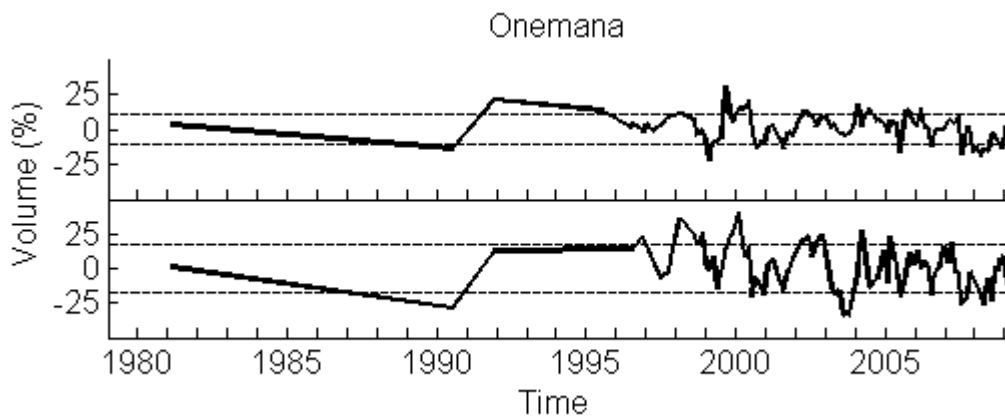


Figure VII.16: Onemana Beach volume timeseries. The horizontal dashed lines represent one standard deviation above and below the mean.

- The strong erosion trend in the southern profile was evident from 1995 to 2009. Both profiles showed a long term trend of erosion. A strong seasonal signal was also prevalent at the southern site.

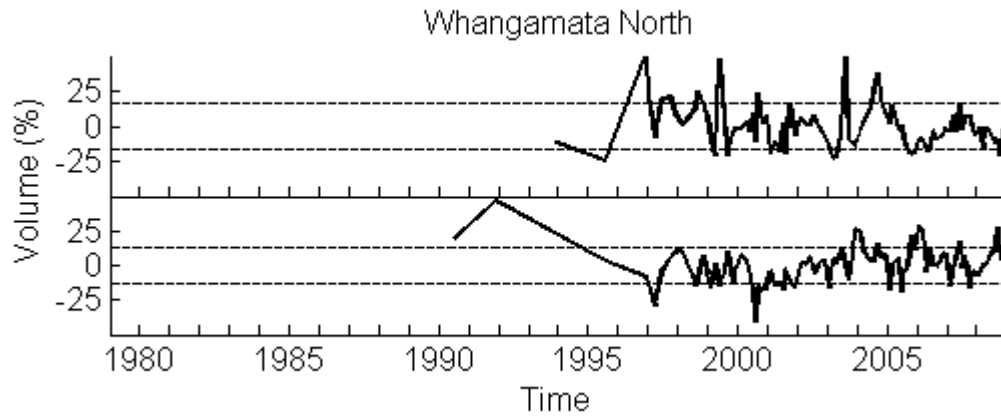


Figure VII.17: Whangamata North Beach volume timeseries. The horizontal dashed lines represent one standard deviation above and below the mean.

- The two profiles on this beach did not show uniform behaviour. The highly variable nature of the northern profile was attributed to being located adjacent to Whangamata Harbour. The southern profile showed a steady increase in overall beach volume since 1997. The large volume at this site in 1991 was due to a large berm formation and overall profile. The MSL contour was located more than 20 m further seaward than any profile in the proceeding 10 years to 2001.

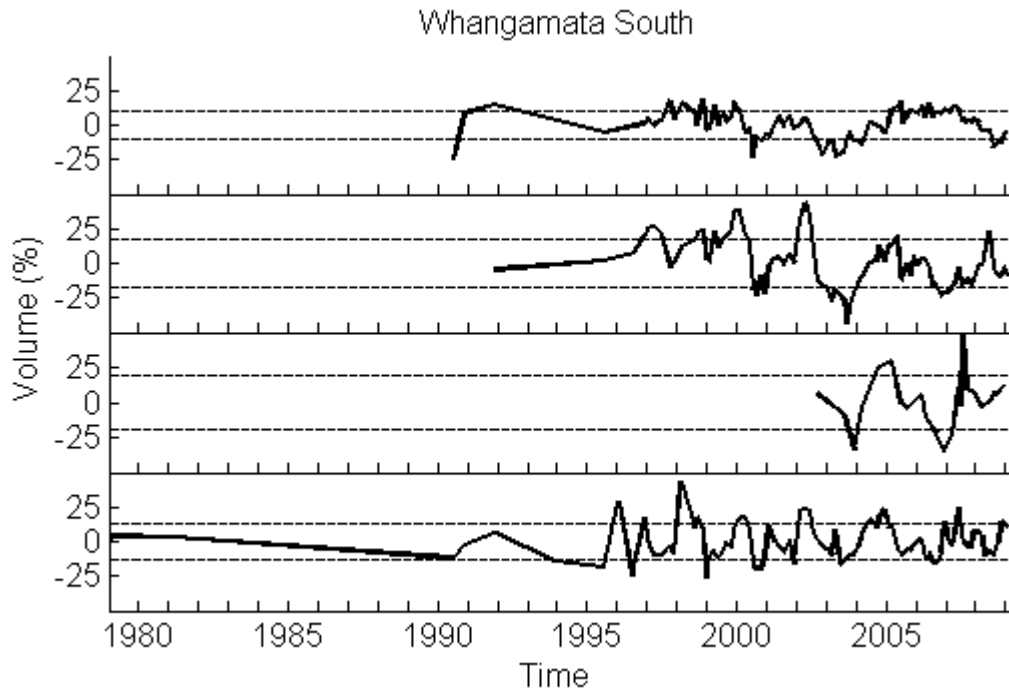


Figure VII.18: Whangamata South Beach volume timeseries. The horizontal dashed lines represent one standard deviation above and below the mean.

- Of particular interest was the evidence of the biennial oscillation in the data at the southern profile site and profile second from the north. Overall the beach appeared very stable with no significant long term oscillations or trends.

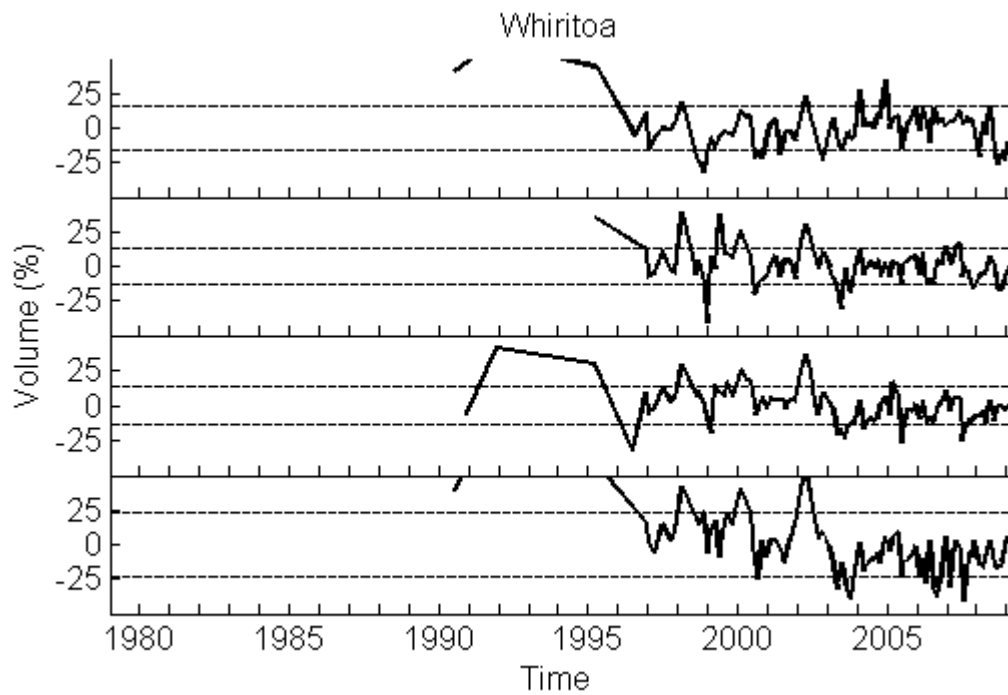


Figure VII.19: Whiritoa Beach volume timeseries. The horizontal dashed lines represent one standard deviation above and below the mean. The apparent missing data is due to the beach volume exceeding 50 % of the mean thus being beyond the axis limits.

- The large volume variations typical of reflective beaches were prevalent when data at the northern and southern profile sites were more than 50 % above the mean during the early to mid 1990's. The northern 3 sites showed relatively stable long term trends, however the profile second from south had a decreasing trend, and the southern profile an apparent significant erosion trend. This was exaggerated by elevated volumes early in the data, however did show significant erosion from the early 1990's to early 2000's. The significant volume decrease was due to a significant landward retreat of the MSL contour of approximately 30 m. The dune region remained very similar.

APPENDIX VIII

MAGNITUDE OF CHANGE RESULTS

This appendix contains the magnitude of change results for each individual profile. The beach average data shown in Figures 3.11 to 3.14 were derived from the individual profile data shown here. The data were normalised as discussed in Section 3.3.2, therefore three profiles with short datasets were excluded, those being: Tairua CCS36-2; Pauanui CCS38; and, Whangamata South CCS57-2. All graphs in this appendix maintain the same visual properties regarding profile locations. The beaches and profiles are plotted from north to south (refer Table II.1) with the following colour scheme in each figure: solid black line (northernmost); dotted blue line; dashed green line; dash-dot red line; and, solid magenta line with circle marker points. The y axis data are the frequencies of occurrence of each bin of magnitude of change data. The x axis magnitude of change data were grouped into 0.2 m³.m⁻¹.day⁻¹ bins. of beach volume and a common unit of m³.m⁻¹ was used. The key findings from the results in addition to those discussed in Chapter 3 were:

- Rings Beach and Maramaratotara were identified as outlier beaches. The individual profile analysis showed that these two profiles had the lowest volume variations compared to all other sites on the Coromandel Peninsula;
- There was one exception in which CCS22-1 at Wharekaho Beach which was similar, and this was identified in Figure 3.15 also which was attributed to the sheltered location of the profile.

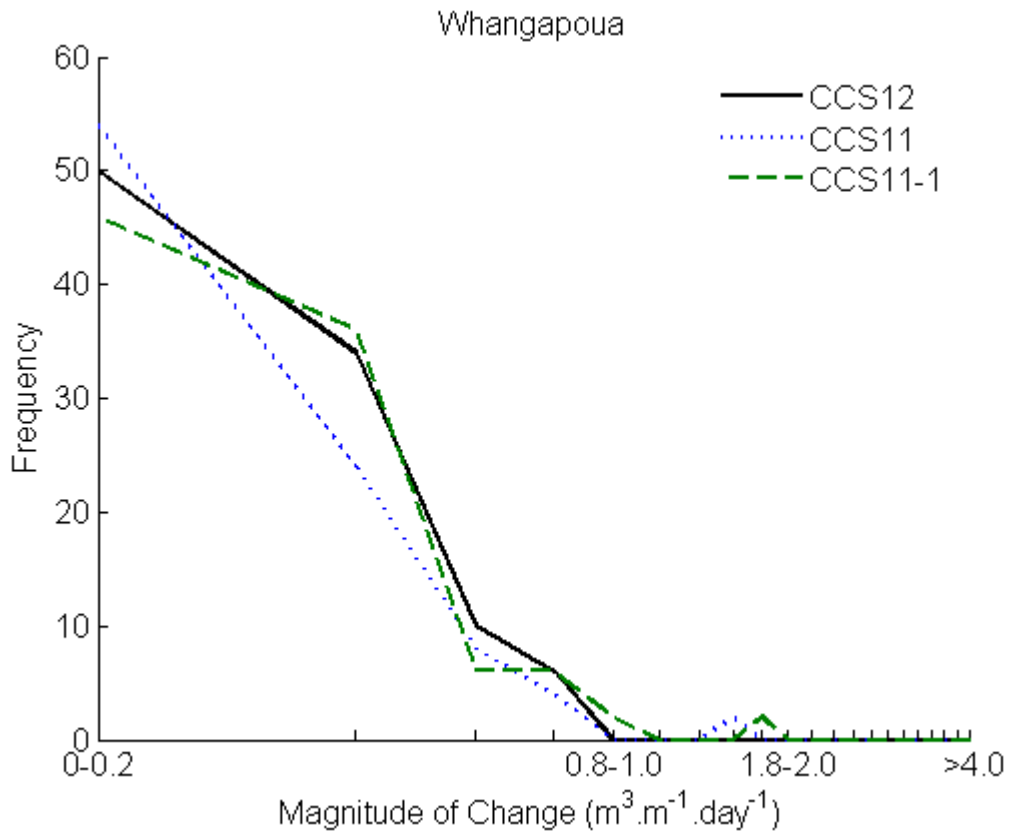


Figure VIII.1: Whangapoua Beach magnitude of change data for each profile.

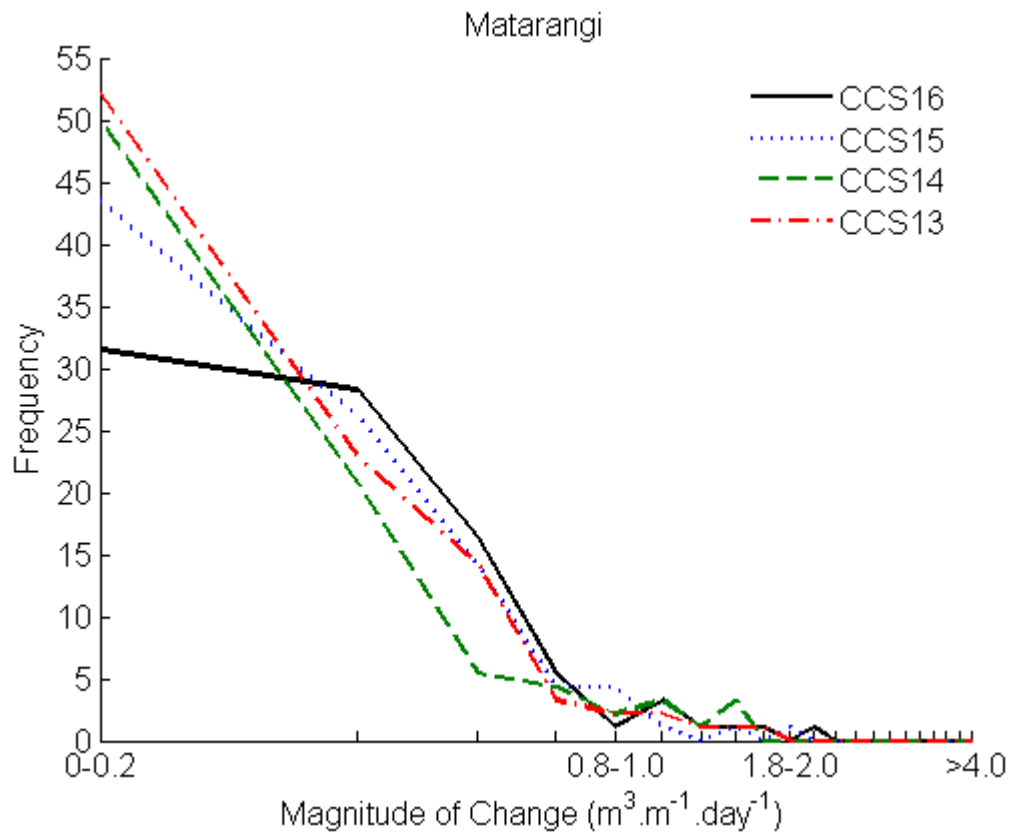


Figure VIII.2: Matarangi Beach magnitude of change data for each profile.

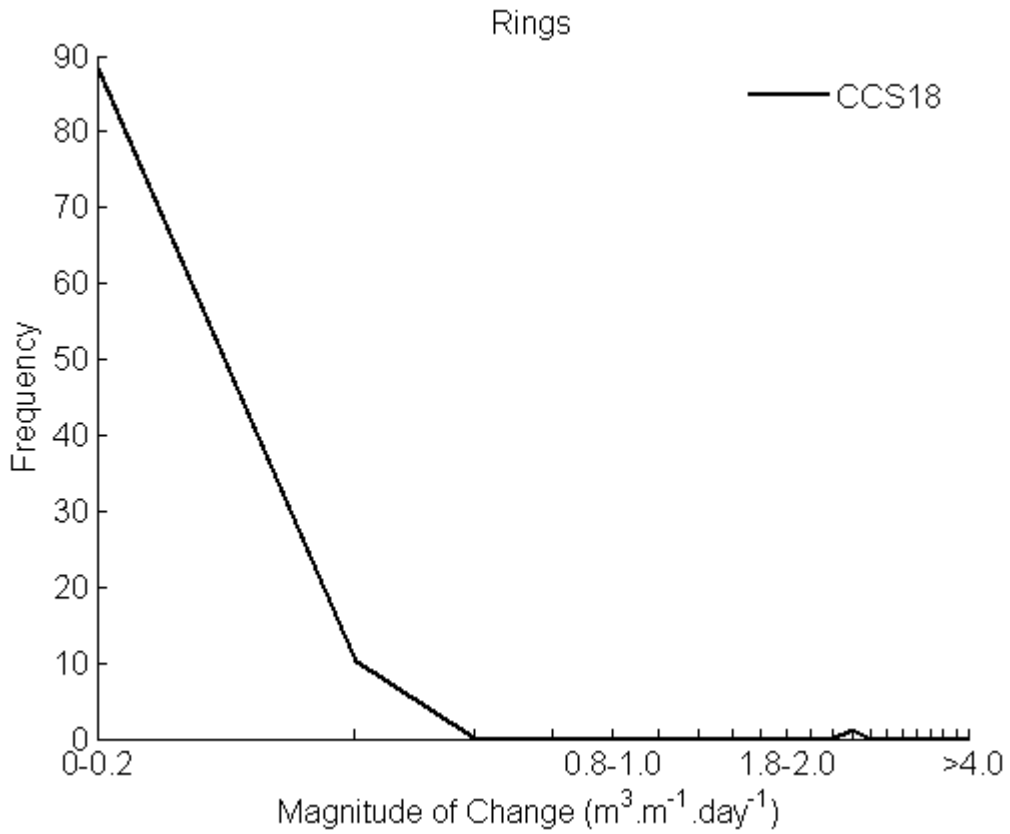


Figure VIII.3: Rings Beach magnitude of change data for each profile.

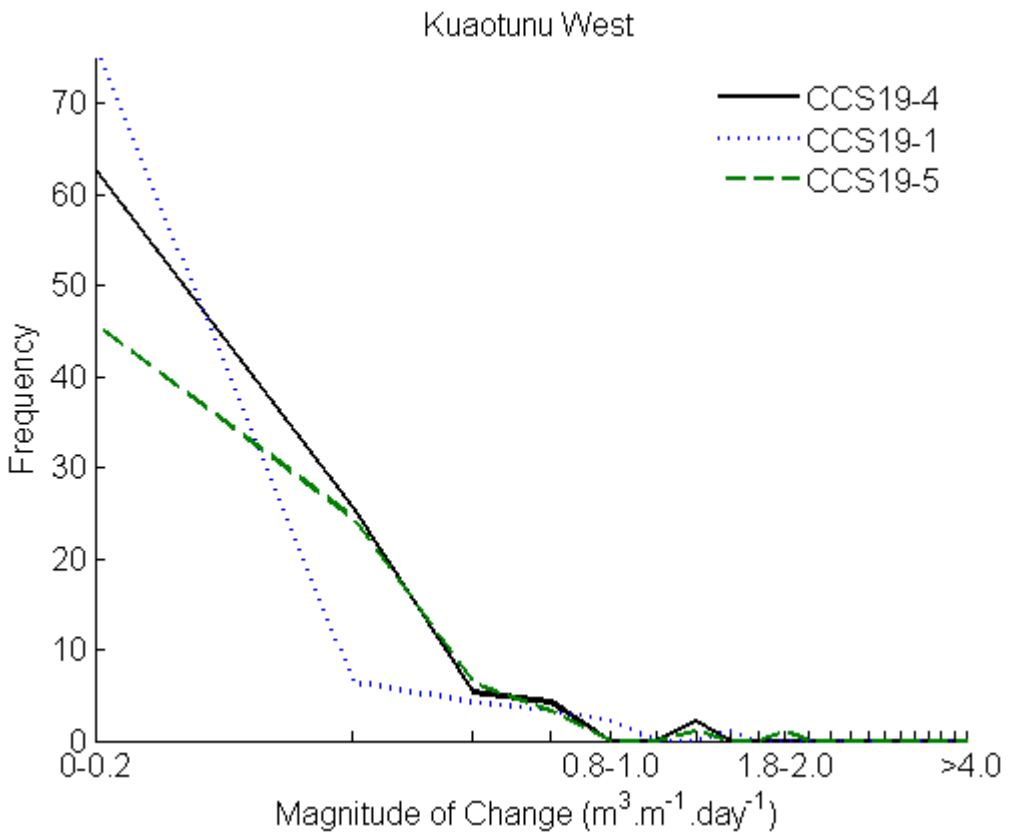


Figure VIII.4: Kuaotunu West Beach magnitude of change data for each profile.

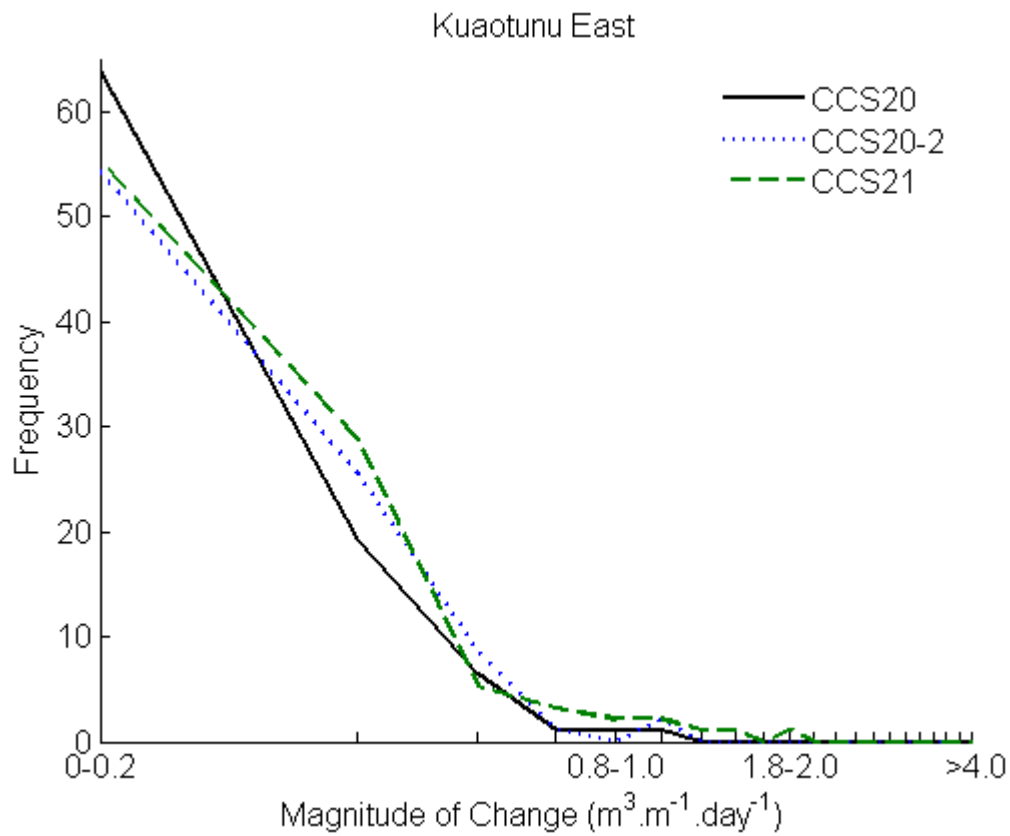


Figure VIII.5: Kuaotunu East Beach magnitude of change data for each profile.

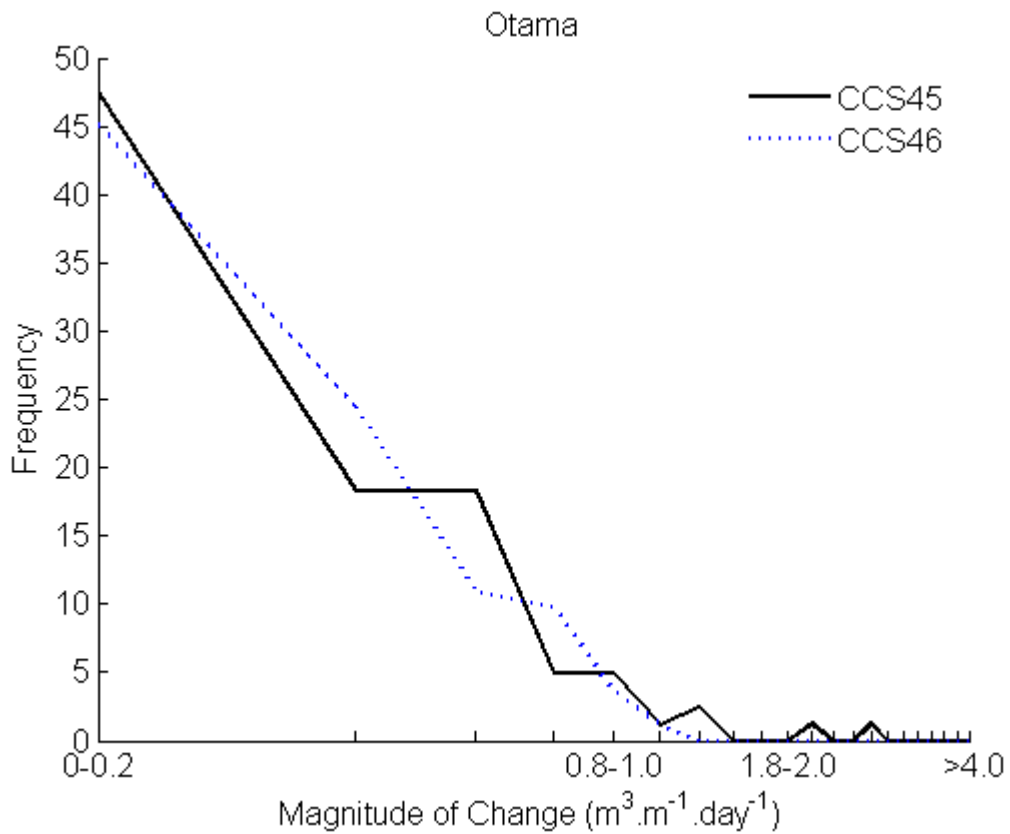


Figure VIII.6: Otama Beach magnitude of change data for each profile.

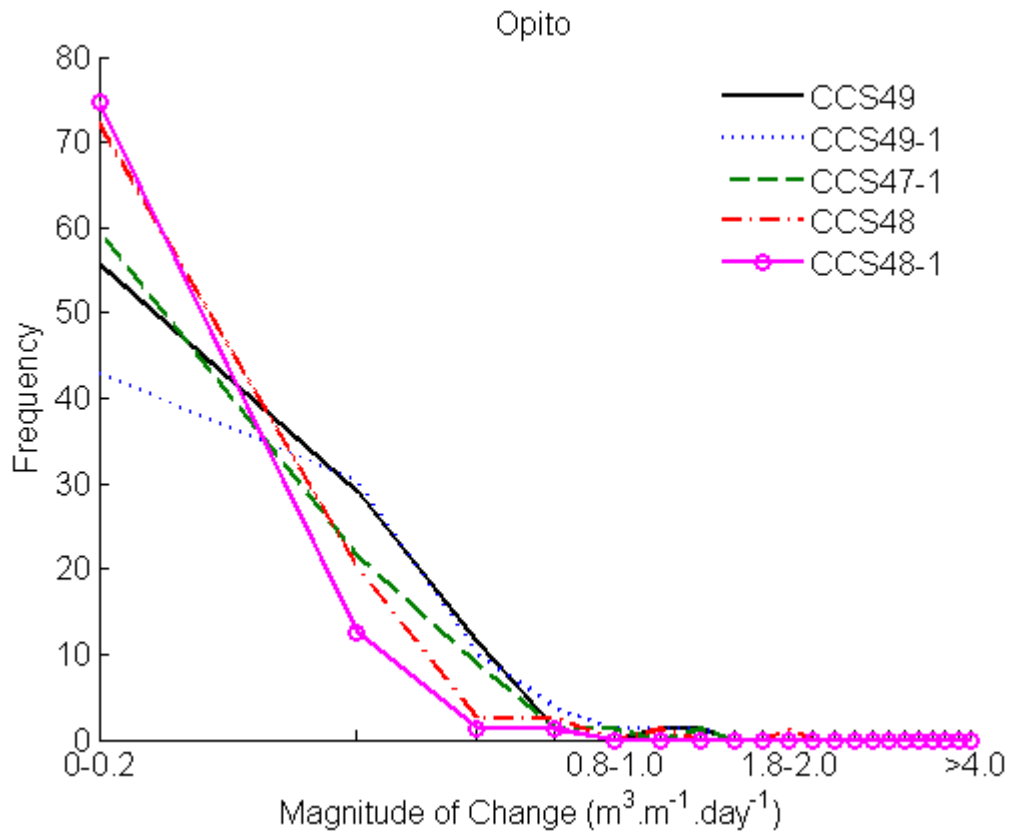


Figure VIII.7: Opito Beach magnitude of change data for each profile.

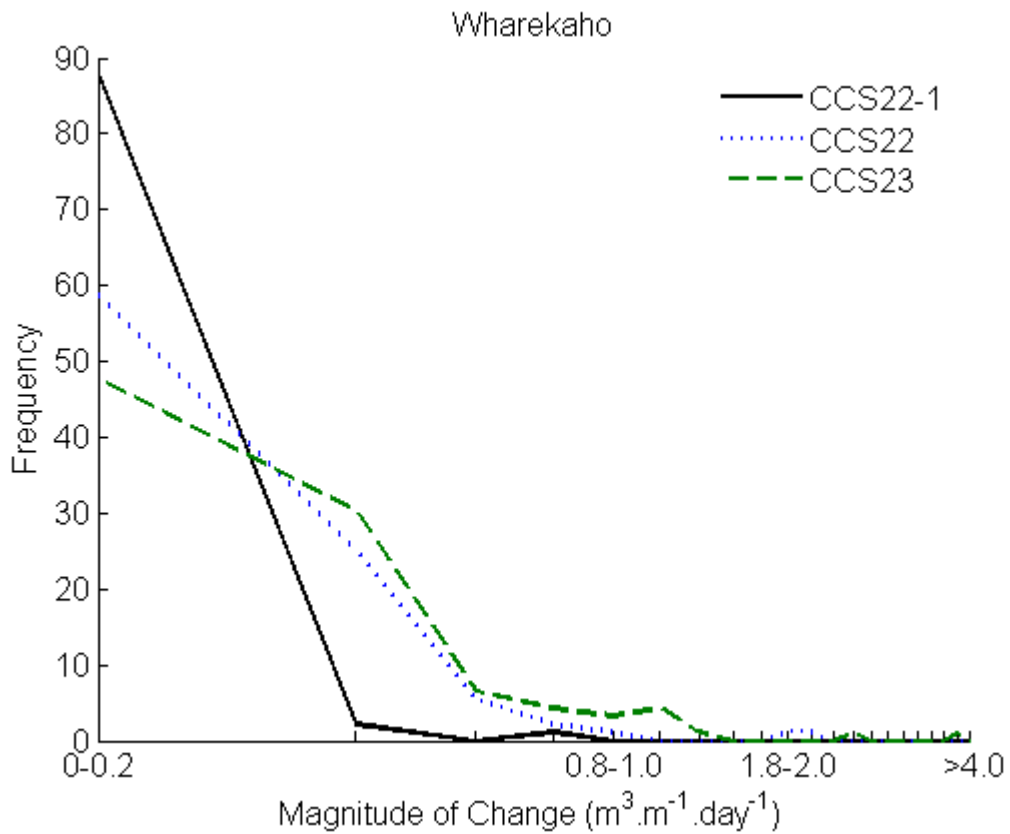


Figure VIII.8: Wharekaho Beach magnitude of change data for each profile.

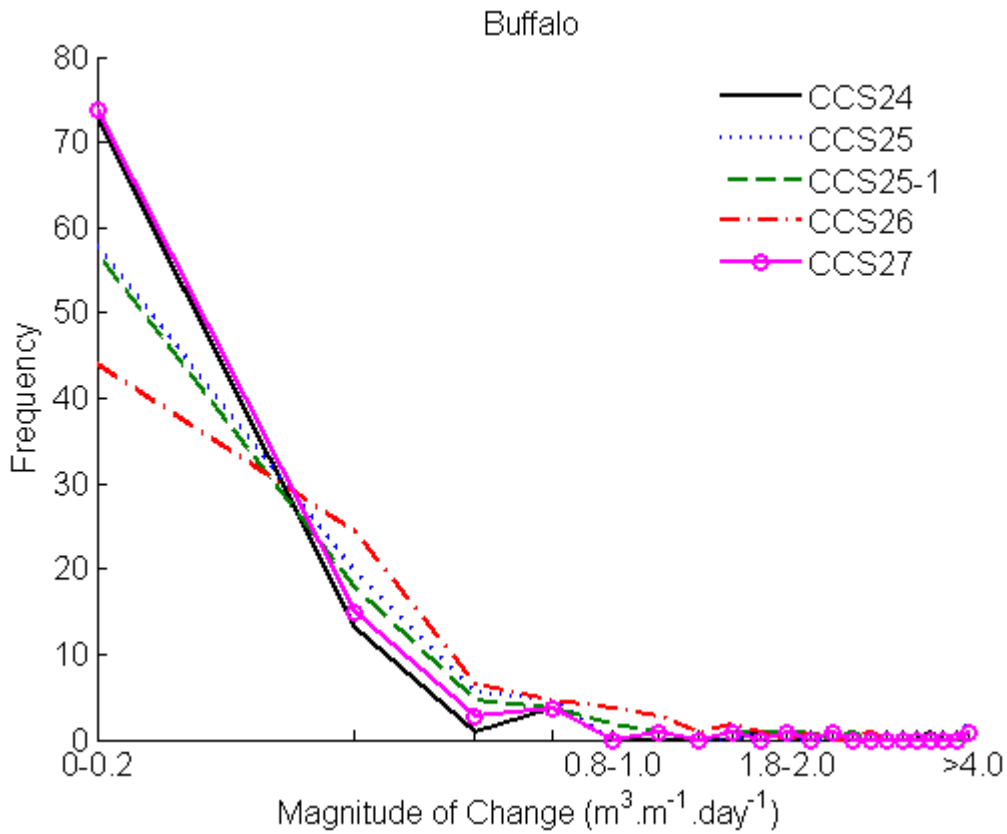


Figure VIII.9: Buffalo Beach magnitude of change data for each profile.

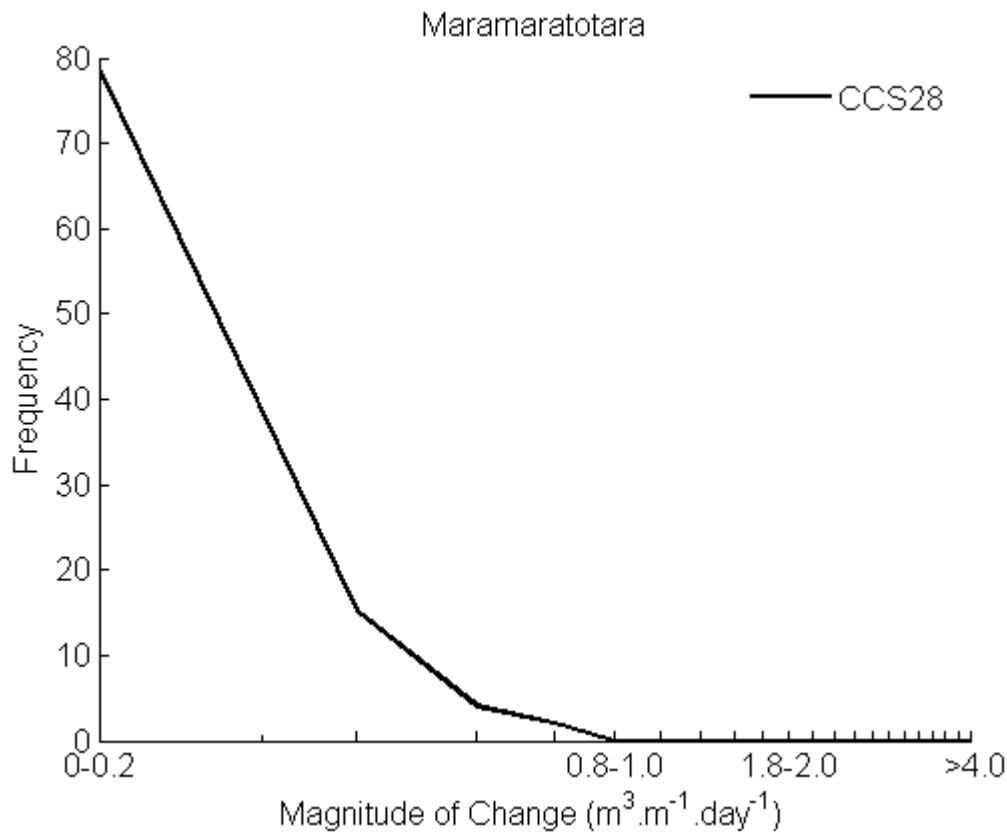


Figure VIII.10: Maramaratotara Beach magnitude of change data for each profile.

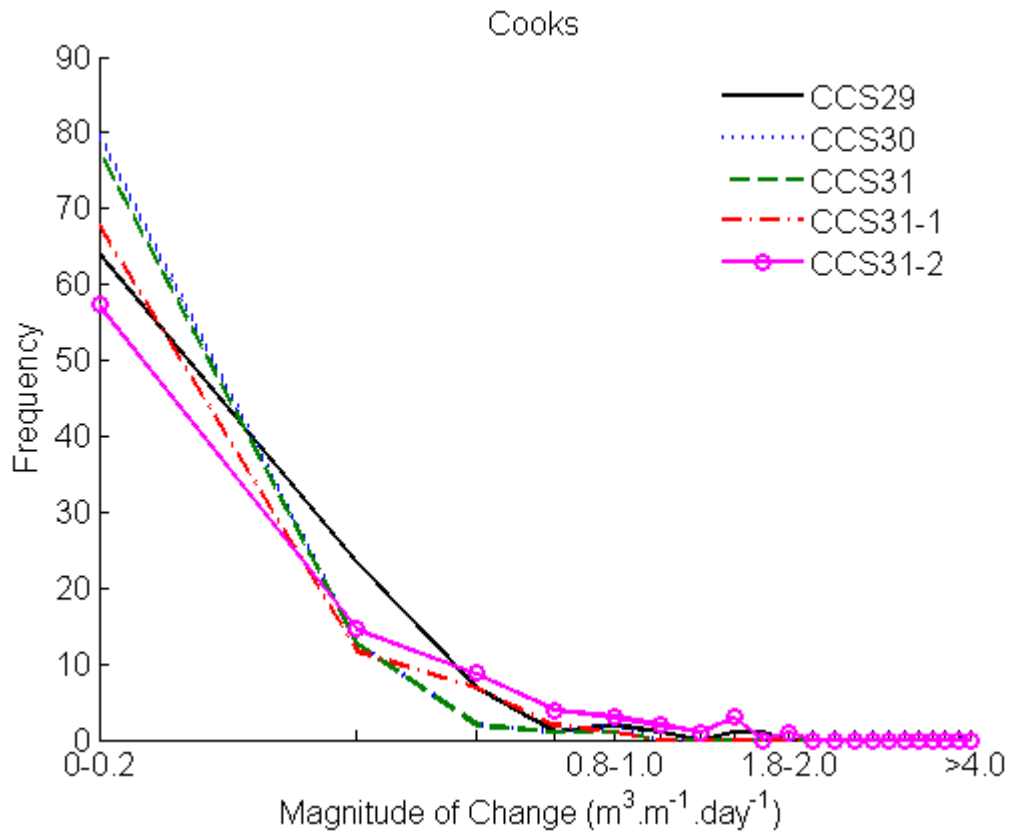


Figure VIII.11: Cooks Beach magnitude of change data for each profile.

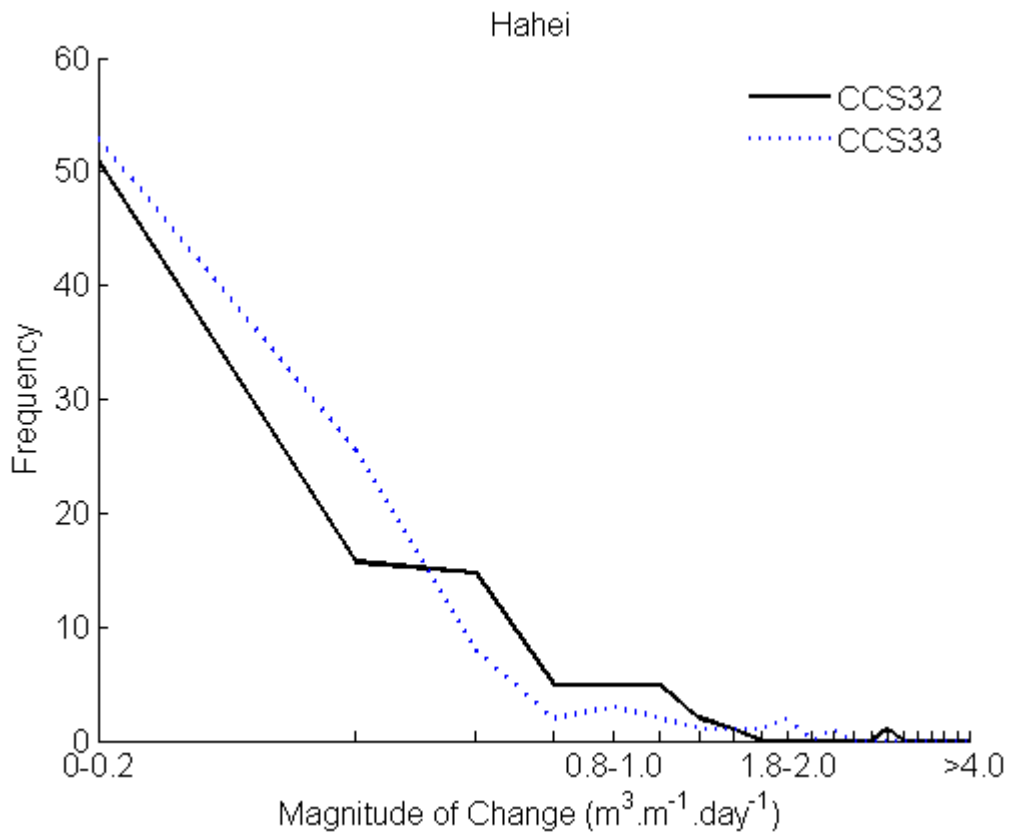


Figure VIII.12: Hahei Beach magnitude of change data for each profile.

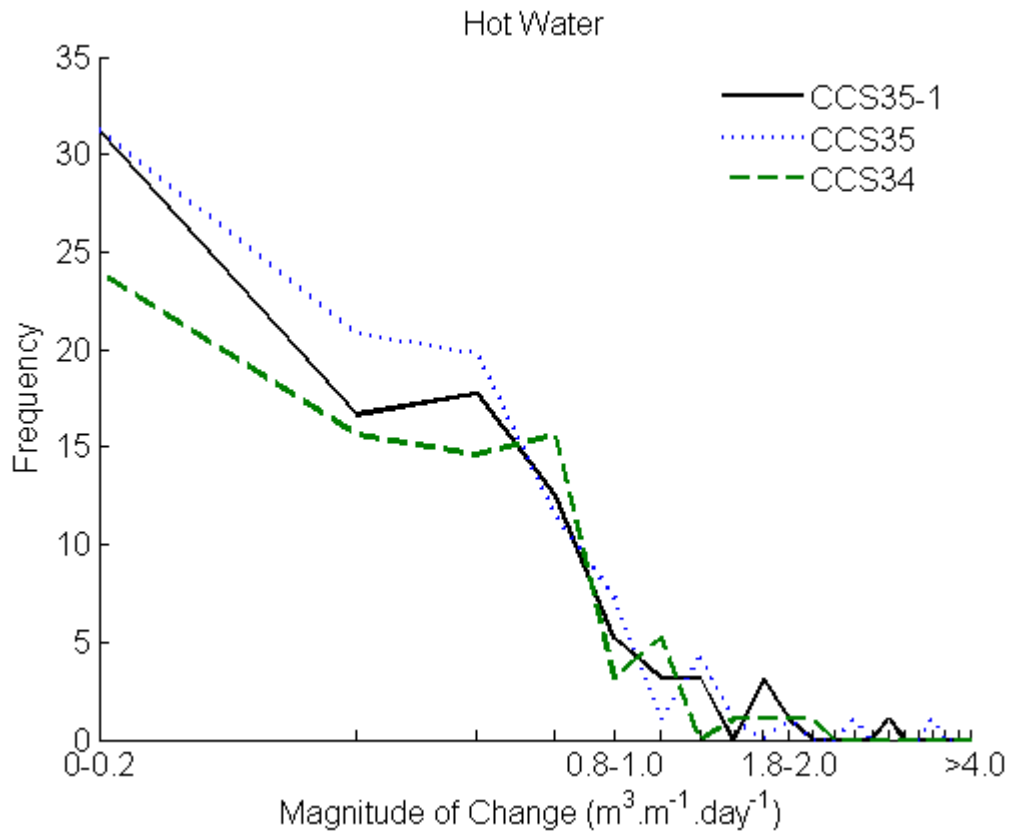


Figure VIII.13: Hot Water Beach magnitude of change data for each profile.

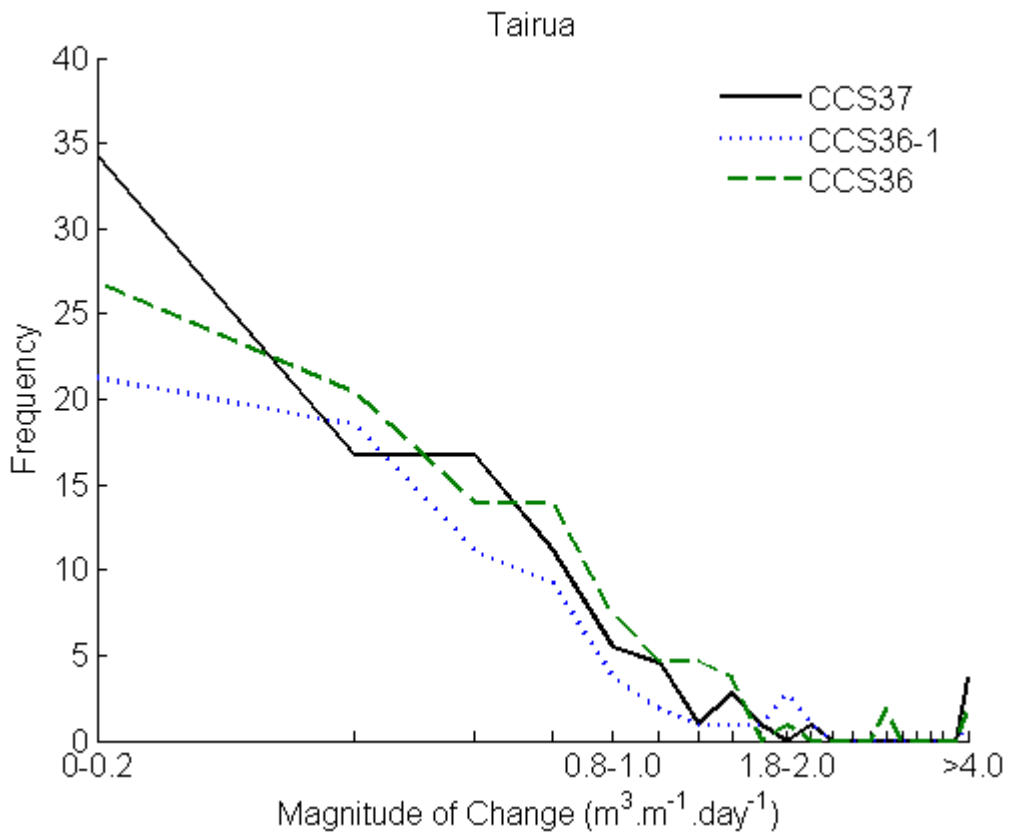


Figure VIII.14: Tairua Beach magnitude of change data for each profile.

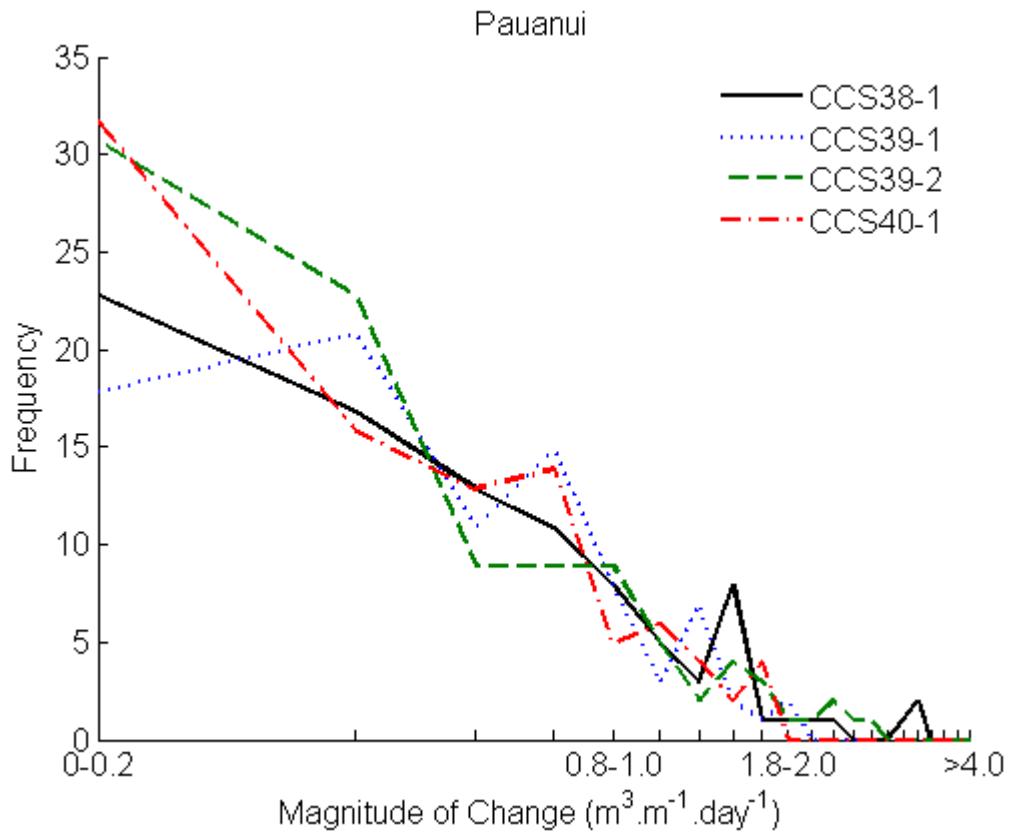


Figure VIII.15: Pauanui Beach magnitude of change data for each profile.

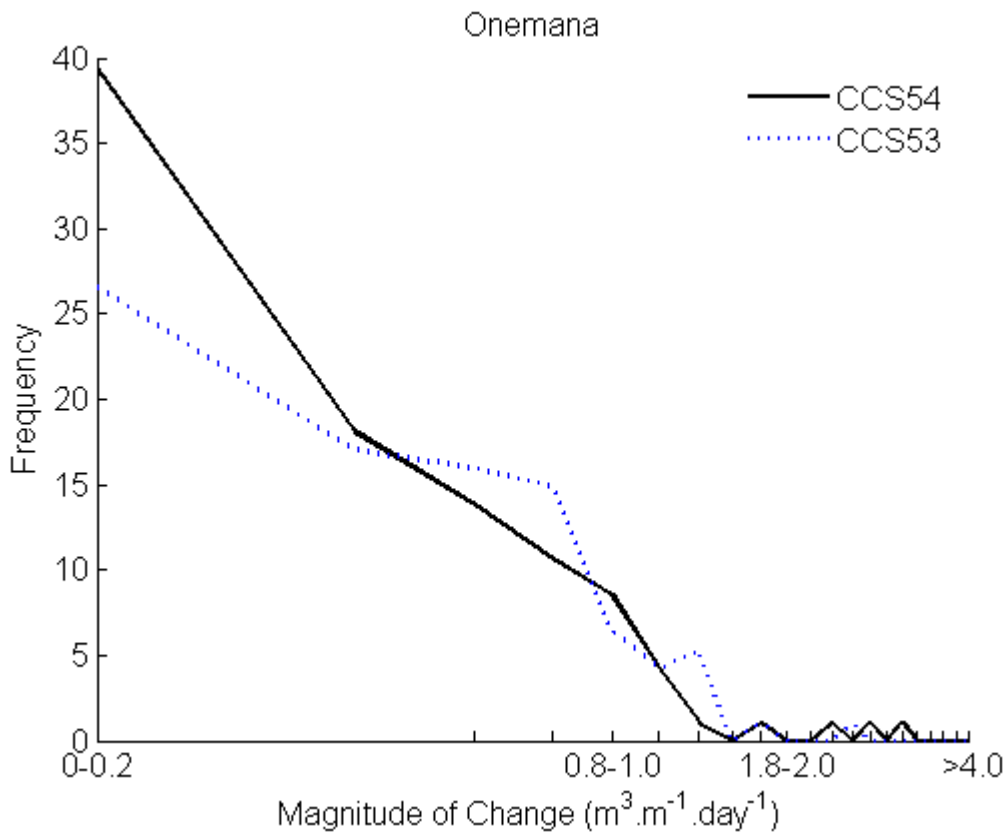


Figure VIII.16: Onemana Beach magnitude of change data for each profile.

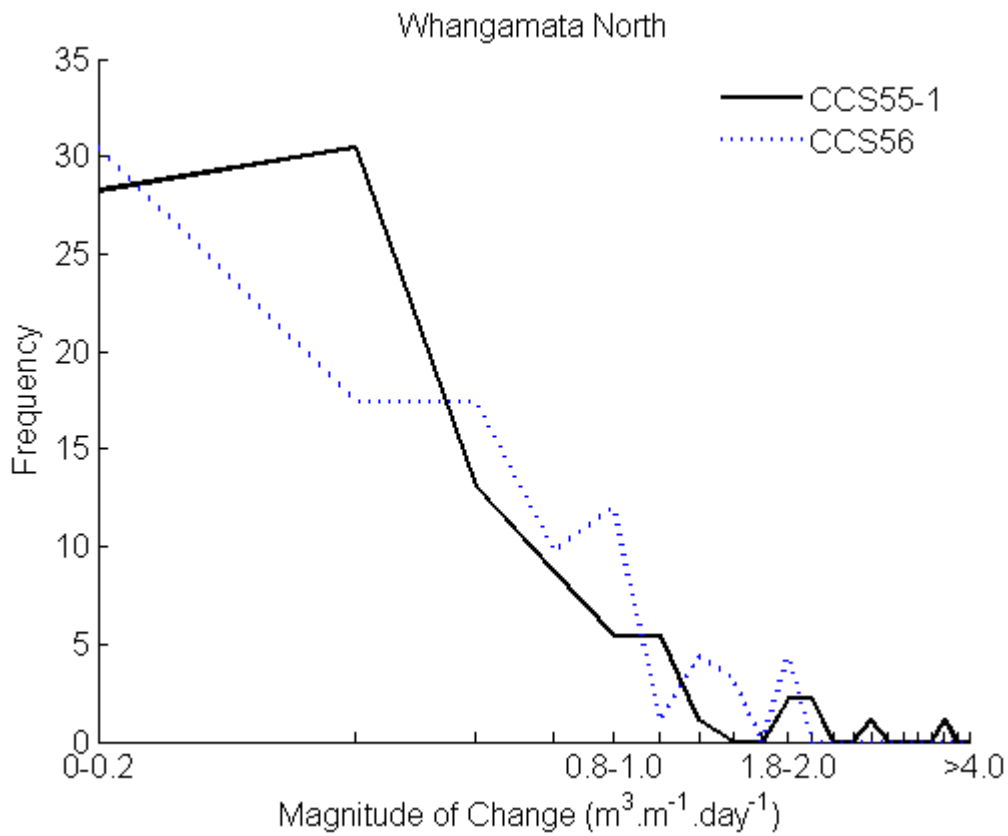


Figure VIII.17: Whangamata North Beach magnitude of change data for each profile.

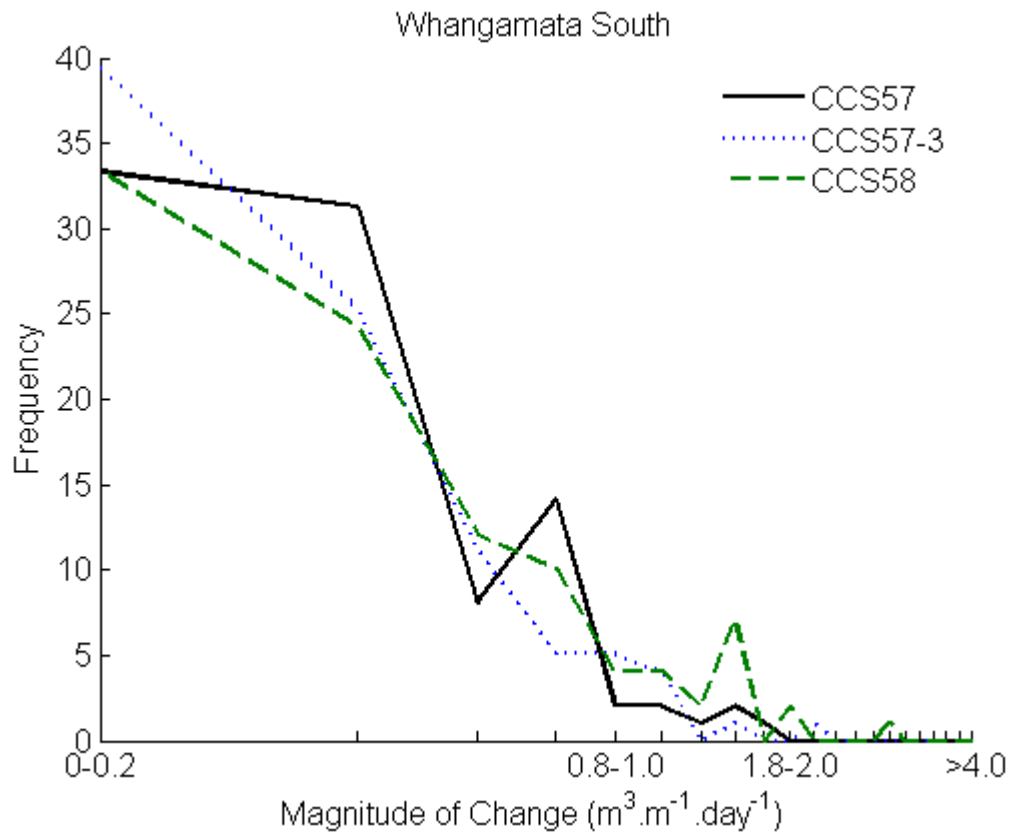


Figure VIII.18: Whangamata South Beach magnitude of change data for each profile.

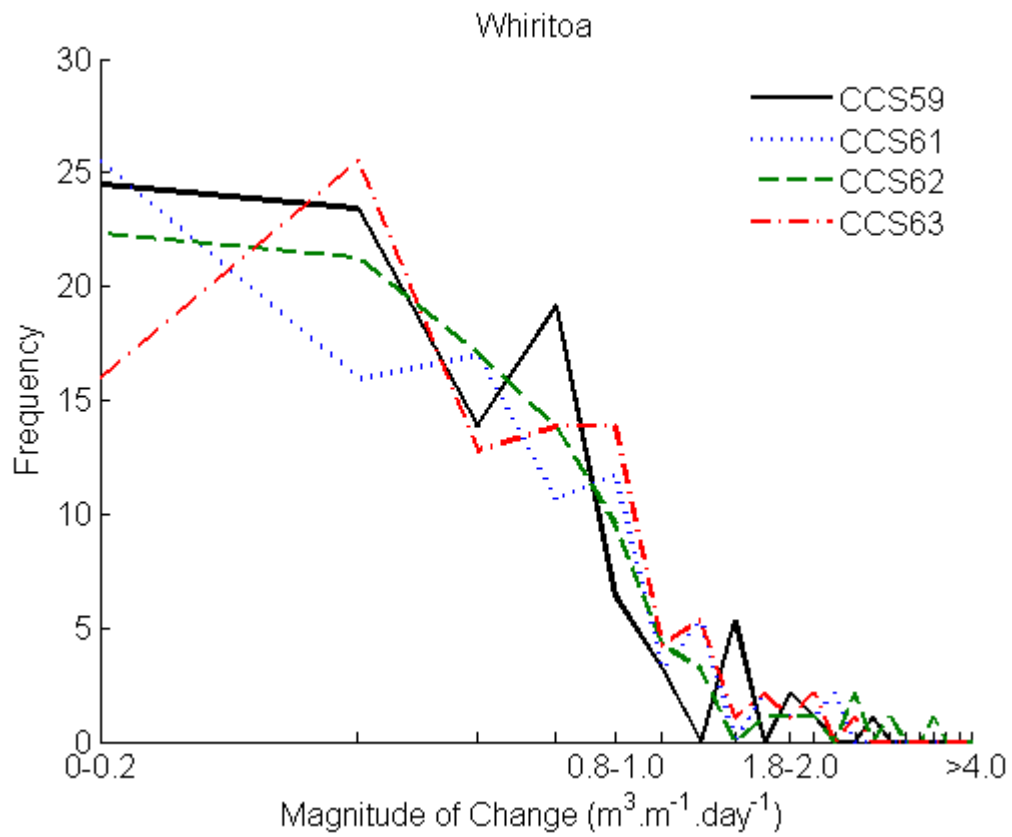


Figure VIII.19: Whiritoa Beach magnitude of change data for each profile.